



University
of Glasgow

Neckebroeck, Albane (2019) *Novel cyclopropane-based β -turn mimetics: evaluation within simple and complex peptide systems*. PhD thesis.

<http://theses.gla.ac.uk/77882/>

Copyright and moral rights for this work are retained by the author

A copy can be downloaded for personal non-commercial research or study, without prior permission or charge

This work cannot be reproduced or quoted extensively from without first obtaining permission in writing from the author

The content must not be changed in any way or sold commercially in any format or medium without the formal permission of the author

When referring to this work, full bibliographic details including the author, title, awarding institution and date of the thesis must be given

Enlighten: Theses

<https://theses.gla.ac.uk/>
research-enlighten@glasgow.ac.uk

Novel Cyclopropane-Based β -Turn Mimetics: Evaluation within Simple and Complex Peptide Systems

Albane Neckebroek

M.Sci., Ingénieur chimie organique, bioorganique et thérapeutique

Thesis submitted in fulfilment of the
requirements for the Degree of Doctor of Philosophy



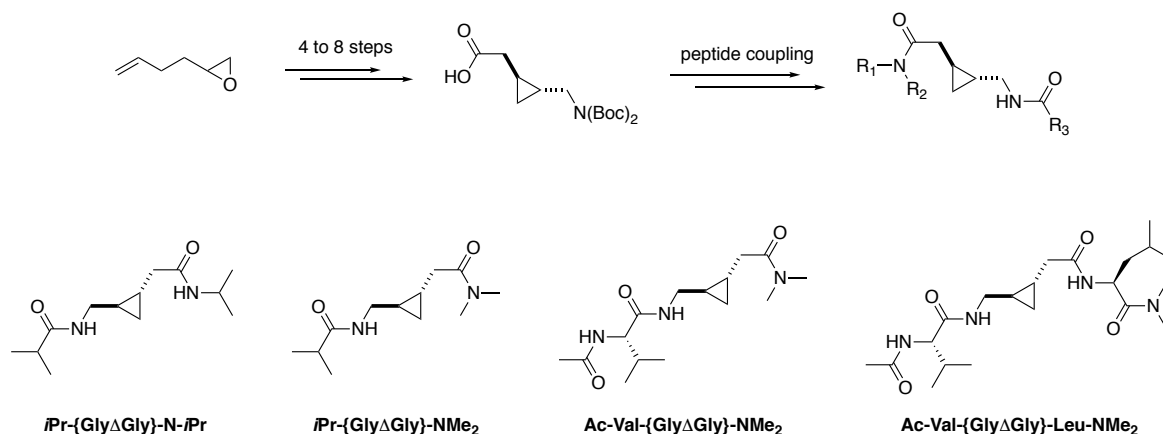
School of Chemistry
College of Science and Engineering
University of Glasgow
September 2019

Abstract

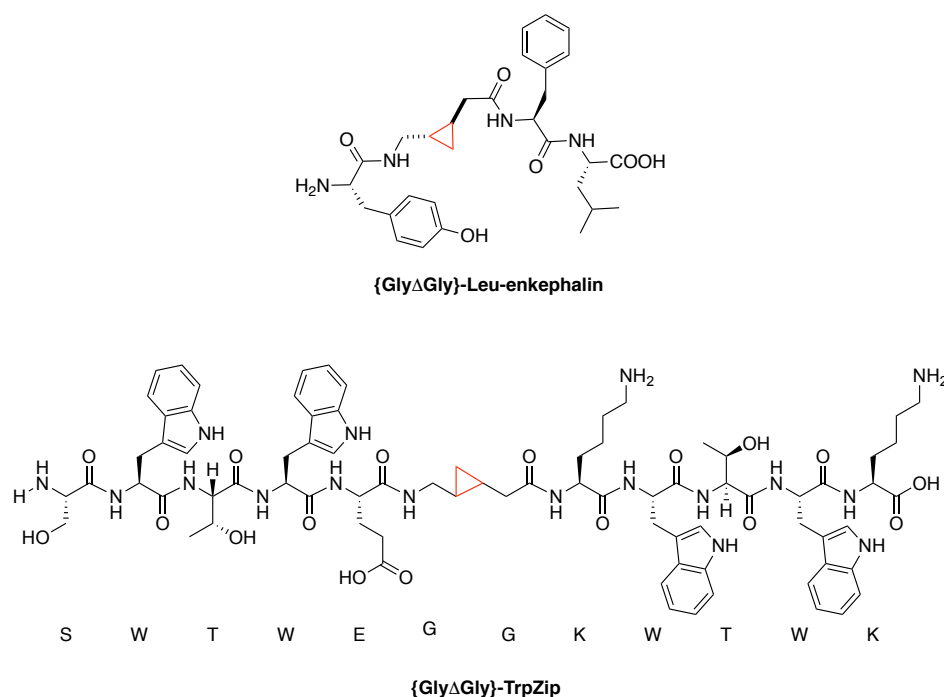
Peptides are crucial in biological processes: depending on their structure and location in the body they play different important roles. *In vivo*, peptides can be cleaved by proteases that degrade and reduce their activity. Studies have shown that peptide bonds can be mimicked in order to prevent cleavage *in vivo* while retaining bioactivity and increasing the solubility as well as the ability to control the folding of the peptide. Furthermore, synthetic targets that mimic conformational features of biologically active protein' domains have raised an intense interest for organic and medicinal chemists. The target in peptidomimetics nowadays is to get a better biological activity than natural occurring peptides by mimicking their structure.

This project focuses on the synthesis of peptidomimetics containing a cyclopropane as an amide bond isostere. Incorporation of a cyclopropane allows the molecule to be constrained conformationally, bringing hydrogen bond donor and acceptor groups together and facilitating reverse turn formation. To demonstrate this concept, the racemic and enantioenriched {GlyΔGly} dipeptide replacement units were synthesised and then incorporated at the centre of different short peptide chains. Optimisation and development of a new strategy is described in this thesis along with spectroscopic analyses to identify the secondary structure adopted by the peptides.

IR, concentration-dependant NMR, 2D NOESY NMR and circular dichroism (CD) analyses were conducted to prove the formation of this secondary structure. The studies were performed on peptides with different lengths, in order to demonstrate the propensity of β -turn formation depending on number of residues (from two to five) but also depending on the solvent. Intramolecular hydrogen bond formation was determined by NMR and IR spectroscopy, which allowed identification of the conformation. 2D NMR and CD spectroscopy allowed to isolate precisely the conformation adopted by the mimics.



Promising results from these model systems were obtained and applied to the synthesis of novel cyclopropane-based Leu-enkephalin and TrpZip peptide analogues. Those peptides are known to form β -turn and β -hairpin respectively, so controlling hydrogen bonding and the folding properties is particularly important.



Herein is described the synthesis of the longer analogues using the Gly-Gly surrogate designed and their full conformational analysis. CD and 2D NMR conformational analysis were conducted in order to identify the folding pattern of the analogues designed.

This project was achieved with the kind help of Dr. Drew Thomson and his PhD student Selma Crecente Garcia who provided MD calculation and helped with the acquisition of the different NMR experiments followed by the assignments of protons of the TrpZip peptides; Dr. Brian Smith who kindly provided the 600 MHz NMR spectrometer and his expertise in

protein conformational analysis; and Dr. Sharon Kelly for the CD measurements and interpretation.

Table of Contents

Abstract	<i>i</i>
Table of Contents	<i>iv</i>
Acknowledgements	<i>vii</i>
Declaration	<i>ix</i>
Abbreviations	<i>x</i>
Introduction	<i>1</i>
1.1. Proteins and peptides: structure and function	<i>1</i>
1.2. The peptide bond: generality and isosteres	<i>4</i>
1.3. Structure of proteins and peptides	<i>7</i>
1.3.1. Interactions stabilising the folding of a protein/peptide	<i>7</i>
1.3.2. Primary and secondary structure	<i>10</i>
1.3.3. Tertiary and quaternary structure	<i>13</i>
1.4. β-turn, generality and medicinal chemistry target	<i>15</i>
1.4.1. Definition and interest	<i>15</i>
1.4.2. Conformational analysis tools for β -turn identification	<i>17</i>
1.5. β-Turn peptidomimetics	<i>21</i>
1.5.1. Introduction to peptidomimetics and examples	<i>21</i>
1.5.2. β -Turn peptidomimetics, synthesis and analysis	<i>24</i>
1.5.3. Cyclopropanes: generality and synthesis	<i>43</i>
1.6. Introduction to the design and synthesis of β-turn mimics in the Clark group	<i>48</i>
1.6.1. Previous work in the group	<i>48</i>
1.6.2. Aim of this work	<i>56</i>
Results and discussion	<i>57</i>
2.1. Compounds Naming and Abbreviations	<i>57</i>
2.2. Strategy	<i>57</i>
2.3. Boc-{Gly Δ Gly}-OH Synthesis	<i>60</i>
2.3.1. Retrosynthetic Analysis	<i>60</i>

2.3.2.	Towards the Synthesis of 2-Ethenyl-cyclopropanemethanol Precursor for N-terminus Installation	61
2.3.3.	N-Terminus Functionalisation	66
2.3.4.	C-Terminus Installation	69
2.4.	Synthesis of Single Enantiomer Mimics by Resolution of Racemic Intermediates	73
2.4.1.	Early Stage Resolution	73
2.4.2.	Alcohol Resolution by Steglich Esterification	74
2.4.3.	Amide Coupling Resolution on Protected Amine.....	76
2.4.4.	Resolution of Carboxylic Acid Intermediates	77
2.4.5.	Summary	79
2.5.	Synthesis of Model Peptides Containing the Dipeptide Mimic	80
2.5.1.	Capped Dipeptide Synthesis	80
2.5.2.	Synthesis of Tri- and Tetra-peptide Hybrids that Contain the Mimic	83
2.6.	Synthesis of Ester Analogous of the Turn Mimics	86
2.7.	Conformational Analysis of Peptide Hybrids that Contain Turn Mimics	88
2.7.1.	Preliminary Results, NH Chemical Shift Comparison	88
2.7.2.	Hydrogen bond formation analysis.....	92
2.7.3.	Use of Circular Dichroism to Probe Peptide Structure.....	102
2.7.4.	NMR analysis of tetrapeptides 77 and 78	107
2.8.	Towards Leu-Enkephalin Mimicry.....	110
2.8.1.	Synthesis of {Gly Δ Gly}-Leu-enkephalin 132 and 133	111
2.8.2.	Conformational Analysis of {Gly Δ Gly}-Leu-enkephalin 132 and 133	112
2.8.3.	Towards the Synthesis of {Tyr Δ Gly}-Leu-enkephalin 134 and 135	116
	<i>Tryptophan Zipper, turn replacement and analysis</i>	<i>122</i>
3.1.	Introduction.....	122
3.2.	Synthesis of the TrpZip and its analogues.....	126
3.3.	Circular dichroism	127
3.3.1.	Materials and methods.....	127
3.3.2.	Results and discussion	127
3.4.	MD calculation, a tool to understand the stability and folding pattern of peptides	134
3.5.	NMR conformational analysis	142
3.5.1.	Material and method	142
3.5.2.	Results and discussion	142
3.6.	Conclusion	147

<i>Conclusions</i>	<i>148</i>
<i>Experimental</i>	<i>154</i>
<i>LIST OF REFERENCES</i>	<i>251</i>

Acknowledgements

Firstly, I would like to thank Prof. J. Stephen Clark for giving me the opportunity to work on such an interesting project. He always supported me and gave me the advices I needed. I would like to thank him for giving me the freedom in my research and to build strong collaborations to successfully complete this project.

Secondly, I would like to thank Dr. Drew Thomson and his PhD student Selma Crecente Garcia, without whom the TrpZip project wouldn't have been possible. It was good fun and really interesting to work with them. Thank you for all the interesting chats, for letting me use your lab, bench, fume hood and lab equipment I needed to complete the synthesis. Selma was a great help for acquiring NMR and helping me with the painful NMR assignments. I cannot talk about NMR without thanking Dr. Brian Smith. He was speaking Chinese to me in first place, but once I could understand the NMR language, his help was precious. Thank you for your patience and great advices even when I was away. I would also like to thank Dr. Sharon Kelly for her help with the CD, for the late night she had because of me and the nice chat with had.

I would also like to acknowledge the contribution of all of the support staff in the university of Glasgow School of Chemistry. In particular I would like to thank, Ted, Karen, Andy, Jim, Alec for their help and analysis.

I would like to thank all the members of the Clark group, the France group and the Boyer group for the amazing atmosphere in the lab. I wouldn't be able to detail all the fun we had and the number of times I almost died in the office but thank you all for always bringing joy, fun and music. I would like to thank the past members of the groups: Kirsten, Sweet Mickey P (fume hood mate for ever), Gregoor (voyage, voyaaage), Sam (probably running on a mountain), Craig (thanks for introducing me to Scottish accent), David... And the present members: Arwa and Hiba (great to get to know you), Venky, Myron (DMDO you can do it), Jess (the woman of the lab!), Jim, Angus (thanks for your support, and what a time in Florence, open door policy), Destroyer and sugar addicted Dan, Stuart (the Friday inventions will be missed, great time in the France group corner!), Glen Broooodie (your love stories are simply delicious), the Matts, Alistair (thanks for all your advice and the good chats around a pint, or two!), Carolina, Michele and Stefania, Babun, Sean, Selma, Tom, Mike, and all the people who came across my way at Uni.

What would be a PhD without the friendship you build! Alex (parties, fun, car rides), Claire (hike hike hike), Stefan waaaarington, Angelos (all the coffee breaks gossiping), ma Poule (never met such a beautiful person, please be a kid with me forever), LB (nothing can describe how much I love this little Italian woman, same boat, same s***), Falkounet, Antoine (hike, weirdos and crêpes), Aurore, Marge, Petit cul, Kiko, Isa, and Mickey P. I don't know how to thank them for everything they gave me over the past few years. Your friendship is precious to me and please don't stop being crazy. I would also like to thank all my friends from Mulhouse (except Gayzou) and from high school (Nous, Nous et encore Nous) for their support during my PhD (big up to Mais Heu for this) and making my trips back to France always fantastic and full of good memories.

I would like to thank my family and especially Papy. They never understood what I was doing but supported me and helped me when I had stressing times. It was a long process, but I finally managed to finish my studies!

Well done Angus!

Declaration

I hereby declare that the substance of this thesis has not been submitted, nor is concurrently submitted, in candidature for any other degree.

I further declare that all of the work presented in this manuscript is the result of my own investigations. Where the work of other investigators has been used, this has been acknowledged in an appropriate manner.

Albane Neckebroeck

Prof. J. Stephen Clark

Abbreviations

Ac:	Acetyl
ACN:	Acetonitrile
ADME:	Absorption, Distribution, Metabolism, Elimination
Aq:	Aqueous
Arom:	Aromatic
Atm:	Atmosphere
Bn:	Benzyl
Boc:	<i>t</i> -Butyloxycarbonyl
BOP:	(benzotriazol-1-yloxy)tris(dimethylamino)phosphonium hexafluorophosphate
CD:	Circular Dichroism
CRD:	Complementary-Determining Regions
COSY:	Homonuclear correlated spectroscopy
DBU:	1,8-Diazabicycloundec-7-ene
DCC:	<i>N,N'</i> -Dicyclohexylcarbodiimide
DCE:	Dichloroethane
DCM:	Dichloromethane
DEAD:	Diethyl azodicarboxylate
DIAD:	Diisopropyl azodicarboxylate
DIBAL-H:	Diisobutylaluminium hydride
DIC:	<i>N,N'</i> -Diisopropylcarbodiimide
DIPEA:	<i>N,N</i> -diisopropylethylamine
DMAP:	4-(Dimethylamino)pyridine
DMF:	<i>N,N</i> -Dimethylformamide
DMP:	Dimethylpyrrole
DMTMM:	4-(4,6-Dimethoxy-1,3,5-triazin-2-yl)-4-methylmorpholinium chloride
DNA:	Deoxyribo Nucleic Acid
DOR:	δ Opioid Receptor
EDCI:	<i>N</i> -(3-dimethylaminopropyl)- <i>N'</i> -ethylcarbodiimide
Et:	Ethyl
FDPP:	Pentafluorophenyl diphenylphosphinate
Fmoc:	Fluorenylmethyloxycarbonyl
FT-IR:	Fourier-Transform Infrared Spectroscopy

GPCR:	G-protein coupled receptor
HB:	Hydrogen Bond
HBA:	Hydrogen Bond Acceptor
HBD:	Hydrogen Bond Donor
HBs:	Hydrogen Bonds
HBed:	Hydrogen bonded
HIV:	Human Immunodeficiency Virus
HOBt:	Hydroxybenzotriazole
HPLC:	High performance liquid chromatography
HMBC:	Heteronuclear Multi-Bond Connectivity
HSQC:	Heteronuclear Single Quantum Coherence
HRMS:	High resolution mass spectrometry
HSP:	Heat Shock Protein
IC ₅₀ :	Half maximal inhibitory concentration
<i>i</i> -Pr:	<i>Iso</i> -propyl
IR:	Infrared
KOR:	κ Opioid Receptor
LDA:	Lithium diisopropylamide
MCR:	Melanocortin Receptor
Me:	Methyl
MOR:	μ Opioid Receptor
Ms:	Methanesulfonyl
NMO:	<i>N</i> -Methylmorpholine <i>N</i> -oxide
NMR:	Nuclear magnetic resonance
NOE:	Nuclear Overhauser Effect
NOESY:	Nuclear Overhauser Effect spectroscopy
PCNA:	Proliferating Cell Nuclear Antigen
PMB:	Para-methoxybenzyl
PPACK:	Phe-Pro-Arg Chloromethyl Ketone
PyBOP:	(Benzotriazol-1-yloxy)tripyrrolidinophosphonium hexafluorophosphate
RCM:	Ring closing metathesis
RNA:	Ribonucleic acid
SAR:	Structure activity relationship
Su:	Succinimide
T3P:	Propylphosphonique anhydride
<i>t</i> -Bu:	<i>Tert</i> -butyl

TBDPS:	<i>tert</i> -Butylephenylsilyl
TFA:	Trifluoroacetic acid
TFE:	Trifluoroethanol
THF:	Tetrahydrofuran
TLC:	Thin layer chromatography
TrpZip:	Tryptophan Zipper
TOCSY:	Total Correlation Spectroscopy
TPAP:	Tetrapropylammonium perruthenate
UV:	Ultraviolet

Chapter 1

Introduction

1.1. Proteins and peptides: structure and function

Proteins and peptides are of fundamental importance in most biological processes. They perform a variety of important roles both within and outside of the cells of all organisms. The role can be a structural (collagen or elastin),¹ a dynamic function such as transport (myoglobin)², a metabolic control (hormones, receptors),³ muscle contraction agent (myosin),⁴ or catalysis of a chemical reaction (enzymes, Figure 1).⁵

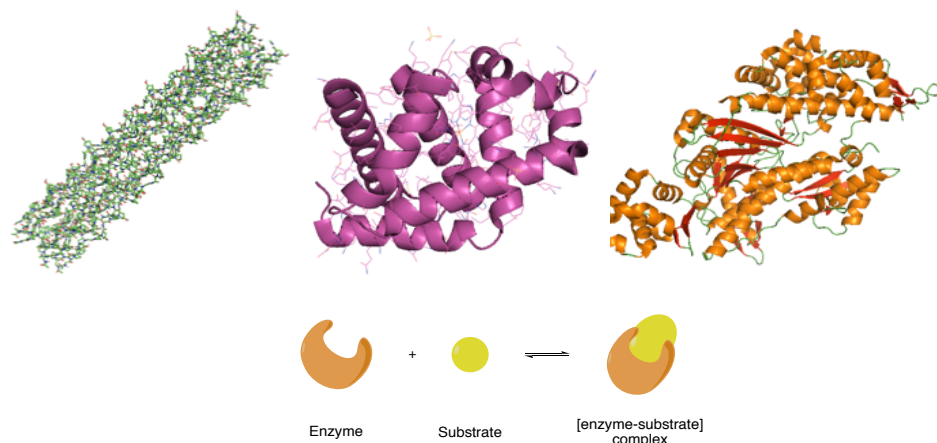
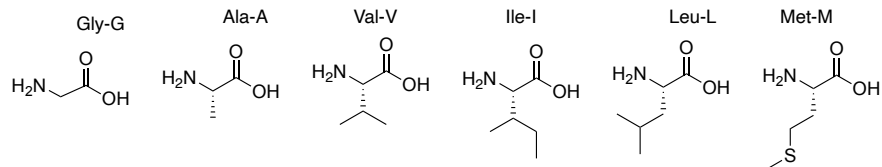


Figure 1: 3D structure of collagen (PDB 4CLG), myoglobin (PDB 3GRK), myosin (PDB 2V26) and enzyme-substrate complex

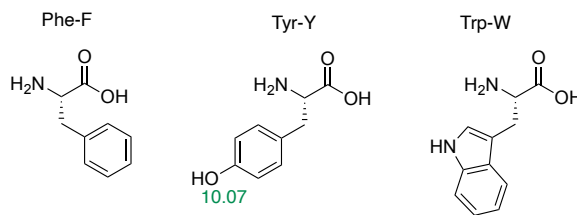
Proteins and peptides are polymers of amino acids linked together by a peptide bond. The large number of natural amino acids means that a vast range of proteins with unique properties is possible. Variation of the sequence of the amino acids, the length of the chain and/or the intramolecular interactions within the protein and therefore the conformation of the protein leads to huge number of peptide and protein structures.⁶ Around 500 different amino acids can be found in nature but 22 are encoded by human codons (Figure 2).⁷ Nine of these amino acids (Phe, Trp, Val, Thr, Met, Leu, Ile, Lys, His) are called essential amino acids, which means that they must be supplied in the diet to have a sufficient production of them. A further six (Arg, Cys, Gln, Pro, Gly, Tyr) are considered “conditionally essential amino acids” meaning that the synthesis can be disturbed by some pathologic conditions.⁸ The rest (Ala, Asp, Asn, Glu, Ser) are non-essential amino acids because they can be

synthesised in the body in sufficient quantities. The last two (Sec and Pyl) are present in proteins by a specific mechanism.^{9,10} Peptides differ from proteins on the basis of size and are defined as having a chain of 50 or fewer amino acids.¹¹ The structure that comes from the assembly of the amino acids will determine the function and the location of the protein in the body.

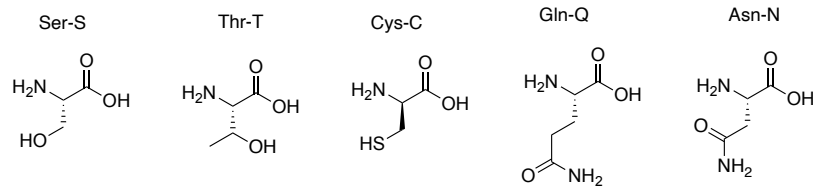
Hydrophobic



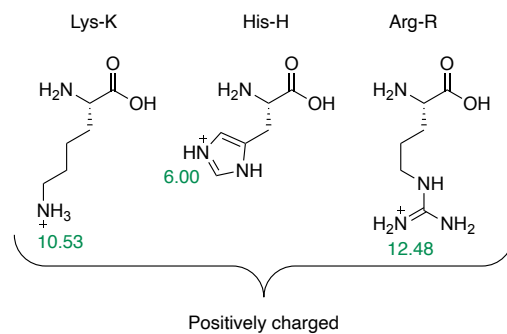
Aromatic



Polar



Charged



Special case

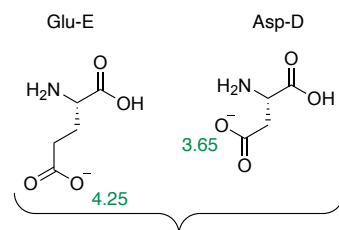
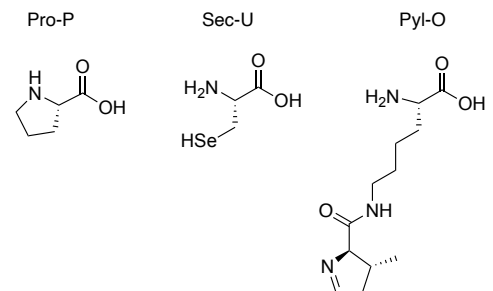


Figure 2: 22 natural α -amino acids and side chains' pK_a value.

An amino acid is a small molecule or monomer, with a carboxylic acid (C-terminus) and a primary amine (N-terminus) functional groups (except for Pro), connected by carbon that bears a side chain of variable length depending on the nature of the specific amino acid. Natural amino acids (those encoded by the genome) have the side chain located on the α -position relative to the carboxylic acid as the *S*-enantiomer (except Gly), and so they are therefore referred as α -amino acids.¹² The amino acids are classified depending on the properties of their side chains as shown below and each is designated by a three-letter or single-letter code.

Since the discovery of amino acids, peptides and proteins in the 19th century,¹³ various methods have been developed to synthesise natural or non-natural proteins/peptides and in recent years the use peptide synthesizers or genetically modified organisms has come to the fore. The advantage of using proteins as potential therapeutic agents, is that they can be more selective for their targets than conventional drugs with fewer side effects. Unfortunately, in most cases, proteins fail to meet the criteria of Lipinski's rule of five because they usually have a molecular weight above 500 Da, and possess too many hydrogen-bond donors/acceptors.¹⁴ The Lipinski's rule of five describes the five key physiochemical parameters and the molecular properties that confer favourable pharmacokinetic properties (absorption, distribution, metabolism and excretion) on a drug and make it likely to be orally active. The components are: the molecule must have five or fewer hydrogen bond donor groups (HBD), 10 or fewer hydrogen bond acceptor groups (HBA), a molecular weight of less than 500 Da, and a logP (a measure of the lipophily, thus the membrane permeability of molecules) of 5 or less. By using this method of "Lipinski rule of five" it was possible to categorised compounds as drug-like or lead-like molecules and filter libraries to remove poor candidates.^{15,16} Moreover, proteins usually bear a charge at physiological pH \sim 7.4 [pKa(C-ter) \sim 1.7–2.3, pKa(N-ter) \sim 7–9,¹⁷ the pKa of the side chains substituent can vary between 3 and 12], thus their ability to cross the membrane is reduced. That is why research is conducted into small peptides and peptidomimetics in order to satisfy the Lipinski's rule of five by synthesising smaller and more cell permeable molecules. In addition, small peptides and peptidomimetics can represent a biologically active section of a protein of interest and be used without the need to synthesise and purify an entire protein (which can be expensive and time consuming).¹⁸

1.2. The peptide bond: generality and isosteres

Proteins and peptides are polymers of amino acids joined through amide linkages. The resonance energy of the peptide bond is around 16 kcal/mol (in comparison benzene has a resonance energy of 46 kcal/mol) and possesses extra stability as a consequence of its partial double bond character (Figure 3). This is due to the delocalisation of the nitrogen lone pair into the antibonding orbital π^* of the carbonyl group. The energy required for rotation about a single C–C bond is approximately 3 kcal/mol and about 60 kcal/mol for a C=C double bond. Rotation around an amide C–N bond with its partial double-bond character requires greater energy, which limits rotation about this bond.^{6,19} Due to this partial double bond character, the entire amide group is planar and so there are two possibilities: *trans*- or *cis*-conformation.

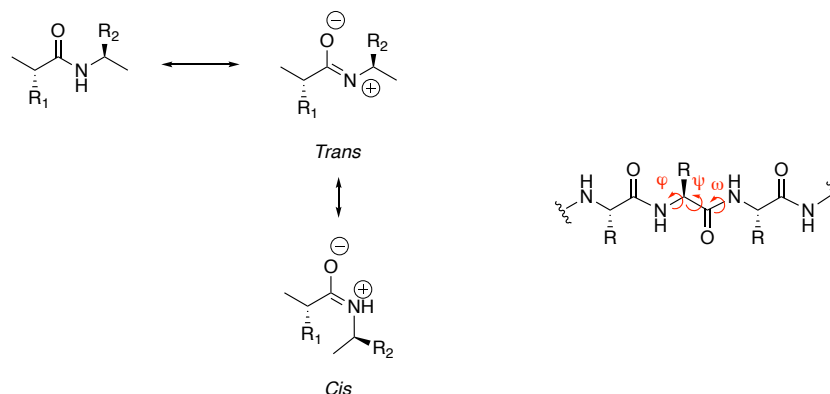


Figure 3: peptide bond resonance structures and dihedral angles

The *trans*-conformation is the conformer that usually occurs in all open peptide chains,²⁰ implying that the side chains of adjacent amino acids lie on opposite sides of the main chain.²¹ The *cis*-conformation is less stable as a consequence of the steric hindrance between the side chains; nevertheless, it can be found in peptide bonds between any amino acids and Pro (Xaa-Pro). A peptide bond is defined by three dihedral angles: ϕ , ψ and ω . The ϕ angle of the i residue is defined by the torsion $C_{i-1}-N_i-C\alpha_i-C_i$, ψ by the torsion $N_i-C\alpha_i-C_i-N_{i+1}$, and ω by the torsion $C\alpha_i-C_i-N_{i+1}-C\alpha_{i+1}$. These angles are an important feature for protein folding analysis.²² By definition, the *trans*-conformation is that in which the dihedral angle ω ($C\alpha$ -C-N- $C\alpha$ angle) is 180° and the *cis*-conformation is the one where ω is 0° .²³

The peptide bond presents a paradox in terms of its stability when one considers how it behaves chemically: vigorous conditions are required (concentrated acid or base at elevated temperature) to promote hydrolysis but on the other hand protease-mediated *in vivo* by

hydrolytic cleavage occurs under mild conditions (physiological pH and temperature). Proteases comprise four different mechanistic classes: serine proteases, cysteine proteases, aspartyl proteases and metalloproteases (Figure 4).²⁴

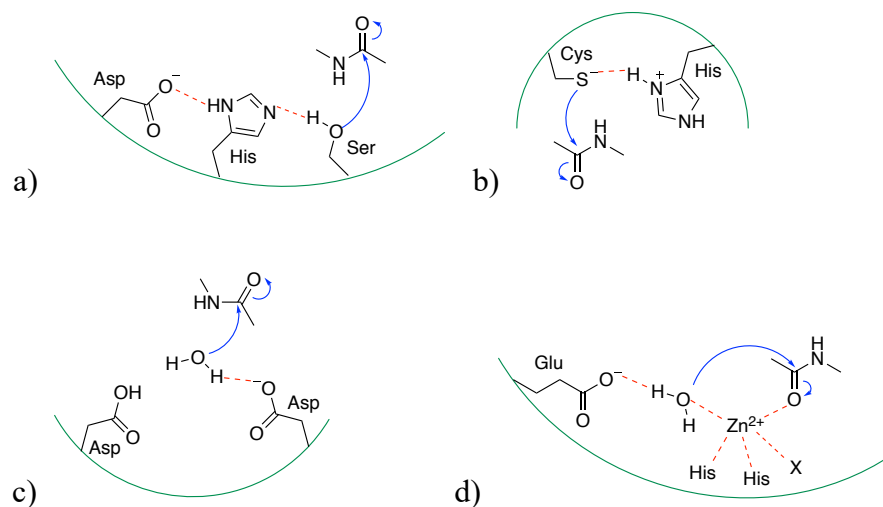


Figure 4: proteases and their mechanism. a) Serine protease, b) cysteine protease, c) aspartyl protease, d) metalloprotease

In serine proteases (Figure 4a) there is a catalytic triad formed by Asp, His and Ser amino acids in the active site. His deprotonates the Ser-OH, with the help of the proton-withdrawing Asp, and allows nucleophilic attack of the nucleophilic Ser onto the carbonyl group of the peptide bond. The cysteine proteases (Figure 4b) work in a similar way to the serine proteases, but in this case a strongly nucleophile sulphur atom on the Cys residue is deprotonated by His in the active site. Aspartyl proteases (Figure 4c) function via acid-base mechanism in which a water molecule serves as a nucleophile. In this case, water coordinates with the Asp carboxylate and is then activated by the abstraction of a proton and the polarised water can now attack the carbonyl of the peptide bond. Metalloproteases (Figure 4d) use a coordinated metal, usually Zn, in the catalytic mechanism. The metal coordinates to the imidazole groups of two His residues and an acidic side chain, or with the imidazole groups of three His residues and a water molecule hydrogen bonded to a Glu residue, the activated water can then attack the carbonyl group.

In addition to its stability, the peptide bond possesses two hydrogen-bond acceptors and one hydrogen-bond donor. Hydrogen bonds play a critical role in stabilizing secondary structure, facilitating inter- and intramolecular interactions and protein-protein recognition processes (enzyme-substrate for example).²⁵ In principle, the folding and shape, and thus consequently intramolecular interactions, of a protein can be controlled in order to increase its specificity

and/or the mode of action, by replacement of the peptide bond with a suitable isostere. An isostere is a functional group with similar chemical or physical properties to the group that it replaces; a molecule containing an isostere should produce the same biological response as the natural substrate. In medicinal chemistry, isosteres are used frequently in drug design to improve the pharmacodynamic and pharmacokinetic properties of a drug.²⁶ In order to avoid degradation by peptidase, some studies have been focused on replacing the peptide bond by different isosteres.

For example, the peptide bond can be replaced by another functional group such as a urea, without modification of the synthesis strategy commonly employed for peptide synthesis.²⁷ Liskamp *et al.* have demonstrated that a peptidomimetic can be synthesised using the Fmoc protection strategy in a peptide synthesiser. Every peptide bond was replaced by a urea moiety and every residue was replaced by its β -equivalent without significant losses in the overall yield or purity (Figure 5).

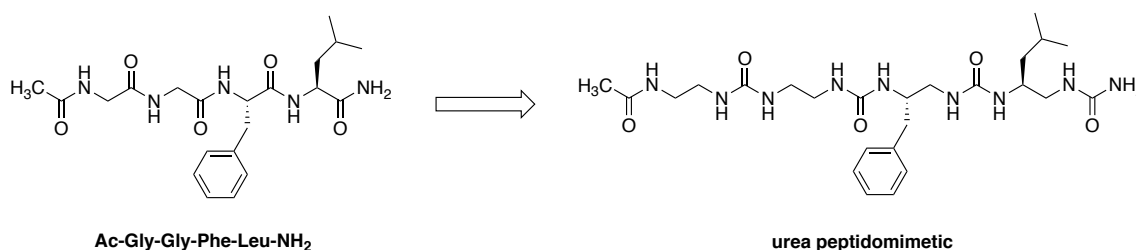


Figure 5: urea peptidomimetic

Other researchers have reported that replacement of a peptide bond by a triazole unit does not alter the biological activity of the compound.²⁸ V. D. Bock *et al.* have synthesised mimics of the natural product cyclo-[Pro-Tyr-Pro-Val] (Figure 6).

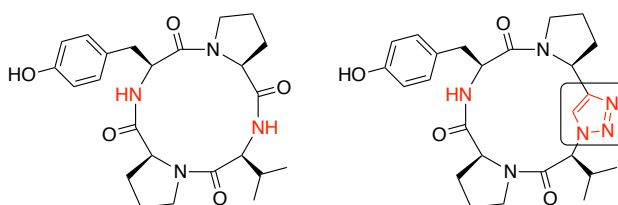


Figure 6: cyclo-[Pro-Tyr-Pro-Val] peptide and one of the analogues

In this study, three peptidomimetics were synthesised. In two of them, a triazole was used to replace one peptide bond on each side (red in Figure 6), and in the third one both peptide bonds were replaced with triazoles. The inhibitory effect of these analogues was then evaluated on mushroom tyrosinase and compared to the activity of the natural product. The

inhibitory activity was not only retained but increased for two of the analogues. Nonetheless, in most cases replacement of a peptide bond resulted in a loss of a hydrogen bond, which could be crucial for inter- and/or intramolecular interaction, making the mimics a good tool for the understanding of such interactions.²⁹

1.3. Structure of proteins and peptides

Proteins and peptides can be described in terms of their level of organisation by use of the term primary, secondary, tertiary and quaternary to describe structure. The general folding of a protein is stabilised by multiple weak interactions and so it is essential to describe them before discussing the different levels of organisation. These weak interactions are non-covalent and reversible.

1.3.1. Interactions stabilising the folding of a protein/peptide

1.3.1.1. *Hydrophobic interactions*

Hydrophobic interactions occur between non-polar groups. In peptides and proteins, this corresponds to the interactions between the hydrophobic side chains of non-polar residues (such as Ala, Val, Phe *etc.*). Water can repel these hydrophobic residues causing them to be buried in the native state of the protein (*i.e.* the folded protein). An example of a hydrophobic interaction in a peptide is aromatic-aromatic side chain interaction stabilising β -hairpin formation.³⁰

1.3.1.2. *Ionic interactions*

Ionic interactions are electrostatic interactions between two charged or partially charged groups of opposite polarity. These interactions occur between two groups having significant electronegativity differences. In peptide stabilisation, ionic interactions correspond to the interactions between paired anionic and cationic amino acid side chains (e.g. between Lys and Asp).

1.3.1.3. Van der Waals interactions

Van der Waals and hydrogen bonding interactions are crucial for the stability and function of molecules.³¹ They are weak electrostatic interactions between two permanent or induced dipoles. They have three major contributions and are distance dependant:

Permanent dipole-dipole interaction, or Keesom force: this interaction can be attractive or repulsive; the dipole of opposite signs will be attracted and dipoles of opposite signs will be repelled. This is represented in the figure 7 by the dipole moment of a molecule (a carbonyl group for example).

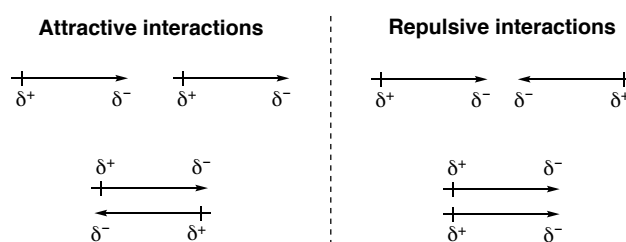


Figure 7: Keesom force

Dipole-induced dipole interactions, or Debye forces: these attractions result when a polar molecule induces a dipole in a nonpolar molecule/atom by disturbing the arrangement of electrons around it (induction or polarisation). They are always attractive and depend on the polarizability of a molecule.³² For instance, a carbonyl group with a dipole moment can induce a dipole in an adjacent aromatic ring (Figure 8) because π -electrons are more polarizable than σ -electrons.

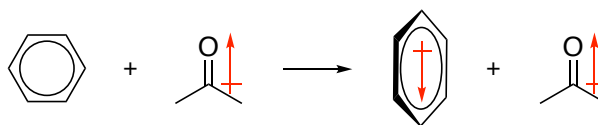


Figure 8: Debye force

Dispersive interactions, or London forces: they correspond to attractive interactions between any pair of molecules or atoms caused by the instantaneous multipole interactions. As in the case of Debye forces, they depend on the polarizability of molecules. In a folded protein, there are numerous dispersive interactions (mainly involving aromatic residues) that make important contributions to its overall stability.³²

1.3.1.4. Hydrogen bonds

A hydrogen bond is an electrostatic attractive interaction between a hydrogen atom that is covalently bonded to an electronegative atom (N, O, S, F) and the lone pair of an electronegative atom (N, O, S, F). These groups are called, respectively, the hydrogen bond donor (HBD) and the hydrogen bond acceptor (HBA). A hydrogen-bonding interaction is weaker than a covalent bond or an ionic interaction but is stronger than hydrophobic or van der Waals interaction. The electronegative bonding partner pulls the electrons away from the hydrogen in the HBD and the hydrogen nucleus is exposed on the back side, which becomes electron deficient (δ^+). This allows an electrostatic interaction to be established with a Lewis basic electron pair of an electronegative atom which is partially negatively charged (Figure 9).

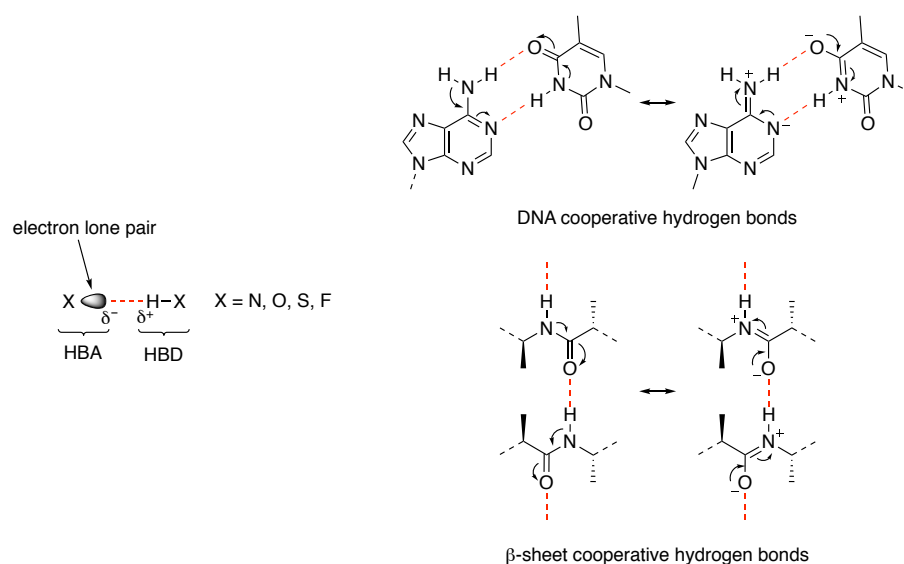


Figure 9: Hydrogen bond and cooperativity of hydrogen bonds

In biology, the hydrogen bonds are responsible for base pairing in DNA and RNA, the formation of elements of secondary structure in proteins/peptides and intermolecular protein-protein interactions. In biological systems, hydrogen bonds can have a cooperative character, which means that the strength of a hydrogen bond will be increased by an adjacent hydrogen bond (Figure 9). The hydrogen bond increases the acidity of the proton and the basicity of the oxygen (or any electronegative atom). This greatly stabilises base pairing and protein folding.

1.3.2. Primary and secondary structure

The primary structure corresponds to all the amino acids linked together by peptide amide bonds. It is the denatured state where the peptide/protein is unfolded and inactive. With 20 different natural amino acids, an infinite combination of these is possible, allowing huge diversity in primary structure. For example, a dipeptide involves two residues, thus $20^2 = 400$ different combinations are possible. However, a sequence of amino acids will not usually adopt a linear, extended conformation, but instead will fold into a complex three-dimensional structure of lower energy, stabilised by hydrogen bonds and other intramolecular interactions (electrostatic, π -stacking, hydrophobic etc.). The structure based on this hydrogen bonded arrangement is the secondary structure. It includes turns, α -helices and β -sheets.

1.3.2.1. α -helix

Linus Pauling was the first to report the α -helix conformation in 1951.³³ It is described as right-handed helical conformation with 3.6 residues per turn and a distance of 5.4 Å. In this structure, the peptide C=O bond of the i^{th} residue points towards the peptide N–H group of the $i-4^{\text{th}}$ residue to generate a 13-membered pseudocyclic structure (Figure 10). α -Helices represent the most prevalent type of the secondary structure in proteins (about 30% in globular proteins),³⁴ and could play an important role in the early stage of protein folding. Pace *et al.* observed that certain amino acid residues are more frequently found in α -helices such as Ala, Leu and Glu because of their favourable enthalpic contribution of between 0–0.4 kcal/mol (0–1.67 kJ/mol) compared to Gly which contributes around ~1 kcal/mol (4.18 kJ/mol) as a consequence of its greater flexibility, which reduces its propensity to stabilise α -helices. Proline does not stabilise an α -helix because it does not have a free N–H to form a peptide bond with another residue.

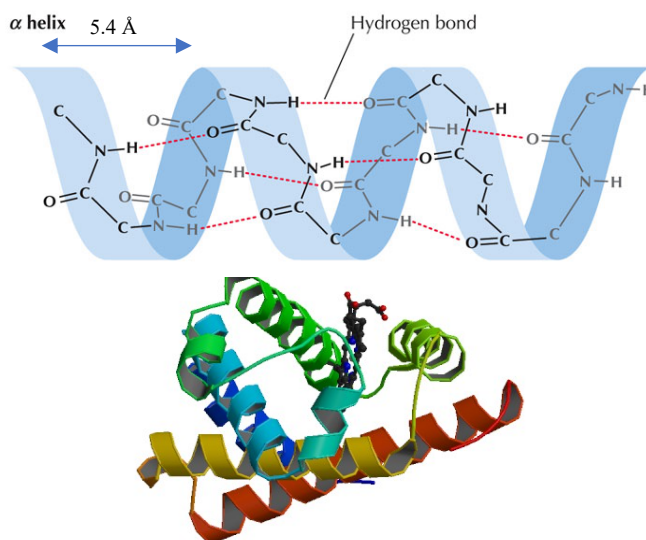


Figure 10: structure of an α -helix and of myoglobin protein

α -Helices perform a variety of functional roles, such as recognition (protein-protein or protein-nucleic acid),^{35,36} membrane spanning and other mechanical properties,³⁷ which means that the α -helix is a good target for medicinal chemistry research.

1.3.2.2. β -sheet

Another prominent secondary structure unit is the β -sheet, it is formed by successive β -strands joined by a turn. A strand is an almost fully extended chain of amino acids (3 to 10 residues). The dihedral angles ϕ and ψ of the strands' residues are near 135° and -135° respectively, whereas these angles are at 180° and -180° in an extended conformation, which gives a characteristic twist in the sheet conformation.³⁸ The two β -strands, comprising the β -sheet, are stabilised by cross-strand hydrogen bonds between peptide bonds. They can align themselves to be parallel or antiparallel (Figure 11a and b). Hydrogen bonds are planar (HBA and HBD in front of each other, the hydrogen bond is perpendicular to the strands) in an anti-parallel β -sheet, and non-planar (HBA and HBD slightly deviated), therefore slightly less stable, in a parallel β -sheet. The strands don't necessarily follow each other in the sequence and may be located at different regions of the protein/peptide. β -hairpin corresponds to the simplest motif of the β -sheet consisting of two β -strands joined by a loop (Figure 11c).

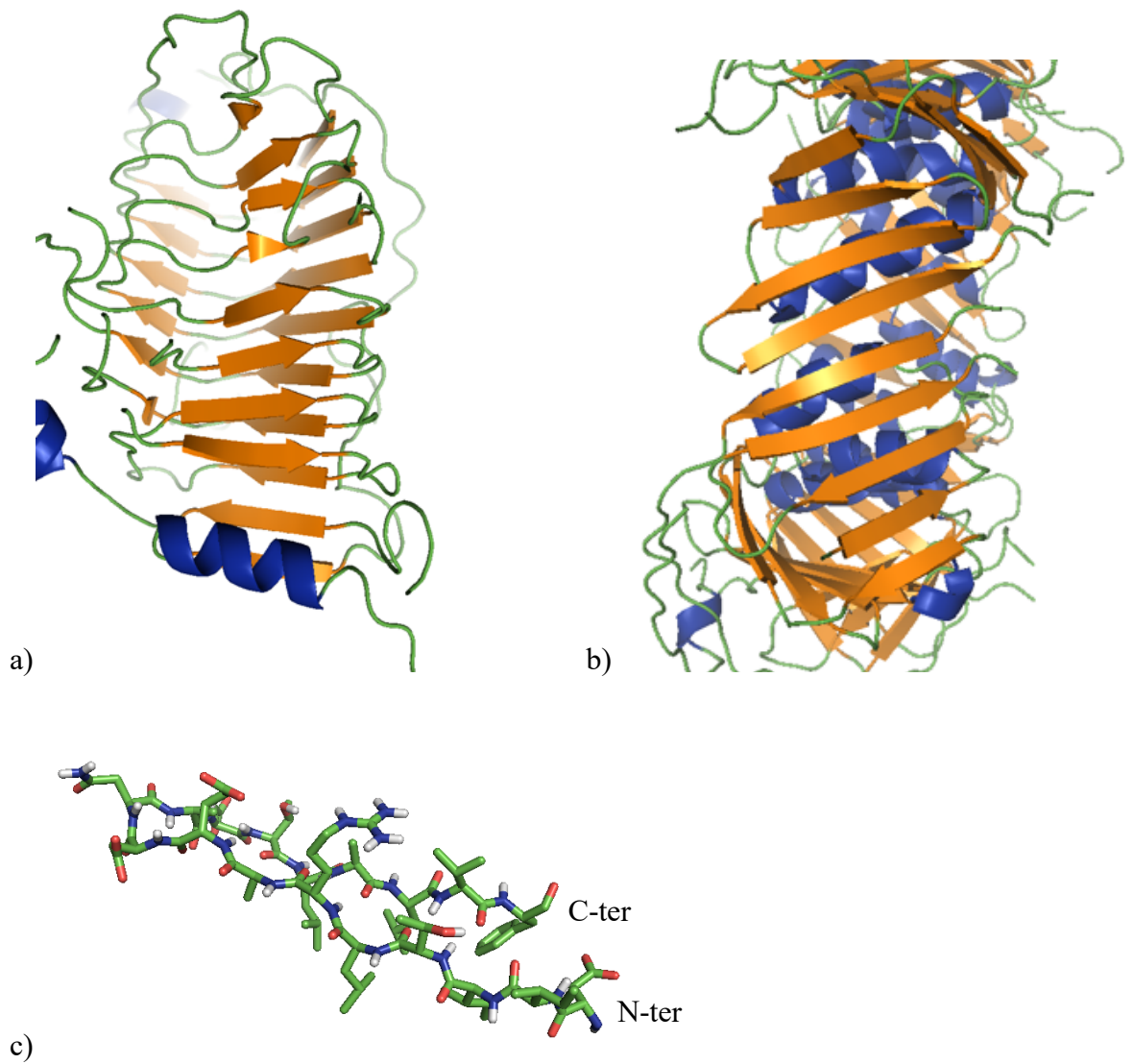


Figure 11: a) parallel β -sheet from pectate lyase, b) anti-parallel β -sheet from human PCNA, c) zoom on anti-parallel β -hairpin.

In both parallel and anti-parallel, the side chains along the strands alternate above and below the plane (Figure 11c), while the side chains of the opposite residues on neighbouring strands lie in the same plane and in close proximity, facilitating interactions across the strands.

1.3.3. Tertiary and quaternary structure

The tertiary structure is the overall folded form of the protein where the energy is usually minimised and includes the three-dimensional arrangement of the protein including orientation of the side chains. It is an assembly of secondary structures and disordered conformations in a protein/peptide. The formation of tertiary structure depends on the interactions between amino acids in close proximity to each other to form secondary structure, and also between side chains of distant amino acid residues in the primary sequence by ionic, hydrophobic, disulfide or other interactions.

Many proteins are composed of a single chain protein but some feature more than one subunit forming a stable folded structure. The subunits can be strictly identical in their amino acid sequence (Tobacco mosaic virus, Figure 12a), relatively similar (α and β subunits of the haemoglobin, shown in blue and red in Figure 12b) or completely different (aspartate transcarbamylase, Figure 12c). Once completely folded, the protein is in its so-called “native state”, this is the quaternary structure of proteins.

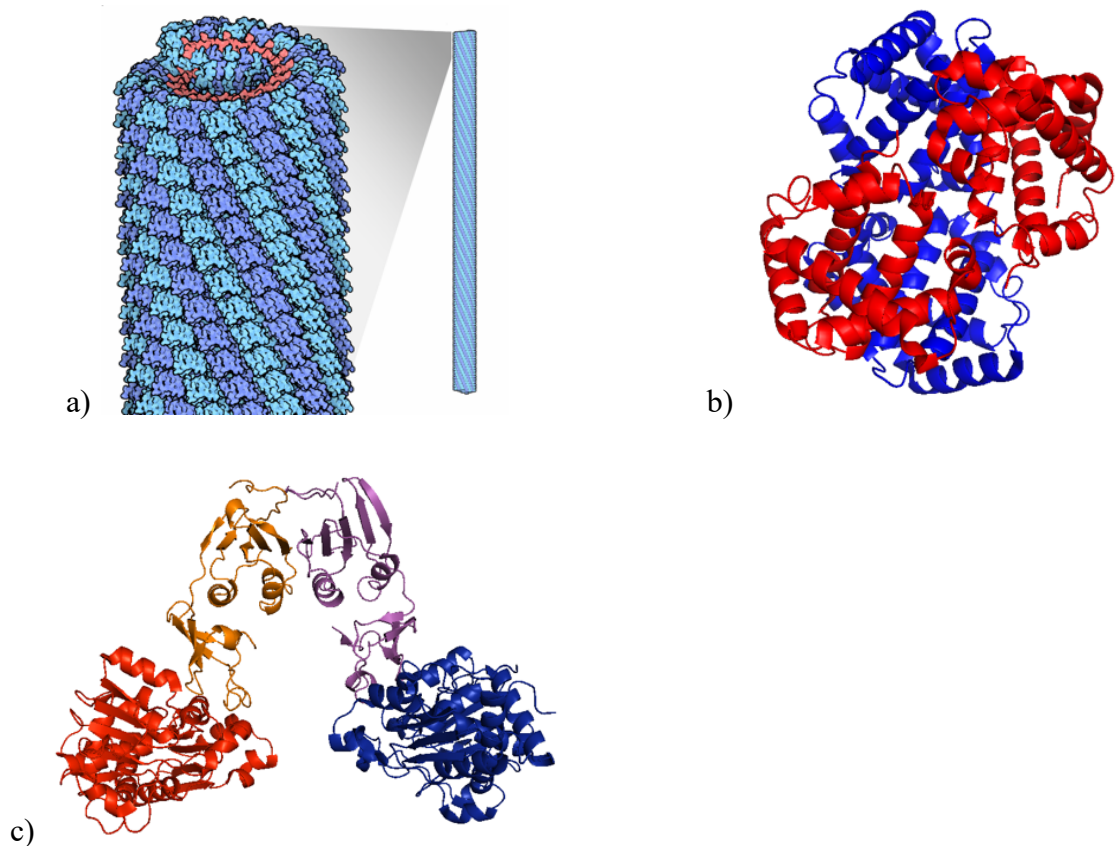


Figure 12: quaternary structure of a) tobacco mosaic virus, b) haemoglobin, c) aspartate carbamylase

Many large proteins do not fold spontaneously and instead are assisted by proteins called chaperones. These chaperones help the newly formed proteins to fold and avoid misfolding or aggregation, which can result in the formation of proteins that are potentially toxic. Molecular chaperones are described as “any protein that interacts with, stabilises or helps another protein to acquire its functionally active conformation, without being present in its final structure”.³⁹ Some of these proteins are known as heat-shock protein (HSP), as they are upregulated under conditions of stress, in which more aggregated intermediates are formed. Chaperones are then classified accordingly to their molecular weight given in kilodaltons (e.g. HSP40, HSP70 etc.).

Combinations of amino acids (the primary sequence) and their interactions will produce the three-dimensional shape of the protein on folding and are therefore responsible for the functionally active conformation.⁴⁰ This will determine the role and location of the protein in the body. Elements of secondary structure, such as the β -turn, have piqued a keen interest of medicinal chemists in recent decades as possible target sites for drug development because they often play a critical role in protein folding, stability and molecular recognition.

1.4. β -turn, generality and medicinal chemistry target

1.4.1. Definition and interest

Segments with regular secondary structures such as α -helices or β -sheets are usually joined by stretches of polypeptide (typically 4 residues) that promote abrupt changes of direction, which are referred to as U-turns or reverse turns. Depending on the number of residues involved in the turn, a variety of distinct types of turn can form: γ -turns involve three residues, β -turns involve four residues and α -turns involve five residues. Consequently, NH-OC hydrogen bonded pseudo-rings of various sizes can be formed: 7-, 10- or 13-membered rings correspond to γ -, β - and α -turns respectively (Figure 13).⁴¹

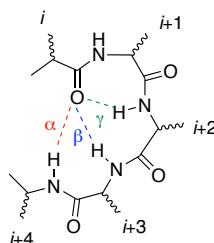


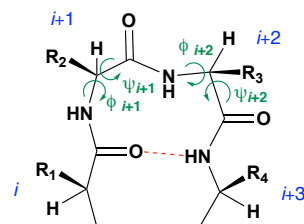
Figure 13: different types of reverse turn

Another characteristic of turns is that the distance between Ca_i and Ca_{i+4} has to be less than 7 Å. The most common and stable turn found in peptides and proteins is the β -turn. The work presented in this thesis will focus only on a mimic of the β -turn.

β -Turns are classified according to the value of the dihedral angles of the $i + 1$ and $i + 2$ residues (central residues of the turn, Table 1). Nine established β -turn conformations have been reported by Thornton *et al.*⁴² All turns have specific, well-defined torsion angles (or dihedral angles) with the exception the type IV β -turn, in which the dihedral angles are not well-defined but a stable turn structure is formed nevertheless.

Table 1: β -Turn types and their corresponding dihedral angles and general representation of a β -turn stabilised by a hydrogen bond

β -Turn type	Dihedral angles ($^{\circ}$)			
	ϕ_{i+1}	ψ_{i+1}	ϕ_{i+2}	ψ_{i+2}
I	-60	-30	-90	0
I'	60	30	90	0
II	-60	120	80	0
II'	60	-120	-80	0
VIa1	-60	120	-90	0
VIa2	-120	120	-60	0
VIb	-135	135	-135	160
VIII	-60	-30	-120	120
IV	All other values			



All types of β -turn are stabilised by a hydrogen bond between the oxygen atom of i^{th} residue and NH of the $i + 3^{\text{th}}$ residue. In most cases β -turns are composed of hydrophobic residues such as Gly (also gives more flexibility), Pro or Asn.⁴³ A β -turn with strands on N-terminus and C-terminus sides is known as β -hairpin (basic component of a β -sheet), it is stabilised by cross-strand hydrogen bonds between opposite residues. It is important to note that β -hairpins do not necessarily involve a β -type turn, it could be any type of turn.^{44,45}

β -Turns are often composed of hydrophobic amino acids and they occur between regions of regular secondary structure (such as helices and sheets), consequently they tend to be located at the surface of the protein, and play a role in ligand-receptor or substrate-enzyme interaction recognition, making it a potentially interesting motif and target for novel medicinal agents.^{41,46} β -Turns are also thought to play an important role in the process of protein folding where formation of stable secondary structures is initiated by turns, which position strands in close proximity so that they interact with one another.⁴⁷ In contrast, it is possible that β -turns form passively during the process of protein/peptide folding and arise as a consequence of folding rather than functioning as folding promoters. Hydrophobic side chains can interact with each other across strands and this will allow a turn to be formed, this is known as hydrophobic collapse.

β -Turns are an important feature in protein secondary structure as well as in the native state of proteins (in GPCR ligands for example),⁴¹ which makes it a challenging and important target in peptidomimetic research. Within the last few decades many studies concerning β -turn mimicry have been conducted, especially in relation to the use of carbon-carbon single or double bonds as peptide bond replacements.

1.4.2. Conformational analysis tools for β -turn identification

1.4.2.1. Infrared spectroscopy

Vibrational spectroscopy is a particularly useful method for the detection of hydrogen bonded structures in peptides, thanks to the strong infrared (IR) bands of the amide group present.⁴⁸ In the early 50s, Elliot and Ambrose demonstrated that IR spectroscopy could provide useful data about the secondary structure of proteins and peptides.⁴⁹ The method has evolved in the decades since then, with the arise of the Fourier-transform infrared spectroscopy (FT-IR). The advantage of using FT-IR, is that high quality spectra can be obtained with relatively small amounts (1 mM is usually enough) of the protein/peptide under investigation in a variety of environments (aqueous, miscellaneous or organic). Furthermore, IR spectroscopy relies on vibrational bond energy, so no external probes are required for the conformational study (unlike NMR or CD). The bands arising in IR spectra as a consequence of the vibration of the peptide groups provide information about the secondary structure of peptides and proteins, an additional chromophores are not required.⁵⁰ The IR spectrum of a protein is characterised by nine different absorption regions known as amide modes, which means a planar CONH group would give nine amide bands, commonly called amide mode A, B, I to VII (table 2).⁵¹

Table 2: Amides mode and their approximate frequencies

Amide	Approximate Frequency (cm^{-1})
A	3300
B	3100
I	1650
II	1550
III	1300
IV	725
V	625
VI	600
VII	200

Amide mode A arises from NH stretching, amide mode I from C=O stretching vibrations, amide mode II from NH bending with a contribution from CN stretching. Amide mode III is usually weak and rarely seen in conventional IR spectra but arises from NH bending and CN stretching. The other modes, are usually not used to interpret IR spectra and most conformational studies based on IR spectroscopy have been performed with reference to amide I and A bands exclusively.^{52,53}

The wavenumber corresponding to each amide vibrational mode can be influenced by the environment of the peptide/protein. Hence, the wavenumber can be influenced by the intermolecular interactions between various molecules or interactions with the solvent, and by intramolecular interactions. The major type of bond that can be analysed with IR spectroscopy is the hydrogen bond, because bonding of this type changes the vibrational characteristics and dipole moment of a bond. Typically, in the case of hydrogen bond formation, the amide modes A and I will shift to lower wavenumbers, while amide mode II will shift to a higher wavenumber.

With this technique, it is possible to analyse whether or not the NHs of a small peptide are involved in intramolecular hydrogen bonds in various solvents; in the event of a β -turn study, it is possible to analyse the formation of the 10-membered hydrogen bonded system by use of an appropriate model, as described in a following section.⁵⁴

1.4.2.2. Circular dichroism

Circular dichroism (CD) is an essential tool for probing the structure of peptides. The technique was developed in the 1970s for the structural analysis of the secondary structure of peptides/proteins.⁴⁸ CD results as a consequence of the interactions of polarised light with chiral molecules. Proteins, which are composed by chiral amino acids, are chiral by definition and display a unique spectrum depending on their 3D conformation. Indeed, it is important to note that the CD spectrum of a protein is not simply the sum of the CD spectra of its residues but is the result of a chiral macromolecule greatly influenced by its the 3D structure, and therefore the secondary structure. CD allows secondary structures (α -helix, β -sheet, β -turn) to be analysed in solution with great accuracy because each secondary structure unit results in the generation of a specific CD spectrum (Figure 14).⁵⁵

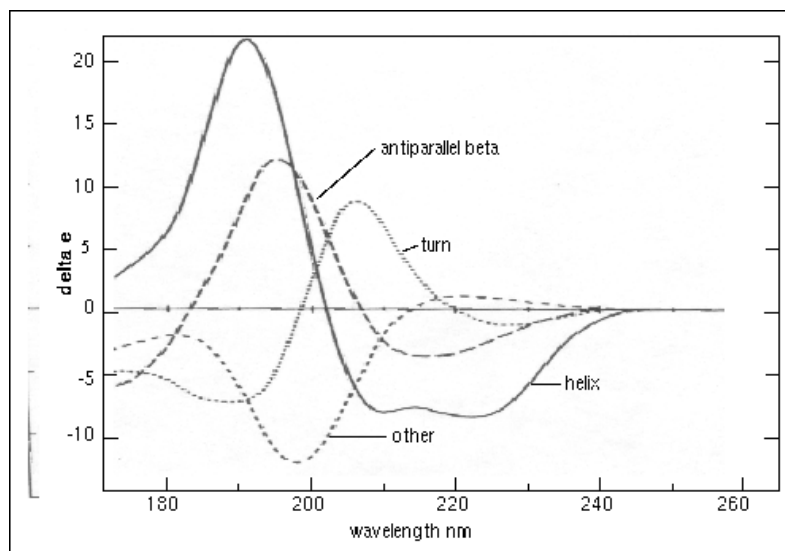


Figure 14: CD spectra in the far-UV of “pure” secondary structures⁵⁶

The far-UV (180–260 nm) corresponds to the region of the spectrum where there is a great sensitivity to the backbone conformation of peptides/proteins.⁵⁷ Near-UV (250–320 nm) acquisition can provide information about the contribution of aromatic side chains to the folding process.

α -helix has a high positive peak around 190 nm followed by two negatives at 210 and 225 nm. β -sheet and β -turn present a positive at respectively 195 and 205 nm followed by a negative curve. In early studies, β -turns were overlooked in terms of their contribution to the folding of a protein,⁵⁸ thus CD spectra were not recorded. Within the past few decades CD spectra of type I and II β -turns have been obtained and it is now known that they are the most found in proteins.^{59,60,61}

1.4.2.3. Nuclear Magnetic Resonance

All chemists are aware of the power of the NMR spectroscopy for the determination of molecular structure and conformation but also for the elucidation of the selectivity and stereocontrol of some reactions. NMR is also a major tool for the determination of the 3D structure of macromolecules such as proteins or peptides.

The folding pattern of a peptide/protein can be analysed through by the use of various NMR techniques. In the case of relatively small peptides (less than 10-12 residues), it is possible to study the formation of intramolecular hydrogen bonds between amides within the peptide directly. Concentration-dependent NMR studies provide good evidence to indicate the

presence and strength of both intra- and inter-molecular hydrogen bond formation. In this study the chemical shift of a selected NH of the peptide is targeted. If the chemical shift changes with the log of the concentration, it indicates that this NH is involved in an intermolecular hydrogen bond.⁶² Indeed, the higher the concentration the more the molecules will interact with one another. If the chemical shift does not change significantly with the concentration, this provides evidence that the NH is intramolecularly hydrogen bonded because the degree of hydrogen bonding is not dependent on concentration in this case.⁶³ The same observation can be made with data from temperature dependant NMR studies. In this case, the chemical shift-temperature dependence ratio $\frac{\Delta\delta}{\Delta T}$ is measured and the lower it is, the stronger the intramolecular hydrogen bond.⁶⁴ Another NMR experiment that is used to detect hydrogen bond formation consists of calculating the exchange rate between a hydrogen and deuterium present in a protic NMR solvent. The hydrogen concerned is usually the NH of an amide bond, but it can also be from an acidic side chain (attached to N, O or S atom as C-H exchange very slowly with the solvent).⁶⁵ The rate is calculated over time and is a good indicator of the formation of a hydrogen bond and how stable it is. Indeed, if an NH does not appear in a deuterated solvent (D₂O, MeOD, d-TFE etc.) it means that it is exchanging rapidly with the solvent so is solvent-exposed and not protected by an intramolecular hydrogen bond. The techniques described above are useful for the detection of hydrogen bonds, but NMR spectroscopy can provide much more information about the overall 3D structure of a peptide or protein thanks to 2D NMR.

Homonuclear 2D NOESY (Nuclear Overhauser Effect) NMR is important for the determination of the structure of organic and biological molecules. Indeed, cross-peaks in the 2D spectrum correspond to the interaction between protons that are close in space. This is a powerful tool for the identification of the stereochemistry of complex molecules, but also the general configuration of a peptide. By identifying the cross-peaks between protons at the α -position of the residues composing the peptide, it is possible to tell, for instance, in a four-residue peptide, if H α of residue *i* is interacting with H α of residue *i*+3. If it is, this suggests that the peptide is adopting a turn conformation.

1.5. β -Turn peptidomimetics

1.5.1. Introduction to peptidomimetics and examples

Natural peptides and proteins should be, by their structure and function, attractive drug-candidates because they are essential to every biochemical process. Even though large peptides have great stability and are more specific than small-molecule drugs with respect to their targets and fewer side effects, they do have several disadvantages: they have poor bioavailability (short half-life), are rapidly degraded by proteases in the blood stream, suffer rapid clearance and have poor oral absorption characteristics.⁶⁶ These parameters are the pharmacokinetic properties of ADME (Absorption, Distribution, Metabolism, Excretion). Low ADME means that a molecule is not a good drug-candidate. For instance, some natural peptide-derived inhibitors such as pepstatin, a pepsin inhibitor (pepsin is a protease found in the stomach that degrades proteins into smaller peptides), have shown promising hypertensive activities in biological tests, but their low bioavailability and lack of target selectivity have precluded their further development.⁶⁷ Wiley and co-workers defined a peptidomimetic as “a small nonpeptide structure that can mimic the activity of a native peptide or protein”. Nowadays, the challenge is to find a low-molecular-weight molecule with desired pharmacokinetic properties (superior to those of native peptides) that would bind specifically to a target receptor. Expansion of our knowledge of proteins and their domains has allowed the peptidomimetic field to develop. Indeed, determining the 3D structure of a key point of contact between the protein and the receptor is important as this develops understanding of exactly which structural features and functional groups are important for activity to take place.⁶⁸ The structure-based design of molecules that can mimic the binding site to a specific target (structurally and functionally) or so-called structure-activity relationship (SAR) has developed rapidly over the past few decades and is essential for designing new peptidomimetic drug candidates.^{69,70} Once the targeted conformation for biological activity is known, a small molecule can be designed to form and stabilise the required conformation with the same functional group in place for interactions. A library of similar compounds can then be synthesised following a generic synthetic route and screened for biological activity. Features that improve or decline the activity can then be identified and the structure refined for a better biological activity. Peptidomimetics that possess peptide bond surrogates or transition state analogues have been developed in which the main polyamide chain is absent or interrupted by a non-peptidic group, which makes the molecule less susceptible to proteolytic degradation.⁷¹

Hanessian and Auzzas have reported the synthesis of conformationally constrained azacyclic peptidomimetics that contain proline and pipecolic acid building blocks (with a 5- and 6-membered ring respectively, Figure 15).⁷²

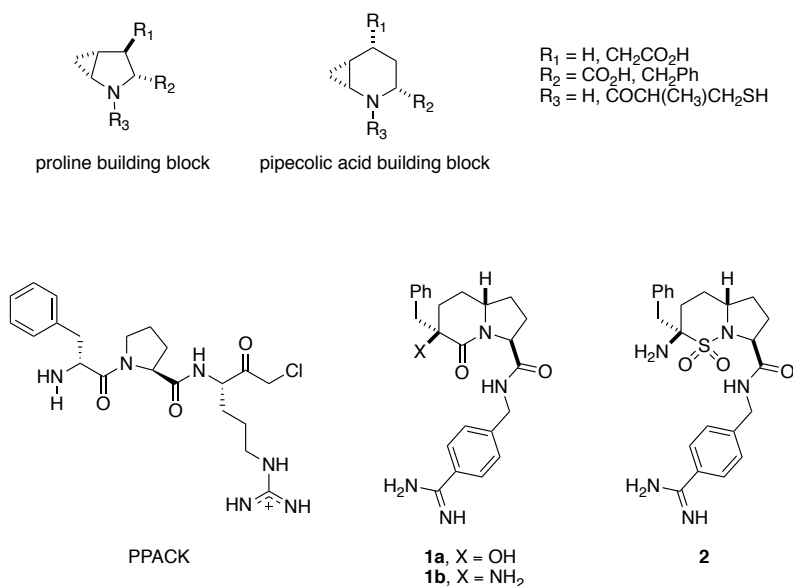


Figure 15: Proline and pipecolic acid building block and PPACK peptidomimetics.

In spite of the synthetic challenges presented by these constrained amino acids, the researchers pursued the synthesis of the polycyclic proline analogues **1a,b** and **2**, which are peptidomimetics of PPACK (Phe-Pro-Arg chloromethyl ketone) peptides. PPACK is a potent inhibitor of thrombin, a serine protease that is involved in the coagulation process, with an IC_{50} of 110 nM. The synthesis of **1a** and **b** proved to be challenging but the compound was obtained with good stereocontrol. The three analogues were tested against thrombin and the hydroxyl analogue **1a** was found to be five-fold less active than the amine analogue **1b** ($\text{IC}_{50} = 4 \text{ nM}$ *in vitro*). Co-crystallisation of **1a** with thrombin followed X-ray analysis revealed that the peptidomimetic was interacting with the protease at the same amino acid residue as the native peptide and therefore has the same binding mode.

G-protein-coupled receptors (GPCRs) are a large family of proteins with seven transmembrane helices as a common structural motif. They are located at the surface of cells and are implicated in the transduction of extracellular signals into intracellular responses. The natural ligands of the GPCRs are extremely diverse, ranging from hormones to nucleosides or lipids and Ca^{2+} ions. Such a variety of ligands indicates a great diversity of actions, and GPCRs are potential targets for various disorders, such as allergies, hypertension, cancer and asthma, etc. (Figure 16).⁷⁰ Around 50% of the drugs that have been

launched on the market recently target GPCRs. These receptors are attractive targets for medicinal chemists and amenable to the development of peptidomimetics.⁷³

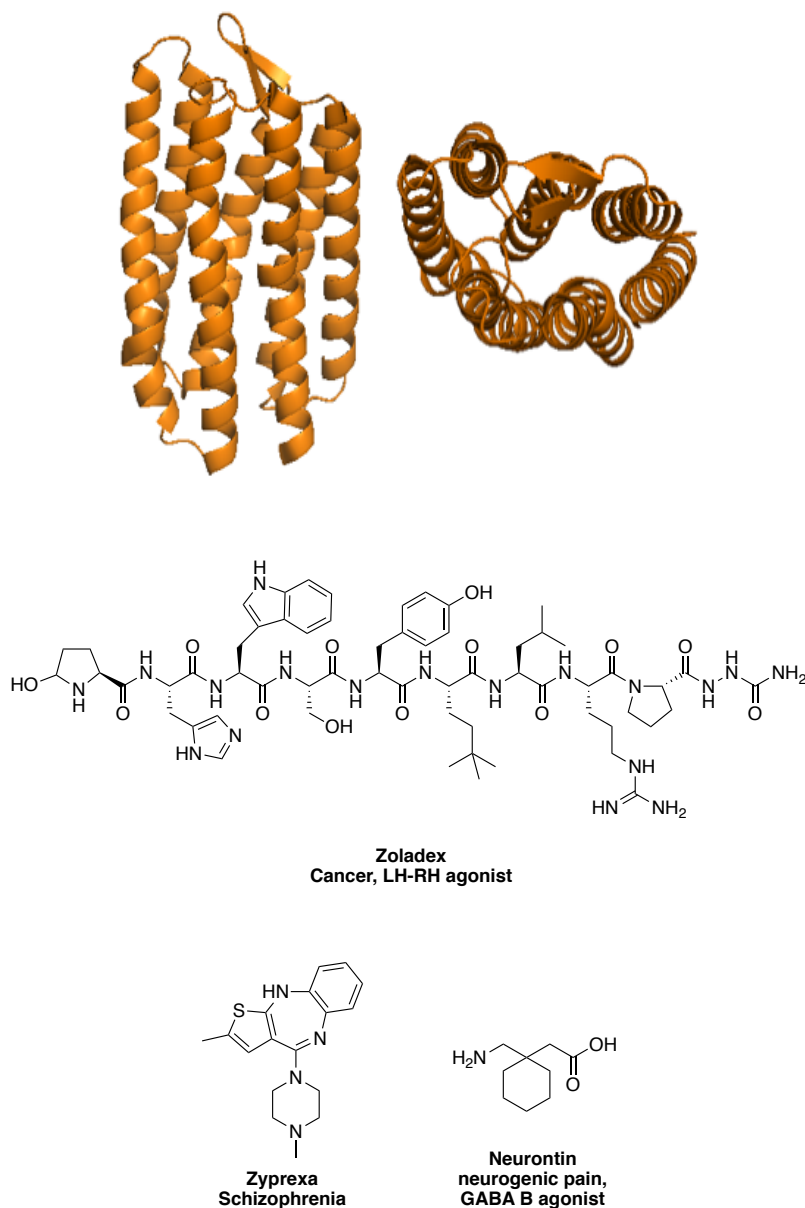


Figure 16: rhodopsin GPCR and some examples of drugs targeting GPCRs

It has been demonstrated that GPCR ligands often interact with the receptor via a turn structure,⁴¹ implying that the turn is generally located at the surface of the protein. Therefore, they are interesting targets to study in order to gain an understanding about the molecular interactions between receptors and ligands as well as other interactions involved in biological process.

1.5.2. β -Turn peptidomimetics, synthesis and analysis

1.5.2.1. Robinson's work on synthetic vaccines

The application of peptidomimetics is not only drug design and development but is also in the field of synthetic vaccines. Natural peptides have several weaknesses in this area. They are usually too flexible and unable to preserve a specific conformation that is required for recognition with the antibody. An epitope is the part of the antigen that binds with the antibody and β -hairpin are a known structure found in epitopes. Furthermore, it has been described that the interaction is possible or not depending on the loop sequence. So, constraining the loop to stabilise the hairpin is an important progress in synthetic vaccines. Immunoglobulin contains six domains where the antigens will bind, they are called the complementary-determining regions (CDRs).⁷⁴ Some of them adopt a β -hairpin conformation. Robinson has designed CDRs mimic containing a D-Pro-L-Pro loop to fix the β -turn position in the peptide (Figure 17).⁷⁵

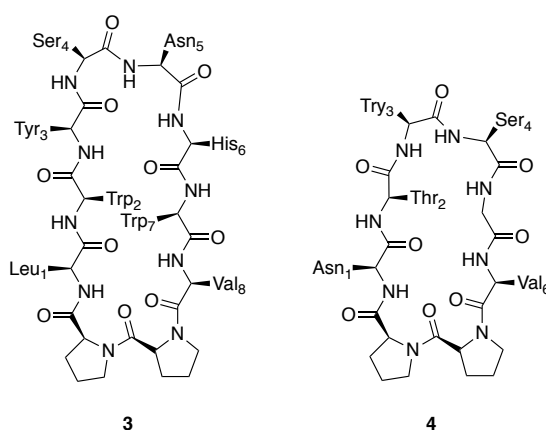
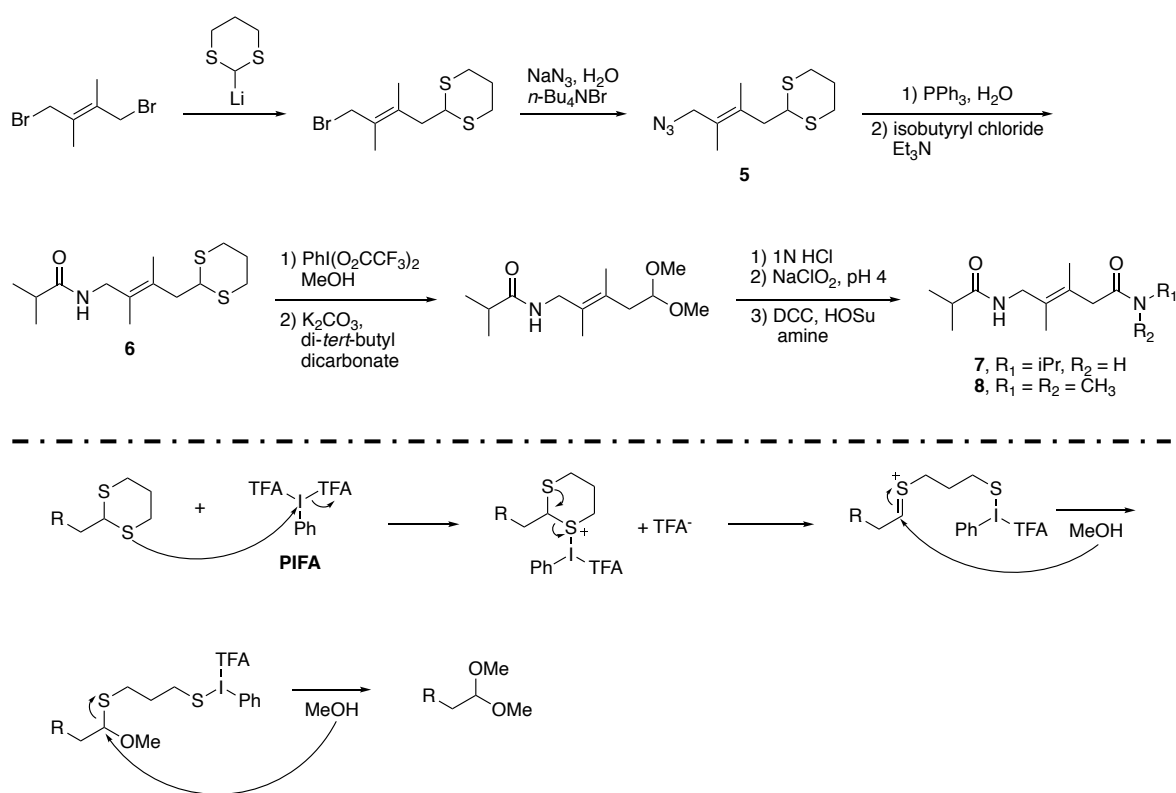


Figure 17: Hairpin mimetic based on CDR loop

3D average conformations extracted from solution NMR study of both cyclic peptides **3** and **4** overlay perfectly respectively with the 3D structure of CDR loops of antibody HC19 (influenza) and antibody TE33 (anticholera). Accurate structural mimetics are possible by replacing a flexible loop by a more rigid moiety such as Pro and could be valuable tool for small molecule antibody mimetics.

1.5.2.2. Gellman *et al.*, alkene as a peptide bond isostere and β -turn initiator

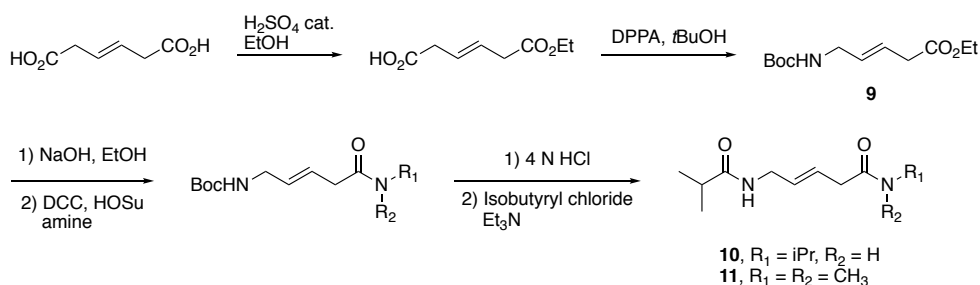
Within the last few decades many studies have been conducted in the field of β -turn mimicry, especially in relation to the use of carbon-carbon single or double bonds as peptide bond replacements. Gellman *et al.* have worked on the use of *trans*-alkenes as peptide bond surrogates and have obtained promising results.⁶³ In order to retain the backbone flexibility of an authentic dipeptide a mimic of the Gly-Gly sequence was chosen because the absence of any stereogenic centres simplified its synthesis. Initially, simple di- and tetra-substituted alkene dipeptide mimics were synthesised and analysed (Schemes 1 and 2):



Scheme 1: Gellman dipeptide mimic synthesis and acetal replacement mechanism

The synthesis of the mimetics **7** and **8** was achieved in 9 steps starting from 1,4-dibromo-2,3-dimethyl-3-(*E*)-butene. The synthesis started with the installation of thioacetal protecting group, followed by nucleophilic substitution using sodium azide. The resulting azide **5** was subjected to a Staudinger reaction to obtain the corresponding amine, which was acylated with isobutyryl chloride to yield the corresponding amide **6**. The dithiane was then replaced by a dimethyl acetal under acidic conditions, which was then cleaved to yield the corresponding aldehyde. Pinnick oxidation afforded the corresponding carboxylic acid, amenable to peptide coupling using DCC and HOSu affording **7** and **8** depending on the

amine used for the final coupling. The disubstituted alkene equivalent was also synthesised in just six steps (Scheme 2).⁷⁶



Scheme 2: disubstituted alkene dipeptide mimetic designed by Gellman et al.

(*E*)-Hex-3-enedioic acid was submitted to a mono-esterification under acidic conditions and subsequent conversion of the remaining carboxylic acid into a Boc protected amine using DPPA afforded **9**. Saponification and coupling followed by *N*-deprotection and acylation of the primary amine afforded the desired disubstituted alkene mimics **10** and **11**.

The conformational studies on the mimics started with an analysis of solvent effects in order to identify the most suitable solvent for NMR studies.⁵⁴ The solvent needed to exhibit no hydrogen bond donor or acceptor behaviour in order to avoid hydrogen bonding between the compound and the solvent. In addition, the compound had to be soluble in the chosen solvent. Acetonitrile (MeCN) and dichloromethane (CH_2Cl_2) were chosen, but unfortunately interactions between the mimic and solvent were apparent when MeCN was used. Therefore, concentration dependent NMR studies of compound **7** (Figure 18) were undertaken in dichloromethane. The variation in NH chemical shift highlighted at different concentrations, from 0.05 mM to 20 mM, is presented in the figure below.

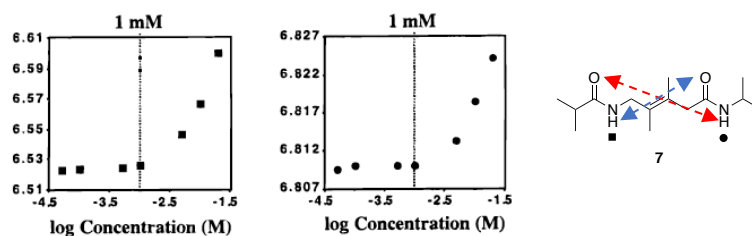


Figure 18: concentration dependent NMR study of ⁷⁷

Both NHs shifted significantly when the concentration was increased above 1mM, meaning that they started forming *intermolecular* hydrogen bond above this concentration. The concentration of 1mM is the highest at which *intramolecular* hydrogen bond formation is

predominant and so this was chosen by Gellman and co-workers as the reference concentration for subsequent IR studies. Two different *intramolecular* hydrogen bonds can be formed in this case, either between the external CO-NH hydrogen bond (red) to form a 10-membered ring, or between the internal CO-NH hydrogen bond (blue) to form an 8-membered ring. In order to understand which hydrogen bond is formed and which stabilises the system best, Gellman and co-workers undertook an IR study on the four mimics synthesised (Figure 19).

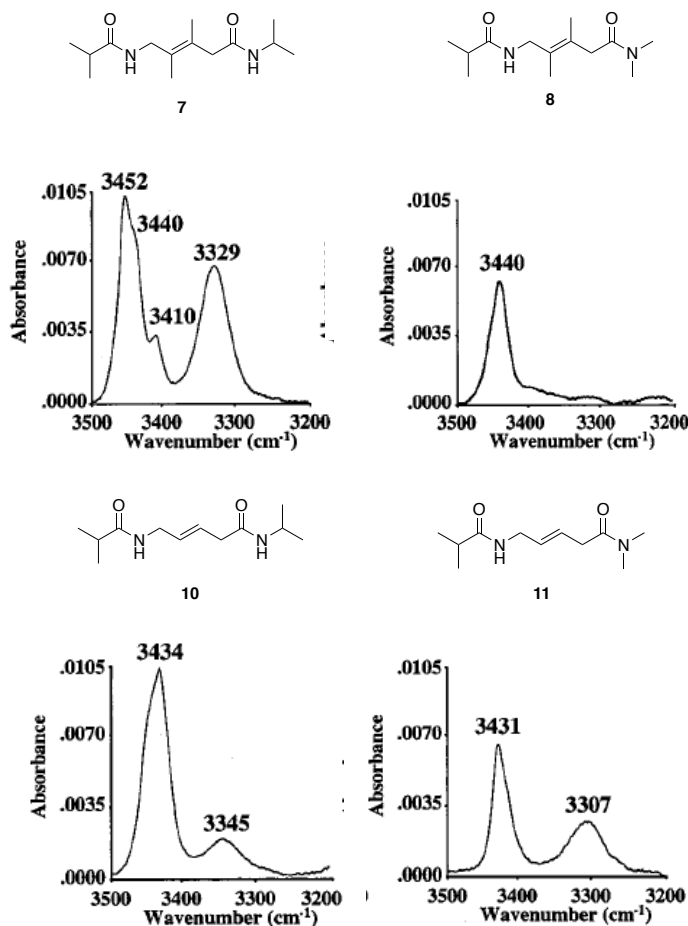


Figure 19: : IR study of tetra and disubstituted alkenes⁷⁷

Compounds **7** and **10** allow understanding of which hydrogen bond is formed, if not both. The mimetics **8** and **11** has the terminal amide capped with two methyl groups, which prevents hydrogen bond from the nitrogen (NH is absent). Consequently, only one hydrogen bond can be formed and that is the one that does so through an 8-membered ring system. Figure 19 shows NH-stretch region in the IR spectrum for these compounds. Four bands were shown for compound **7** – the band at 3329 cm⁻¹ occurs in the region expected for an *intramolecularly* hydrogen bonded NH and the other bands at higher wavenumber correspond to solvated NHs or *intermolecularly* hydrogen bonded NHs. *Intramolecular*

hydrogen bonds were observed in both **7** and **10**, but there is less hydrogen bonding in the disubstituted mimic (smaller area for the band corresponding to the *intramolecularly* hydrogen bonded NH). When the external hydrogen bond was blocked (compound **8** and **11**), only one band at 3440 cm^{-1} was observed, which suggests that there is only interaction with the solvent or *intermolecular* hydrogen bond so the 8-membered ring system is not formed. The system **7** displays extensive 10-membered ring hydrogen bonding but no 8-membered ring hydrogen bonding. The presence of an intramolecular hydrogen bond in compound **11**, as shown by the presence of a band at 3307 cm^{-1} , indicates that the avoidance of allylic strain results in good conformational control.

Encouraged by promising results, Gellman and co-workers extended their study to include the tri- and tetra-peptide mimics of Ac-Val-Gly-Gly-NMe₂ and Ac-Val-Gly-Gly-Leu-NMe₂ that contained the tetrasubstituted alkene. These compounds were synthesised in the same manner as the dipeptides and the same NMR and IR analyses were conducted. The concentration-dependent NMR study showed that both external NHs (NH_{*i*} and NH_{*i+3*}) were concentration independent and so were involved in *intramolecular* hydrogen bond. The peak corresponding to the internal NH started to shift at 5 mM, meaning the 8-membered ring is the less stable hydrogen bonded ring formed.

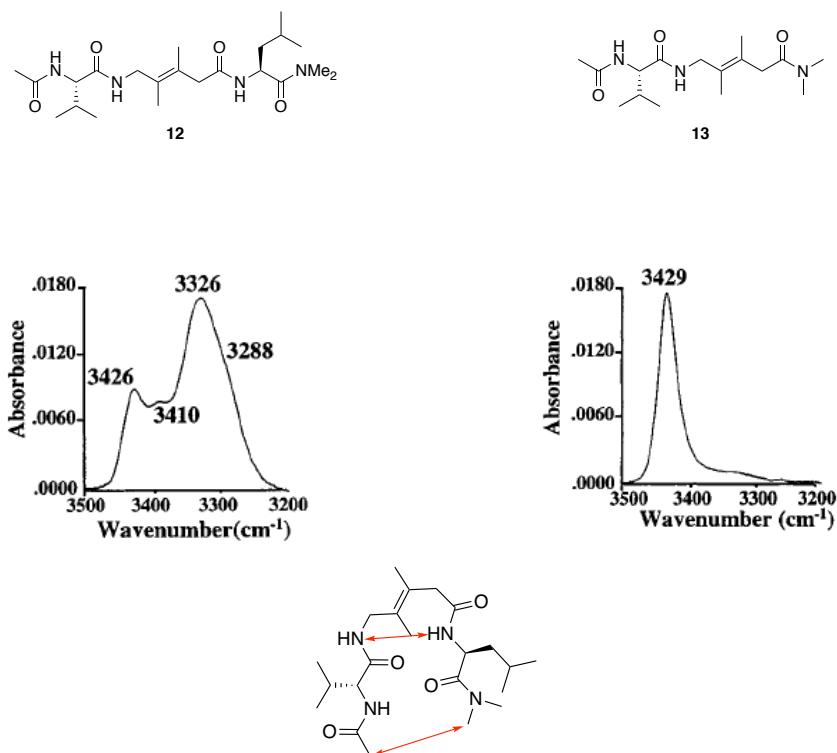


Figure 20: NH-stretch IR of tri- and tetra-peptides and NOE cross peaks observed⁷⁷

The IR spectrum of compound **12** indicates formation of intramolecular hydrogen bond to a greater extent (bigger area in region corresponding to intramolecular hydrogen bond NHs than in the solvent-exposed region, Figure 20) and suggests that probably all NHs are involved in intramolecular hydrogen bond. The mimic **13** was analysed in order to understand which intramolecular hydrogen bond was the driving force of the β -turn formation. In this case, two hydrogen bonds can be formed within the molecule: an 11-membered or an 8-membered hydrogen bonded system. As was the case with the previous results, the 8-membered ring is not favourable and not formed, but neither is the 11-membered ring because the IR spectrum contains only one band at 3429 cm^{-1} , which indicates that the NHs are solvated. Consequently, no intramolecular hydrogen bonds are formed and so a β -turn is not observed for this analogue showing that the 10-membered ring hydrogen bonded system is the driving force of the folding. Additionally, NOESY experiments were undertaken on **12** and long-range NOE cross peaks between the acetamide and the dimethyl groups and between the internal NHs were observed, which demonstrates that the tetrapeptide is adopting a folded conformation in CH_2Cl_2 . The Gly-Gly surrogate placed at the centre of a peptide is useful for the development of an understanding of β -turn formation.

1.5.2.3. Leu-enkephalin analogues by Dory et al.

Enkephalins are endogenous pentapeptides that bind to opioid receptors. Three classes of opioid peptides have been described: enkephalins, endorphins and dynorphins (Figure 21). They are naturally produced in the central nervous system by the action of peptidases and by post-translational modification.⁷⁸

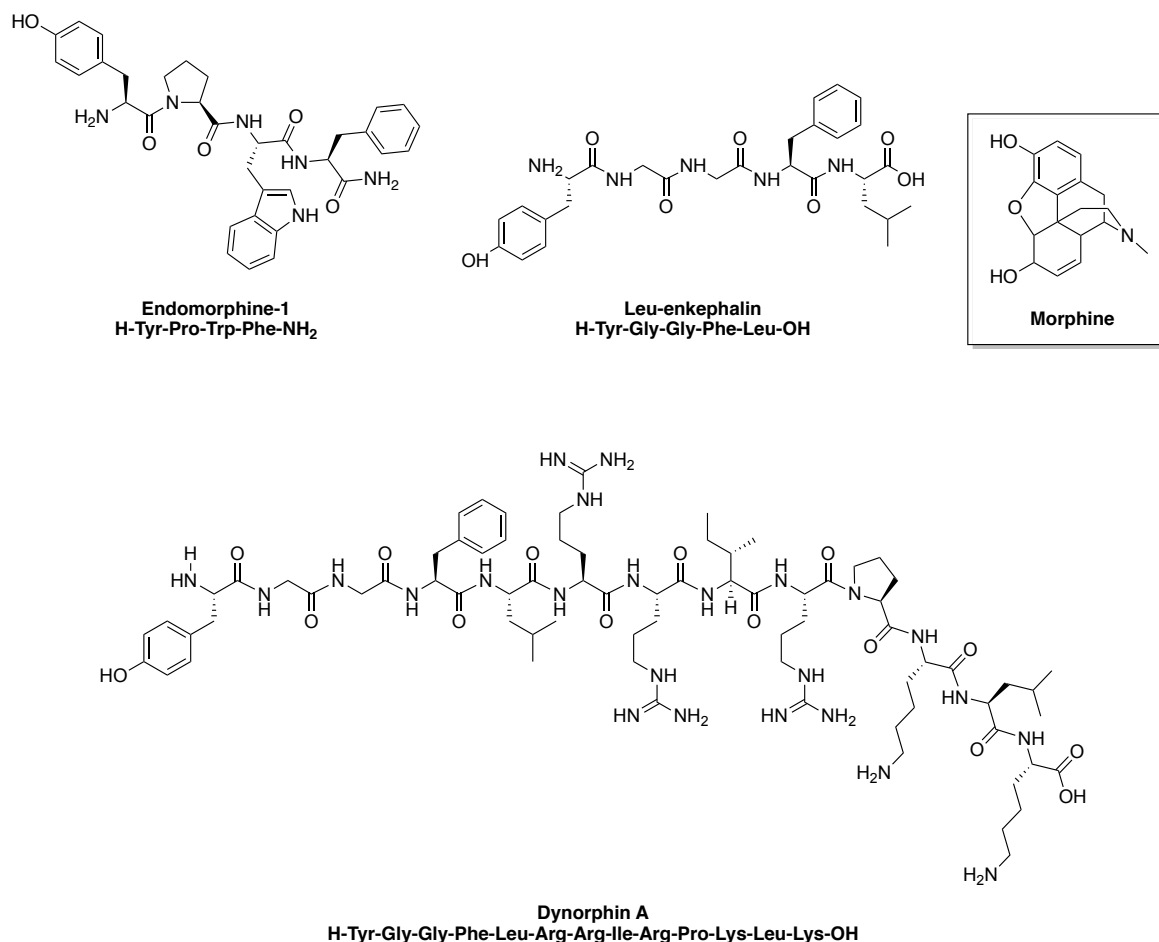


Figure 21: endogenous opioids peptides and structure of morphine

Opioid receptors belong to the superfamily of GPCR described earlier.⁷⁹ They can be activated by endogenous or exogenous agents (such as morphine or heroin). Opioid receptors can be divided into three categories: μ -opioid receptors (MOR), activated by compounds such as morphine an opiate analgesic; δ -opioid receptors (DOR) and κ -opioid receptor (KOR)s. These last two receptor types have also been targeted for the development of analgesic agents, which have fewer side effects than compounds binding to MOR. Indeed, MOR is also responsible for tolerance to and dependence on narcotics and opioid drugs.⁸⁰

Enkephalins were discovered in the 1970s as endogenous agonists with high affinity for DOR and MOR, with a preference for the DOR.⁸¹ Two pentapeptides differing in their last residue were isolated from pig brain and were named Leu-enkephalin and Met-enkephalin. The ratio between them in the body seems to depend on the species. Once the structure of Leu-enkephalin had been elucidated, it was shown by X-ray crystallography that it can adopt two kinds of β -turn in its unbound form ($4 \rightarrow 1$ or $5 \rightarrow 2$), stabilised by antiparallel hydrogen bonding between Tyr-Phe or Gly-Leu residues (Figure 22).^{82,83} Aside from the X-ray crystallography data, there is no evidence that this conformation is the one adopted by Leu-enkephalin when interacting with its receptor. Furthermore, there is no spectroscopic data (IR, CD, NMR) to indicate β -turn formation of this peptide in solution.

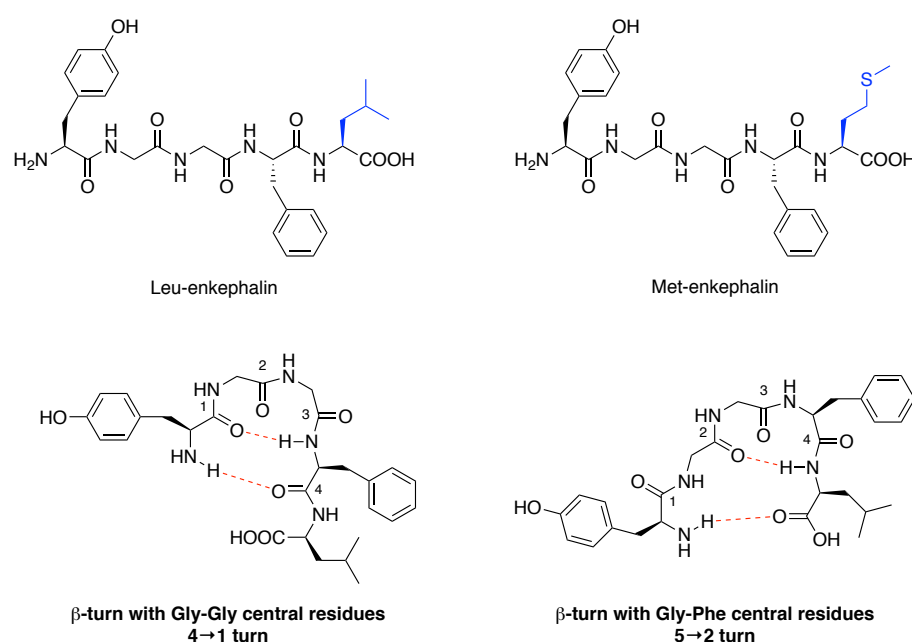


Figure 22: enkephalins and β -turn conformation stabilised by hydrogen bond

Recently, Dory and Gendron investigated the replacement of the peptide bonds in Leu-enkephalin by either a *trans*-alkene or a triazole, and studied the affinity and activity of the resulting conformationally constrained analogues towards DOR.^{84,85} Initially, each peptide bond was replaced with an (*E*)-disubstituted alkene to analyse the roles that the various amide bonds play in binding affinity to DOR or MOR (Figure 23).

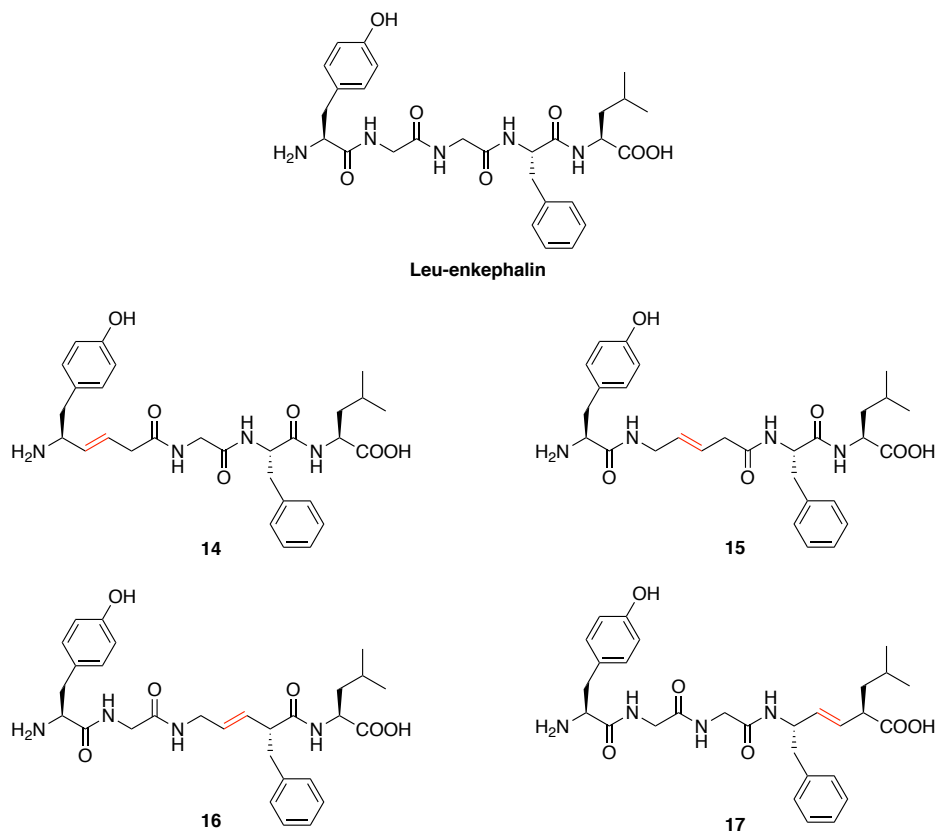


Figure 23: Leu-enkephalin and the alkene analogues

Binding affinity tests showed that the replacement of the Gly-Gly or Gly-Phe and Phe-Leu amide bonds (**15**, **16** and **17**) resulted in a significant decrease in affinity for the DOR (K_i values were 761 ± 32 nM, 587 ± 19 nM and 196 ± 29 nM respectively compared to 6.3 ± 0.9 nM for the native peptide), this indicates that these amide bonds are essential for efficient binding to the receptor. The replacement of the first amide bond (**14**) does not change the affinity for the receptor significantly. The hybrid peptides **14**, **16** and **17**, are still active to DOR, albeit to a lesser extent, while compound **15** is completely inactive, proving once more that this amide bond is essential for the binding and activity of the agonist. The sequential replacement of amide bonds by an *E*-alkene is an efficient way to understand the role and nature of interactions involving peptide bonds. The loss of affinity and activity for all analogues might be due to the loss of a crucial hydrogen bond to the binding pocket of the DOR. In order to address this issue, Dory *et al.* replaced selected peptide bonds with a triazole in order to retain rigidity in the system and provide two hydrogen bond donors; consequently, the hydrogen bonds could still be formed with the binding site of the receptor (Figure 24).

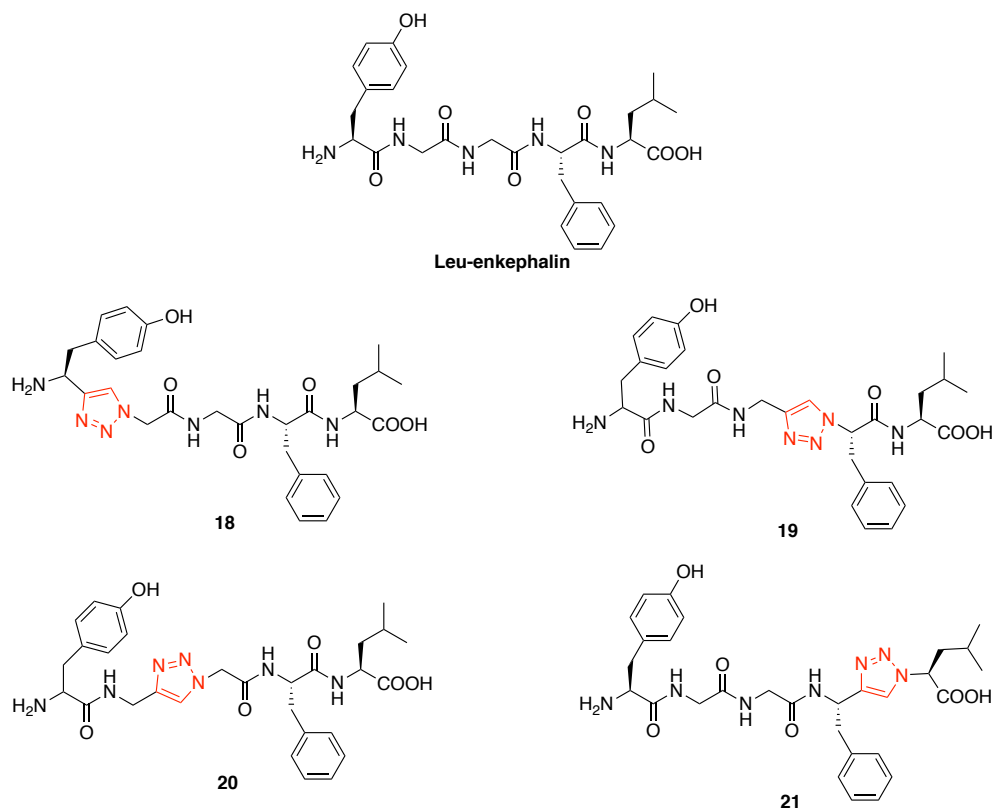


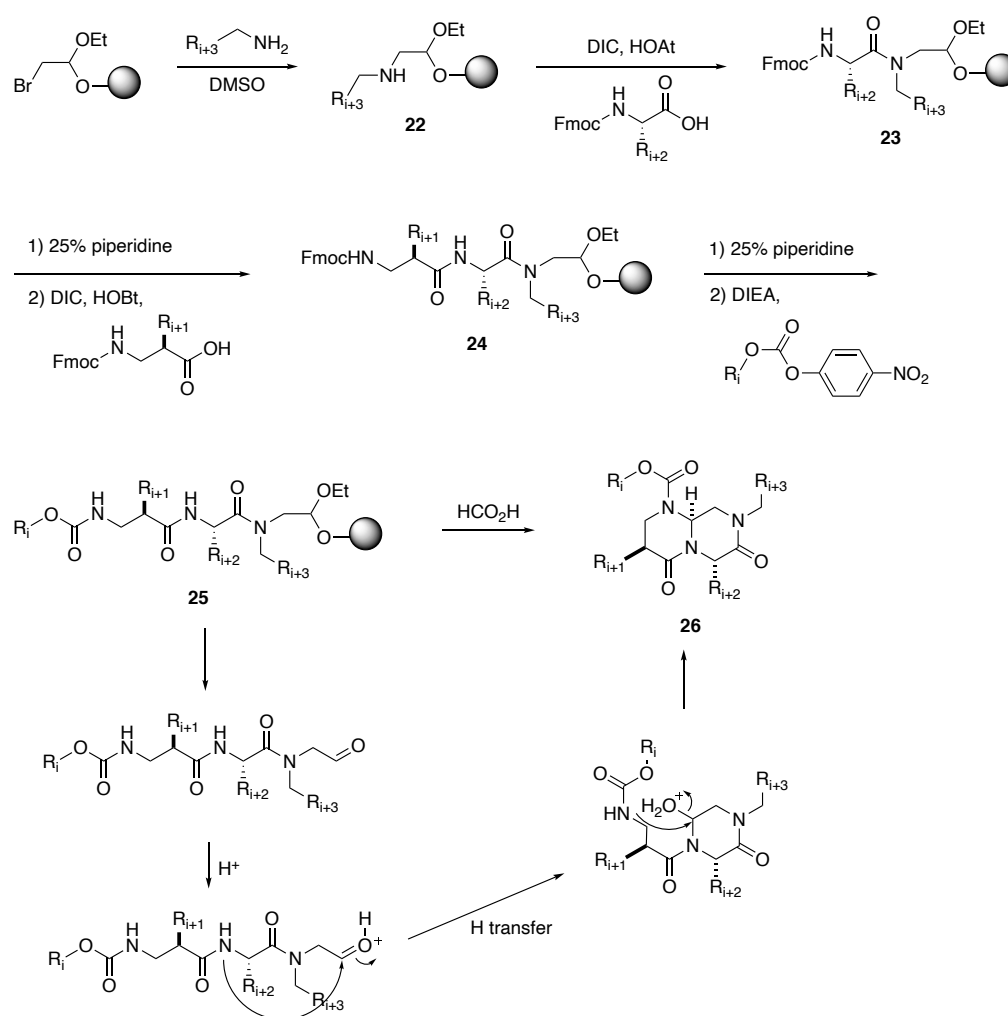
Figure 24: Leu-enkephalin and its triazole analogues

The affinities and potencies of the analogues towards DOR were tested. In all cases, it was found that the affinity is greatly diminished even more than the analogues with an alkene isoster. Only the analogue **21** in which the final amide bond was replaced with a triazole showed a modest affinity and activity ($K_i = 89 \pm 12$ nM, $EC_{50} = 830 \pm 66$ nM), but even this compound was almost 13-fold less active than the native peptide. This study showed that a triazole is not a good peptide bond isostere because all analogues demonstrate lower activity and affinity for the DOR than the native peptide.

These examples suggest that the replacement of peptide bonds by more rigid moieties may be useful for pharmaceutical and molecular design application. However, it is clear that careful design of the mimic is required and replacement of an amide bond can result in the loss of important hydrogen bonds or produce unfavourable steric interactions.

1.5.2.4. Enkephalin and endorphin mimetics by Kahn et al.

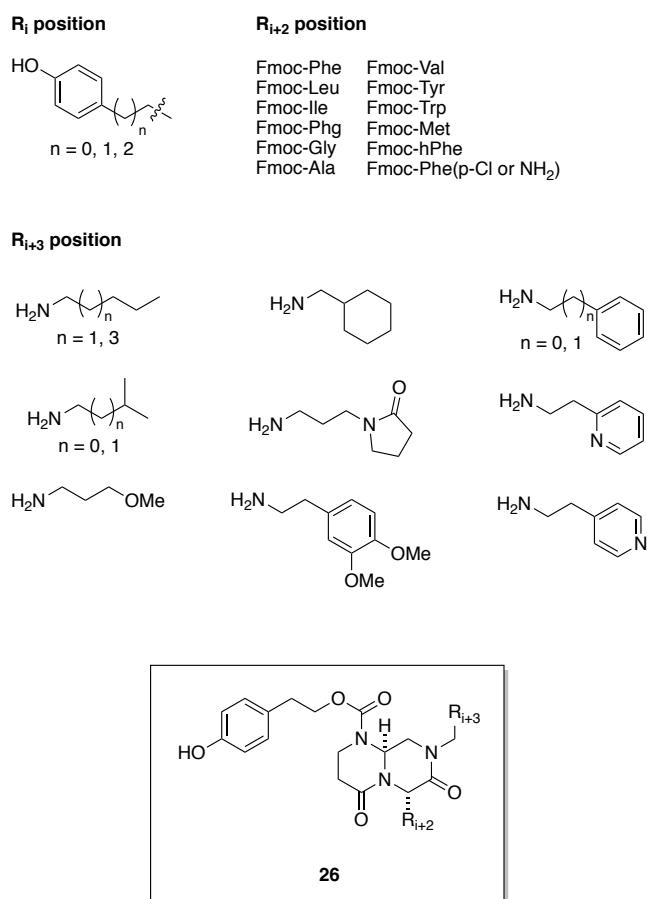
Opioids analogues are a widely described target for peptidomimetics and β -turn mimics. The examples exposed by Dory and Gendron exhibited a decrease of the affinity and activity when a peptide bond is replaced by an alkene or a triazole. Other studies were investigated towards the replacement of the turn sequence by a more constraint peptide in which a bicyclic core is used (Scheme 3). This peptide developed by Kahn and co-workers has the advantage to have four different sites readily accessible by solid phase synthesis.⁸⁶ The aim of this study was to find a potent and selective ligand towards one of the opioid receptors (MOR, DOR or KOR).



Scheme 3: β -Turn and its bicyclic analogue general synthetic route

The synthesis started from the commercially available bromoacetal resin which underwent nucleophilic substitution with various primary amine to afford the corresponding secondary amine **22**. This is then submitted to peptide coupling with the Fmoc-protected amino acid to yield peptoid **23**. Fmoc is then removed using 25% piperidine following by coupling with

β -alanine and HOBt leading to **24**. After deprotection the amine was treated with the corresponding aryl *p*-nitrophenyl carbonates in the presence of DIEA to afford **25**. Treatment with formic acid allowed cleavage of the acetal resin followed by cyclisation via aldehyde-amide condensation to give the bicyclic peptide **26**.⁸⁷ With this general synthesis a library of compound could be accessed easily with various substituents (Figure 25). Binding affinity study was then undertaken by looking at competitive selective binding on radioligand [³H]naloxone for relatively nonselective opioid receptors in rat cerebral cortex.



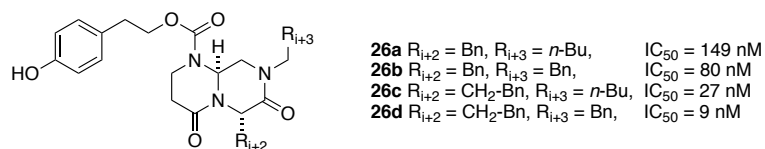
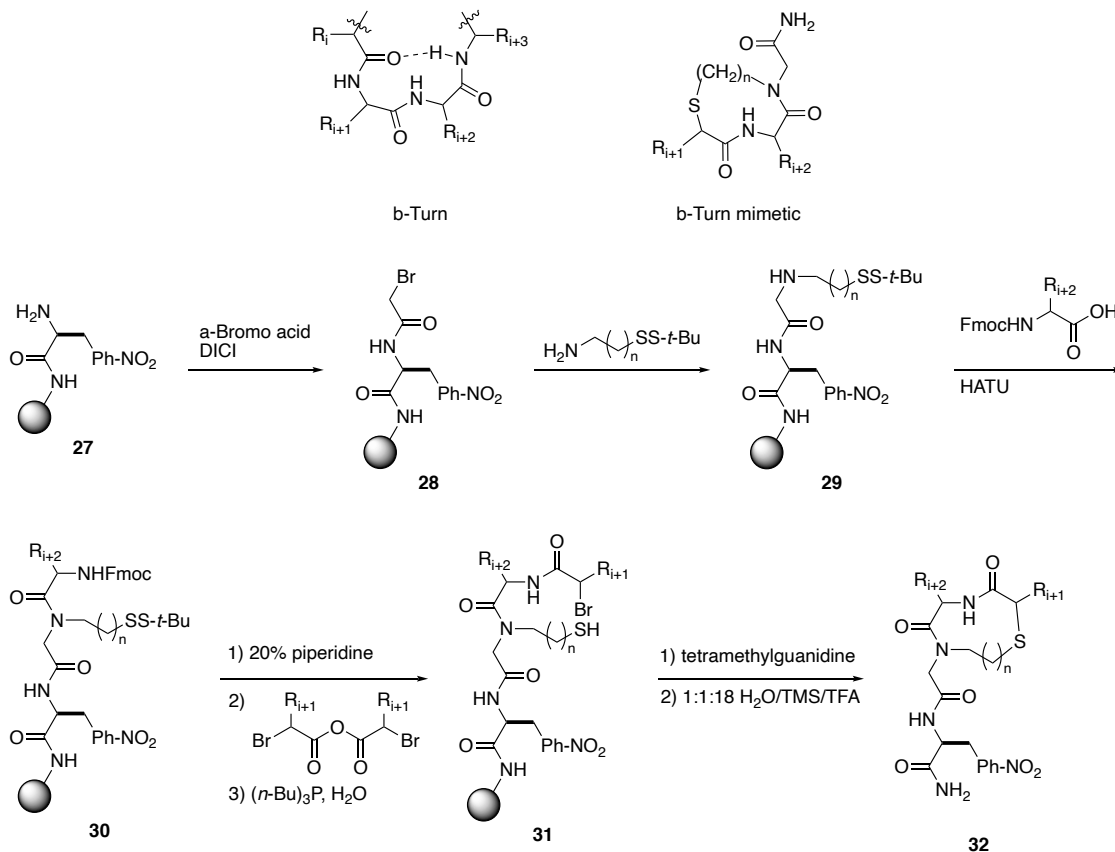


Figure 26: Four selected analogues and their IC_{50}

The replacement of an alkyl chain in $i + 3$ position by an aromatic improved the inhibitory activity almost two-time fold (**26b**). When the $i + 2$ position is modified from benzyl to phenethyl (one more carbon in the alkyl chain, **26c**), the activity greatly improved from 149 to 27 nM, and can be further enhanced three-time fold by changing the $i + 3$ position with a benzyl group (**26d**, $\text{IC}_{50} = 9 \text{ nM}$). The two last compounds were further studied in order to examine the receptor selectivity and both compounds exhibited an excellent selectivity towards MOR. Conformational analyses allowed to identify that **26d** was adopting a type III β -turn. This study undertaken by Kahn and co-workers allowed the optimisation of a general synthesis for a large library of compounds and identify by SAR four potent analogues. Among these four peptides, two were further tested and showed high affinity towards MOR at nanomolar concentration and their binding conformation has been determined as a type III β -turn.

1.5.2.5. Ellman's cyclic β -turn mimetic library

Following the same scheme developed by Kahn *et al.* with the general synthesis of enkephalin and endomorphin analogues, Ellman and co-workers have designed a library of β -turn mimetics by solid phase synthesis with various side chains functionality (Scheme 4).⁸⁸ A variety of analogues was synthesised via this method.



Scheme 4: Ellman's analogues and their general synthesis

Compound **27** was obtained by treatment of rink amide resin with standard conditions for SPPS. Bromo acetic acid was coupled to it using DIPEA, which then underwent nucleophilic substitution with disulphide amine to obtain peptide **29**. Further coupling on secondary amine using HATU and corresponding amino acid yielded **30**. Upon Fmoc deprotection coupling with symmetric anhydride, the mixed disulfide was cleaved using tributylphosphine in a mixture of polar solvents to give **31**. Rapid cyclisation using tetramethylguanidine followed by resin cleavage using H₂O/TMS/TFA cocktail afforded **32**. 11 compounds were synthesised following this route (Table 3).

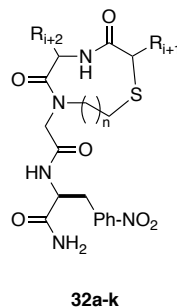


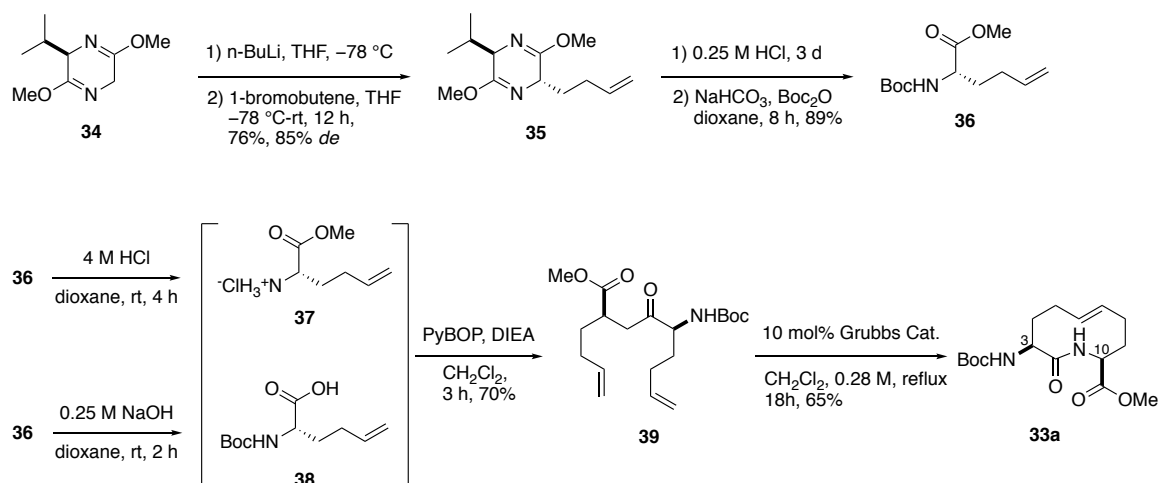
Table 3: analogues synthesised by Ellman and co-workers

32	R_{i+1}	R_{i+2}	n
a	CH ₃	CH ₂ -Ph	2
b	CH ₃	CH ₂ -Ph	2
c	CH(CH ₃) ₂	CH ₂ -Ph	2
d	CH ₂ CO ₂ H	CH ₂ -Ph	2
e	CH ₃	(CH ₂) ₄ NH ₂	2
f	CH ₃	CH ₂ CO ₂ H	2
g	H	CH ₂ -Ph	2
h	H	CH ₂ OH	2
i	CH ₃	CH ₂ C ₆ H ₄ -4-OH	2
j	CH ₃	CH ₂ -Ph	1
k	CH ₂ C ₆ H ₄ -4-OH	CH ₃	1

With this method they accessed to a rapid construction of turn mimic with a low level of epimerisation occurring. A 9-membered β -turn mimetic without the *p*-nitrophenyl alanine chromophore and Me chains at $i + 1$ and $i + 2$ positions was chosen as a model compound for conformational analysis. The $^3J_{\text{NH-H}\alpha}$ of the central amide with H α of $i + 2$ residue was 9.5 Hz, which corresponds to a dihedral angle Φ_{i+2} of $-120^\circ \pm 20^\circ$ (using Karplus equation). On the basis of comparison with different types of turn and computational analysis, the lowest energy conformer adopted a type II' β -turn conformation.⁸⁹

1.5.2.6. Katzenellenbogen's type I β -turn mimic

Constraint cyclic β -turn mimic were largely studied in the past decades. A highly constrained ten-membered lactam **33** was developed by Katzenellenbogen et al. that proved to be a good mimic of a type I β -turn mimic by molecular mechanic conformational searching.⁹⁰ Two different routes were investigated to obtain mimic **33**, via curtius rearrangement and macrolactamisation or by ring closing metathesis (RCM). The Second route proved to be more efficient and represented the first example of a ten-membered lactam cyclised using RCM (Scheme 5).



Scheme 5: Spiro-bicyclic β -turn mimic synthesis

The synthetic approach started by the alkylation of Schöllkopf's auxiliary **34** with 1-bromobutene affording alkene **35** in good yield and *de*. Diastereoisomers were then separated by column chromatography and hydrolysis of the auxiliary under acidic conditions afforded the corresponding amine which was then protected yielding protected amino acid **36**. Boc group was removed under acidic conditions affording **37** and **36** was saponified to afford corresponding carboxylic acid **38**. **37** and **38** were coupled using standard coupling conditions (PyBOP and DIEA) to RCM precursor **39**. Optimisation of the RCM afforded the desired macrolactam in 65% yield. The other diastereoisomer could be obtained following the same scheme. With the core turn mimic in hand, tetrapeptide derivatives were prepared for conformational analysis (Table 4).

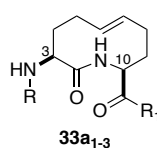


Table 4: tetrapeptides analogues obtained

33a	R	R ₁
1	Boc-Phe-	-Met-NH ₂
2	Boc-Phe-	-Phe-OMe
3	Boc-Ala-Phe-	-Phe-OMe

The conformational analysis consisted in temperature dependent, concentration and solvent dependent NMR studies and MD calculations. **33a₂** was analysed and an intramolecular hydrogen bonds were identified between the carbonyl of the Boc group and the ring amide proton and between the Boc carbonyl and the NH of the N-ter Phe indicating the formation of a β -turn in solution. Vicinal ³J coupling constant were then measured and dihedral angles

extracted with the Karplus equation and used the value for torsional constraint for molecular modelling, the torsion angles measured were within 30° of the ideal angles for a type I β -turn. 1D NOE experiment was also undertaken and expected β -turn cross-peaks were observed. The spectroscopic data proved that peptide **33a₂** was experiencing a type I β -turn conformation in solution. Coupling constant was then compared between **33a₁**, **33a₂** and **33a₃** and no significant difference was observed meaning that all derivatives have a similar conformation under various conditions. The bicyclic core was a good choice of mimetic to stabilise a turn conformation.

1.5.2.7. Examples of β -turn peptidomimetics including cyclopropane moiety

A small number of research groups have considered using a cyclopropane as a β -turn or β -strand inducer. Shuto *et al.* reported the synthesis of conformationally restricted peptidomimetics based on the structural features of cyclopropane.⁹¹ Depending on whether the substituents on the cyclopropane are in a *trans*- or a *cis*-configuration, the system could mimic either a β -turn or a β -strand (Figure 27).

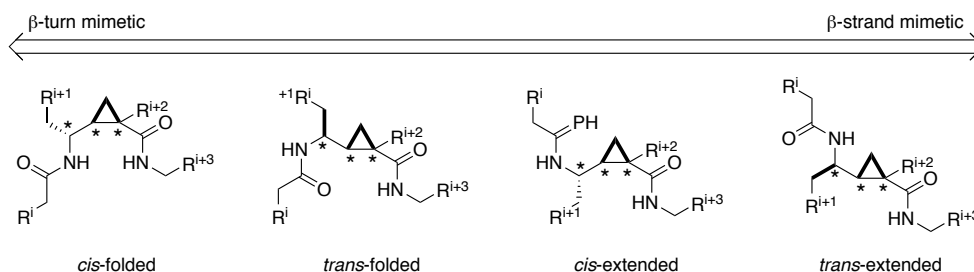


Figure 27: β -turn or β -strand mimicking regarding cyclopropane configuration

The natural melanocortin receptor (MCR) ligand possess the key sequence Ac-His-Phe-Arg-Trp-NH₂, which plays an important role in its receptor binding affinity. Considering this, a synthesis of analogues of this sequence was developed including *cis*- or *trans*-cyclopropane by Shuto and co-workers (Figure 28).

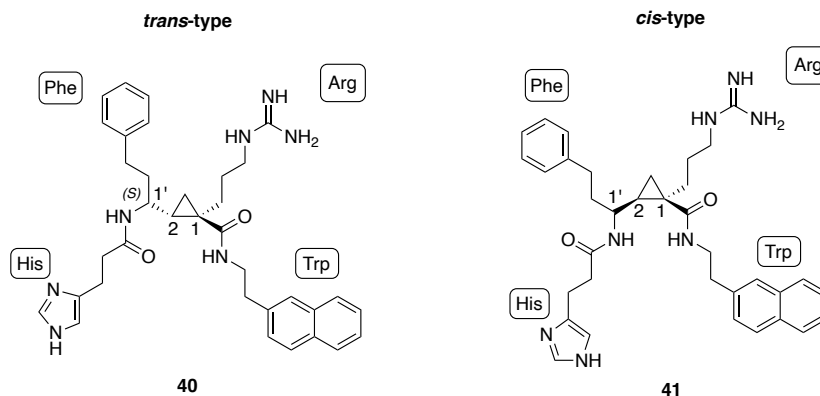


Figure 28: Designed analogues of MCR ligand

Biological assays showed that *trans*-cyclopropane **40** exhibited a higher affinity for the MCR than the corresponding *cis*-cyclopropane **41**. *Trans*-isomer **40** also showed better activity and specificity for one of the MCR receptors – hMC4R ($K_i = 0.37\text{--}0.88\text{ }\mu\text{M}$) – and also possesses a longer half-life than the original tetrapeptide ($t_{1/2} > 24\text{ h}$ and about 1.7 h respectively in human serum). Thus, utility of cyclopropane-containing peptidomimetics to identify non-peptidic analogues of bioactive peptides as novel lead compounds was demonstrated.

Martin *et al.* have also explored the use of cyclopropane unit as a rigid peptide bond replacement because of its potential ability to preorganise the resulting hybrid peptide into a conformation that is similar to the bound conformation of the original more flexible peptide⁹². A part of the peptide bond was substituted, either the NH of the i^{th} amide (modification a) or the C=O of the $(i + 1)^{\text{th}}$ amide (modification b, Figure 29):

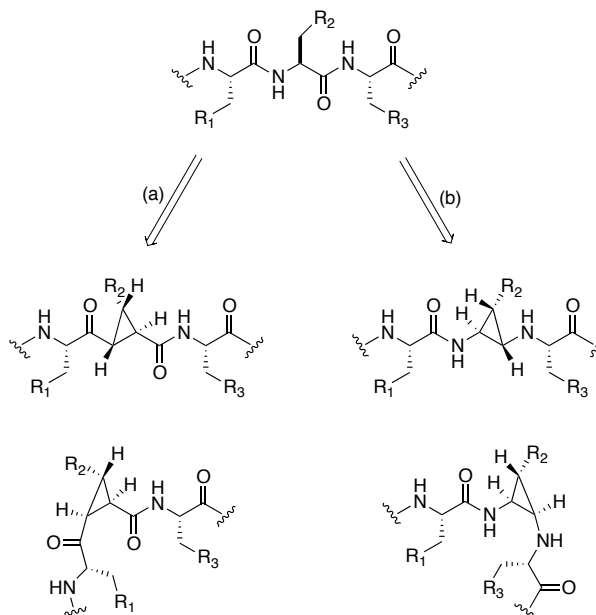


Figure 29: peptidomimetics with cyclopropane

Various peptidomimetics were synthesised and tested on several biological targets (Renin, Matrix Metalloprotease, HIV-protease inhibitor and enkephalin assays).⁹¹ The results showed that the cyclopropyl group enforced an extended or turned conformation in each case whilst projecting the amino acid side chains into well-defined positions. In some cases, cyclopropyl peptidomimetics were highly active and more potent than the flexible analogues, but in other cases it was detrimental to change the peptide amide bond because crucial hydrogen bonding was lost. This hydrogen bonding is needed because it allows the peptide to bond with the target and thereby inhibit or activate it, as seen with Leu-enkephalin analogues. In all cases, a *trans*-cyclopropane unit appears to be more compatible with locally extended structures than a *cis*-cyclopropane.

1.5.3. Cyclopropanes: generality and synthesis

All carbons of a cyclopropane lie on the same plane and all the C–C bonds have the same length which means the three carbons are at the corner of an equilateral triangle. This structure is considerably strained due to the bond angle (60°) deviating greatly from the optimum tetrahedral angle of 109.5° . Any rotation around a simple C–C bond in a cyclopropane is impossible, so all of the C–H bonds are forced to be eclipsed (Figure 30). The C–C bonds of cyclopropane are bent and can be considered to be intermediate in character between σ - and π -bonds. In fact, it has been shown that a cyclopropane attached to a carbonyl group has roughly the same spectroscopic properties as an α,β -unsaturated carbonyl.⁹³ These properties make the cyclopropane much more reactive than other cycloalkanes such as cyclohexane and cyclopentane as an amide bond surrogate.

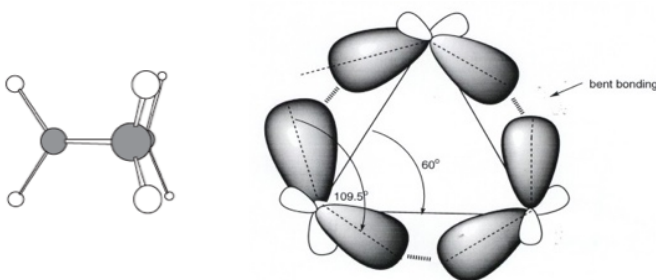


Figure 30: View along C–C bond and orbitals arrangement in cyclopropane

Cyclopropanes are present in many natural compounds. Indeed, everyone is familiar with the ‘salty’ smell of the sea which is actually the dictyopterene (Figure 31), a family of volatile cyclopropanes used by female algae to attract male gametes.⁹⁴ A cyclopropane is also present in hypoglycin,⁹⁵ a blood sugar level lowering agent from the ackee tree. More than a hundred pharmaceutical agents contain a cyclopropyl group, such as the antidiabetic drug Saxagliptin and U-106305,^{96,97} which is a potential therapeutic agent for coronary heart disease.

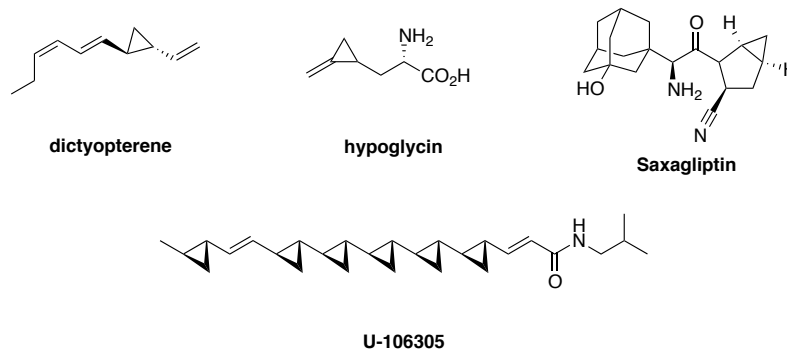
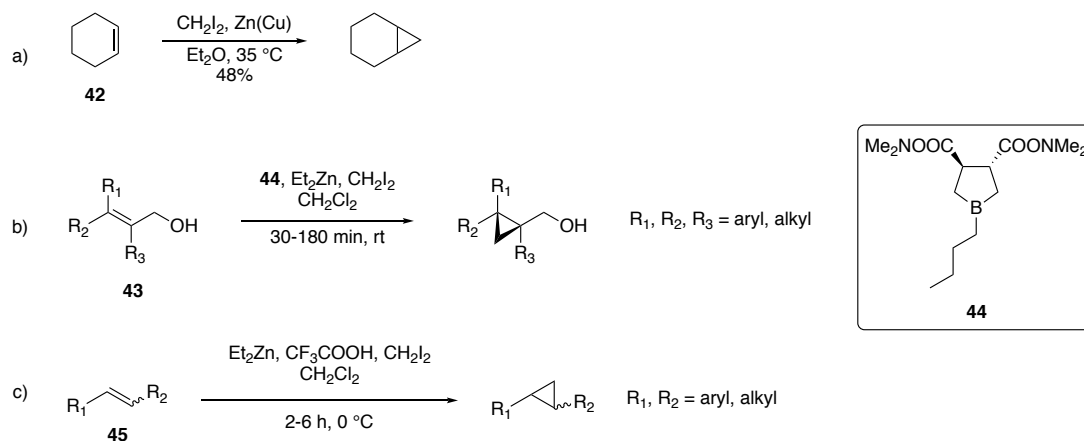


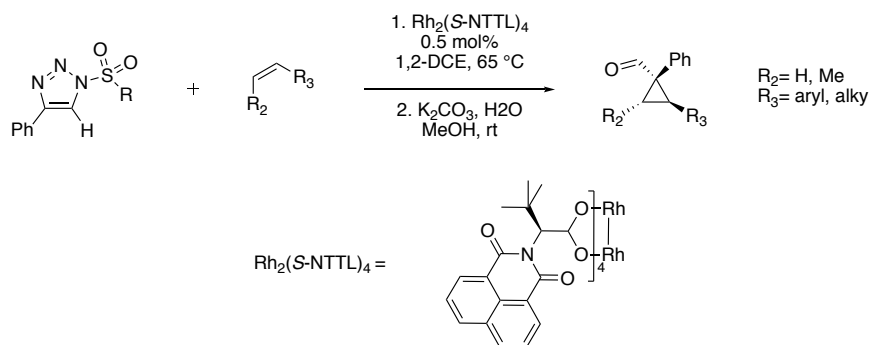
Figure 31: natural and synthetic compound containing cyclopropyl group

The synthesis of cyclopropane was first reported by August Freund in 1881 who treated 1,3-dibromopropane with sodium leading to the cyclopropane by a Wurtz reaction.⁹⁸ Most chemical syntheses of cyclopropanes involve the addition of a carbene or a carbenoid to an alkene. This is well demonstrated by the Simmons-Smith reaction in which an alkene **42** reacts with a zinc carbenoid species that has been formed *in situ* from diethylzinc and diiodomethane (Scheme 6a).⁹⁹ In 1998, Charette *et al.* developed an asymmetric cyclopropanation reaction in which one equivalent of the boronate ligand **44** was used as chiral auxiliary and used this method to complete the total synthesis of U-106305.^{100,101} A yields of more than 80% were obtained and good enantiomeric excesses (>90%) were achieved for a wide range of allylic alcohols **43** (Scheme 6b) by use of this method. Allylic alcohols undergo cyclopropanation much faster than the corresponding unfunctionalised alkenes because of the coordination between the zinc and the Lewis-basic oxygen of the hydroxyl group in the transition state; coordination also explains the high levels of stereoselectivity. In 2003, Shi *et al.* reported the use of modified zinc carbenoids employing trifluoroacetate.¹⁰² This method increases the rate of conversion considerably via a [2+1] pathway at room temperature when a conjugated or symmetric alkene **45** in reacted (Scheme 6c).



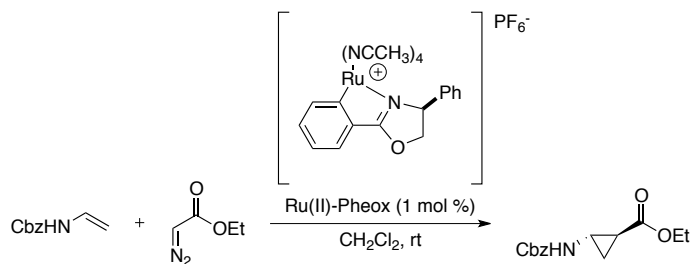
Scheme 6: Simmons-Smith reaction and its variations

An alternative cyclopropane synthesis has been developed recently that involves a different transition metal mediated reaction to generate the carbenoid. Fokin *et al.* developed a reaction that involves *in situ* generation of a rhodium carbenoid from a triazole or sulfonyltriazole (Scheme 7).¹⁰³ When a chiral complex such as $\text{Rh}_2\{(\text{S})\text{-NTTL}\}_4$ was used, cyclopropanes were obtained with yields of up to 99% and with high enantioselectivity (*ee* > 96%) and diastereoselectivity (*dr* 1:20). However, this method could be only used to produce trisubstituted cyclopropanes enantioselectively.



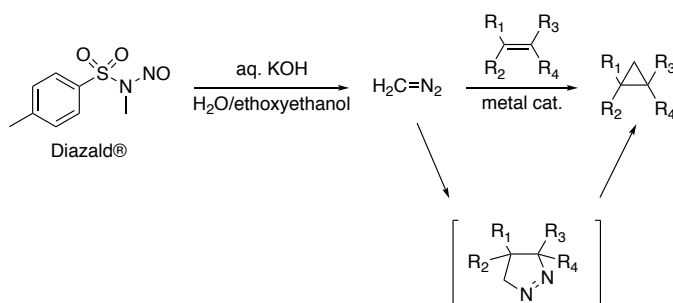
Scheme 7: Fokin's enantioselective cyclopropanation

Ruthenium was also reported as an excellent transition metal for the generation of carbenoids from diazoesters. Indeed, Iwasa and co-workers found that $\text{Ru}(\text{II})$ -Pheox could be used to catalyse the reaction of ethyl diazoacetate with an enamine to form a cyclopropylamine within 5 h in 99% yield and good selectivity (ratio *trans/cis* 7:3) (Scheme 8).¹⁰⁴ In contrast, the use of rhodium acetate as the catalyst resulted in poor stereoselectivity. However, it is possible to epimerise from the *cis*-isomer to the *trans*-isomer in a further step which will be described in a future section.



Scheme 8: cyclopropanation using diazoester and Ru catalyst

Despite its explosiveness and toxicity diazomethane has been found to be a good reagent for cyclopropanation. Diazomethane is usually generated in situ or immediately prior to use by the reaction of Diazald® and a solution of KOH in water (Scheme 9).¹⁰⁵



Scheme 9: cyclopropanation using diazomethane generation in situ

Table 5 summarise some of the conditions that have been described for the formation of cyclopropanes from diazomethane. In most of the procedures, alkene possesses an electron-withdrawing substituent.

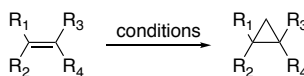


Table 5: Cyclopropanation using diazomethane reported in literature

Entry	Alkene	Cat.	Ligand	Results
1	$R_1 = \text{Ph}, R_2 = R_3 = \text{H}, R_4 = \text{CO}_2\text{Me}$	$\text{CuOTf} \cdot 0.5\text{PhCH}_3$		40-80% yield 48-77% <i>ee</i>
2	$R_1 = \text{H or Me}, R_2 = \text{Aryl}, R_3 = R_4 = \text{H}$		-	64-89% yield Open to air
3	$R_1 = \text{H}, R_2 = \text{Aryl}, R_3 = \text{H or CONMeOMe}, R_4 = \text{H or CO}_2\text{Me}$	$\text{Pd}(\text{OAc})_2$	-	64-99% for <i>trans</i> -alkene 15-73% for <i>cis</i> -alkene

Charette *et al.* have described the use of a bis-(oxazoline) ligand and copper triflate to generate a cyclopropanation catalyst (Table 5, entry 1).¹⁰⁶ They noticed that CuOTf or Cu(OTf)₂ were equally effective for catalyst formation. They reported decent yields with acceptable levels of stereocontrol for the *trans*-cyclopropane formed. Carreira and co-workers improved the use and formation of diazomethane *in situ* by using an iron catalyst (Table 5, entry 2).¹⁰⁷ Indeed, the use of this catalyst combined with very slow addition of Diazald® in the pre-mixture allowed the reaction to be performed in open air. This method gave relatively good yields and selectivities for formation of *trans*-cyclopropanes, but an asymmetric variant of the reaction was not reported. Cyclopropanation of alkenes with diazomethane has also been used for the synthesis of therapeutic targets (Table 5, entry 3).¹⁰⁸ In this case, the synthesis of *trans*- and *cis*-cyclopropane in a relatively good yield was reported.

1.6. Introduction to the design and synthesis of β -turn mimics in the Clark group

1.6.1. Previous work in the group

1.6.1.1. Ynamides and alkynes Leu-enkephalin peptidomimetics

The first approach of the Clark group towards a β -turn mimetic was to synthesise macrocyclic ynamides or alkynes that would mimic the turn conformation of the pentapeptide Leu-enkephalin (Figure 32).¹⁰⁹

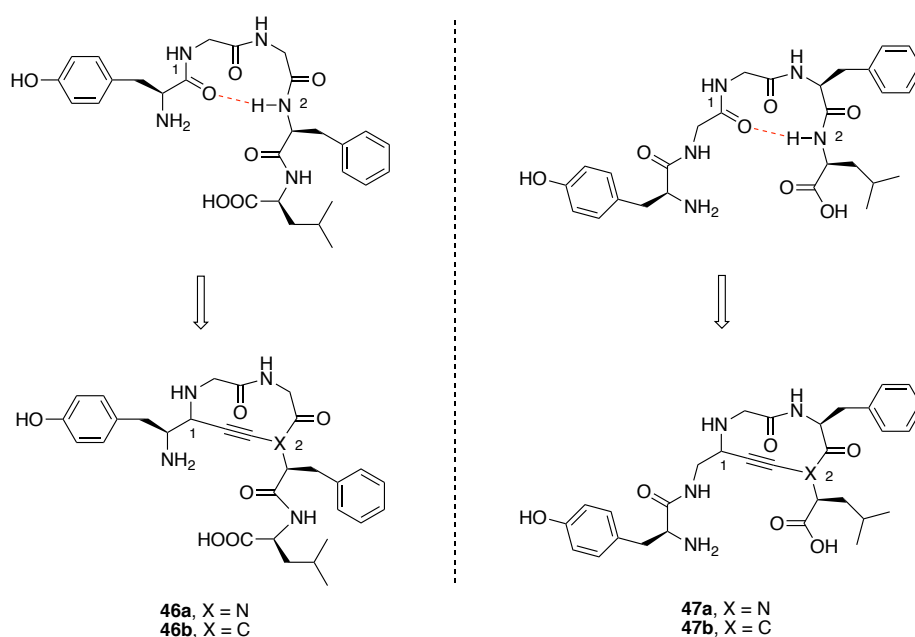


Figure 32: Ynamides and alkyne peptidomimetics

As shown in Figure 32, it was intended that an ynamide or alkyne would replace the hydrogen bond by a covalent bond, restraining the system and forcing it to adopt the turn conformation. Those units were chosen for several reasons. Firstly, almost all the functional groups remain and the only group to be replaced is the hydrogen bonded carbonyl; secondly, the bond distance between atoms 1 and 2 in the figure is similar (Table 6).

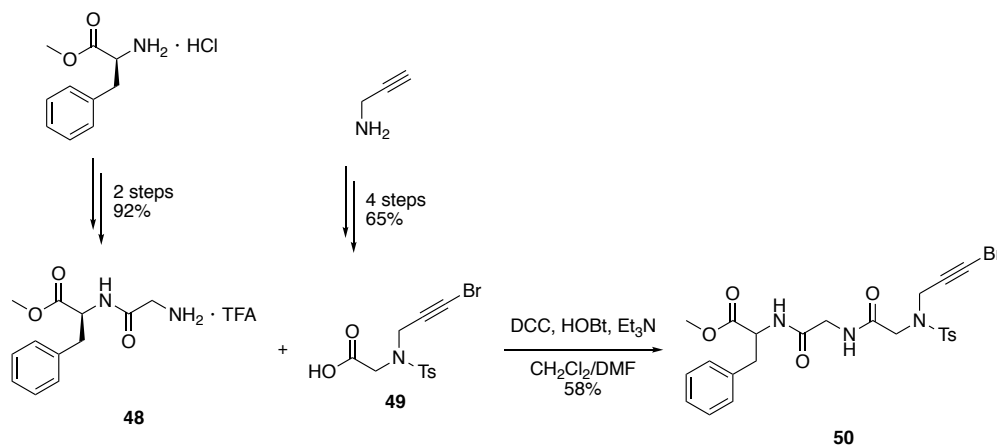
Table 6: bond lengths of mimetics

Structure	Distance (Å)
	4.21 ⁸³
	4.14 ^a
	4.21 ^a

^a using known average bond lengths summed up

The bond length is relatively similar to that in the hydrogen bonded structure, which makes the surrogates good choices for use in β -turn mimicry.

Various models were used in order to explore reactions required to prepare the ynamide and alkyne and effect the macrocyclization reaction. The initial strategy involved formation of the ring by intramolecular ynamide synthesis from precursor **50**, which was obtained by coupling between **48** and **49**. TFA salt **48** was obtained in two steps from Phe methyl ester hydrochloride by amide coupling with Boc-Gly and subsequent deprotection. Alkyne **49** was obtained by tosylation of propargyl amine followed by *N*-alkylation using *t*-butyl bromoacetate affording the desired acetylenic fragment. Bromination of the alkyne with NBS and AgNO₃ followed by ester cleavage afforded **49** in 65% over 4 steps (Scheme 10).



Scheme 10: precursor 50 synthesis

The synthesis of compound **50** meant that the intramolecular cyclisation reaction could be explored. The initial attempt to construct the ring was performed using Hsung's second generation amidation condition (Table 7, entry 1).¹¹⁰ This revised amidation reaction involves the use of copper sulphate pentahydrate as catalyst, phenanthroline as ligand and K₃PO₄ as base. When the loading and temperature described by Hsung was followed, there was no reaction. When, loadings of the catalyst and ligand were increased and the reaction temperature was raised, decomposition of the substrate was observed.

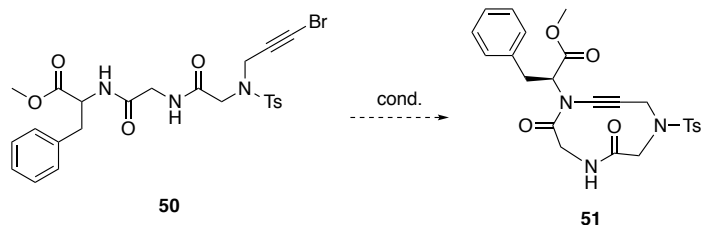
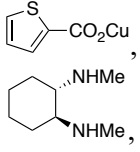
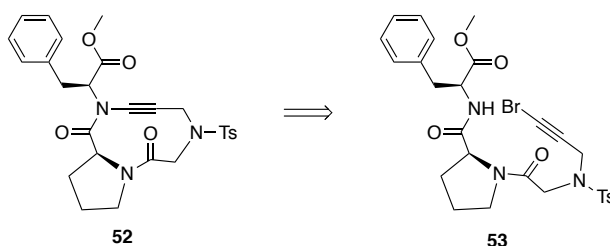


Table 7: macrocyclisation attempts for ynamide formation

Entry	Conditions	Results, comments
1	10-20 mol% CuSO ₄ ·5H ₂ O 20-40 mol% 1,10-phenanthroline, K ₃ PO ₄ Toluene, 70 °C	Slow or no conversion Decomposition with high loading and temperature
2	FeCl ₃ ·6H ₂ O DMEDA, K ₂ CO ₃ Toluene 90 °C	No conversion SM recovered
3	CuI KHMDs, Pyridine THF, rt	No conversion SM recovered
4	CuCN K ₃ PO ₄ , Pyridine Toluene, 90 °C	No conversion SM recovered
5	10 mol% CuSO ₄ ·%H ₂ O 20 mol% 1,10-phenanthroline, K ₃ PO ₄ , Ni(acac) ₂ Toluene, 70 °C	Little conversion Decomposition with time
6	 Toluene, 85 °C	Dimerisation of SM

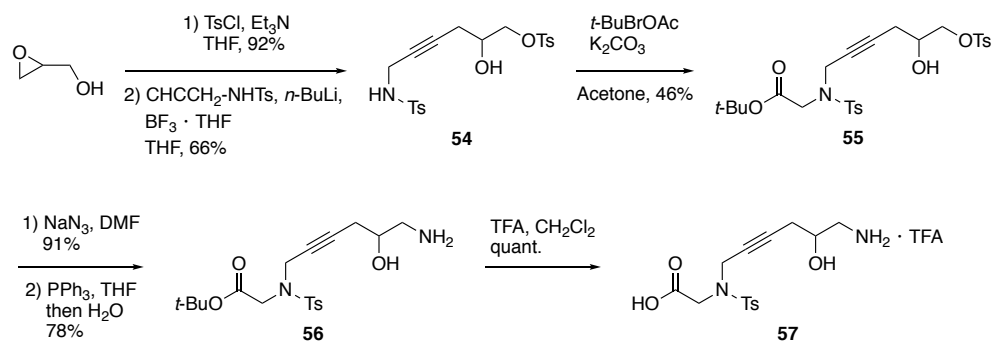
The reaction was then performed using conditions described by Zhang *et al.* using Iron(III) chloride hydrated (Table 7, entry 2).¹¹¹ These workers had used the reaction to couple oxazolidinones, sulfonamides and lactam substrates, but had not explored intramolecular amidation. Intramolecular cyclisation did not occur under these conditions and starting material was recovered. Danheiser and co-workers had reported amidation promoted by a stoichiometric amount of CuI.¹¹² Unfortunately, under Danheiser's conditions, no reaction occurred and almost all of the starting material was recovered (Table 7 entry 3). Following these disappointing results, Hsung's first generation conditions were employed in which CuCN was used as the copper sources instead of CuSO₄ (Table 7 entry 4). This reaction resulted in no conversion of the starting material and so attempts were made to optimise the reaction conditions, by changing the ligand, the metal, the alkyne, the solvent and the reaction temperature. The use of Ni as additive showed promising results for intermolecular coupling reaction between (bromoethynyl)benzene and protected Gly (73% yield) and so the reaction was tested on substrate **50** (Table 7 entry 5). Unfortunately, this reaction resulted in decomposition of the starting material over time and the required product was not obtained.

The reaction was then investigated further using various ligand and catalyst combinations (Table 7 entry 6), via an allenamide intermediate. In this case, the catalyst was copper thiophenecarboxylate (CuTC) and 1,2-dimethylaminocyclohexane was employed as the ligand. This procedure produced interesting results for the synthesis of ynamide using alkynyl bromide.¹¹³ Unfortunately, reactions performed in toluene delivered an undesired compound, which appeared to be a dimer of **50**. Attempts were made to conformationally constrain the system by installing a Pro residue in the peptide chain (Scheme 11) in the expectation that this would orientate the alkynyl bromide and the amide for cyclisation and reduce the entropic penalty in the transition state.



Scheme 11: Proline analogue and its precursor

Compound **53** was synthesised in four steps with yield of 34% by a series of deprotection and amide coupling reactions. This substrate was then submitted to macrocyclisation under the conditions of Hsung's second general protocol and also reaction with CuTC catalyst. The former reaction resulted in no reaction with recovery of the starting material and the latter reaction produced an undesired compound that appeared to be the dimer by NMR analysis. As a consequence of these negative results and the failed attempts to achieve prepare target **53** by an amidative cross-coupling reaction, the target was revised and the precursor **55** was synthesised (Scheme 12).



Scheme 12: synthesis of precursor 57

The synthesis of **57** started from commercially available glycidol. Epoxide opening was accomplished using optimised Yamaguchi-Hirao alkylation conditions with *n*-BuLi and $\text{BF}_3 \cdot \text{THF}$ complex.¹¹⁴ This reaction afforded the alkyne **54** in 66% yield. *N*-Alkylation gave **55** followed by azide displacement of the tosylate and a Staudinger reaction afforded amine **56**. Subsequent ester cleavage using TFA, produced the cyclisation precursor **57** in 22% yield over 6 steps. Efforts were then focused on the cyclisation by amide coupling by use of conditions that are summarised in Table 8.

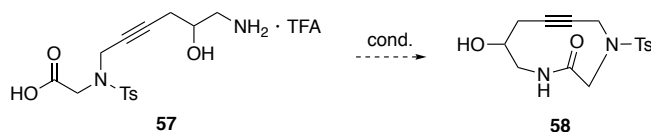


Table 8: amide coupling screening

Entry	Conditions	Results
1	BOP, HOBT, DIPEA $\text{CH}_2\text{Cl}_2/\text{DMF}$	No conversion
2	EDCI, DMAP $\text{CH}_2\text{Cl}_2/\text{DMF}$	No conversion
3	FDPP, DIPEA DMF	Decomposition
4	DMTMM, DIPEA DMF	Decomposition
5	PyBOP, DIPEA DMF	Decomposition
6	$\text{Co}_2(\text{CO})_8$, CH_2Cl_2 Then amide coupling reagents	No to poor conversion

Common coupling reagents were used (table 8, entries 1, 2 and 5, Figure 33) in attempts to affect the cyclisation reaction. Unfortunately, the required lactam was not obtained, even after extended reaction times of several days and addition of further amounts of the coupling reagent(s).

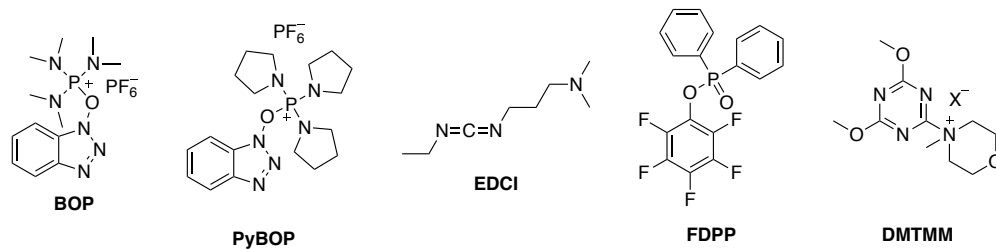


Figure 33: coupling reagents used for the screening

It had been reported that pentafluorophenyl diphenylphosphinate (FDPP) and 4-(4,6-dimethoxy-1,3,5-triazin-2-yl)-5-methylmorpholinium (DMTMM) were efficient coupling agents for peptides containing macrolactams.¹¹⁵ Precursor **57** was then submitted to amide coupling using FDPP or DMTMM (Table 8, entries 3 and 4) but only decomposition of the starting material was observed by NMR of the reaction mixture. A hypothesis that could account for the failure of these reaction conditions was that the precursor might be too constrained by the triple bond, which prevented cyclisation. In order to address this issue, it was decided to form a cobalt-alkyne complex with the expectation that triple bond would show more double bond type character and a less strained ring-system would be produced.¹¹⁶ The cobalt complex of **57** was prepared and isolated, but the subsequent amide coupling reaction did not deliver the required target **58** (Table 8, entry 6). The various coupling reagents listed in table 5 were used as well, but none gave promising results.

Optimisation of both ynamide synthesis and alkyne cyclisation reactions to give the desired peptide mimic were unsuccessful. The replacement of the non-covalent hydrogen bond by a covalent triple bond was considered to be a good strategy considering the atom distance mentioned earlier, but another target was required in order to avoid the macrocyclisation step, which seemed to be impossible to achieve.

1.6.1.2. Trans-cyclopropane peptide bond isostere

The Clark group strategy moved towards the synthesis of a completely different class of analogues. It was decided that replacement of a peptide bond by a rigid group such as cyclopropane would be better than replacement of the hydrogen bond by a covalent linker. This would constrain the system more than in a regular peptide bond and increase the stability of the mimic under physiological conditions by preventing proteolytic cleavage at this position.

Initial studies towards the synthesis of the protected *cis*- or *trans*-cyclopropane-containing Gly-Gly surrogate (Figure 34) were undertaken.

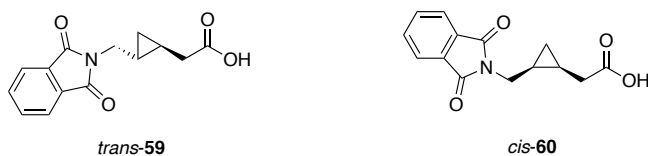
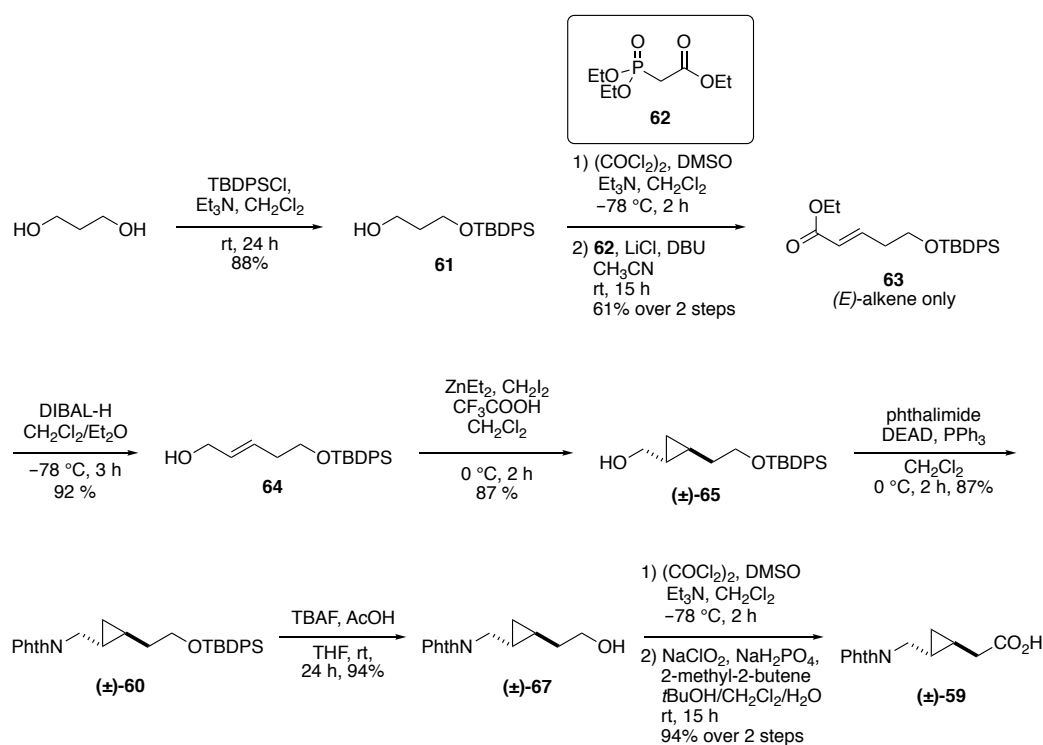


Figure 34: *trans*- and *cis*- cyclopropane targets

Several route towards these compounds were investigated. The synthesis of the *trans*-**59** was accomplished in 9 steps with an overall yield of 36% starting from the commercially available propan-1,3-diol (scheme 13).¹¹⁷

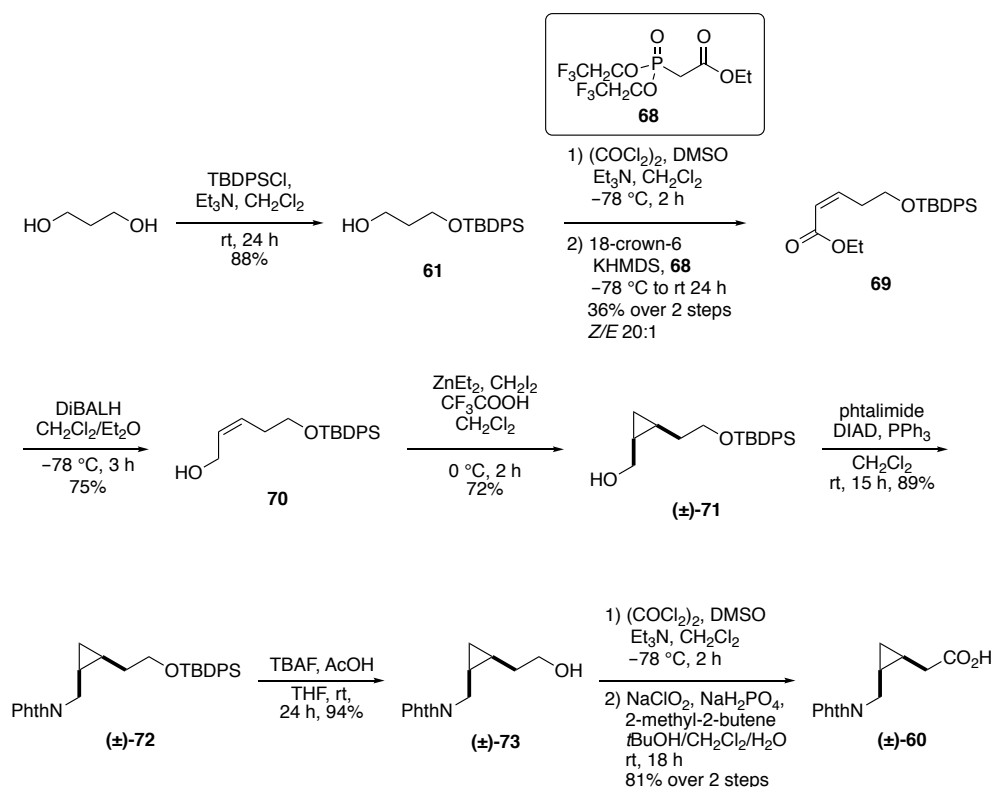


Scheme 13: *trans*-59 synthesis via HWE olefination and Shi cyclopropanation

The synthesis started with mono-protection of propan-1,3-diol with a TBDPS group. Subsequent Swern oxidation delivered the corresponding aldehyde necessary for the Horner-Wadsworth-Emmons (HWE) olefination.¹¹⁸ This reaction involved the phosphonate **62** and resulted in the stereoselective formation of the (*E*)-alkene **63**. Ester reduction with DIBAL-H afforded the allylic alcohol **64** and a Simmons-Smith reaction was undertaken using Shi's conditions to give the *trans*-cyclopropane **65**.¹¹⁹ From the alcohol **65**, a Mitsunobu reaction was performed using phthalimide to introduce the desired protected amine functionality and

deliver the imide **66**. The silyl ether was cleaved and the resulting alcohol **67** was oxidised to the corresponding carboxylic acid *trans*-**59** via stepwise Swern and Pinnick oxidation reactions. The synthesis of the racemic protected amino acid *trans*-**59** was completed in 9 steps.

An analogous route was used to synthesise *cis*-**60**.¹²⁰ Previously, cyclopropanation of the (*E*)-alkene **64** had resulted in formation of the *trans*-cyclopropane, but in this case a Still-Gennari olefination reaction was used instead of the HWE reaction to access to (*Z*)-alkene **69**.¹²¹ *cis*-Cyclopropane **71** was installed in the next step using the conditions described in scheme 14. The synthesis was completed by the same sequence of reactions as above to give the racemic target compound *cis*-**60** in 9 steps and in a 10% overall yield.



Scheme 14: *cis*-60 synthesis via Still Gennari olefination

The Still-Gennari modification employs two electron-withdrawing trifluoroalkoxy substituents on the phosphonate **68** rather than the ethoxy group on the phosphonate **62** which produced the (*Z*)-alkene **69** with *Z/E* a ratio of 20:1. The subsequent steps followed the same procedure as described for the synthesis of *trans*-**59**.

This work was promising in that it produced dipeptide mimics that are similar to those described by Gellman *et al.* but in which an alkene is used to replace the amide bond instead

of a cyclopropane.⁷⁶ Both dipeptides were synthesised as racemic mixtures and no analyses concerning intramolecular hydrogen bond formation were undertaken. Analysis of hybrid peptide that contain cyclopropane-containing peptide mimics to establish whether intramolecular hydrogen bonding is present was to be one of the main challenges of the work presented in this thesis.

1.6.2. Aim of this work

Using the concept of cyclopropane peptidomimetics, the Clark research group was interested in synthesising cyclopropane derivatives where a cyclopropane is used to replace a peptide bond (Figure 35) in order to induce β -turn formation. The first objective was to synthesise both racemic and enantioenriched dipeptide surrogates containing a cyclopropane moiety. Following their successful synthesis, the next step was to be the incorporation of these isosteres into various peptides. Various NMR and IR spectroscopy techniques would then be used to perform conformational analysis to verify formation of intramolecular hydrogen bond and identify general conformations adopted by the peptides.

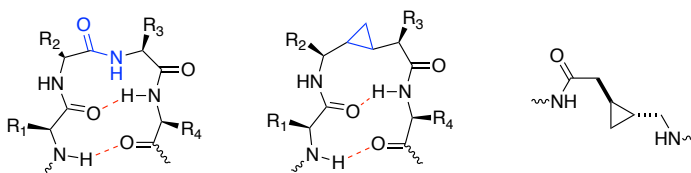


Figure 35: β -turn in a peptide, hypothetical β -turn mimicry, structure of the desired dipeptide surrogate

The length of the peptide was to be varied from 2 to 12 residues in order to understand the stability of the peptides and their propensity to adopt the desired conformations. The peptides were to be analysed by IR, NMR and CD methods in order to prove β -turn formation.

Chapter 2

Results and discussion

2.1. Compounds Naming and Abbreviations

Abbreviations have been used throughout this thesis to simplify the naming of the compounds that have been synthesised. Peptides and proteins are named from the N-terminus to the C-terminus so the nomenclature is consistent. The dipeptide mimic **74** will be named PGN-{Gly Δ Gly}-OH, where PG is the protecting group installed (Figure 36) and Δ refers to the cyclopropane that replaces the peptide bond.

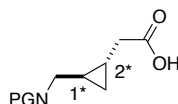


Figure 36: PGN-{Gly Δ Gly}-OH

The stereocenters are named from N-terminus to the C-terminus, carbon 1 represents the CH of the cyclopropane located on the N-terminal side, carbon 2 the CH located on the C-terminal side. For example, (*R,S*)-NPG-{Gly Δ Gly}-OH corresponds to carbon 1 with *R*-configuration and carbon 2 with *S*-configuration. In the case of racemic mixtures, the peptide will be named (\pm)-NPG-{Gly Δ Gly}-OH. In the event of longer peptides, the residue will be incorporated in the name as in the official nomenclature; *e.g.* (*R,S*)-PGN-X₁-{Gly Δ Gly}-X₂-OH. The stereochemical assignments given in brackets correspond only to the configuration of the cyclopropane, the configuration of the natural amino acids X₁ and X₂ will not be included.

2.2. Strategy

β -Turn mimetics have proven to be promising tools in medicinal chemistry as well as synthetically challenging targets in organic and peptidomimetic chemistry. Over the past few decades, they have allowed chemists and biologists to develop a better understanding of protein-protein interactions in biological processes.^{84,91} From natural peptides to constrained peptidomimetics, research in the area of β -turn mimetics has grown rapidly in recent decades and promising results have been obtained in the field of drug discovery.^{122,123,124}

The objective of this project was to demonstrate that β -turn-like structures could be generated in small peptides by the synthesis non-natural hybrid peptide analogues that contain an amide bond replacement group. Constrained peptides have been shown to be capable of β -turn mimicry and at the outset of the project, Gellman *et al.* had demonstrated that it was possible to detect intramolecular hydrogen bonds in non-natural hybrid peptide analogues using FTIR and NMR spectroscopy (cf. section 1.6.1.2). In Gellman's case, a combination of FTIR and NMR spectroscopy was used to identify formation of the β -turn in hybrids in which a peptide bond between two Gly residues had been replaced by a (*E*)-alkene (Figure 37).^{125,126} Hydrogen bonds between the amide groups present in the compounds were identified. Tetrasubstituted alkenes were found to be effective amide bond surrogates and enhanced the formation of a β -turn in small peptides. The challenge was to identify differences when the peptide bond is replaced by a non-planar moiety such as a *trans*-cyclopropane instead of an alkene. Analogues of the model peptides designed by Gellman and co-workers were synthesised and analysed using the same conditions by IR and NMR in order to provide a benchmark for our own analogues (Figure 37).

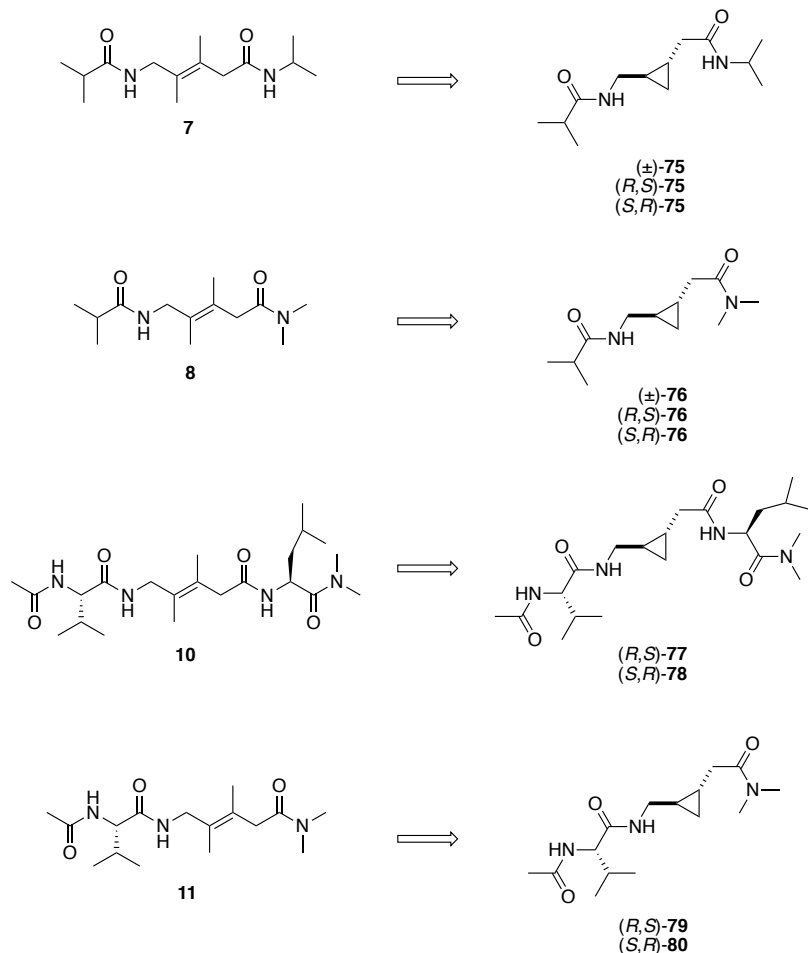
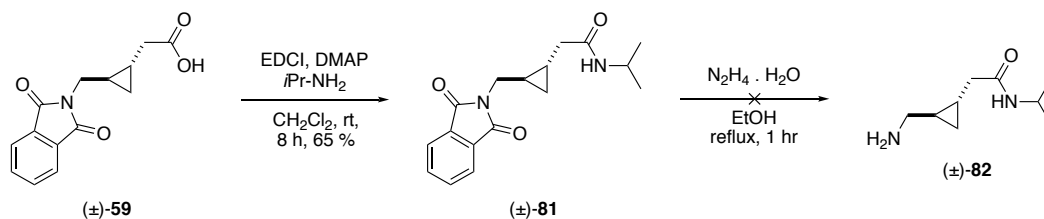


Figure 37: Gellman peptidomimetics and our analogues

The strategy was to prepare the *trans*-cyclopropane at the start of the synthesis by an efficient route that would permit access to significant quantities of both enantiomers. After enantioenriched compounds had been obtained, the Gly-Gly surrogates PGN-{GlyΔGly}-OH were to be synthesised. Before revisiting the first-generation route previously developed in the group, the readily available racemic dipeptide mimic (±)-NPhth-{GlyΔGly}-OH **59** was subjected to peptide coupling to produce the first analogue (±)-**75** (Scheme 15).



Scheme 15: Towards the dipeptide mimicry for IR study

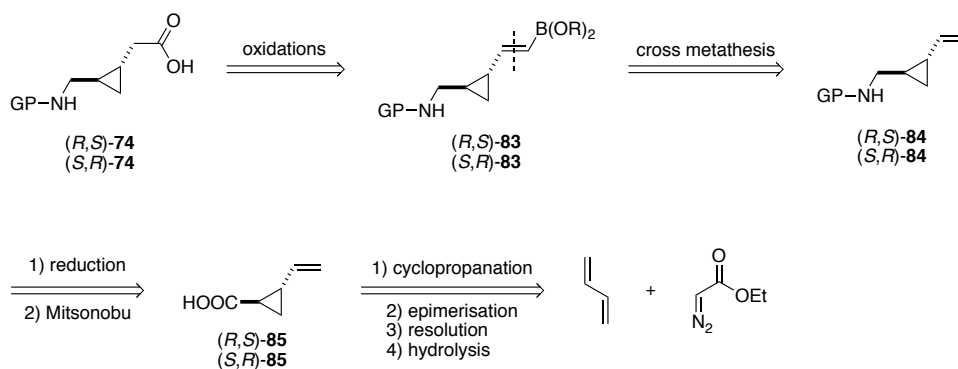
Peptide coupling using EDCI and DMAP was performed to give the amide (±)-**81** in 65% yield. Cleavage of phthalimide protecting group was attempted using hydrazine but this

reaction did not succeed. Consequently, the Boc group was chosen for *N*-protection in the revised route because the removal of this group does not require harsh conditions.

2.3. Boc-{GlyΔGly}-OH Synthesis

2.3.1. Retrosynthetic Analysis

An optimised route towards the *trans*-PGN-{GlyΔGly}-OH was designed and the functionalised cyclopropane was constructed first so that cyclopropanation of a more complex alkene substrate was avoided. Diastereoselective cyclopropanation of butadiene has been well described and various methods are available to accomplish this reaction, so this was an attractive starting point for synthetic work.^{127,128,129,130}

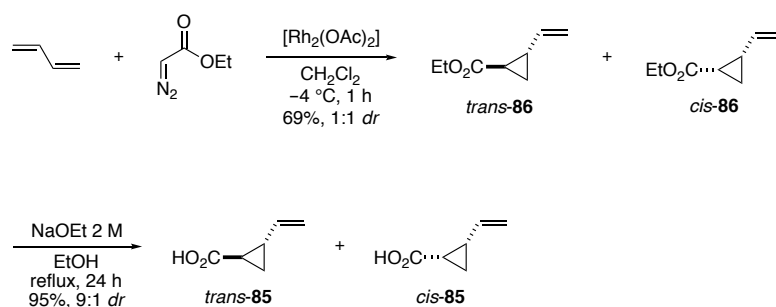


Scheme 16: Retrosynthesis

Preliminary retrosynthetic analysis suggested that PGN-{GlyΔGly}-OH **74** could be obtained from the boronate ester **83** by successive oxidation reactions (scheme 16).¹³¹ The boronate ester **83** could be installed by performing a cross metathesis reaction on the terminal alkene **84**,¹³² which possesses a protected amine functionality. The amine could be introduced by reduction of the carboxylic acid **85** to the corresponding alcohol, followed by a Mitsunobu substitution reaction with a suitable *N*-nucleophile. The carboxylic acid **85** could be obtained by cyclopropanation of butadiene using diazoester to yield a mixture of *cis*- and *trans*-cyclopropanes. It was anticipated that a reaction epimerisation would be used in order to obtain mainly the *trans*-isomer and subsequent resolution of the racemic carboxylic acid using a chiral amine would deliver two separable diastereoisomers, which would then be hydrolysed to give sufficient quantities of the enantioenriched compounds.

2.3.2. Towards the Synthesis of 2-Ethenyl-cyclopropanemethanol Precursor for N-terminus Installation

The first challenge was the synthesis of *trans*-cyclopropane motif with high distereoselectivity (scheme 17). It is known that it is difficult to achieve high levels of diastereocontrol when metal carbenes bearing chiral non-racemic ligands are used to promote the reaction of diazo compounds with disubstituted alkenes.¹³³ Consequently, the decision was made to use Rh₂(OAc)₄ as catalyst for the cyclopropanation reaction and then epimerise the resulting mixture of cyclopropanes to give the more stable *trans*-isomer as describe in literature.¹³⁴



Scheme 17: Synthesis of 2-ethenylcyclopropane-1-carboxylic acid **85**

The synthesis of cyclopropane **86** was performed by reaction of ethyldiazoacetate with butadiene under Rh₂(OAc)₄ catalysis. When ethyldiazoacetate was added too quickly, diethyl fumarate and maleate were obtained as side-products due to dimerization of the diazoester. Indeed, the reaction of dimerization of the diazoester is faster than the cyclopropane formation. Therefore, optimisation of the reaction conditions was undertaken to avoid the formation of these by-products (Table 9).

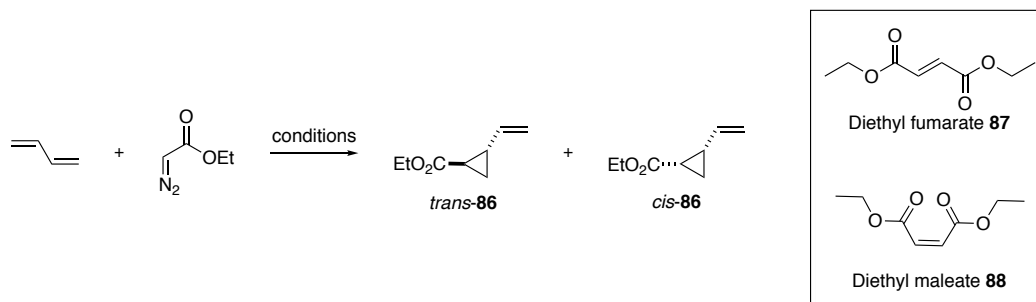


Table 9: Optimisation of the cyclopropanation reaction of butadiene

Entry	Butadiene in CH ₂ Cl ₂ (M)	Ethyldiazoacetate in CH ₂ Cl ₂ (M)	Addition rate (mL.h ⁻¹)	Reaction time	86:87–88 ratio ^a	<i>trans</i> : <i>cis</i> ratio ^a
1	11.4	neat	14	4 h	0:1	-
2	10.5	neat	7	4 h	1:1	1:1
3	10.5	1.75	10	2 h	2.5:1	1:1
4	10.5	1.75	8	1 h	1:0	1:1

^aDetermined by ¹H NMR

In the first experiment, neat ethyldiazoacetate was added at a rate of 14 mL/h (Table 9, entry 1), but in this case only diethyl fumarate **87** and maleate **88** were isolated. When the reaction mixture was diluted slightly and the rate of addition was reduced to 7 mL/h (Table 9, entry 2), a ratio 1:1 of side-products to products was obtained. The isomers were differentiated by NMR by measuring the coupling constant on the CH of the cyclopropane. Separation of the isomers by column chromatography was attempted but both compounds and side-products eluted together so attempts were made to further optimise the reaction. Ethyldiazoacetate addition rate and concentration seemed to be the main issue so it was added as solution in CH₂Cl₂ (Table 9, entries 3 and 4). The best result was obtained with the slowest flow rate (Table 9, entry 4) and in this case only the cyclopropanes were obtained in good yield (69%, 1:1 *dr*). The next objective was to perform base-mediated epimerisation of the diastereomeric mixture to obtain a *trans*-cyclopropane (Table 10).

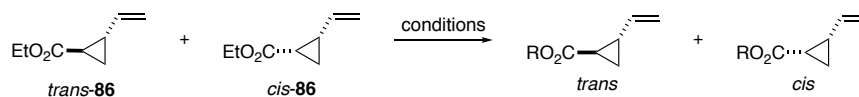
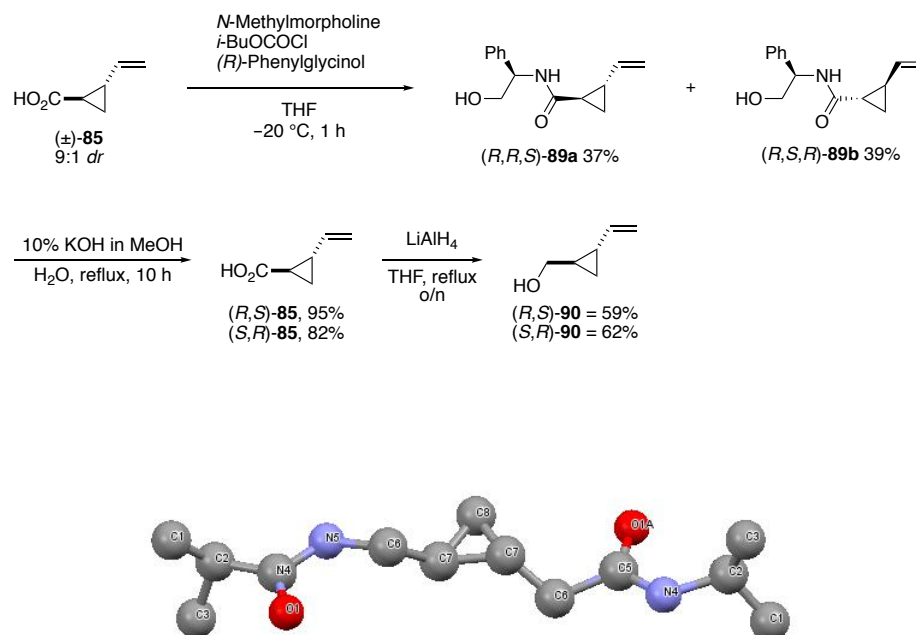


Table 10: Epimerisation Optimisation

Entry	Base	Time (days)	Product	<i>trans:cis</i> ^a
1	NaOEt <i>in situ</i> (from NaH and EtOH)	1	R = OEt, 86	3:7
2	DBU	6	R = OEt, 86	3:2
3	NaOEt <i>in situ</i> (from NaH and EtOH)	4	R = OH, 85	3:2
4	NaOEt 2 M (from Sigma Aldrich)	7	R = OEt, 86	3:2
5	NaOEt <i>in situ</i> (From Na solid and EtOH)	1	R = OH, 85 , 95%	9:1

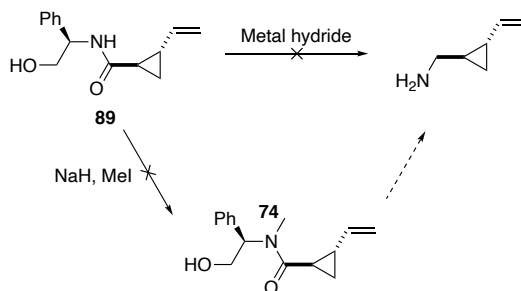
^a Determined by NMR

DBU is commonly used as a base for epimerisation,¹³⁵ but the observed ratio of 3:2 did not improve after 6 days (Table 10, entry 2). Sodium ethoxide (NaOEt) is also a common based used for epimerisation and EtOH has a similar pKa to that of *t*-BuOH. NaOEt can be generated *in situ* or used as a commercially available solution. When it was generated *in situ* from NaH and ethanol (Table 10, entries 1 and 3), slow epimerisation occurred after a day and a ratio 3:7 of isomers was obtained which favoured the *cis* isomer. After a longer time of reaction (4 days) the *trans:cis* ratio was improved to 3:2 and an acidic work up gave the corresponding carboxylic acid instead of the ester, which obviated subsequent ester hydrolysis. This was contrasted with the case in which commercially available solution of NaOEt was used (Table 10, entry 4).¹³⁴ However, the ratio observed after seven days was no better than that which had been obtained previously. When NaOEt was formed *in situ* using sodium metal dissolved in EtOH (Table 10, entry 5), epimerisation and hydrolysis occurred with an acidic work-up to give the carboxylic acid with a 9:1 *dr* and in 95% yield after only one day. Freshly prepared NaOEt was essential for the epimerisation to occur rapidly and the source of sodium was essential for *in situ* generation to produce good quality reagent. At this stage of the synthesis it was impossible to establish the configuration on the cyclopropane, the compound being an oil and the cyclopropyl hydrogens overlapping on the NMR spectrum, no data could be collected towards the obtention of the *trans* compound. However, crystal structure could be obtained from racemic peptide **75** synthesised later (Scheme 18). It was clear that this peptide synthesised from the cyclopropanation using carbene chemistry described earlier was *trans*. As no epimerisation could occur along the route designed, it was possible to state that *trans*-cyclopropane was obtained and isolated.



Scheme 18: Resolution of carboxylic acid (±)-85 and hydrolysis of the resulting amide and X-ray crystal structure of peptide 75.

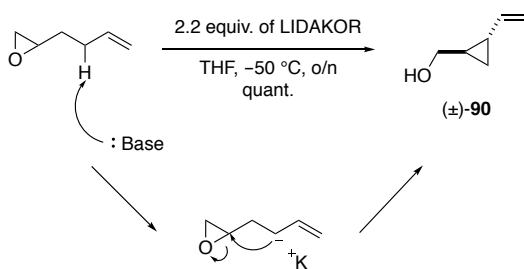
The diastereoenriched carboxylic acid **(±)-85** was now available in reasonable quantities and so separation of the enantiomers by formation of diastereoisomeric amides with (*R*)-phenylglycinol could be investigated (scheme 18).¹³⁶ The carboxylic acid was deprotonated with *N*-methylmorpholine and converted to its mixed anhydride using *i*-BuOCOCl. Nucleophilic attack of (*R*)-phenylglycinol on the activated electrophile gave the resulting amides **89**. The diastereoisomers were obtained in a 1:1 ratio and were easily separable by careful column chromatography. Once separated, the synthesis of the dipeptide mimic was pursued using both enantioenriched compounds in parallel. Hydrolysis of the amide using 10% KOH in MeOH afforded **(R,S)-85** and **(S,R)-85** in yields of 95% and 82% respectively. Acidic hydrolysis reactions using various concentrations of sulfuric acid were also attempted but only decomposition of the substrate was observed. Reduction of the carboxylic acid was performed using LiAlH₄ to give the primary alcohols **(R,S)-90** and **(S,R)-90** in good yield but the reaction solvent had to be removed carefully by distillation owing to the volatility of the products. Overall, enantioenriched alcohols **(R,S)-90** and **(S,R)-90** were synthesised in 5 steps in yields of 9% and 14% respectively.



Scheme 19: Amide reduction attempts

Attempts were made to reduce the amide **89a-b** directly to the corresponding primary amine in order to avoid the hydrolysis steps (Scheme 19). Various metal hydrides (LiAlH_4 , LiBH_4 , Red-Al) were tested in small scale reactions but they were unsuccessful. *N*-Alkylation of the amide was undertaken, in order to discover if tertiary amides would be more prone to reduction.¹³⁷ Unfortunately, attempts to alkylate the amide were ineffective and only the alcohol was alkylated. At this stage, this route was abandoned and alternative approaches were considered.

The difficulties in reproducing some of the steps in good yield combined with the low overall yield prompted the design of an alternative synthesis. The new route was designed to avoid low-yielding and unnecessary steps such as the epimerisation and resolution reactions. An attractive approach to the synthesis of the cyclopropane was evident from the work of Brandi and co-workers who has described a 3-*exo*-cyclisation of an allylic anion generated using the superbasic reagent LIDAKOR, (scheme 20).¹³⁸ The LIDAKOR base is generated from *n*-BuLi, diisopropylamine and potassium *tert*-butoxide and is similar to the Schlosser's base ($\text{BuLi}/t\text{-BuOK}$) except that diisopropylamine is added to the equimolar mixture. The presence of a dialkylamine makes the base less nucleophilic and in this case prevents elimination of the epoxide directly. This allows LIDAKOR to deprotonate the substrate at the α -position of the alkene. The resulting allylic anion undergoes a 3-*exo*-cyclisation with opening of the epoxide to give the thermodynamically stable *trans*-cyclopropane exclusively at low temperature.

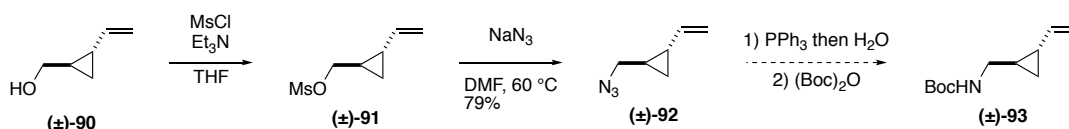


Scheme 20: LIDAKOR Cyclopropanation and mechanism

In this case, use of the previously reported reaction conditions gave the cyclopropane **90** in quantitative yield (Scheme 20). It was found that the reaction was amenable to scale-up (20 g) by use of very concentrated 11 M *n*-BuLi commercially available. Comparison with the NMR of enantioenriched alcohol **90** obtained via carbene chemistry allowed to identify that only the *trans* isomer was obtained.

2.3.3. N-Terminus Functionalisation

The aim was to convert alcohol **90** into the corresponding primary amine bearing an appropriate protecting group. The first approach was installation of the amine by use of a Staudinger reaction and subsequent Boc-protection (Scheme 21).



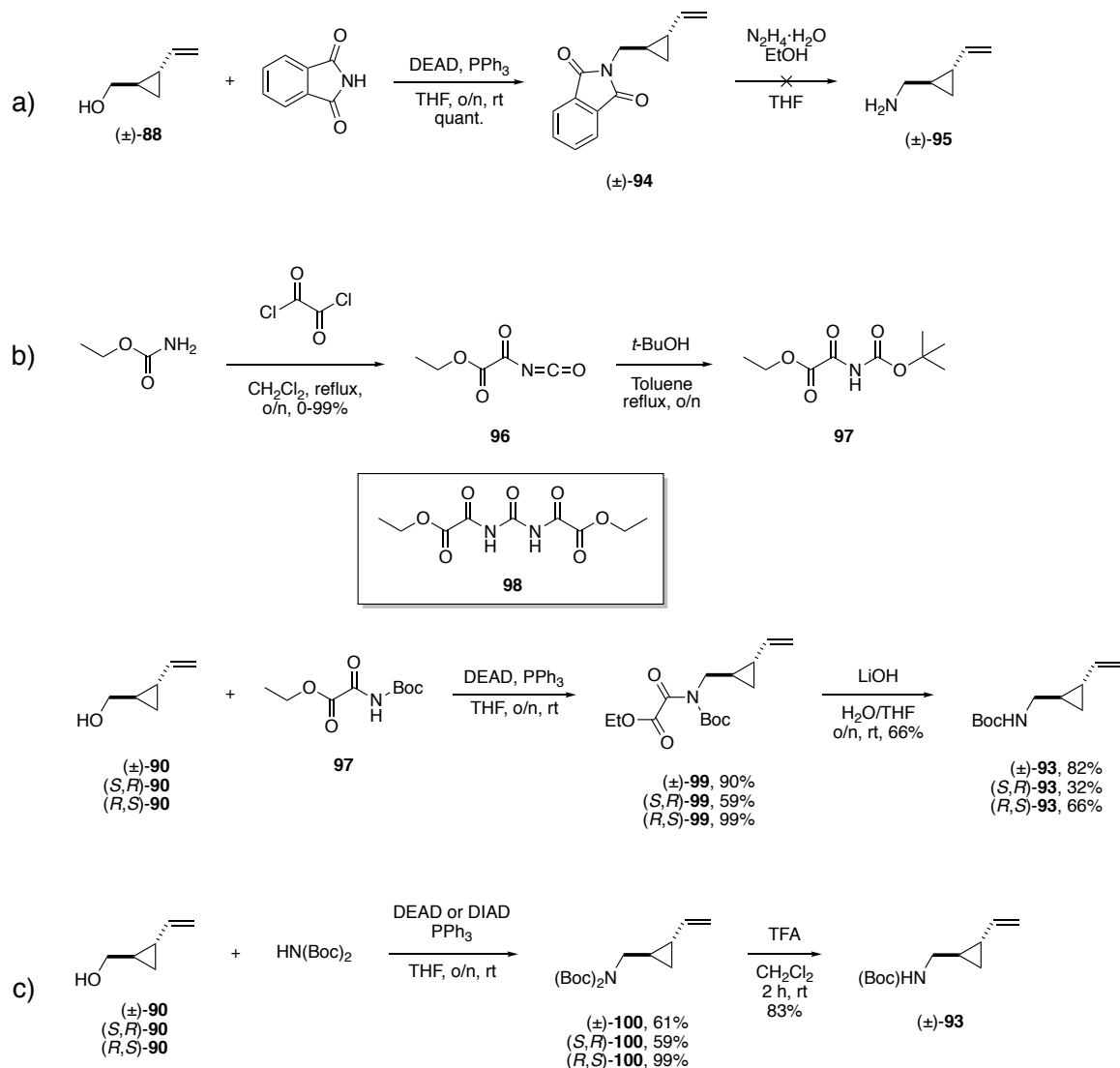
Scheme 21: Towards Staudinger reaction for amine installation

Elaboration of the alcohol **90** commenced with the activation of the alcohol to generate a good leaving group. Generation of a tosylate was attempted but the reaction led to decomposition of the starting material.¹³⁹ It was possible to prepare the mesylate **91** but it was unstable and had to be used immediately. Azide substitution using sodium azide was successful and the reaction delivered compound **92** in 79% yield over 2 steps.¹⁴⁰ Unfortunately, Staudinger conditions did not deliver the corresponding protected amine **93**. This method was not only unsuccessful but also considered to contain too many steps for efficient installation of the amine.

An alternative approach, in which the protected amine would be installed by a Mitsunobu reaction in a single step, was very attractive (Scheme 22). Reaction with phthalimide was explored first and previously described Mitsunobu conditions were employed, the required

compound **94** was obtained in quantitative yield (Scheme 22a).¹⁴¹ Conditions for phthalimide removal are known to be harsh and it proved very difficult to remove this group. It was impossible to remove the protecting group in good yield even when the imide **94** was heated at reflux in neat hydrazine; only starting material was recovered. The phthalimide cleavage reaction was attempted at later stages of the synthesis but was never successful.

Le Corre *et al.* has reported *N*-Boc ethyl oxamate to be compatible with Mitsunobu conditions because of its low NH pKa (pKa = 8.3 in H₂O, Scheme 22b).^{142,143,144} It seemed likely that this compound could serve as an *N*-nucleophile during a Mitsunobu reaction with the alcohol **90**. The synthesis of *N*-Boc ethyl oxamate **97** started from the commercially available ethyl oxamate, which was treated with oxalyl chloride to produce the isocyanate **96** in variable yields. Subsequent treatment of the product with 1.1 equivalents of *tert*-butanol led to **97**. However, the reaction to form the isocyanate was very difficult to reproduce and the main product in each case was the bis-oxalate **98** because of the highly reactive isocyanate reacting quickly with another isocyanate. Altering of several of the reaction parameters (scale, solvent, order and time of addition, temperature of reaction, concentration) did not improve matters. Even when reactions were performed under identical conditions and in parallel, varying amounts of products were observed by ¹³C NMR analysis. In spite of the poor reproducibility of the reaction, sufficient quantities of the isocyanate **96** were obtained over the course of this study (Scheme 22b). The Mitsunobu reaction with alcohol **90** afforded **99** in very good yield and the oxamate was cleaved by treatment with LiOH in H₂O/THF to afford the Boc protected compound **93** in a respectable yield.

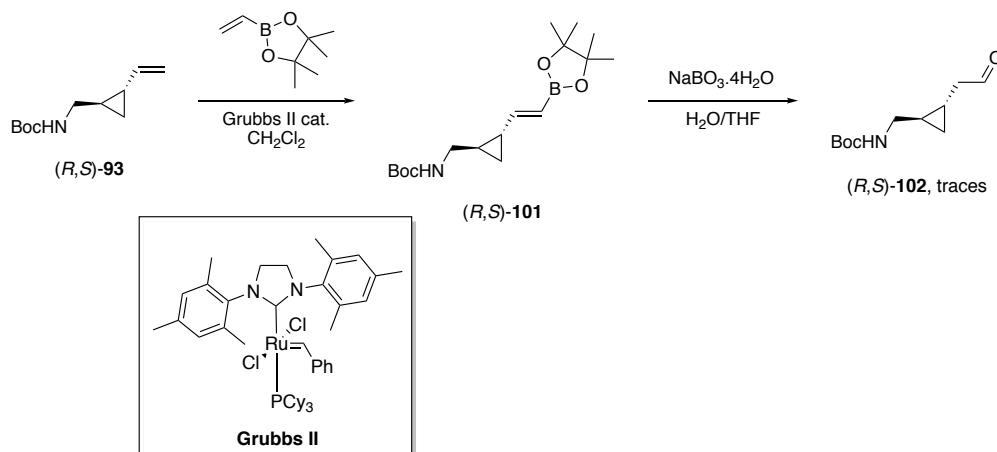


Scheme 22: Mitsunobu reaction

The synthesis of the oxamate nucleophile required for the Mitsunobu reaction was impractical so $\text{NH}(\text{Boc})_2$ was investigated as an alternative nucleophile (Scheme 22c). $\text{NH}(\text{Boc})_2$ is less acidic than the phthalimide or *N*-Boc ethyl oxamate but is still sufficiently acidic to participate in the Mitsunobu reaction.¹⁴⁵ The substitution reaction proceeded to give the bis protected amine **100** but in slightly lower yield than before owing to the higher pKa. As described previously,¹⁴⁶ mono-Boc removal was performed by treatment of the bis-carbamate **100** with 1.5 eq. of TFA to afford the mono-deprotected amine **93** in 83% yield after purification by column chromatography. Although, one Boc group could be cleaved efficiently, both Boc groups were retained at this stage because of efficiencies later in the synthesis.

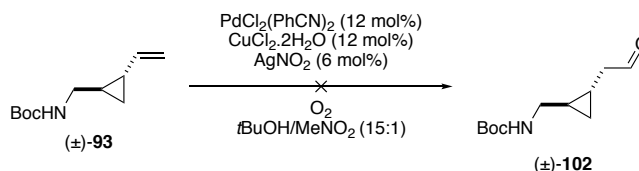
2.3.4. C-Terminus Installation

Cross metathesis between terminal alkene and vinylboronate and subsequent oxidation is known to be an efficient method for the generation of aldehydes from terminal alkenes. Frey *et al.* have also demonstrated that it is possible to perform cross metathesis reactions on cyclopropane-containing substrates.¹⁴⁷ The cross metathesis reaction was applied to the alkene **93** (Scheme 23).



Scheme 23: Cross metathesis using vinyl boronic pinacolic ester

The substrate was treated with the pinacol vinylboronate as the cross metathesis partner in presence of 5 mol% of Grubbs II catalyst. However, little conversion was observed over the course of two days and the product **101** degraded rapidly on column chromatography. Only traces of the desired aldehyde **102** were obtained when oxidation was performed on the crude reaction mixture using sodium perborate.¹⁴⁸ A potential alternative way to obtain the required aldehyde **102** from alkene **93** with anti-Markovnikov selective Wacker oxidation (Scheme 24).¹⁴⁹



Scheme 24: Selective Wacker oxidation

The alkene **93** was subjected to Wacker oxidation under a flow of oxygen overnight. However, only traces of aldehyde were detected by NMR analysis of the crude reaction mixture and so another approach had to be adopted. The third option was to introduce the

carboxylic acid by hydroboration of the alkene and then oxidation of the resulting alcohol (Table 11).¹⁵⁰

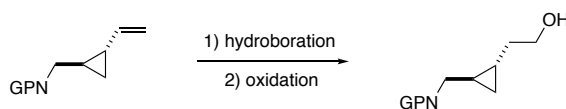


Table 11: Hydroboration optimisation

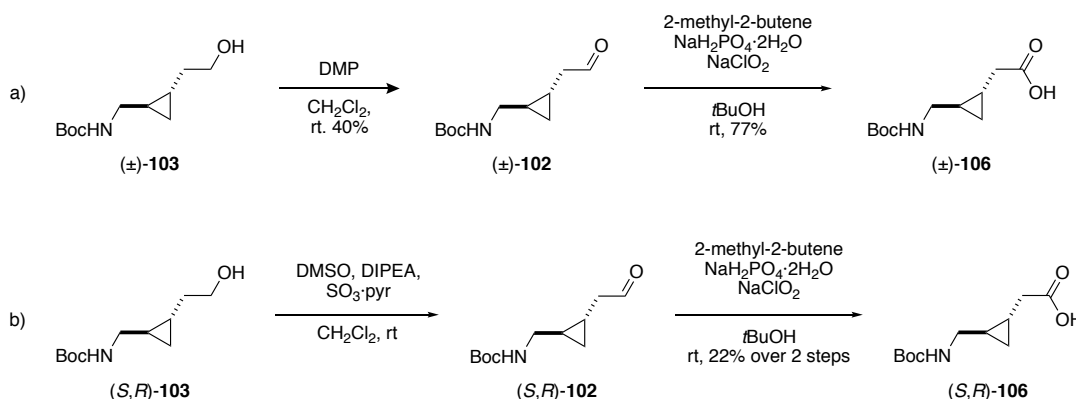
Entry	SM	NPG	Borane source	Oxidising agent	Product, Yield
1	(±)- 93	NHBoc	9-BBN (2 equiv.)	NaOH/H ₂ O ₂	103 , SM recovered ^a
2	(<i>R,S</i>)- 93	NHBoc	9-BBN (3 equiv.)	NaBO ₃ ·4H ₂ O	103 , 35% SM recovered ^a
3	(<i>R,S</i>)- 93	NHBoc	BH ₃ ·THF	NaBO ₃ ·4H ₂ O pH7 buffer	103 , 63%
4	(±)- 93	NHBoc	BH ₃ ·THF	NaBO ₃ ·4H ₂ O pH7 buffer	103 , Quant.
5	(<i>S,R</i>)- 93	NHBoc	BH ₃ ·THF	NaBO ₃ ·4H ₂ O pH7 buffer	103 , 61%
6	(±)- 94	Phth	BH ₃ ·THF	NaBO ₃ ·4H ₂ O pH7 buffer	104 , 80%
7	(±)- 100	N(Boc) ₂	BH ₃ ·THF	NaBO ₃ ·4H ₂ O pH7 buffer	105 , 97%
8	(<i>R,S</i>)- 100	N(Boc) ₂	BH ₃ ·THF	NaBO ₃ ·4H ₂ O pH7 buffer	105 , 91%
9	(<i>S,R</i>)- 100	N(Boc) ₂	BH ₃ ·THF	NaBO ₃ ·4H ₂ O pH7 buffer	105 , 91%

^aDetermined by NMR

When hydroboration was performed by treatment of the alkene with two equivalents of 9-BBN and oxidation of the resulting borane with hydrogen peroxide (Table 11, entry 1),¹⁵¹ poor conversion of the starting material was observed. The reaction was repeated with a larger excess of 9-BBN and sodium perborate as oxidant, but once again the required alcohol was not produced and some decomposition had occurred (Table 11, entry 2).¹⁵² The borane source was then replaced by 1 M borane tetrahydrofuran complex solution and oxidation was performed with sodium perborate at pH 7 (phosphate buffer).¹⁵³ This method proved to be very efficient and a good yield of the alcohol was obtained which was of sufficient purity that it could be used in the next step without any purification. These conditions were then applied on the various protected amines used in the course of the project (Table 11, entries 4 to 9) to give primary alcohols **103-105**.

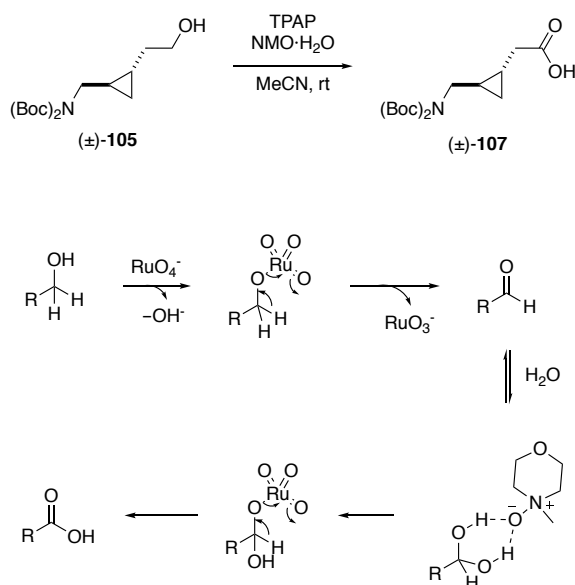
The next step was oxidation of the primary alcohol **103** to give the C-terminal carboxylic acid **106** (Scheme 25). In a two-step process, DMP oxidation gave a poor yield and purification of the aldehyde by column chromatography resulted in degradation of the product (Scheme 25a). Pinnick oxidation afforded the Boc-protected amino acid **106** in 77% yield (31% over two steps). Oxidation of the alcohol **103** under Parikh-Doering conditions

gave only a trace amount of aldehyde after purification.¹⁵⁴ When aldehyde **102** was not isolated but instead submitted directly to the subsequent Pinnick oxidation reaction, the carboxylic acid **106** was obtained in 22% yield over two steps (Scheme 25b).¹⁵⁵



Scheme 25: Two-step oxidation of the alcohol 103 to access to the carboxylic acid 106

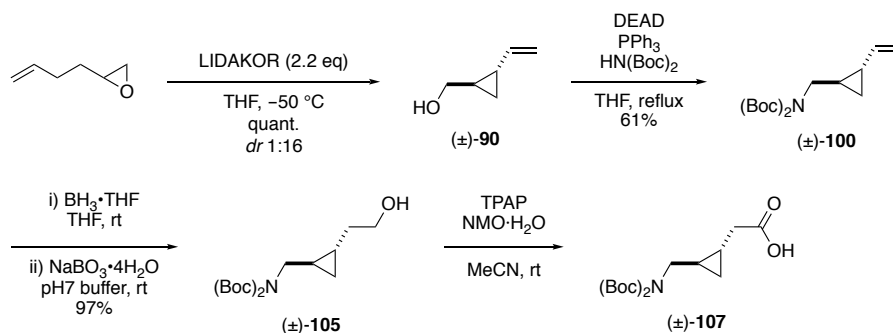
TPAP oxidation is commonly used to oxidise primary alcohols to give aldehydes and, in this case, dry NMO is usually used as the stoichiometric oxidant. In this case, hydrated NMO was used as the oxidant to stabilise the resultant aldehyde by forming a 6-membered ring (Scheme 26), which activates the aldehyde to further oxidation to the carboxylic acid. NMO plays a dual role in this reaction: as a Lewis-base to stabilise the aldehyde hydrate and as a co-oxidant to recycle the catalyst.¹⁵⁶ This single-step oxidation of the alcohol **106** to give the carboxylic acid **107** was performed to avoid dealing with sensitive intermediate aldehyde **102**.¹⁵⁷



Scheme 26: TPAP Oxidation and its mechanism

Slow and controlled addition of TPAP was necessary because of the exothermic character of the reaction, especially when working on big scale. After optimisation, an addition rate of 20 mg/20 min resulted in the the best conversion. Carboxylic acid **107** was unstable and decomposed during chromatographic purification, so the product was used immediately for the next step without purification.

In summary, the Gly-Gly surrogate was synthesised in good yield and on multigram scale by a route that involved sequential super-base-mediated rearrangement of 1,2-epoxy-5-hexene, Mitsunobu, hydroboration and oxidation (Scheme 27). The key cyclopropane peptide mimic (±)-Boc₂-{GlyΔGly}-OH **106** was now available for incorporation into various peptides to give hybrid compounds

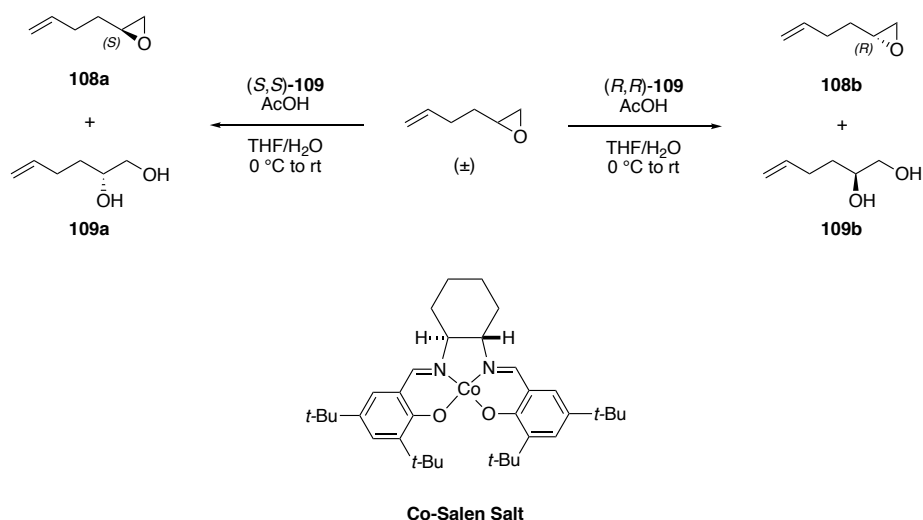


Scheme 27: Synthesis of the racemic mixture of (±)-Boc₂-GlyΔGly-OH 107

2.4. Synthesis of Single Enantiomer Mimics by Resolution of Racemic Intermediates

2.4.1. Early Stage Resolution

Now that an efficient route to racemic Boc₂-{GlyΔGly}-OH **107** had been developed, the next challenge was to find the optimal method to resolve the enantiomers. The resolution of epoxides to provide enantioenriched building blocks is a well-established strategy in organic chemistry,^{158,159} and so it seemed likely that the terminal epoxide starting material could be resolved and each enantiomer could be taken through the whole synthesis separately with the main challenge being chirality transfer during the LIDAKOR-mediated rearrangement reaction. The kinetic resolution procedure developed by Jacobsen was selected because it has been used on similar substrates to generate an enantiopure epoxide and an enantiopure diol (Scheme 28).

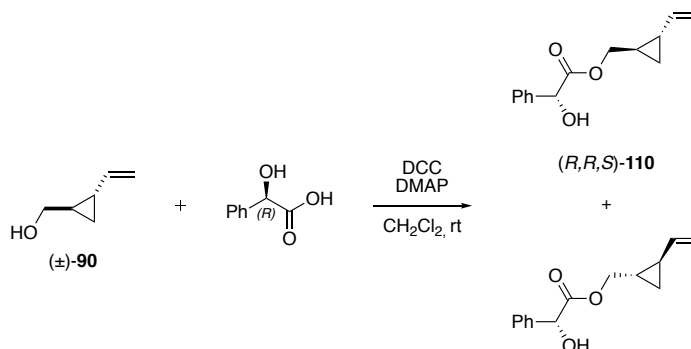


Scheme 28: Jacobsen resolution

The epoxide was subjected to resolution with both (*S,S*)- and (*R,R*)-Co-salen catalyst in parallel. After a reaction time of 8 h, the NMR analysis showed that a mixture of epoxide **108** and diol **109** had been generated in a 2:1 ratio when either enantiomer of the catalyst was used. Unfortunately, the epoxide was difficult to handle due to its volatility and separation of the epoxide from the diol could only be achieved by column chromatography (100% EtOAc) because distillation was unsuccessful on both a small and large scale. The epoxide could not be obtained without traces of water, which was an issue for the LIDAKOR reaction, and so this approach was abandoned.

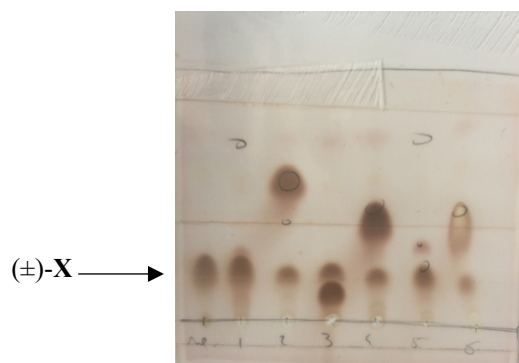
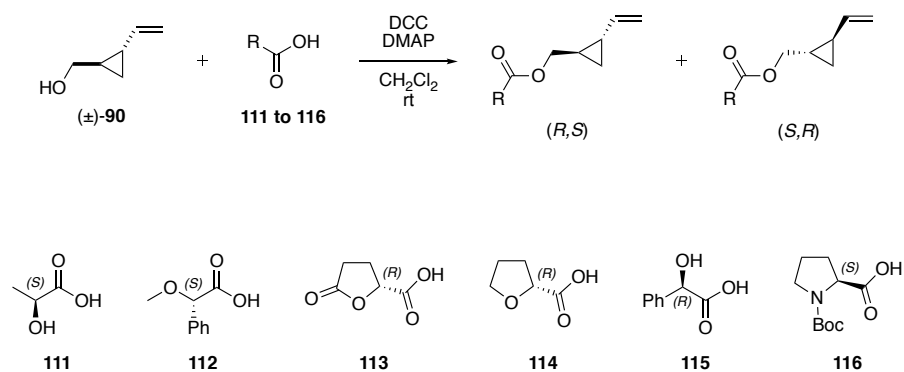
2.4.2. Alcohol Resolution by Steglich Esterification

Another method to resolve racemic intermediates was investigated. The Steglich esterification reaction is often used to resolve alcohols into diastereoisomeric esters with chiral acids and coupling agents.^{160,161} Alcohol **90** was subjected to Steglich esterification using enantiomerically pure (*R*)-mandelic acid to produce diastereomeric esters (Scheme 29).



Scheme 29: Steglich esterification on alcohol 90

The esterification reaction was performed at room temperature overnight but several products were obtained following purification of the crude product by column chromatography. The small amount of the required ester that was obtained suggested that separation of the diastereomers would be difficult and so various chiral acids were explored as resolving agents (Scheme 30).



Scheme 30: Resolution optimisation on alcohol **88 by Steglich esterification and TLC of the scope**

Six chiral carboxylic acids (**111** to **116**) were used for the resolution reaction. Unfortunately, as shown by TLC, the starting material (alcohol **90**) was still present in all reactions after heating overnight at reflux and there was little conversion. Furthermore, only one other spot was visible in all of the reactions. HPLC analysis of one of the reactions (that performed with acid **114**) showed both diastereoisomeric esters had been formed but they were inseparable by chromatography. Altering TLC eluent (PET/EtOAc 1:1, 6:1, 6:2, 8:2, 1:2) did not make any difference to the separation.

2.4.3. Amide Coupling Resolution on Protected Amine

Resolution of the racemate by ester formation was unsuccessful and so attention was turned to the formation of diastereoisomeric amides because these had been successful earlier (Table 12).

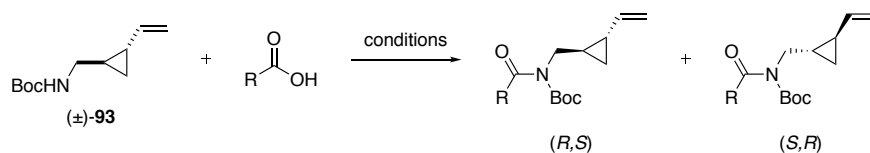


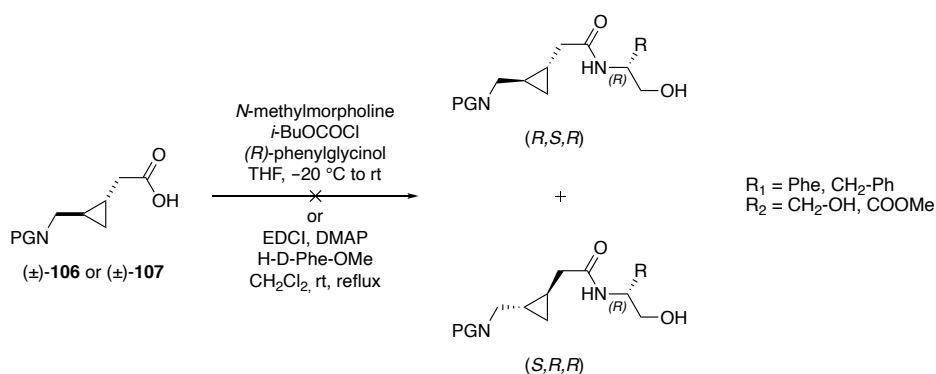
Table 12: resolution of 93 by amide coupling

Entry	Chiral acid	Conditions	Results
1	(<i>R</i>)-mandelic acid 	<i>N</i> -methylmorpholine <i>i</i> -BuOCOC1	decomposition
2	(<i>S</i>)-(+)- <i>α</i> -methoxyphenyl acetic acid 	<i>N</i> -methylmorpholine <i>i</i> -BuOCOC1	decomposition
3	(<i>R</i>)-mandelic acid 	HOBt, EDCI, DIPEA	no conversion
4	(<i>S</i>)-(+)- <i>α</i> -methoxyphenyl acetic acid 	HOBt, EDCI, DIPEA	no conversion

The mixed anhydride method used for the resolution of carboxylic acid **85** was performed on **93** using *N*-methylmorpholine and *i*-BuOCOC1.¹³⁶ This method led to decomposition of the product (Table 12, entries 1 and 2). Amide formation mediated by HOBt and EDCI was attempted because these reagents are known to give efficient formation of tertiary amides.¹⁶² Attempts to form an amide with either (*R*)-mandelic acid or (*S*)-(+)-*α*-methoxyphenyl acetic acid (Table 12, entries 3 and 4) did not result any conversion of the starting material into the required products. At this stage, resolution of the initial epoxide, the alcohol **90**, and the protected amine **93** had failed and so attention was turned to resolution of (±)-BocH-{GlyΔGly}-OH.

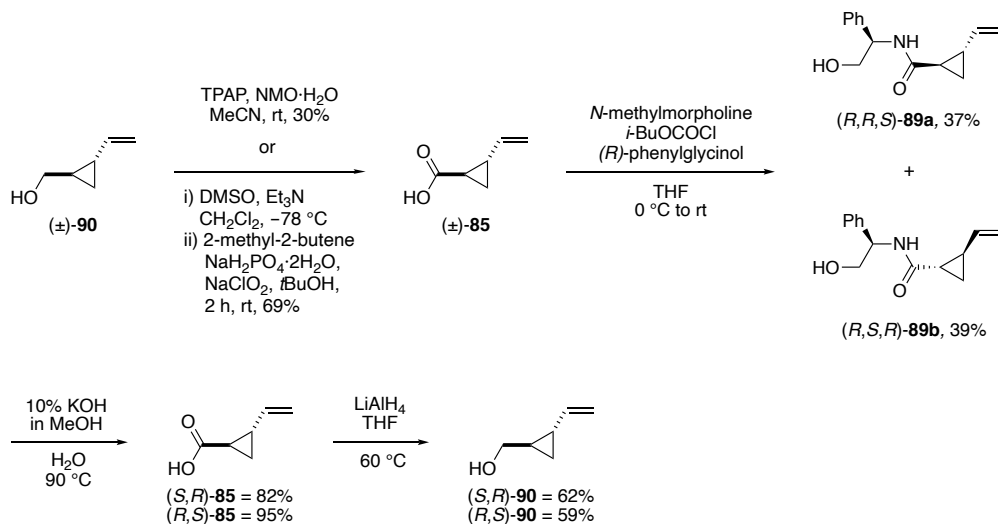
2.4.4. Resolution of Carboxylic Acid Intermediates

Instead of using the amine to form an amide suitable for resolution, the carboxylic acid on C-terminus of final dipeptide mimetic was considered as a site for diastereomer formation. Under the same procedure as before, mono protected (\pm)-Boc- $\{\text{Gly}\Delta\text{Gly}\}$ -OH **106** or bis protected (\pm)-Boc₂- $\{\text{Gly}\Delta\text{Gly}\}$ -OH **107** were treated with *N*-methylmorpholine, *i*-BuOCOC₂H₅ and (*R*)-phenylglycinol. After a reaction time of several hours, there was no evidence that amide coupling had occurred (scheme 31).



Scheme 31: Resolution on final dipeptide mimic

Next, resolution was attempted by coupling of a carboxylic acid intermediate with a chiral amino acid by use of common amide coupling procedures (EDCI, DMAP, Scheme 31). As previously discussed, the amide obtained after purification was subjected to HPLC analysis and was found to be a mixture of diastereoisomers. Finally, attention was reverted to the previously successful method (cf. Scheme 18). To explore this method, it was necessary to oxidise the alcohol **90** to produce the carboxylic acid **85** (Scheme 32).

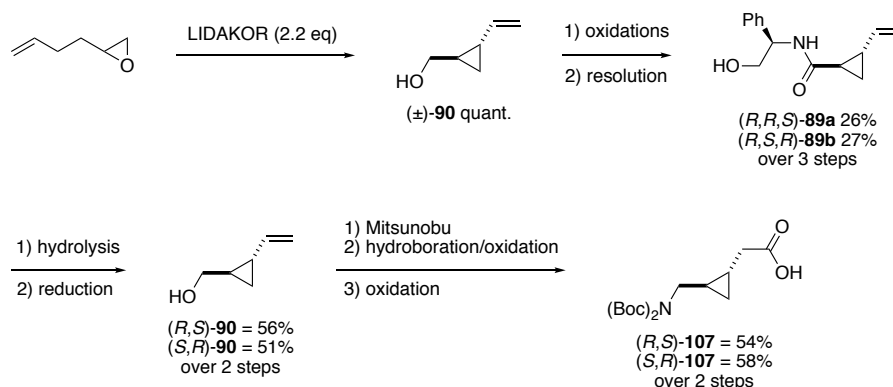


Scheme 32: Resolution of enantioenriched alcohol 90 at an early stage in the synthesis

The alcohol $(\pm)\text{-90}$ was submitted to a TPAP oxidation in the presence of water in order to obtain the corresponding carboxylic acid $(\pm)\text{-85}$ directly. Addition of 20 mg/20 min of TPAP was required to control the exothermic character of the reaction and so the procedure was time consuming on large scale. It was found that Swern oxidation followed by a Pinnick oxidation was more practical on larger scale (≥ 20 mmol of alcohol).¹⁶³ The carboxylic acid $(\pm)\text{-85}$ was obtained by use of these two methods in yields of 30% and 69%, respectively. The racemate reacted with (R) -phenylglycinol as chiral agent to produce two diastereoisomers $(R,R,S)\text{-89a}$ and $(R,S,R)\text{-89b}$ that were separable by column chromatography. Absolute configuration was determined as in the initial route by their $[\alpha]_D$. Each diastereomer was then hydrolysed to yield the enantioenriched carboxylic acids $(R,S)\text{-85}$ and $(S,R)\text{-85}$. The enantioenriched carboxylic acids were then reduced using LiAlH_4 to provide the alcohols $(R,S)\text{-90}$ and $(S,R)\text{-90}$ in 14% yield over 4 steps.

2.4.5. Summary

The initial route designed started with a cyclopropanation using carbene, a mixture of diastereoisomer was obtained (*cis/trans* ratio 1:1) and required epimerisation followed by resolution to get only the *trans* enantioenriched cyclopropane which was considered to be too many steps. The challenge of the cyclopropanation reaction was overcome by using a superbase-mediated rearrangement reaction to produce the racemic *trans*-cyclopropane **90** in a very good yield. Resolution of the racemic mixture at various stages of the synthesis was attempted and the best method was found to be the amide coupling of the acid **85**, obtained by two-stage oxidation of the alcohol **90**, to (*R*)-phenylglycinol as described in the initial route. The diastereoisomeric amide were easily separable by column chromatography and were obtained in reasonable yields (scheme 33).



Scheme 33: Summary of the synthesis of the enantioenriched dipeptide

Synthesis of the enantioenriched carboxylic acids allowed the dipeptide mimics **107** to be achieved in 5 steps by sequential Mitsunobu reaction to install the bis-protected N-terminus, optimised hydroboration and subsequent oxidations at the C-terminus. This new route was designed and optimised to reduce the number of steps and improve the overall yield from 1% to 8%. The enantioenriched mimic $\text{Boc}_2\text{-}\{\text{Gly}\Delta\text{Gly}\}\text{-OH}$ **107** was obtained in 8 steps (9 in the initial route).

2.5. Synthesis of Model Peptides Containing the Dipeptide Mimic

2.5.1. Capped Dipeptide Synthesis

In order to investigate the formation and extent of intramolecular hydrogen bonds within cyclopropane-containing peptide hybrids, two molecules were designed (Figure 38). The targets selected were analogues of the peptides used by Gellman *et al.* to demonstrate the formation of intramolecular hydrogen bonds in systems where the peptide bond has been replaced by an alkene (cf. section 1.6.1.2, Scheme 1).

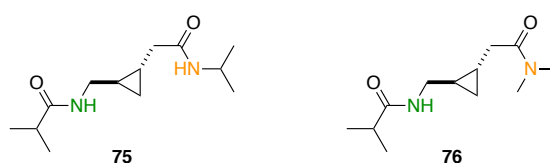
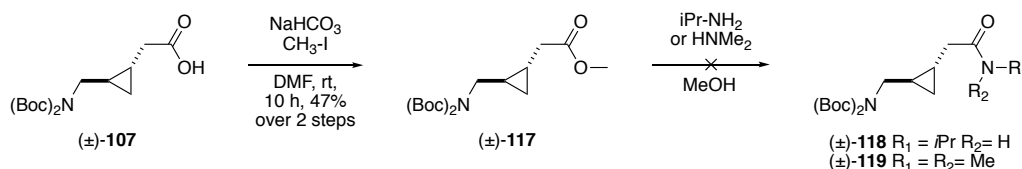


Figure 38: Dipeptide mimics

β -Turns are stabilised by a 10-membered hydrogen bonded ring (cf Figure 13); and so the systems were designed to explore formation of this type of hydrogen bond. The peptide **75** contains two amide bonds that are able to form hydrogen bonds (Gly-NH and NH-*i*-Pr). In contrast, the peptide **76** is capped with a dimethylamino group at the C-terminus to removal hydrogen bond donor capability at this position and allow only one hydrogen bond to be formed.

Unfortunately, the polar Boc₂-{Gly Δ Gly}-OH dipeptides decomposed during purification due to the presence of a free carboxylic acid and the corresponding methyl ester **117** was prepared to enable purification (Scheme 34).¹⁶⁴



Scheme 34: Methyl ester formation and attempted amide synthesis

The ester **117** was prepared by treatment of the carboxylic acid (±)-**107** with sodium bicarbonate and iodomethane in solution at reflux. The reaction was performed overnight and methyl ester was obtained after column chromatography in 47% yield over two steps.

Attempts to perform amide formation directly by treatment of the ester **117** with isopropylamine were unsuccessful.¹⁶⁵ Consequently, the carboxylic acid **106** was used in subsequent coupling without purification to avoid problems encountered during chromatography.

The peptide coupling reaction of crude Boc₂-{GlyΔGly}-OH **107** with isopropylamine and dimethylamine was investigated under a variety of conditions (Table 13).

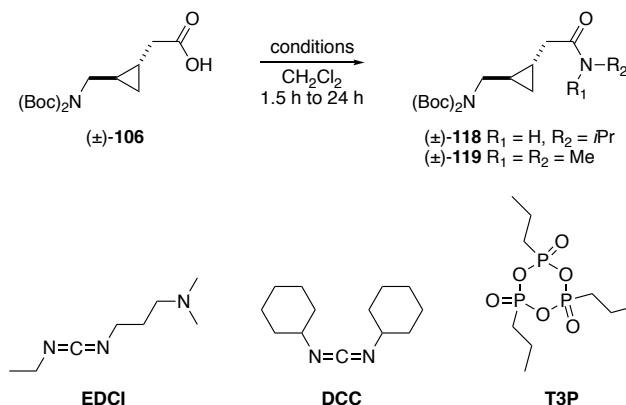


Table 13: First amide coupling optimisation

Entry	Amine	Coupling agent	Base	Product	Yield
1	HNMe ₂ ^(a)	DCC	HOSu	(±)- 119	— ^(b)
2	<i>i</i> PrNH ₂	DCC	HOSu	(±)- 118	— ^(b)
3	<i>i</i> PrNH ₂	EDCI	DMAP	(±)- 118	31%
4	HNMe ₂ ^(a)	T3P	Et ₃ N	(±)- 119	33%
5	HNMe ₂ ^(a)	T3P	Et ₃ N	(±)- 119	37%
6	<i>i</i> PrNH ₂	T3P	Et ₃ N	(±)- 118	46%

^(a) 2 M in THF

^(b) hard purification, impure after column chromatography

Initially, DCC coupling agent was used in presence of hydroxysuccinimide (HOSu) as an additive in order to avoid side reactions.^{166,167} However, reaction of the carboxylic acid **107** with dimethylamine or isopropylamine in THF (Table 13, entries 1 and 2) afforded coupled product that was contaminated with undetermined impurities and HOSu. When EDCI was used in combination with DMAP (Table 13, entry 3), the formation of water-soluble by-products facilitated purification of the product. Unfortunately, a low yield of the coupled product **118** was obtained and so the use of T3P (propylphosphonic anhydride) instead of a carbodiimide was explored (Table 13 entries 4,5 and 6).¹⁶⁸ The yield was improved when the coupling reaction was performed with dimethylamine over a longer reaction period. The amides **118** and **119** were produced in a satisfactory yield and sufficient pure material was

obtained for the next coupling reaction. These conditions were used for the synthesis of all N-terminus amide (Table 14, T3P coupling).

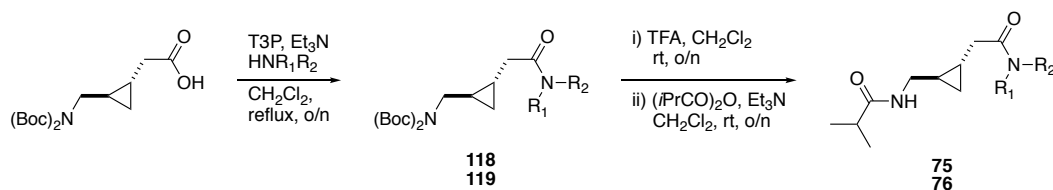


Table 14: summary of dipeptide synthesis

Entry	Isomer	R ₁ , R ₂	T3P coupling yield	Final product, yield
1	(±)	R ₁ = H, R ₂ = <i>i</i> Pr	(±)- 118 , 46%	(±)- 75 , 69%
2	(<i>S,R</i>)	R ₁ = H, R ₂ = <i>i</i> Pr	(<i>S,R</i>)- 118 , 52%	(<i>S,R</i>)- 75 , 17%
3	(<i>R,S</i>)	R ₁ = H, R ₂ = <i>i</i> Pr	(<i>R,S</i>)- 118 , 35%	(<i>R,S</i>)- 75 , 31%
4	(±)	R ₁ = R ₂ = Me	(±)- 119 , 37%	(±)- 76 , 7%
5	(<i>S,R</i>)	R ₁ = R ₂ = Me	(<i>S,R</i>)- 119 , 48%	(<i>S,R</i>)- 76 , 65%
6	(<i>R,S</i>)	R ₁ = R ₂ = Me	(<i>R,S</i>)- 119 , 74%	(<i>R,S</i>)- 76 , 40%

N-Deprotection was performed using 10 equivalents of TFA to afford the free amine which was then treated (*i*PrO)₂O and trimethylamine to give the analogue of interest. The final capped dipeptide mimics were obtained in low to reasonable yield (from 7 to 69% over 2 steps), but sufficient material was produced to undertake the intended spectroscopic analyses. Racemic and enantiomerically enriched (both antipodes) samples of both peptides were synthesised and then used to explore hydrogen bond formation in the hybrid model turn mimics (Figure 39).

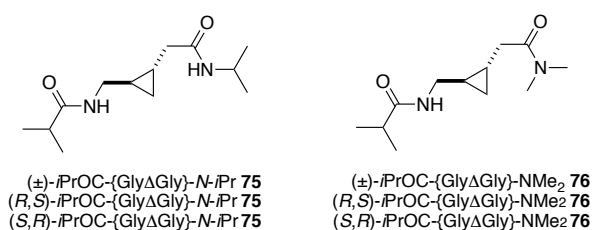
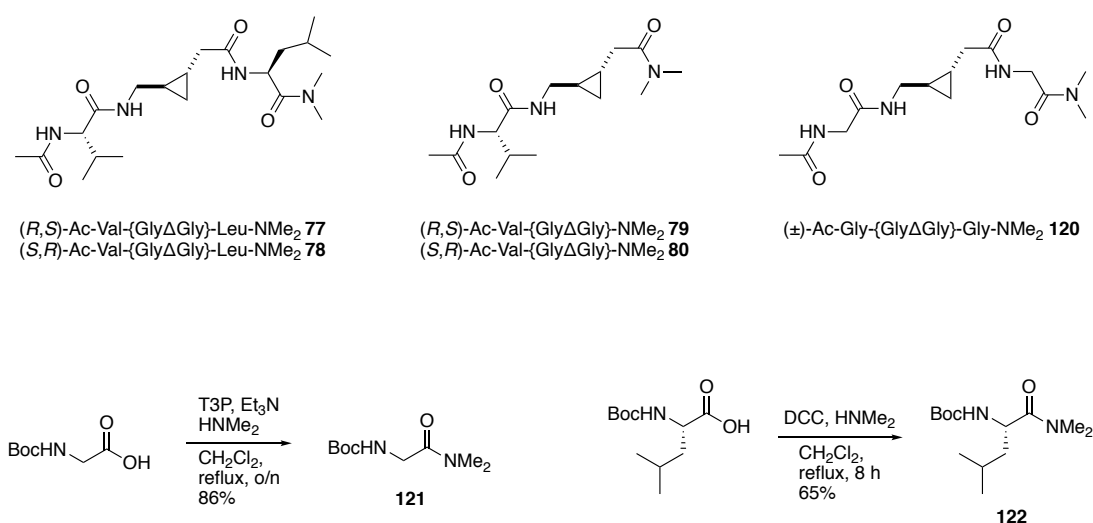


Figure 39: Dipeptide mimics

2.5.2. Synthesis of Tri- and Tetra-peptide Hybrids that Contain the Mimic

Longer peptides were synthesised in order to mimic the loop section of a β -hairpin, with the {Gly Δ Gly} surrogate mimicking the $i + 1$ and $i + 2$ turn residues and the two external residues (i and $i + 3$) playing the role of the strands. The influence of the lengths of the peptide and the addition of extra amide bonds on the stability of the conformation adopted by the hybrid was analysed and the contribution of the side chains was also studied.

To this end the hybrid peptides Ac-Val-{Gly Δ Gly}-Leu-NMe₂ **77** and **78** and Ac-Val-{Gly Δ Gly}-NMe₂ **79** and **80** were synthesised.⁵⁴ The principle was to study hydrogen bond formation and discover whether the analogues possessed the hydrogen bonding arrangement observed in the native dipeptide system. The more flexible analogue Ac-Gly-{Gly Δ Gly}-Gly-NMe₂ **120** was also synthesised and studied in order to understand how the side chains contribute to the folding process. The synthetic strategy adopted was similar to that used to prepare the simple dipeptides and amino acids were modified beforehand if needed (scheme 35).



Scheme 35: Tri- and tetra-peptides 77-80 and modified amino acid 121 and 122 synthesis

Boc-Gly-NMe₂ **121** was synthesised in 86% yield following the approach used to prepare the dipeptide mimics described previously and using T3P as the coupling reagent. Boc-Val-NMe₂ **122** was synthesised in a 65% yield by use of a DCC coupling reaction.¹⁶⁹

Two coupling reactions were performed on the C-terminus of Boc₂-{Gly Δ Gly}-OH **107** (Table 15). T3P was used for the first coupling reaction in all cases (Table 15, 1st coupling,

entries 1–6) and the corresponding C-terminal amide was obtained with variable yields (48–85%). The TFA mediated deprotection of the N-terminus proceeded without incident and the resulting crude amine was used directly in the second peptide coupling reaction, which was performed using the same coupling agent (Table 15, 2nd coupling, entry 1). The product **120** was found to be sensitive and further purification was performed by trituration using cold pentane twice after column chromatography.

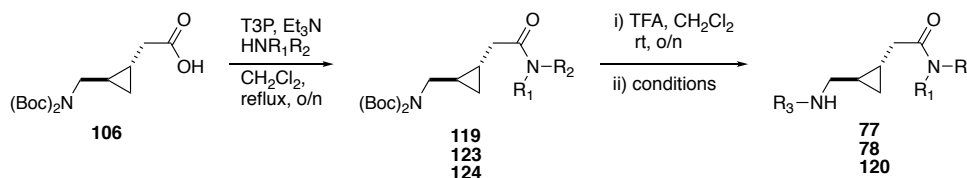


Table 15: Tri- and tetrapeptide synthesis

Entry	isomer	1 st coupling		2 nd coupling		
		Amine	Yield	Acid, coupling agent	Product	Yield ^(a)
1	(±)	Boc-Gly-NMe ₂ 123	63% ^(a)	Ac-Gly-OH, T3P	120	52%
2	(<i>S,R</i>)	R ₁ = R ₂ = Me 119	48%	Ac-Val-OH, T3P	80 ^(b)	– ^(b)
3	(<i>S,R</i>)	Boc-Leu-NMe ₂ 124	72% ^(a)	Ac-Val-OH, T3P	78 ^(b)	– ^(b)
4	(<i>S,R</i>)	R ₁ = R ₂ = Me 119	48%	Ac-Val-OH, HATU	80	12%
5	(<i>R,S</i>)	R ₁ = R ₂ = Me 119	74%	Ac-Val-OH, HATU	79	14%
6	(<i>S,R</i>)	Boc-Leu-NMe ₂ 124	72% ^(a)	Ac-Val-OH, HATU	78	76%
7	(<i>R,S</i>)	Boc-Leu-NMe ₂ 124	85% ^(a)	Ac-Val-OH, HATU	77	17%

^aYield over two steps

^bepimerisation occurred, ratio 3:2 of diastereoisomers observed

Submission of substrates **123** and **124** to the second peptide coupling reaction under these conditions resulted in a doubling of peaks in the NMR spectra (Table 15, 2nd coupling, entries 2–3). This observation could have resulted from restricted rotation around one of the amide bonds giving rise to rotamers or epimerisation at the acidic α position of Val after activation with T3P and oxazolone formation. Techniques such as variable-temperature NMR, solvent switching and selective NOE NMR have been used to determine whether conformers or diastereomers are present and so careful NMR analyses were performed on the mimics **78** and **80**.^{170,171} Samples were prepared in various solvents of differing polarity (CDCl₃, CDCl₂, CD₃CN, MeOD) and their ¹H NMR spectra were compared (Figure 40). The peaks highlighted correspond to the H_α of the Val residue. Doubling of peaks was observed in all spectra (except those obtained for samples in MeOD, where peaks overlapped) and the ratios of isomers / rotamers were compared. The polarity of solvent would be expected to influence the population of rotameric conformers, but in these experiments all solvents gave a consistent 3:2 ratio.

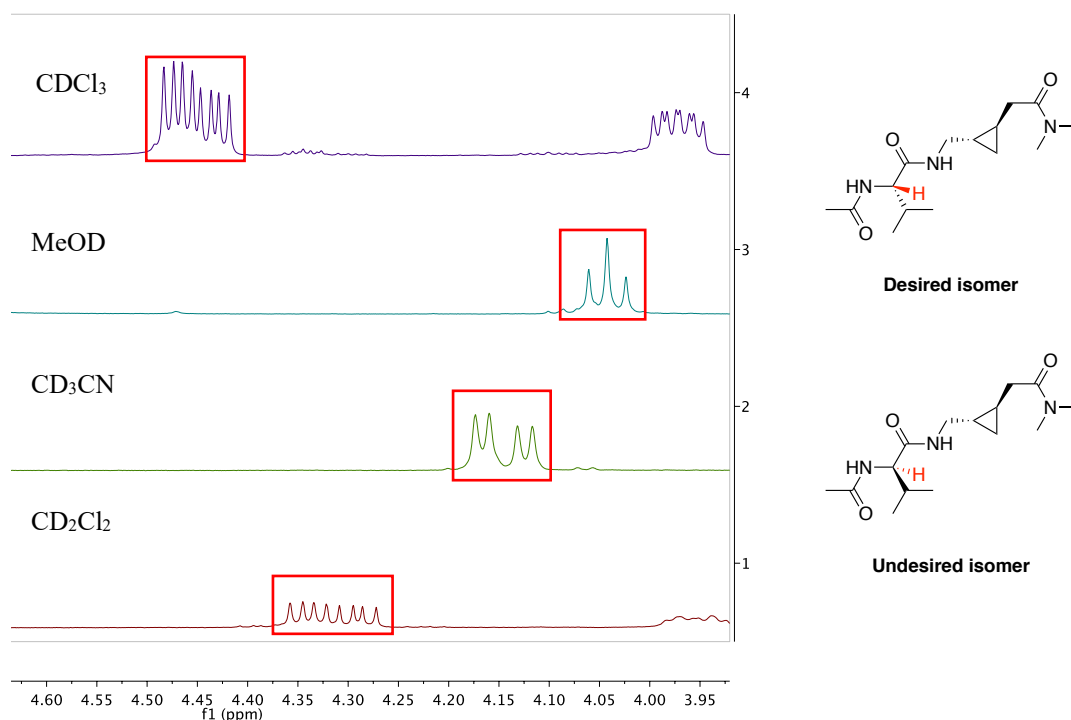


Figure 40: ^1H NMR spectrum of 78 in different solvents

Variable temperature NMR analyses were also undertaken. The barrier to rotation around the amide bond generally decreases with increasing temperature. However, the ^1H NMR spectra were obtained at 20 °C and 50 °C and the ratios of the key peaks were the same at both temperatures. Consequently, it was concluded that epimerisation had occurred when T3P was used to facilitate the second peptide coupling reaction and a diastereoisomeric mixture of products had been formed.

In an attempt to avoid this problem, the use of HATU as an alternative coupling agent was explored.¹⁷² The reaction sequence was repeated as before but the yields obtained for the tripeptides were lower than before and the reactions suffered from poor reproducibility (Table 15, 2nd coupling, entries 4–7). Importantly, there was no doubling of peaks in the NMR spectra of the final products, which indicated that epimerisation had been avoided by the use of HATU as a coupling reagent.

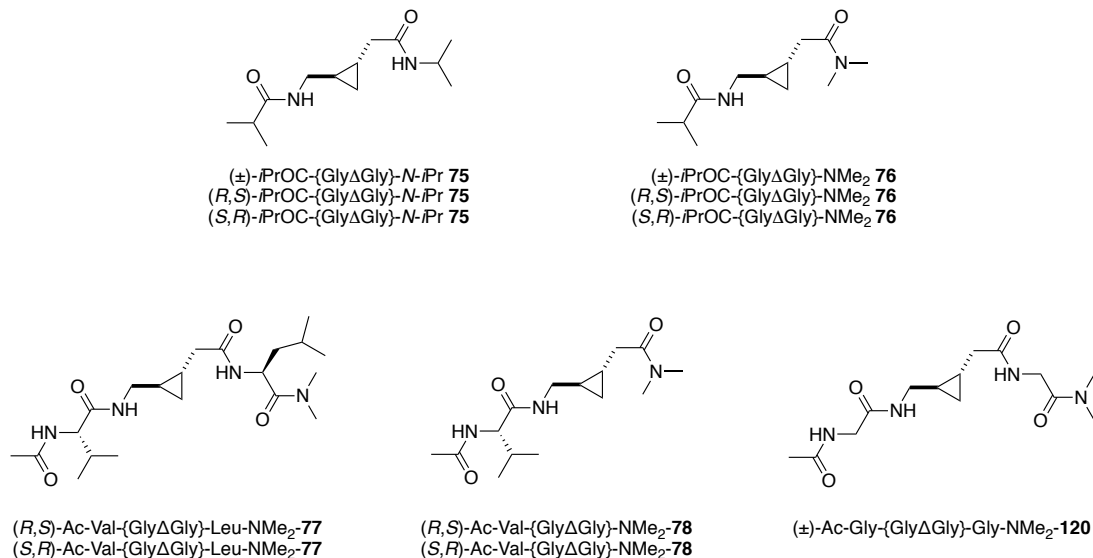
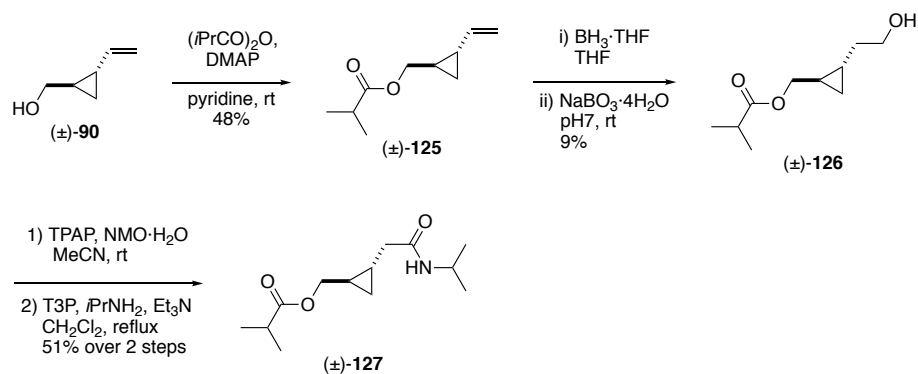


Figure 41: Peptidomimetics synthesised based on Gellman's work

Although the sequence was not fully optimised, sufficient material was obtained for the conformational analysis to be undertaken. Five peptides were synthesised, including enantioenriched (both antipodes) and racemic variants (Figure 41)

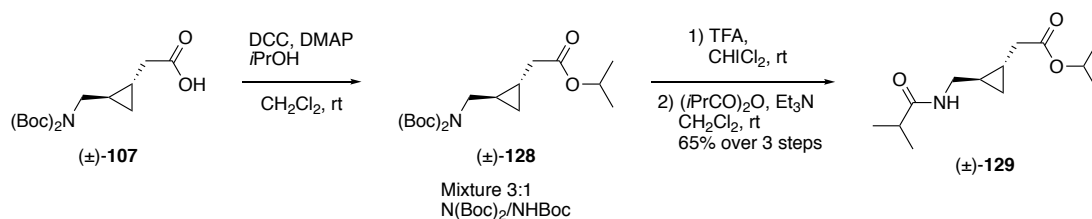
2.6. Synthesis of Ester Analogous of the Turn Mimics

An alternative way in which the hydrogen bonding network within a peptide can be probed is by selective replacement of amides with the corresponding esters. The ester and amide have similar conformations but have different hydrogen bonding properties: an amide bond can act as hydrogen bond donor whereas an ester cannot and an ester is a much weaker hydrogen bond acceptor than an amide. A series of esters was designed to probe the deletion of single hydrogen bonds. The N-terminus amide was the first to be replaced by an ester group (Scheme 36).



Scheme 36: Synthesis of *iPrCOO*-{*GlyΔGly*}-*N-iPr* 127

The key ester bond was introduced when alcohol **90**, obtained from the original LIDAKOR rearrangement reaction, was esterified using $(i\text{PrCO})_2\text{O}$ to produce the ester **125** in 48% yield. Subsequent alkene hydroboration and oxidation, following the same conditions described for $\text{Boc}_2\text{-}\{\text{Gly}\Delta\text{Gly}\}\text{-OH}$ synthesis, delivered the alcohol **126** in a very poor yield. The alcohol was then oxidised directly to the corresponding carboxylic acid using TPAP and hydrated NMO. The carboxylic acid was not purified but instead was submitted to the T3P-mediated amide coupling reaction with isopropylamine to give the amide **127** in 51% yield over two steps. A second analogue, in which the ester and amide functionality are reversed, was synthesised from $\text{Boc}_2\text{-}\{\text{Gly}\Delta\text{Gly}\}\text{-OH}$ (**106**) (Scheme 37).



Scheme 37: *iPrCO*-{*GlyΔGly*}-*OiPr* Synthesis 129

The protected amino acid was subjected to Steglich esterification with isopropanol to produce the ester **128** as a mixture 3:1 of N(Boc)_2 and NHBoc compounds. Global deprotection of the mixture by treatment with 10 equivalents of TFA afforded the corresponding amine, which was submitted for amide formation by reaction with isobutyric anhydride. Analogue **129** was obtained in 40% yield over 7 steps. Only a racemic mixture was prepared because the spectroscopic properties of the individual enantiomers were expected to be the same.

2.7. Conformational Analysis of Peptide Hybrids that Contain Turn Mimics

2.7.1. Preliminary Results, NH Chemical Shift Comparison

In ^1H NMR spectroscopy, the chemical shift of the signal for a given proton is sensitive to its chemical environment.¹⁷³ In particular, the ^1H NMR signal of an N-H or O-H can display an important variation in its chemical shift depending on its environment and interaction with polar groups. Therefore, by considering the various NMR spectra in a library of related peptides, it should be possible to explore the presence or absence of hydrogen bonds.

In this study, performed at 1 mM in CD_2Cl_2 , the reference values of N-H chemical shifts were compared between the β -turn mimics and compounds that could not form turns, either because there was no hydrogen bond donor on the C-terminus available to form a 10-membered ring (esters **129**, and dimethyl amides **76** and **78**) or the main chain was too short for a turn to form (Ac-Val-NHMe **130** and Ac-Leu-NMe₂ **131**). It was anticipated that a significant difference in NH chemical shift value would indicate the presence of a hydrogen bond. In particular, when a NH is involved in an *intramolecular* hydrogen bond the chemical shift tends to move downfield. The NH chemical shift of Ac-Val-NHMe, Ac-Leu-NMe₂ and alkene analogues had been measured previously by Gellman and co-workers'.⁷⁶

The data in Table 16 indicates extensive folding of tetrapeptide **12** designed by Gellman (the different NH bonds are colour coded for clarity). Val-NH and Gly-NH of peptide **13** have chemical shift values that are similar to those of the reference substrate **130** meaning hydrogen bonds are not formed with the NCO peptide bond and the peptide is in a linear conformation. Therefore, 8- or 11-membered ring hydrogen bonding is not expected in the tetrapeptide **12**. The Val-NH of **12** is shifted downfield by 1.2 ppm relative to **13** and **130**, which suggests that this NH is involved in a strong *intramolecular* hydrogen bond that results in formation of a 14-membered ring.

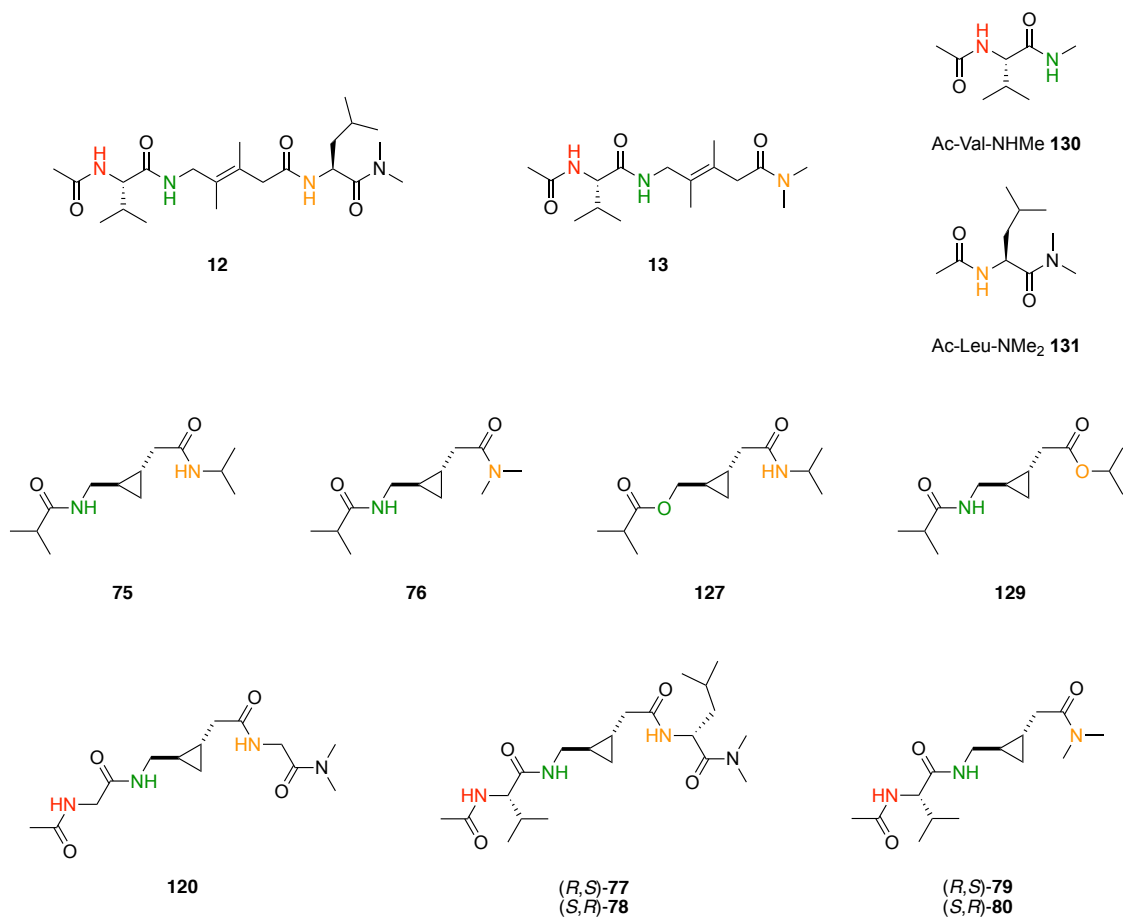


Table 16: Chemical shift comparison

Entry	Peptide	NH	NH	NH
1	Ac-Val-NHMe 130	5.99	5.77	-
2	Ac-Leu-NMe ₂ 131	-	-	6.17
3	Ac-Val-{Gly//Gly}-Leu-NMe ₂ 12	7.24	6.55	6.80
4	Ac-Val-{Gly//Gly}-NMe ₂ 13	6.03	5.73	-
5	(±)-iPrOC-{GlyΔGly}-iPr 75	-	6.79	5.44
6	(<i>R,S</i>)-iPrOC-{GlyΔGly}-iPr 75	-	6.77	5.45
7	(±)-iPrOC-{GlyΔGly}-NMe ₂ 76	-	7.58	-
8	(<i>R,S</i>)-iPrOC-{GlyΔGly}-NMe ₂ 76	-	7.66	-
9	(±)-iPrOC-{GlyΔGly}- <i>O</i> -iPr 129	-	6.40	-
10	(±)-iPrOCO-{GlyΔGly}- <i>N</i> -iPr 127	-	-	5.61
11	(<i>R,S</i>)-Ac-Val-{GlyΔGly}-NMe ₂ 79	6.62	8.12	-
12	(<i>S,R</i>)-Ac-Val-{GlyΔGly}-NMe ₂ 80	6.44	8.11	-
13	(±)-Ac-Gly-{GlyΔGly}-Gly-NMe ₂ 120	6.43	7.51	6.65
14	(<i>R,S</i>)-Ac-Val-{GlyΔGly}-Leu-NMe ₂ 77	6.34	7.70	6.34
15	(<i>S,R</i>)-Ac-Val-{GlyΔGly}-Leu-NMe ₂ 78	6.38	7.70	6.58

As it was expected, racemic and enantioenriched peptides have similar NH chemical shifts, showing that they behaved the same way in terms of their *intramolecular* interactions. The Gly-NH of both variants of **75** is shifted by 1 ppm downfield when compared to the reference compound **130** and the NH-*i*-Pr is shifted upfield of more than 0.7 ppm. This indicates that in the *i*PrOC-{GlyΔGly}-*i*-Pr peptide the Gly-NH is involved in considerable *intramolecular* hydrogen bonding to form an 8-membered ring rather than the expected 10-membered ring. Peptide **75** has only Gly-NH free to interact and the chemical shift for this proton was found to be almost 2 ppm downfield relative to the relevant amide protons in compounds **13** and **130**. The data suggest that a strong *intramolecular* hydrogen bond is formed between Gly-NH and CO group at the C-terminus of the mimic. The NMR data for this dipeptide mimic suggests that the peptide adopts hydrogen bonding arrangement I predominantly (Figure 42).

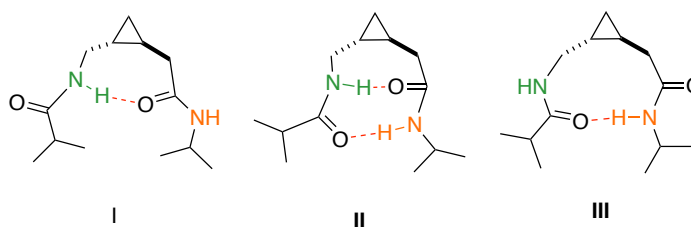


Figure 42: Possible hydrogen bonding arrangements for dipeptide **75**

The ester **129** lacks the hydrogen bond donor required to form the 10-membered ring system. The Gly-NH chemical shift lies 0.7 ppm downfield compared to reference compound **130**, which suggests that the *intramolecular* hydrogen bond observed in peptide **76** is also formed in the ester analogue. In contrast, it is not possible to form an 8-membered hydrogen bonded ring in the ester **127**, but the chemical shift of NH-*i*-Pr is similar to that of **75**, which suggests that *intramolecular* hydrogen bonding with C-ter carbonyl group does not occur. Consequently, conformation III in figure 42 is unlikely to occur in the dipeptide mimic. This data for the dipeptide mimetic suggests that an 8-membered hydrogen bonded ring is formed and this feature would be expected in tetrapeptide **120** and tripeptide **77**.

Each of the two NH chemical shifts of peptides **79** and **80** were found to be shifted downfield by 0.6 and 2.3 ppm when compared to corresponding signals for the compounds **13** and **130**. An incredibly strong *intramolecular* hydrogen bond that involves Gly-NH and C-ter carbonyl group is formed along with a 14-membered hydrogen bonded ring produced by an interaction between Val-NH and the same carbonyl group. So, 8- and 14-membered were expected in tetrapeptides **120**, **77** and **78** and could adopt conformation IV (Figure 43). The

chemical shifts of all three NH of flexible peptide **120** are shifted more than 0.4 ppm downfield compared to the reference peptides which suggests that they were all involved in *intramolecular* hydrogen bonding., Gly-NH is the most strongly hydrogen bonded. Gly-NH and Gly-NH have a similar variation in chemical shift which suggests that they form weaker *intramolecular* hydrogen bonds. Tetrapeptides **77** and **78** could adopt any of the arrangements I, II, III or IV because Val-NH is involved in the strongest hydrogen bonding as shown by data obtained for tripeptide **79** and **80**.

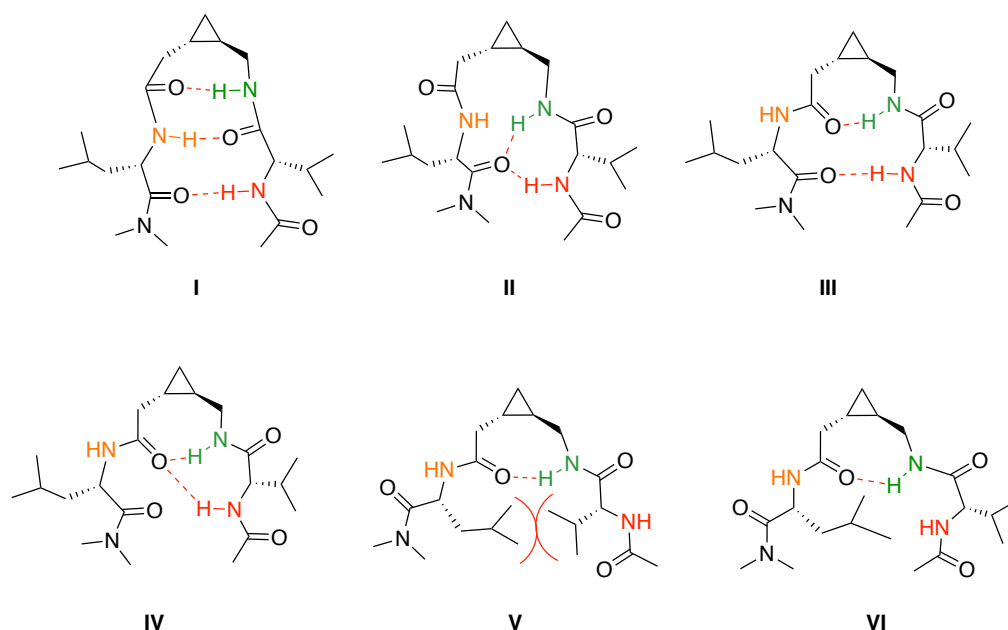


Figure 43: Possible hydrogen bonding arrangements adopted by peptides **77 and **78****

Ac-Val-{GlyΔGly}-Leu-NMe₂ **77** and **78** have chemical shift values that are very similar to the more flexible compound Ac-Gly-{GlyΔGly}-Gly-NMe₂ **120**. These peptides behave similarly and the side chains seem to have little effect and are located on the outside of the turn. This completely excluded conformation V and VI to be adopted. The data obtained for peptides **77** and **78** show that Gly-NH can form an 8- or 11-membered hydrogen bonded ring (conformation I to IV, Figure 43) and it is always involved in *intramolecular* hydrogen bonding as indicated by the large shift downfield when compared to data for reference peptides. These data differ from the observations made by Gellman *et al.* on compounds **12** and **13**. The cyclopropyl mimic was not stabilised by the same *intramolecular* hydrogen bonds, furthermore the 10-membered ring that is supposed to stabilise a β-turn was not the most favoured ring as demonstrated by data for the dipeptide **76** and tripeptides **79** and **80** which suggest that there is a strong *intramolecular* hydrogen bond between Gly-NH and C-ter carbonyl group. It appears that all of the peptides containing the cyclopropyl peptide mimic adopt a folded conformation that is greatly stabilised by the cyclopropyl group.

Moreover, cyclopropyl group constrains the system more than the tetrasubstituted alkene group used by Gellman and co-worker and brings the Gly-NH hydrogen bond donor and the Gly-CO hydrogen bond acceptor into close proximity.

2.7.2. Hydrogen bond formation analysis

2.7.2.1. Dipeptides **75** and **76**

The conformation adopted by a peptide can be determined by measuring the *intramolecular* hydrogen bonds formed. This analysis started with the analysis of the racemic dipeptide turn mimetics **75** and **76**. The C-terminus NH can be involved in a hydrogen bond with the carbonyl at the N-terminus to form a 10-membered ring system and this is the basis for stabilisation of β -turns (Figure 44). The other hydrogen bond network that can be formed is between the N-terminus NH and C-terminus carbonyl group, which results in a less stable hydrogen bonded 8-membered ring system.

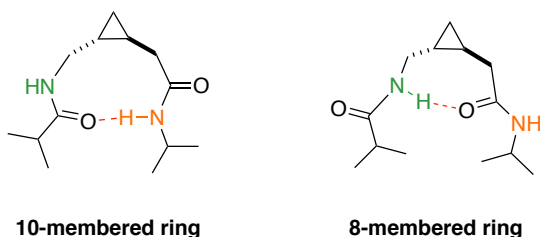


Figure 44: Two intramolecular hydrogen bonds possible in dipeptide **75**

The chemical shifts of both NHs (shown in green and orange in Figure 44) were measured at six different concentrations: 20, 10, 5, 1, 0.5 and 0.1 mM in CD₂Cl₂. Measurements were performed in deuterated dichloromethane CD₂Cl₂ because it is less polar than MeOD or deuterated acetonitrile and because the peptide cannot form hydrogen bonds with the solvent.

The chemical shifts of both the amide protons NH-*i*-Pr and Gly-NH in (±)-*i*PrOC-{GlyΔGly}-*i*Pr **75** varied with the logarithm of the concentration above 1 mM but remained constant at lower concentrations (Figure 45). This suggests that at low concentrations, there are consistent strong *intramolecular* hydrogen bonds and that *intermolecular* hydrogen bonding occur at higher concentrations. The fact that both NH behave in the same way suggests that hydrogen bonded systems that contain 8- and 10-membered rings are formed. It could be that a secondary hydrogen bonded 8-membered ring arises after the formation of the expected 10-membered ring. In the dimethyl equivalent – (±)-*i*PrOC-{GlyΔGly}-NMe₂

76 – no variation of Gly-NH chemical shift was observed across all the concentrations studied. In this case, only one hydrogen bond is possible and this leads to formation of an 8-membered ring. The invariance of chemical shift was surprising because it suggests that the usually less favourable 8-membered ring system was being formed and that the cyclopropane forces the molecule into what would normally be considered to be an unfavourable hydrogen bonding arrangement.

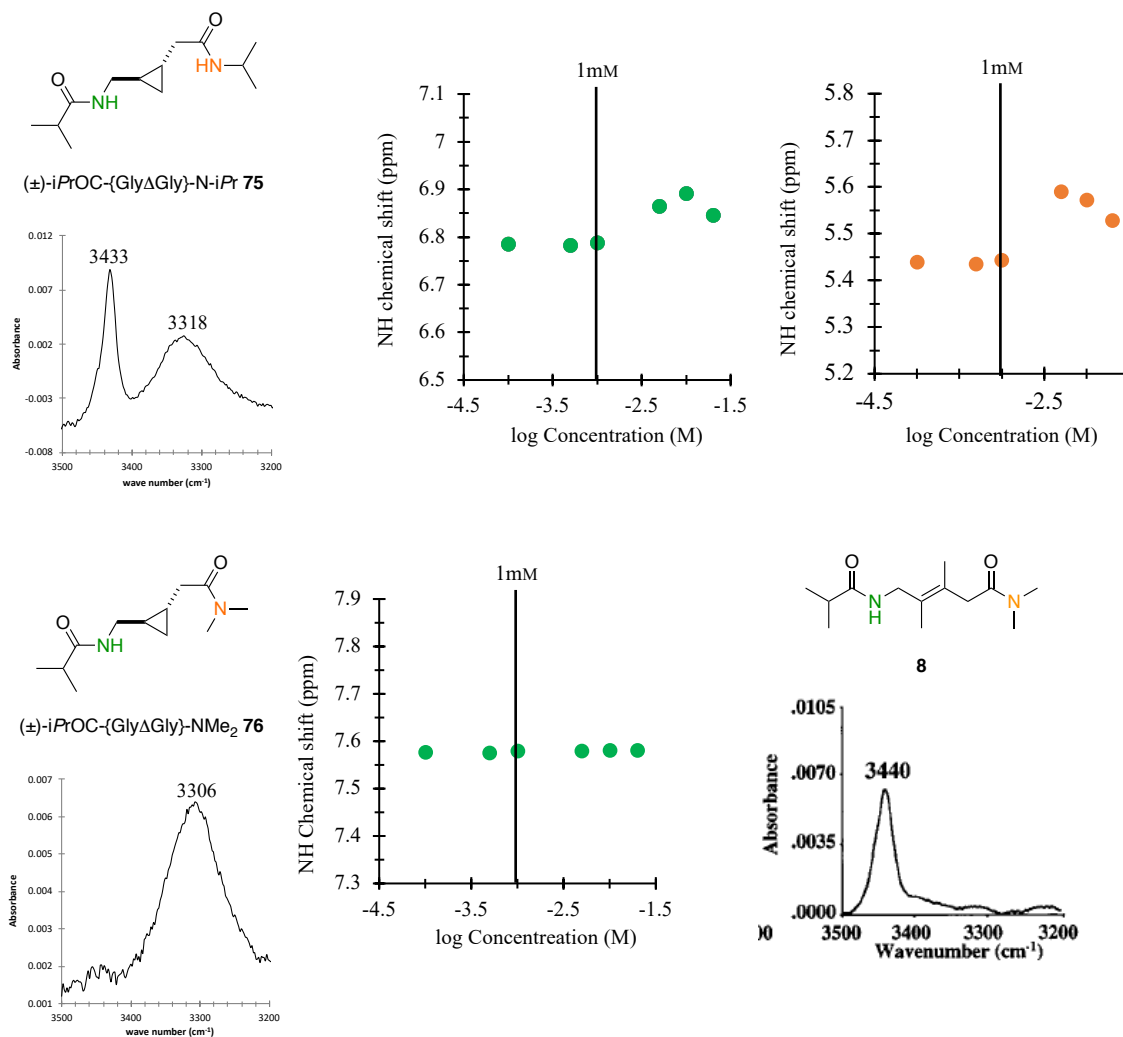


Figure 45: Racemic dipeptides mimic NMR and IR study, and Gellman's analogue IR⁷⁷

The region of the IR spectrum studied corresponds to amide mode A, which is the NH stretch region showing *intermolecular* or *intramolecular* hydrogen bonded NH or solvent-exposed NH. According to the data obtained from the concentration-dependent NMR studies, the *intramolecular* hydrogen bonds were occurring at concentrations below 1 mM for (±)-iPrOC-{GlyΔGly}-N-iPr **75**. This concentration was the optimum one at which to analyse hydrogen bond formation by solution IR spectroscopy. Unfortunately, measurements could not be carried out at 1 or 5 mM due to poor quality data produced by the spectrometer at these concentrations. Consequently, the solution IR spectra of the compounds were

obtained at a concentration of 10 mM in dry CH₂Cl₂. For consistency, this concentration was used for all IR measurements.

(±)-*i*PrOC-{GlyΔGly}-N-*i*Pr **75** displays a strong band at 3318 cm⁻¹, which arises from an *intramolecularly* hydrogen bonded NH, and a band at 3433 cm⁻¹ due to NH exposed to solvent. These data suggest that *intramolecular* hydrogen bonds are still formed in peptide at concentrations above 1 mM and imply that the peptide exists in an equilibrium between a folded conformation (I, II or III in Figure 42) and an open conformation at 10 mM. The IR NH-stretch data for (±)-*i*PrOC-{GlyΔGly}-NMe₂ **76** has only one band at 3306 cm⁻¹, which arises from an NH involved in *intramolecular* hydrogen bonding. This data is supported by the observation made by NMR that this Gly-NH is involved in a strong *intramolecular* hydrogen bond exclusively and excludes the presence of arrangement III (Figure 42) in CH₂Cl₂. In comparison, the IR spectrum of the analogous alkene system **8** synthesised by Gellman and co-workers was reported to have a single band at 3340 cm⁻¹ which corresponds to solvent exposed NH (Figure 45), a finding that implies an absence of *intramolecular* hydrogen bonding in the alkene system. This comparison suggests that the cyclopropane was more effective than an alkene at folding a small hybrid peptide system into a hydrogen bonding arrangement.

Considering these results, it was interesting to determine which of the two possible hydrogen bonds was the strongest and thus responsible driving the folding process. To this end, the two ester analogues (±)-*i*PrOCO-{GlyΔGly}-N-*i*Pr **127** and (±)-*i*PrOC-{GlyΔGly}-O-*i*Pr **129** were analysed by IR spectroscopy (Figure 46). In (±)-*i*PrOCO-{GlyΔGly}-N-*i*Pr **127**, the Gly-NH is replaced by an ester Gly-O and so only the NH-*i*Pr can be involved in *intramolecular* hydrogen bonding to form a 10-membered inner ring. In the case of (±)-*i*PrOC-{GlyΔGly}-O-*i*Pr **129**, the Leu-NH is replaced by an ester O and so only the Gly-NH can be involved in an *intramolecular* hydrogen bond to form an 8-membered ring. However, it is important to note that changing the amide group to an ester group also weakens the hydrogen bond, because esters are generally less effective hydrogen bond acceptors than the corresponding amides.¹⁷⁴

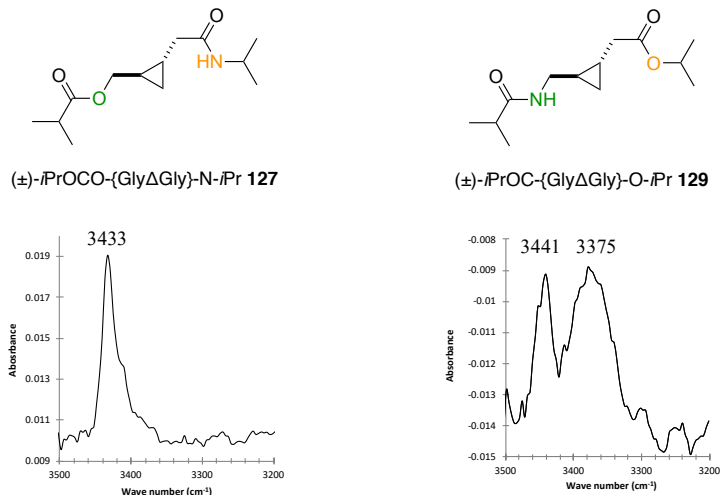


Figure 46: NH-stretch IR of ester analogues 127 and 129

Only one band at 3433 cm⁻¹ was observed for ester (±)-iPrOCO-{GlyΔGly}-N-iPr **127**. This sharp band indicates hydrogen bonding with the solvent, or *intermolecular* bonding with another amide was in operation for **127**. In contrast, two bands were observed for (±)-iPrOC-{GlyΔGly}-O-iPr **129**. The sharp band observed at 3441 cm⁻¹ suggests *intermolecular* hydrogen bonding and the broad band at 3365 cm⁻¹ is attributed to *intramolecular* hydrogen bonding. The presence of two bands suggests an equilibrium is established between folded and unfolded states in the case of this system. Again, the presence of an *intramolecular* hydrogen bond supports the role of the cyclopropane in helping to form a turn motif, especially given the reduced propensity that esters have for hydrogen bond formation.

The spectra of the (*R,S*)-enantiopure variants of the above racemic mixtures were also recorded under the same conditions (Figure 47). The Gly-NH of (*R,S*)-iPrOC-{GlyΔGly}-iPr **75** did not vary significantly with concentration although a small shift was observed at the highest concentrations studied. This suggests that a very strong 8-membered hydrogen bond is formed in this system. The NH-iPr chemical shift was also found to be constant at low concentrations but more variation at higher concentration (> 1 mM). However, this still suggests that a strong *intramolecular* hydrogen bond is formed, but the increased degrees of freedom in the larger 10-membered system make it more susceptible to alternative hydrogen bonding patterns at higher concentrations.

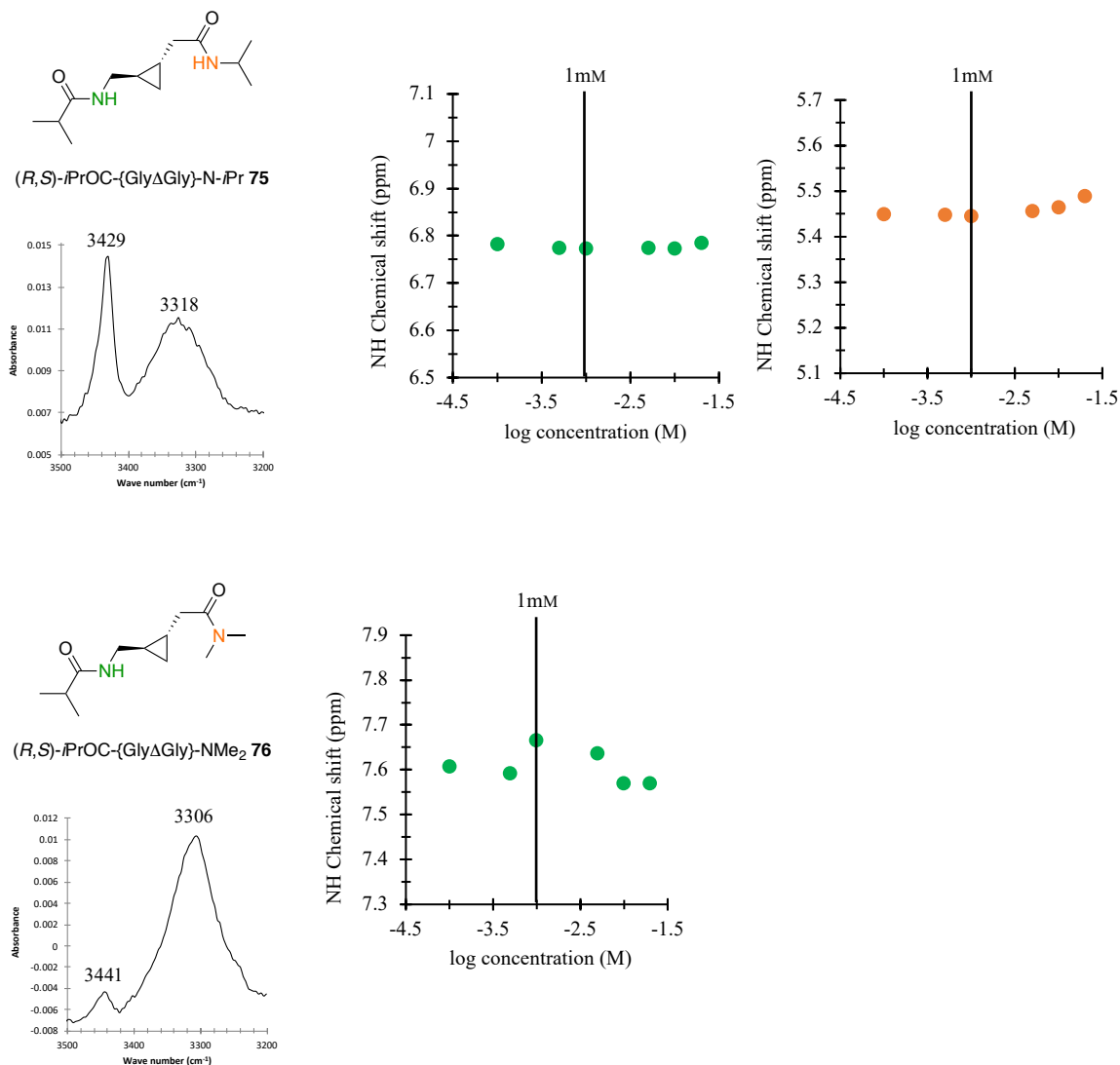


Figure 47: NMR and IR studies of (R,S) -dipeptide mimics 75 and 76

This finding confirmed that conformations I and II were more plausible than conformation III (Figure 42). The IR spectrum acquired was similar to obtained for the racemic mixture showing solvent exposed NHs and *intramolecularly* hydrogen bonded NH with observation of the same bands at 3429 and 3318 cm⁻¹ respectively.

A concentration dependent study of (R,S) -*i*PrOC-{Gly Δ Gly}-NMe₂ **76** showed that the chemical shift varied at between 1 and 5 mM and reverted to the same chemical shift at higher concentration. This implied *intermolecular* hydrogen bonds are not formed but some can be formed with the water present in the NMR solvent. However, the NH can be considered to be *intramolecularly* hydrogen bonded at all concentrations because the chemical shift is the same at very low and high concentrations. Two bands were observed by IR in the NH-stretch region. The one at 3306 cm⁻¹ is suggestive of *intramolecular* hydrogen bonding, and the small peak at 3441 cm⁻¹ indicates that Gly-NH is slightly solvent exposed at 10 mM, a finding which supports the variation observed by NMR.

In summary, the {Gly Δ Gly} surrogate was proven to promote the formation of a turn by spectroscopic measurements. Furthermore, *i*PrOC-{Gly Δ Gly}-NMe₂ variants **76** were shown to be exclusively intramolecularly hydrogen bonded, which implies that an 8-membered cyclic hydrogen bonded system is formed. The size of this hydrogen bonded system is unusual and suggests that the cyclopropane has a propensity to stabilise this type of interaction. Therefore the “ β ” designation could no longer be used for the turn motif adopted by the mimics prepared in the course of this project because the system is stabilised by formation of an 8-membered rather than the usual 10-membered cyclic hydrogen bonded network defined for β -turns.

2.7.2.2. Analysis of Tri- and Tetrapeptide Systems

After completion of studies on the small peptides, attention turned to the analysis of longer peptide systems. This was achieved by extending the amide sequence at both ends with glycine to form a tetrapeptide mimic. Based on the data obtained from the NMR chemical shift studies, it was clear that Gly-NH is involved in the formation of a strong *intramolecular* hydrogen bond that results in the formation of an 8- or 11-membered ring. The two other amide protons – Gly-NH and Gly-NH – have more freedom to rotate and interact either with solvent or *intermolecularly* with another molecule of the hybrid peptide (Figure 48).

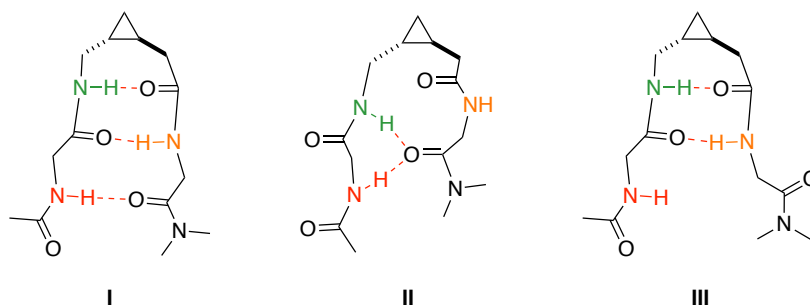


Figure 48: Possible hydrogen bonding arrangements adopted by hybrid peptide **120** in solution

To discover which hydrogen bonded network was formed, concentration-dependant NMR studies were undertaken and solution IR spectra was recorded. The samples were prepared at concentrations that varied between 0.1 and 20 mM and ¹H NMR spectra were recorded in CD₂Cl₂. The solution IR spectrum was recorded at 10 mM in CH₂Cl₂ (Figure 49).

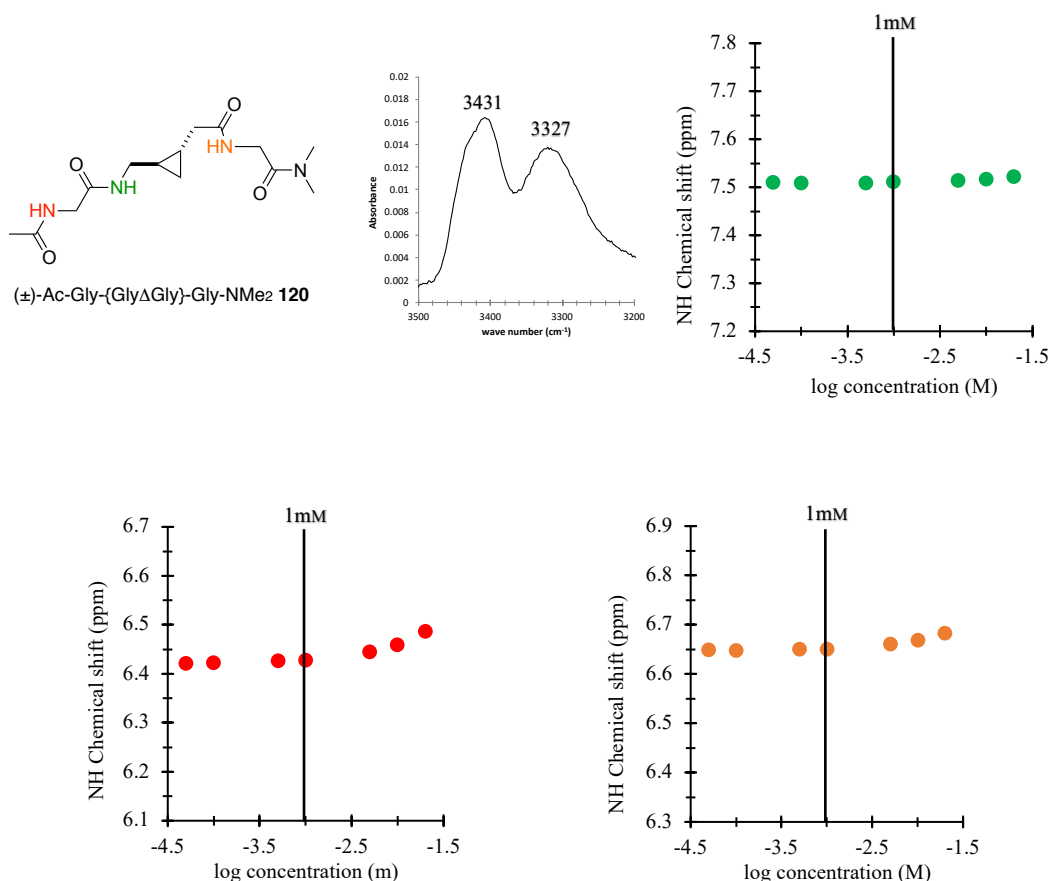


Figure 49: Ac-Gly-{GlyΔGly}-Gly-NMe₂ **120 Hydrogen bond formation analysis**

The Gly-NH slightly varied above 5 mM, which suggests that at high concentration this peptide starts to interact with the solvent or *intermolecularly*. The hydrogen bonded arrangement III is probably the most populated at high concentrations (Figure 48). In contrast, Gly-NH and Gly-NH did not vary with concentration, even at relatively high concentrations, which suggests that they are protected by *intramolecular* hydrogen bonds.

Bands at 3431 and 3327 cm⁻¹ were observed in the NH-stretching region of the IR spectrum. The peak at higher wavenumber arises from NH that is either solvent exposed or *intermolecularly* hydrogen bonded and the other peak arises from *intramolecularly* hydrogen bonded NHs. These data show that there is a population of solvent exposed or *intermolecularly* hydrogen bonded NH and excludes network I as major conformer while showing that an equilibrium between folded and open systems is established. It is important to note that network I (Figure 48) is not the preferred arrangement but is a possible one.

Results suggested formation of a turn structure for the peptide that contains glycine residues at either end so attention was focused on systems bearing more functionalised amino acids. The increased functionality was expected to lead to a decrease in conformational flexibility

of the molecule, which could alter the hydrogen bonding network. (*R,S*)-Ac-Val-{GlyΔGly}-Leu-NMe₂ **77** was analysed first (Figure 50). The concentration-dependent NMR study had the same profile to that observed for (±)-Ac-Gly-{GlyΔGly}-Gly-NMe₂ **120**, which lacks amino acid side chains. The chemical shifts for Leu-NH and Val-NH were found to vary at concentrations above 5 mM in CD₂Cl₂, indicating that they are disposed to form *intermolecular* hydrogen bonds at higher concentrations. In contrast, the chemical shift for Gly-NH was observed to be completely independent of the concentration, which suggests that it is protected by formation of an *intramolecular* hydrogen bond.

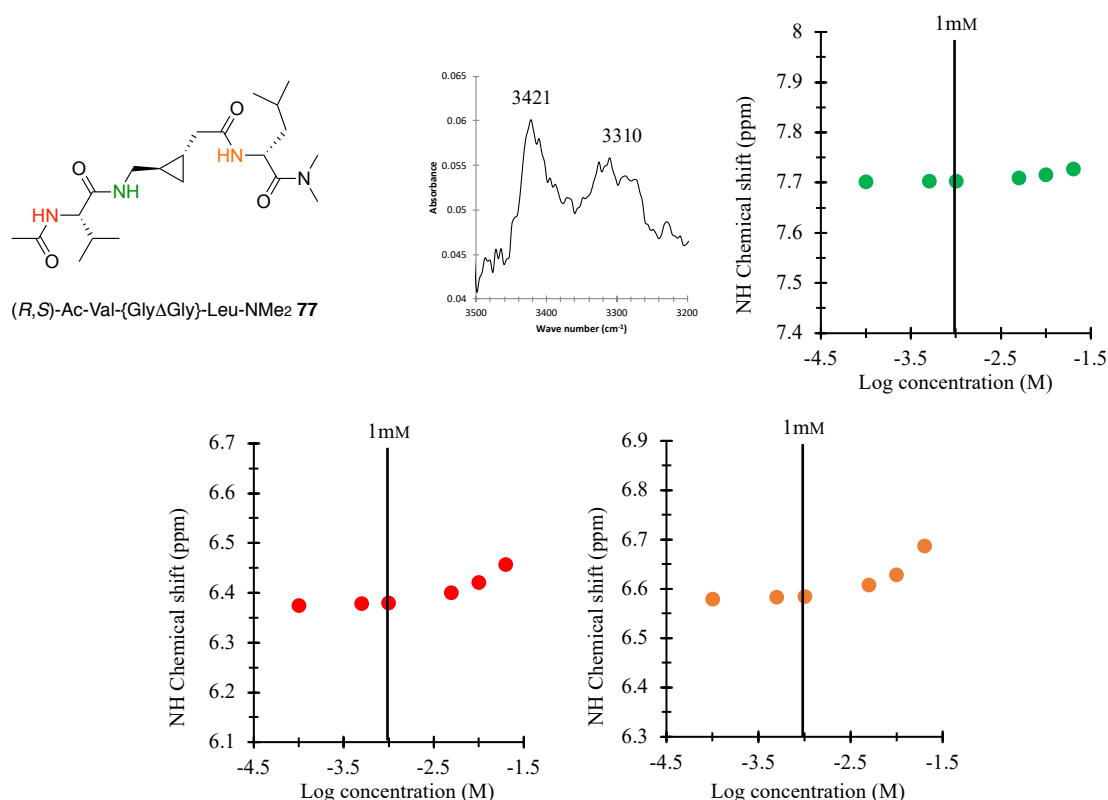


Figure 50: Hydrogen bond analyses on peptide 77

Unfortunately, IR spectra obtained over a range of concentrations were inconclusive. The best acquisition was at 10 mM in CH₂Cl₂. Bands at 3421 and 3310 cm⁻¹ were evident in the spectrum and these arise from solvent exposed / intermolecularly hydrogen bonded NHs and intramolecularly hydrogen bond NHs. Fully hydrogen bonded network I in Figure 48 can be excluded as major contributor. Gly-NH was protected by an *intramolecular* hydrogen bond, consequently networks II, III or IV could be adopted in solution. However, when steric hindrance between the side chains and data obtained from flexible peptide **120** are considered, it is unlikely that the peptide adopts the hydrogen bonded network IV (Figure 43).

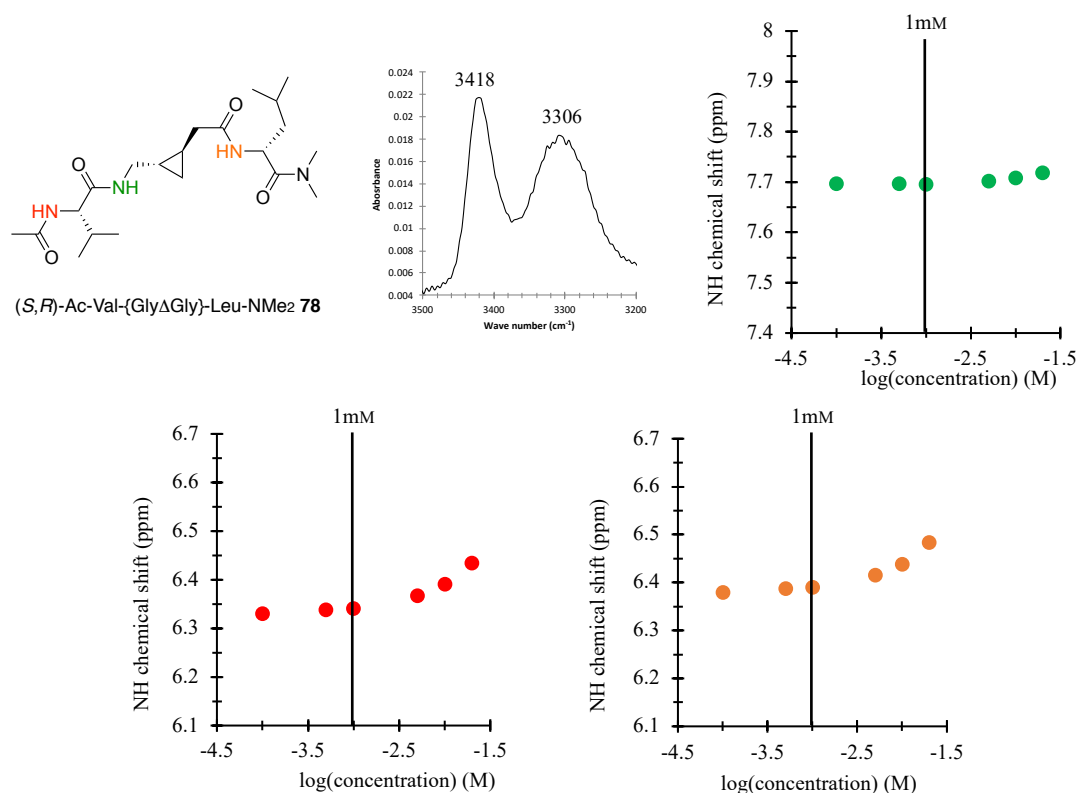


Figure 51: Hydrogen bond formation analysis of peptide 78

The IR spectrum obtained for this peptide was of higher quality than that obtained for compound **77** and these results are supported data obtained by NMR analysis. The bands at 3418 and 3306 cm⁻¹ shows that there is an *intramolecular* hydrogen bonding network in this peptide with some flexibility of both the external residues constituting the strands. In comparison, Gellman and co-workers prepared the analogous tetrasubstituted alkene and observed that Gly-NH was the most exposed to *intermolecular* hydrogen bonding (or interaction with the solvent) and Leu-NH the most strongly *intramolecularly* hydrogen bonded (cf. section 1.6.1.2 Figure 20).

Overall, the data demonstrate that Gly-NH is strongly *intramolecularly* hydrogen bonded in the tetrapeptide. Within the peptide, it is possible for Gly-NH to form two different hydrogen bonds, either with NH-CO or NMe₂-CO (with formation of an 8- or 11-membered ring, II and III Figure 48). Therefore, the tripeptides **79** and **80**, in which one carbonyl group is removed and **hydrogen bond donor sites** are restricted, were considered as a system for exploration of the hydrogen bonded network.

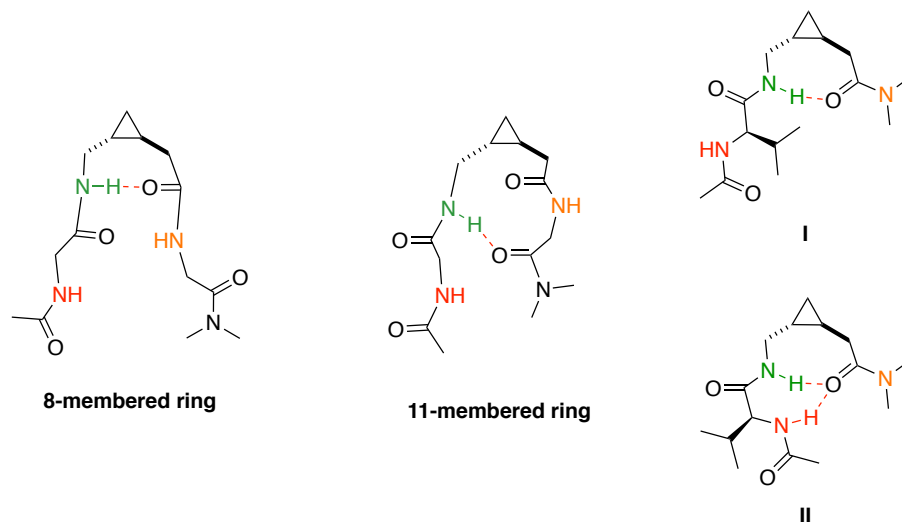


Figure 52: Possible hydrogen bonded ring formed with Gly-NH and possible conformers of 79/80

The enantioenriched variants of the peptides were analysed and similar results were obtained and so only results for (*R,S*)-Ac-Val-{GlyΔGly}-NMe₂ **79** are shown (Figure 53). Analysis of the NMR spectra showed that the chemical shift for Val-NH showed a slight variation with concentration and Gly-NH chemical shift showed no variation. This suggested that these NH were both involved in *intramolecular* hydrogen bonding. Therefore, the two conformations presented in Figure 52 were likely to be in equilibrium in CH₂Cl₂ solution.

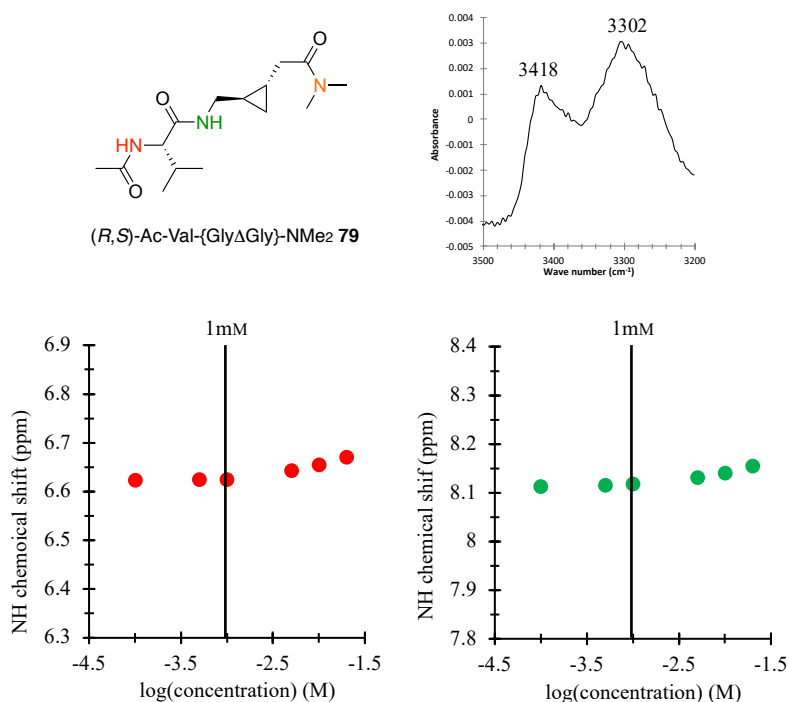


Figure 53: Hydrogen bond formation analysis of peptide 79

Furthermore, when the NH-stretch IR spectrum at 10 mM in CH₂Cl₂ is considered, the band at 3418 cm⁻¹ suggests that *intermolecular* interaction occurring in solution and so the network II is probably not the only one present. This conclusion is supported the NMR chemical shift data.

In this work, cyclopropane-containing peptides have been analysed by NMR and IR spectroscopy. Evidence for intramolecular hydrogen bonds obtained by IR and NMR analysis in dipeptides and in longer peptides. However, the analogues presented in this work have demonstrated an interesting feature: replacement of the peptide bond with cyclopropane seems to favour formation of an 8-membered hydrogen-bonded ring as opposed to more common 10-membered cyclic system observed natural β -turns. Overall, the data suggest that the cyclopropyl unit is an efficient and compact tool to constrain small peptides to adopt a turn conformation stabilised by strong intramolecular hydrogen bonds.

2.7.3. Use of Circular Dichroism to Probe Peptide Structure

Circular dichroism (CD) is an essential tool for structural analysis of the secondary structure of peptides and proteins.¹⁷⁵ Over the past few decades, systems that contain β -turns, especially type I and II turns, have been the subject of structural studies, and characteristic CD spectra have been identified for these types of turn in both MeCN and H₂O.^{176,177,178} For type I β -turns, two different shapes have been described: one has a negative band around 205–210 nm, while the other has a positive band at around 195 nm and large negative band at around 225 nm (Figure 54). Type II turns can be identified by a positive band at around 200 nm going to neutral ellipticity, and β -sheet structure presented the same positive band at 200 nm and a negative band around 210–220 nm.¹⁷⁹

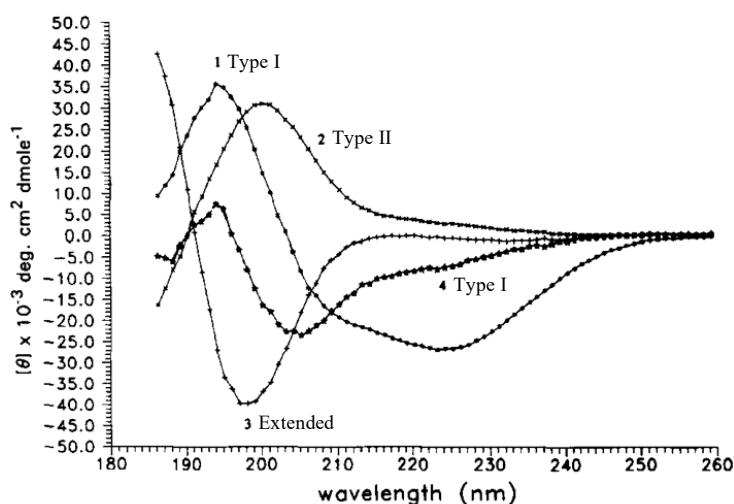
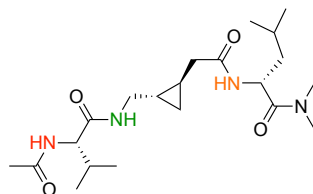


Figure 54: Type I, Type II and extended configuration CD spectra¹⁸⁰

To obtain additional information about our peptide mimics and study their secondary structure, the peptides previously described were analysed by circular dichroism. Previous conformational studies had demonstrated that turn sequence having a Gly in $i + 2$ position was more likely to produce a type II β -turn.¹⁸¹ The analogues designed in this work contained Gly mimic in $i + 1$ and $i + 2$ position, therefore it was possible to compare the results with those reported previously. The CD spectra were recorded and analysed with the help of Dr. Sharon Kelly at the University of Glasgow.

Tri- and tetrapeptide analogues **77-80** were analysed by CD spectroscopy at 1 mg/mL in three solvents with differing polarity. The solvents selected were water, acetonitrile and trifluoroethanol (TFE). Acetonitrile was selected because the peptide should exhibit similar behaviour to that in CH_2Cl_2 (chlorinated solvents are not compatible with CD). Trifluoroethanol (TFE) was selected as a solvent because it enhances intramolecular interactions and secondary structure even in small systems. In water, the peptide was expected to adopt an extended conformation due to extensive solvation.



(*S,R*)-Ac-Val-{GlyΔGly}-Leu-NMe₂ **78**

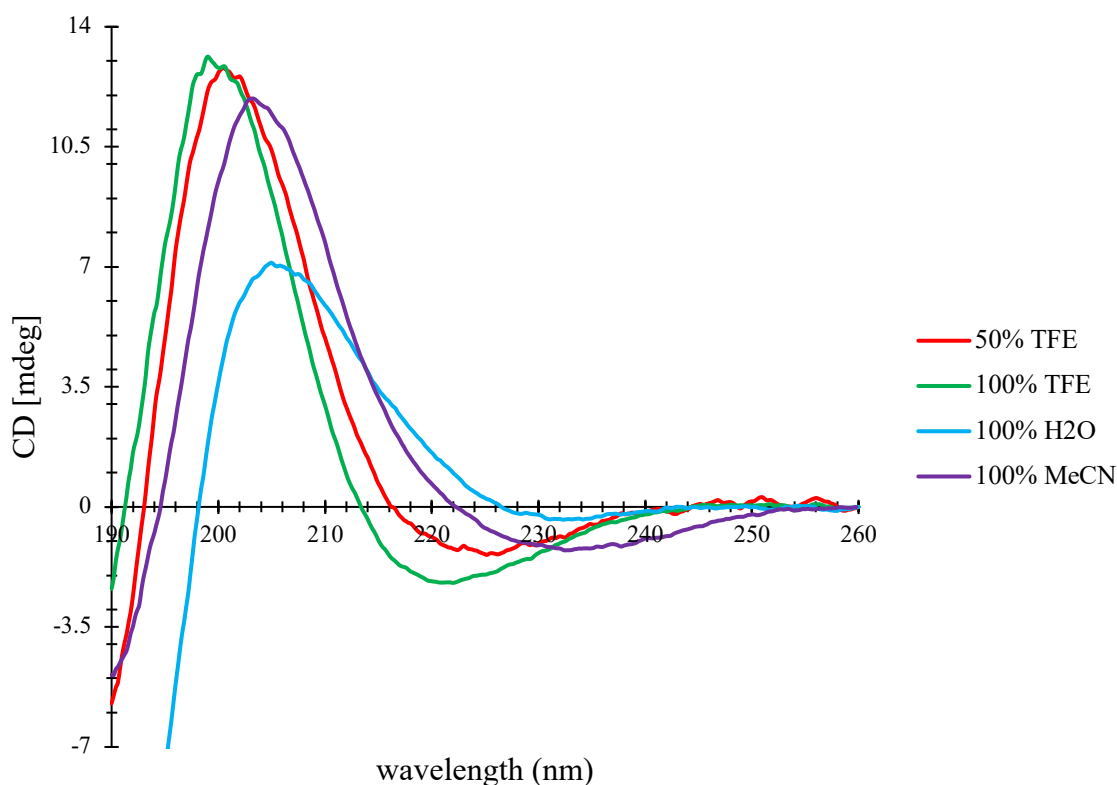


Figure 55: Far-UV CD spectrum of (*S,R*)-Ac-Val-{GlyΔGly}-Leu-NMe₂ **78** as a 1 mg/mL solution in various solvents.

The CD spectrum for tetrapeptide **78** in H₂O (blue in Figure 55) was found to have a large positive band at 205 nm which looks similar to a type II turn shown in Figure 54. However, the peptide was probably sampling some other random conformations given the largely negative peak towards 190 nm. The peptide seems to adopt a turn structure in water, which was not expected for such a small peptide in a polar solvent. In MeCN (purple), the spectrum experienced a more intensive positive and negative peaks at 205 and 235 nm respectively. This CD spectrum suggests that the peptide contains features similar to a type II β -turn and β -sheet in this solvent. The peptide appears to be more structured in trifluoroethanol (1:1 TFE/H₂O in red and 100% TFE in green) with an ellipticity almost two times higher than that in H₂O at 200 nm. Analysis of (*S,R*)-Ac-Val-{GlyΔGly}-Leu-NMe₂ **77** by CD suggests formation of a type II turn in all solvents, but the large negative peaks at around 190 nm in H₂O and MeCN suggest that the peptide experiences other conformations so a complex

mixture of conformers seems to be present in solution. The same conditions were used to analyse (*R,S*)-Ac-Val- $\{\text{Gly}\Delta\text{Gly}\}$ -Leu-NMe₂ **77** and similar results were obtained (Figure 56). Once again, CD data suggests that the peptide is more structured in TFE than in other solvents, and that it displays the characteristic features of a type II β -turn or β -sheet. The CD spectra obtained for samples in H₂O and MeCN suggest that the peptide is probably experiencing another random conformation because a large negative is observed around 190 nm.

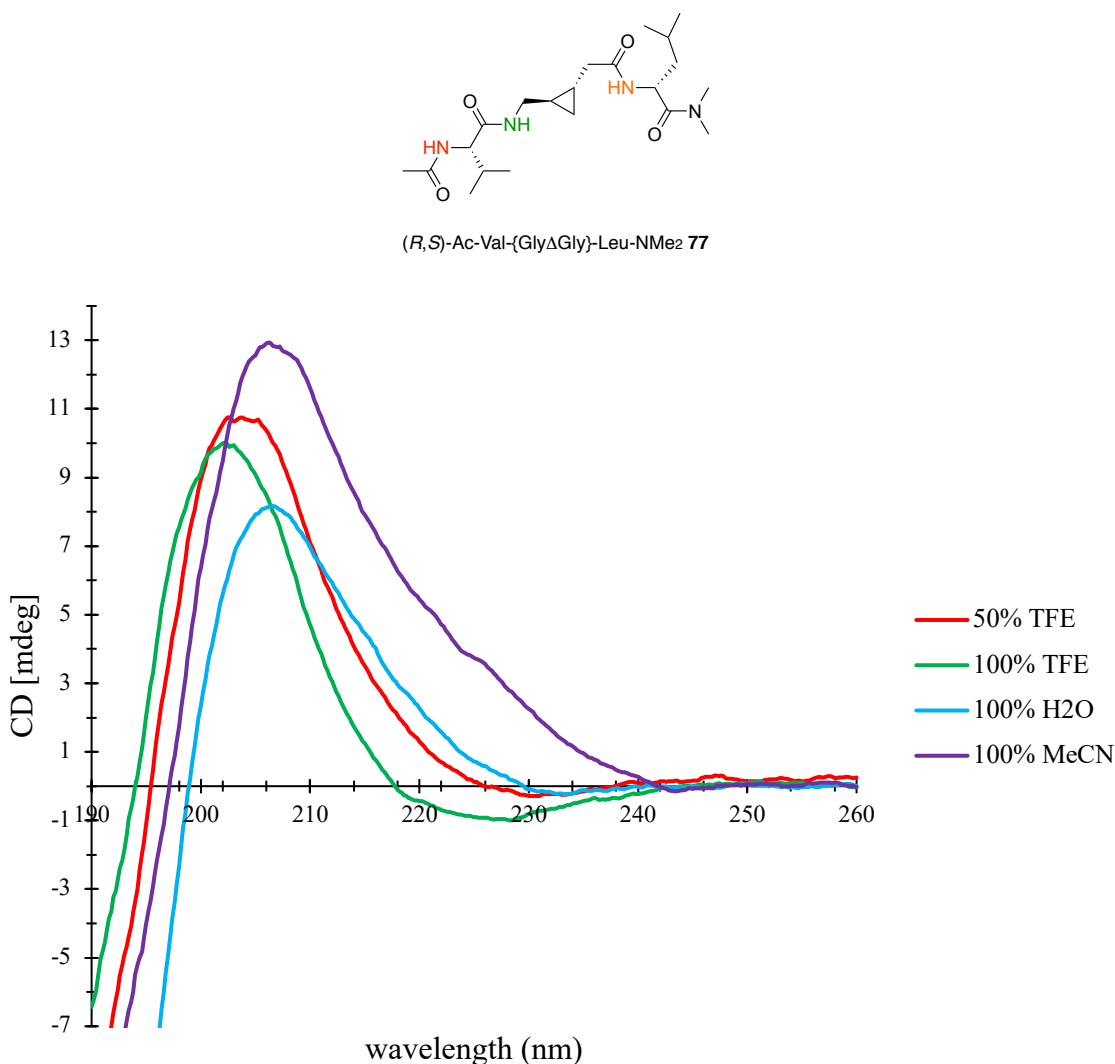


Figure 56: Far-UV CD spectrum of (*R,S*)-Ac-Val- $\{\text{Gly}\Delta\text{Gly}\}$ -Leu-NMe₂ **77** as a 1 mg/mL solution in various solvents.

The formation of turns in the cyclopropyl analogues that had been established by the hydrogen bonding network analysis described previously, was supported by the CD data. In addition, CD spectra provided supplementary information about the folding pattern of the tetrapeptides by displaying features found in a type II β -turn. Nevertheless, in all of the solvents studied, the peptides were found to adopt complex mixtures of conformations.

Variants of the tripeptides **79** and **80** displayed strong *intramolecular* hydrogen bonding as shown by the NMR and IR studies and so it was expected that features indicative of turn formation would be observed by CD spectroscopy. In this case, only solution in H₂O and TFE (1 mg/mL) were used as solvents and features of any type of β -turn were absent in the CD spectra obtained in both solvents (Figure 57). Even in TFE, a solvent in which peptides are supposed to be more structured, negative bands at 198 and 215 nm were observed in the CD spectra of both isomers. These bands correspond to π - π^* and n- π transitions and are usually assigned to random coil formation.¹⁸²

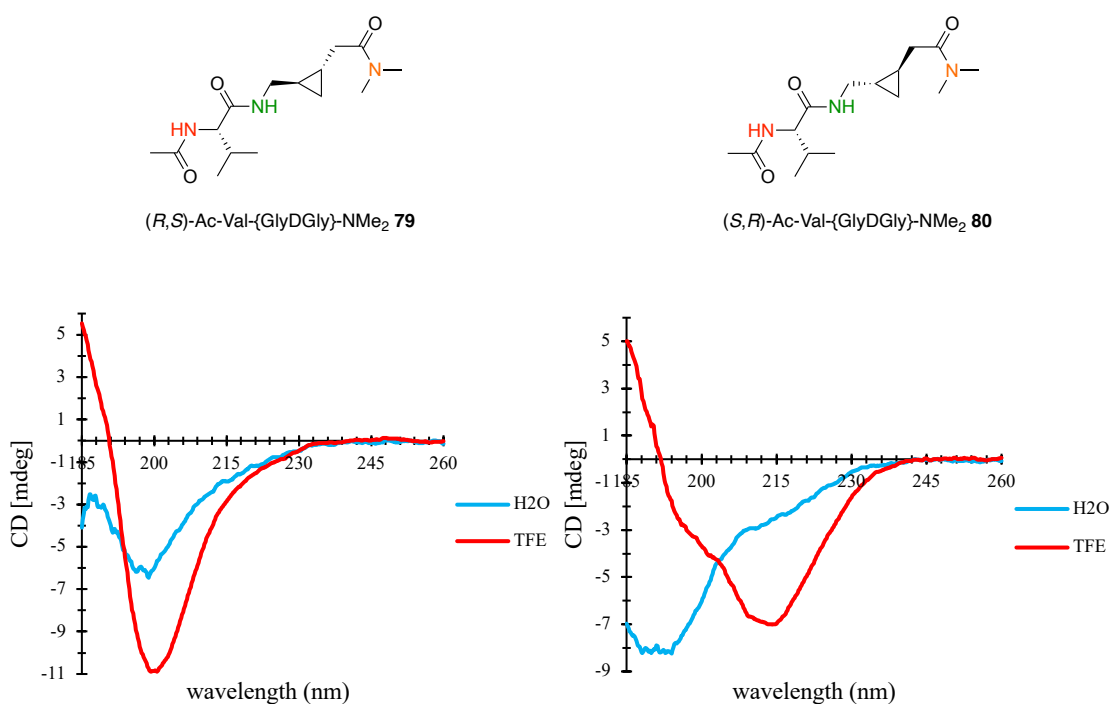


Figure 57: CD Spectra of variants of **79 and **80** in TFE (red) and H₂O (blue) (1 mg/mL)**

However, the peaks were more intense in TFE than in H₂O and, given the small size of the peptides and the intramolecular interactions observed by NMR and IR spectroscopy, we can assume that the peptide is adopting a turn structure but that it is not the preferred conformation adopted by the peptide within the whole population in solution. An equilibrium with a disordered conformation would display this type of spectrum.

2.7.4. NMR analysis of tetrapeptides **77** and **78**

In addition to chemical shift analysis, information can be obtained about molecular conformation by the use of 2D NMR experiments. The compounds described here were analysed by a variety of 2D experiments (COSY, TOSCY, HSQC, HMBC and NOESY). These experiments were performed by Dr Brian Smith at the University of Glasgow. Previous studies have allowed to determine and assign various NOE cross peaks depending on the type of β -turn that was present (figure 58).^{178,183}

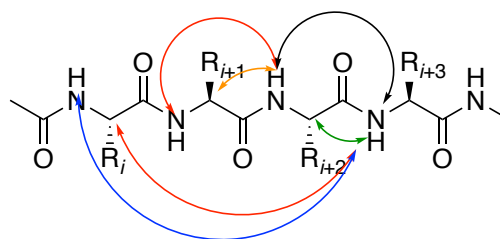
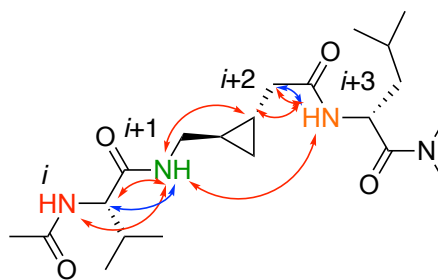


Figure 58: Characteristic NOE cross peaks found in type I (red), I' (blue), II (green) and II' (orange) turn

It is important to remember that in the analogues synthesised for this work a cyclopropane is employed as a peptide bond isostere. As a consequence, the bonds of one NH and one CO have been replaced by CC and CH bonds (that cannot be used to study β -turn) and two atoms in the amide that have sp^2 character have been replaced by sp^3 atoms, which can alter the dihedral angles significantly and thus change the turn adopted. Cross peaks observed with CH protons cannot be used as evidence for β -turn formation. (*R,S*)-**77** and (*S,R*)-**78** were prepared and analysed. The same cross peaks were observed in the two variants and the absolute configuration of the stereocenters in the *trans*-cyclopropane did not influence the folding pattern of the peptide, a finding that supports the data obtained by IR and CD spectroscopy.



(*R,S*)-Ac-Val-{Gly Δ Gly}-Leu-NMe₂ **77**

Figure 59: NOE Cross peaks of **77** measured in 1 mM in CD₂Cl₂ at 293 K (red) and in 1mM H₂O/5 % D₂O at 278 K (blue)

Two interesting cross peaks were observed, NH_{*i*}-NH_{*i*+1} and NH_{*i*+1}-NH_{*i*+3} in TFE (Figure 59). These peaks do not correspond to any features of natural peptides described in literature, but the last interaction establishes the close proximity between Gly-NH and Leu-NH in space and provides further evidence for formation of an 8-membered ring that stabilises the folded conformation of the tetrapeptide. This is also supported by an NH-CH_{*i*+2} cross peak that is observed in spectrum obtained in CD₂Cl₂. Sequential cross peaks NH_{*i*}-H α _{*i*-1} were observed in water and CD₂Cl₂. These cross peaks are characteristic features of β -hairpin strands and of a type II turn (green in Figure 58). This supported the data obtained by CD spectroscopy which showed that the peptide adopts a type II or II' turn (as they differ by rotation of 180° the CD spectrum would be identical). Nevertheless, a NH_{*i*}-NH_{*i*+3} interaction cannot be observed because the peaks for these two NHs have very similar chemical shifts (6.67 and 6.47 ppm respectively), and it was difficult to identify cross peaks in this region.

The NOE interactions within peptide **77** were studied as TFE-d₃ solution. This solvent promotes formation of the strongest *intramolecular* interactions. The NMR experiments were also performed at a lower temperature (278 K) to further enhance intramolecular interactions and obtain clearer signals. It was observed that Leu-NH and Val-NH were exchanging with the deuterium of TFE-d₃ slowly over time (Figure 60, blue t = 0, red t = 20 min, green t = 8 h), whereas Gly-NH exchanged immediately. This can be explained if the Leu-NH and Val-NH are protected from exchange with the solvent because they form *intramolecular* hydrogen bonds, while the Gly-NH was exposed to solvent. This suggested *intramolecular* hydrogen bonding to form of a 10-membered ring, which contrasts with the findings of the NMR shift experiments that had been performed in CH₂Cl₂ described earlier. This finding suggests that *intramolecular* interactions and the conformation adopted by our analogues are highly dependent on the solvent used.

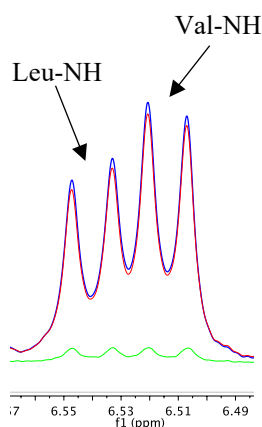


Figure 60: NMR Spectrum of **77** at 10 mM in TFE-d₃ showing H/D exchange of Leu-NH and Val-NH. *t* = 0 min (blue), *t* = 20 min (red), *t* = 8 h (green) at 278 K.

2D NOESY spectra of **77** were also acquired in TFE-d₂ because substrate cannot undergo deuterium exchange with the solvent. The same cross peaks that had been observed in CD₂Cl₂ were observed in this solvent, which was not surprising considering that the CD spectra were similar in all solvents, and suggests the same conformation is adopted. Nevertheless, the *intramolecular* hydrogen bonding pattern is different (Figure 61).

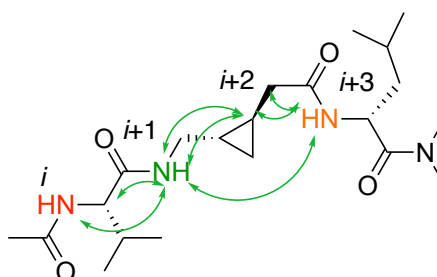


Figure 61: NOE Cross peak of **77** observed at 10 mM in TFE-d₂ at 278 K.

Results were inconclusive and suggested that a defined, exclusive and stable type of turn was not being adopted by these peptides. The spectroscopic data provided evidence for *intramolecular* hydrogen bond formation and suggested that structured and folded conformations are formed but that this varied depending on the solvent. Consequently, it had been demonstrated that replacement of a planar peptide bond by a non-planar cyclopropane was an efficient way to constrain the system and form *intramolecular* hydrogen bonds in organic solvents even in small dipeptide mimics.

2.8. Towards Leu-Enkephalin Mimicry

Leu-enkephalin is a pentapeptide that binds to opioid receptors, with a particular affinity for the δ -opioid receptor.¹⁸⁴ Leu-enkephalin can adopt a β -turn at two different positions with the formation of two hydrogen bonds and so is simple yet biologically important system in which the effectiveness of the cyclopropane dipeptide mimetics in promoting β -turns could be explored (Figure 62). The intention at the outset was to prepare two Leu-enkephalin analogues in which the Gly-Gly or the Tyr-Gly peptide units were replaced with a suitable cyclopropyl mimic.

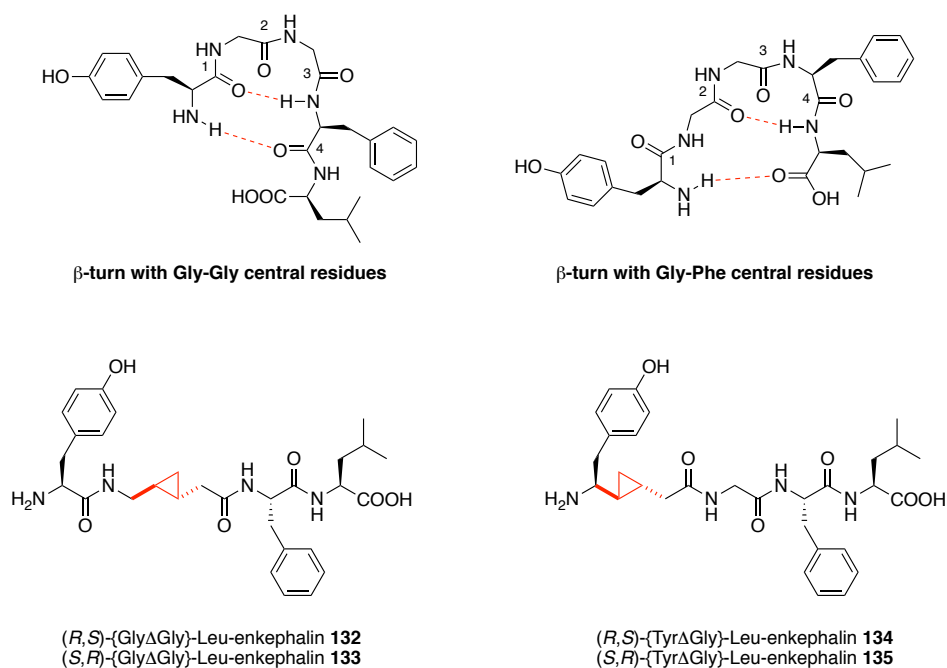
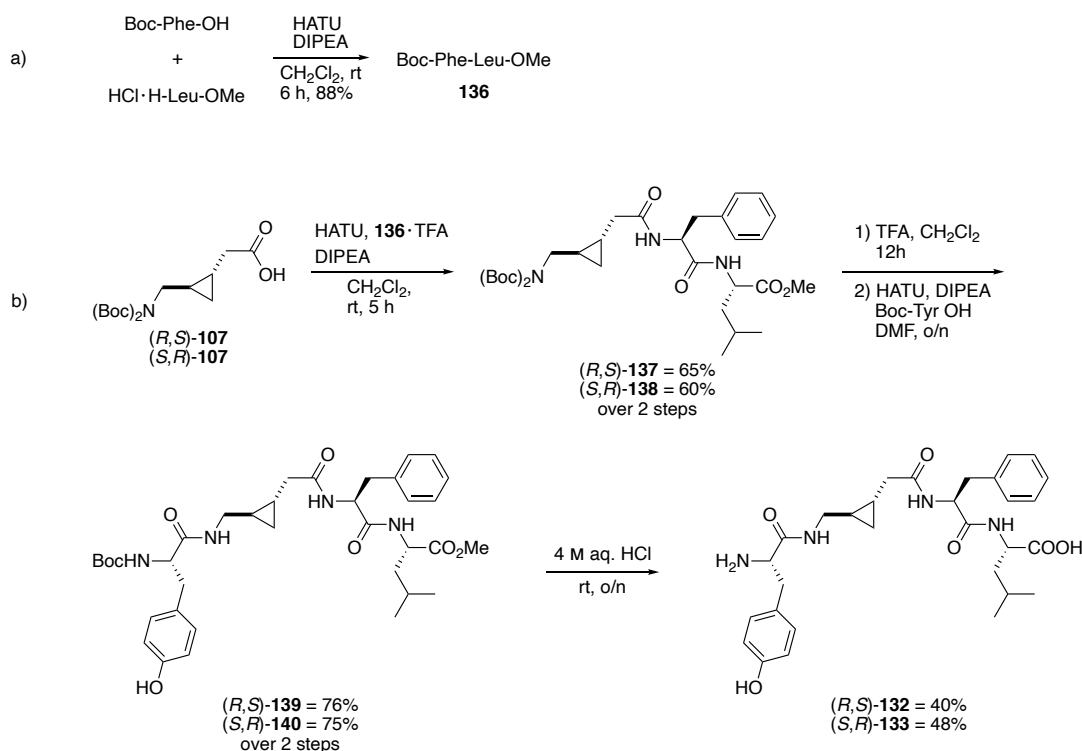


Figure 62: Leu-enkephalin and cyclopropyl analogues

2.8.1. Synthesis of {GlyΔGly}-Leu-enkephalin **132** and **133**

The first targets – {GlyΔGly}-Leu-enkephalin **132** and **133** – were synthesised from the Boc₂-{GlyΔGly}-OH **107** building block. Boc-Phe-Leu-OMe **135** was first obtained in 88% yield by peptide coupling using HATU and DIPEA at rt (Scheme 38a).



Scheme 38: {GlyΔGly}-Leu-enkephalin Analogues synthesis

The synthesis commenced with Boc removal from dipeptide **136** using TFA and then coupling to the acid (*R,S*)- or (*S,R*)-**107** using HATU to give respectively **137** and **138** following the same scheme described for the synthesis of the other analogues (Scheme 38b). Removal of both Boc groups and coupling of the resulting amine to Boc-protected tyrosine afforded the protected analogues **139** and **140** respectively in good yield. The protected peptides were fully deprotected in one pot using 4 M HCl to give (*R,S*)-{GlyΔGly}-Leu-enkephalin **132** and (*S,R*)-{GlyΔGly}-Leu-enkephalin **133** after purification by semi-preparative HPLC in yields of 40% and 48% respectively.

For comparison purposes, natural Leu-enkephalin **141** was also synthesised on a peptide synthesiser using Fmoc-Leu Wang resin (0.84 mmol/g loading) in a 0.1 mmol scale. The peptide was obtained in 43% yield after purification on semi-preparative HPLC.

2.8.2. Conformational Analysis of {GlyΔGly}-Leu-enkephalin **132** and **133**

The conformational studies of the Leu-enkephalin analogues were performed in order to explore whether a β -turn was formed. CD spectra were recorded of solutions in H₂O and TFE at 1 mg/mL (Figure 63). The CD spectra of (*R,S*)-{GlyΔGly}-Leu-enkephalin **132** in water showed a large negative around 190 nm that suggests a random conformation (green, Figure 63). The random population of conformations might be increased by the presence of the free *N*- and *C*- termini. The peptide displayed a more ordered structure in TFE, but it did not correspond to any type of β -turn described previously. This does not mean that the peptide is not adopting the expected conformation but it might adopt a different, currently undefined arrangement at equilibrium. Furthermore, the peptide contains two chromophore residues (Phe and Tyr) which could modify the CD signal due to their intermolecular and / or intramolecular interactions resulting in a unique CD profile. Nevertheless, the positive and negative peaks were observed at around 198 and 220 nm in TFE and H₂O, which suggests similar conformational features are formed in both solvents.

The diastereoisomeric compound, (*S,R*)-{GlyΔGly}-Leu-enkephalin **133** displayed a similar CD spectrum in water, which again suggests that the peptide does not adopt a well-defined structure due to interactions with the solvent (blue, Figure 63). The spectrum obtained from a sample in TFE was slightly different with three sharper positive peaks at 192, 205 and 223 nm, suggesting a better-defined structure in this isomer when compared to the diastereomeric compound.

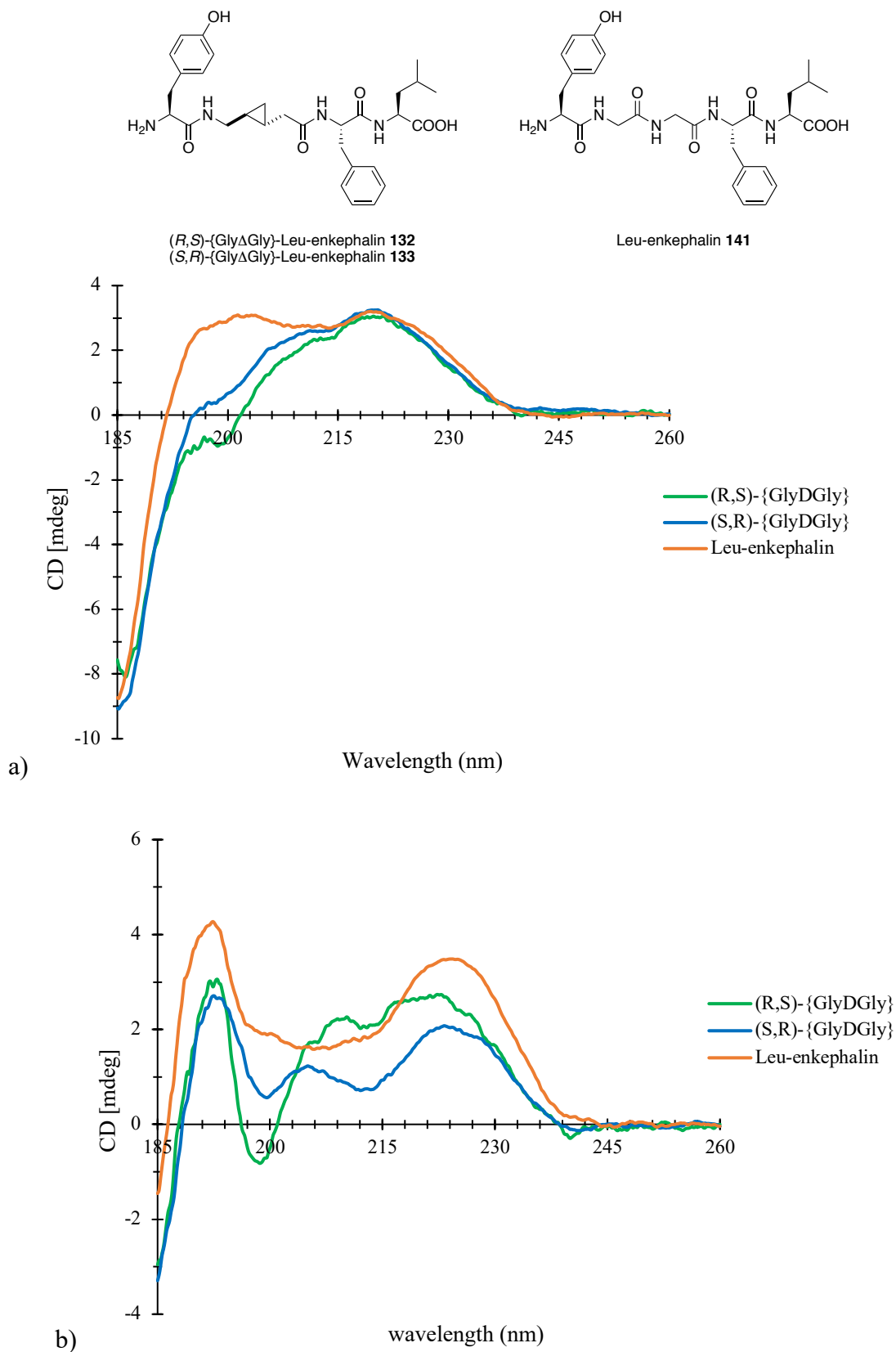


Figure 63: Far-UV CD comparison in a) TFE and b) H₂O of Leu- enkephalin 141 (orange), (*R,S*)-132 (green) and (*S,R*)-133 (blue)

Comparison of the data obtained for the two analogues with the data for the native peptide in TFE (Figure 63a) and H₂O (Figure 63b) was undertaken with a sample concentration of 1 mg/mL. Similar features were evident in the spectra of all three peptides in water, with a large negative peak at 190 nm (suggestive of a random conformation) and a positive peak at around 220 nm was common to all peptides, which suggests that they adopt similar conformations in water. In TFE, the positive peaks at 192 and 220 nm were preserved in all of the peptides, which is evidence for a structure that is better defined for all peptides. However, differences between the conformations were clearly observable in the region of the spectrum around 200 nm. These results indicated that cyclopropane-containing analogues adopted similar conformational features to those found in the native peptide and demonstrated that the cyclopropane moiety is able to stabilise the conformation adopted by the peptide.

Conformational NMR studies were undertaken in order to identify secondary structures that could be adopted by the peptides. Only sequential cross peaks (i.e. those between adjacent residues) were observed for the three peptides, providing no evidence to support any secondary structure adopted by Leu-enkephalin and its analogues. The Leu-NH, Gly₂-NH and Phe-NH had similar chemical shifts in both solvents showing that they are in the very similar chemical environment (Figure 64). However, the downfield shift of the NH peaks when the spectra were recorded in TFE suggests a more ordered conformation. Both isomers of {GlyΔGly}-Leu-enkephalin **132**, **133** and Leu-enkephalin **141** did not exhibit the characteristic features of β -turn when analysed by either NMR or CD spectroscopy. Indeed, no evidence of typical NOE crosspeaks of turns were shown and the CD spectra did not correspond to any type of turn described in literature.

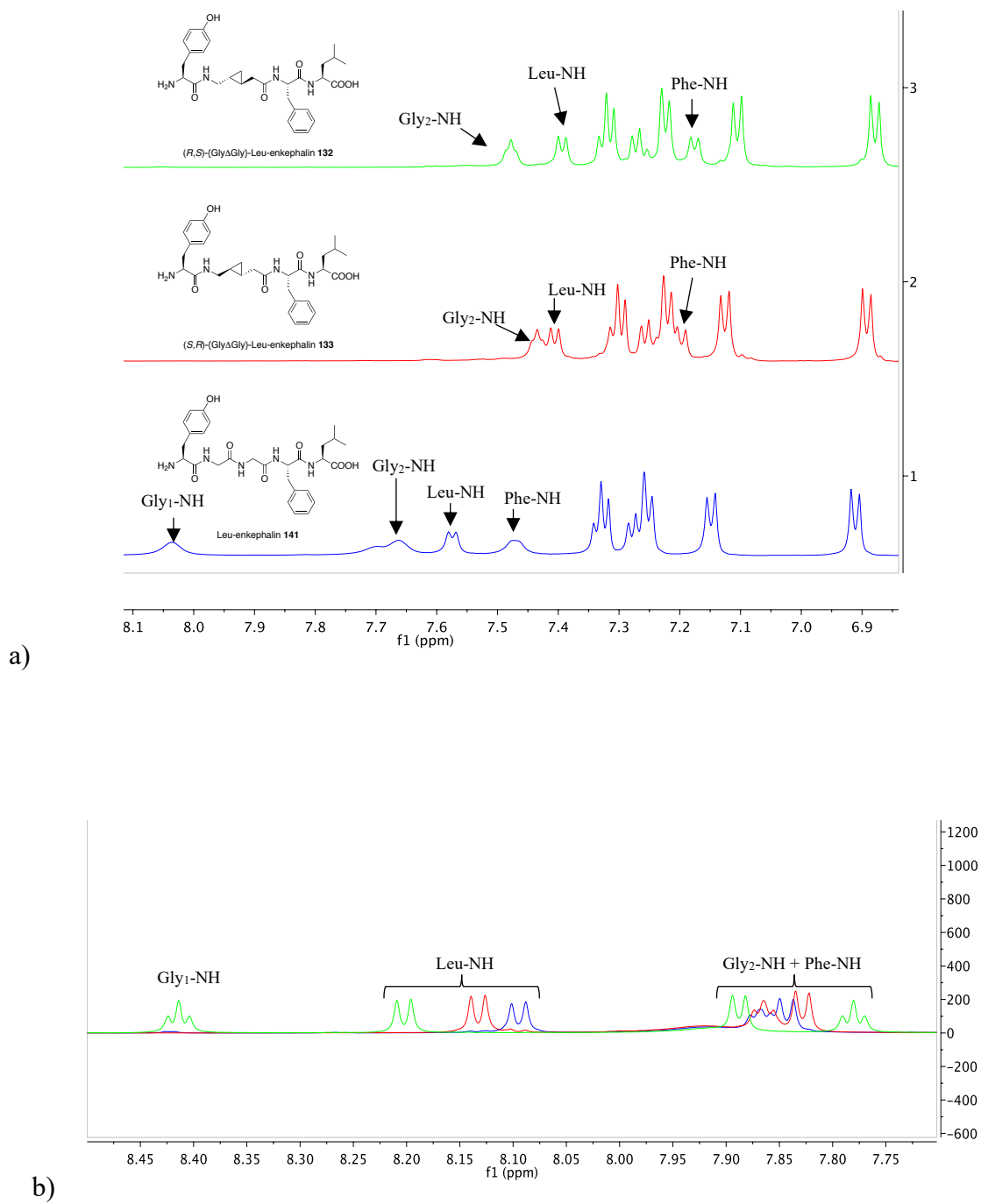
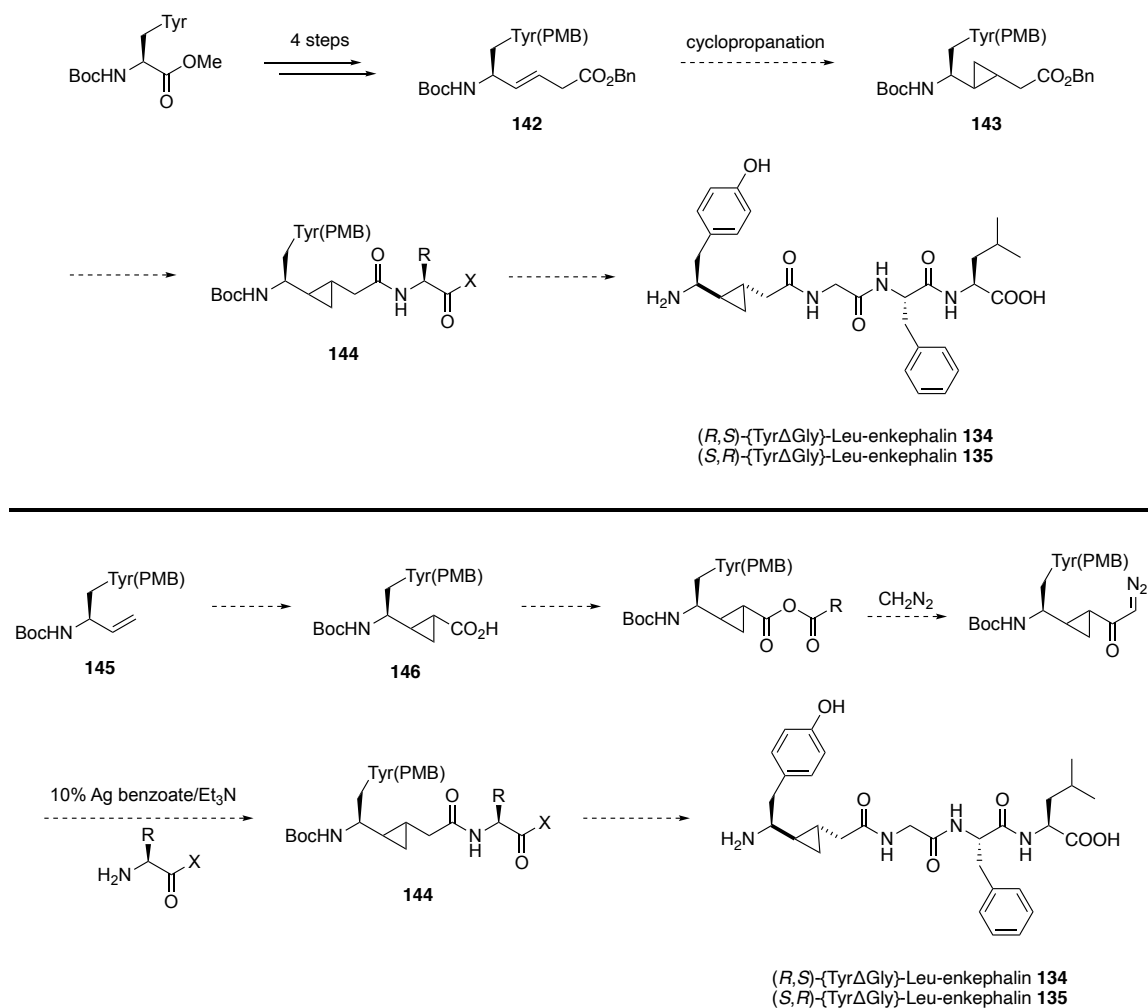


Figure 64: NH Chemical shifts for (R,S)-132, (S,R)-133 and 141 in a) TFE and b) H₂O/5 % D₂O

2.8.3. Towards the Synthesis of {Tyr Δ Gly}-Leu-enkephalin **134** and **135**

Leu-enkephalin contains two glycine residues and the CH₂ bonds within the residues allow free rotation about these bonds. The replacement of glycine with more substituted tyrosine restricts the number of accessible conformations of the molecule. The cyclopropane-containing mimic with a Tyr side chain was also investigated to see if location of the mimic in a different position within the hybrid structure would have an effect. The synthesis commenced with the intermediate alkene **142** which was subjected to stereoselective cyclopropanation reaction (Scheme 39). It was expected that diastereoisomers of **143** would be formed and that separation of the diastereoisomers would be possible. The isomers could then be submitted to peptide coupling to obtain compound **144** and subsequent deprotection in order to obtain Leu-enkephalin analogues. Another approach was to proceed a cyclopropanation on terminal alkene using carbenes chemistry. Once the carboxylic acid **143** obtained, it be submitted to Arndt-Eister homologation to produce the amide **144**.^{185,186} Finally, a standard peptide coupling procedure would be used to deliver the mimic {Tyr Δ Gly}-Leu-enkephalin **134** and **135**.



Scheme 39: Initial strategy for the synthesis of {TyrΔGly}-Leu-enkephalin 134 and 135

Alkene **142** was obtained following the synthesis described by Dory *et al.*⁸⁵ It consisted of sequential PMB protection of the Tyr, DiBAL-H reduction of the ester and Wittig reaction of the aldehyde to give a terminal alkene. This alkene was then subjected to a cross metathesis reaction with benzyl but-3-enoate.

It was expected that cyclopropanation of the alkene would be unselective leading to a mixture of diastereoisomers that could be separated for further study.

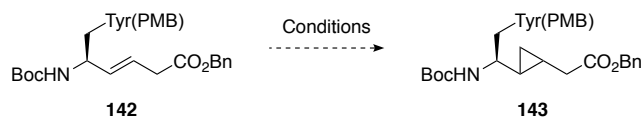


Table 17: Cyclopropanation conditions on alkene 142

Entry	Conditions	Results
1	Et ₂ Zn, CH ₂ I ₂ , CH ₂ Cl ₂ -78 °C to rt	20% conversion
2	CH ₂ N ₂ , Et ₂ O, Pd(OAc) ₂	Decomp.

The general procedure for Simmons-Smith cyclopropanation, in which diethyl zinc is used in combination with diiodomethane, was employed in an attempt to cyclopropanate the alkene **142** but there was poor conversion and the expected product was not obtained (Table 17 entry 1).¹⁸⁷ The use of diazomethane to cyclopropanate vinyl amides has been described.¹⁸⁸ The reaction was attempted on allylic ester **142** using Pd(OAc)₂ as the catalyst (Table 17, entry 2). TLC analysis of the reaction showed that multiple products had been generated but the cyclopropane **143** was not isolated following column chromatography.

After the failure of the reactions above, an alternative cyclopropanation method was explored. Following the success of cyclopropanation of a terminal alkene by a Rh₂(OAc)₄-catalysed reaction with ethyldiazoacetate, these conditions were applied to the functionalisation of the alkene **145** (Table 18, entry 1). A solution of ethyl diazoacetate was added slowly to a solution of the alkene and the catalyst at low temperature and the mixture was stirred for 18 h. The crude product was purified by column chromatography and traces of compound **146** were detected by mass spectroscopy, but the compound could not be further purified to give the required product.

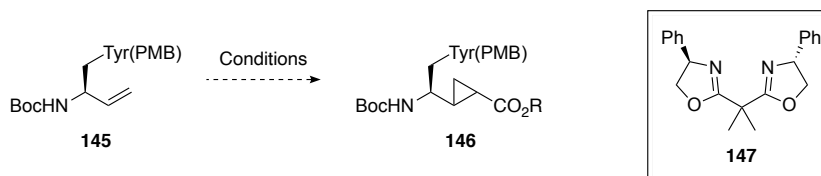
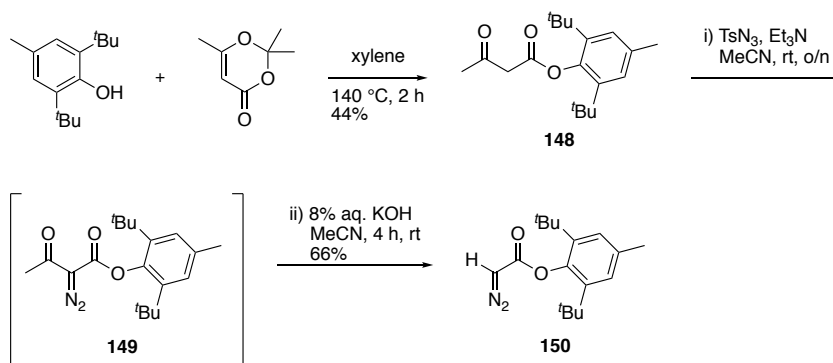


Table 18: Cyclopropanation on terminal alkene

Entry	Diazoester	Cat.	Ligand	Diazoester:143	Results
1	Ethyl	Rh(OAc) ₂ 3 wt%	-	2:1	Traces of 146 ^a
2	Ethyl	CuOTf 1 mol%	147 1 mol%	2:1	Traces of 146 ^a
3	BHT	CuOTf 1 mol%	147 1 mol%	5:1	-
4	BHT	CuOTf 5 mol%	147 5 mol%	5:1	-

^aDetermined by low res. MS

In 1991, Evans *et al.* described the use of a chiral copper(I) bisoxazoline complex to perform the asymmetric cyclopropanation of alkenes with good enantioselectivity.¹⁸⁹ This reaction required the formation of the copper-ligand complex prior to addition of the alkene and diazoester under an inert atmosphere (Table 18, entry 2). This reaction was attempted and a trace of the desired product was detected but it could not be isolated.

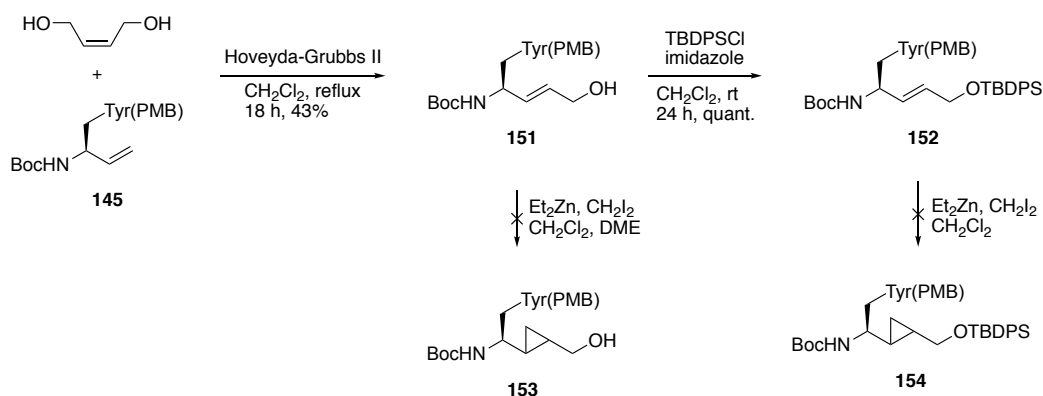


Scheme 40: Synthesis of the BHT diazoester 150

The diazoacetic acid ester derived from BHT has been described as a good substrate for carbene reactions (Scheme 26).¹⁹⁰ The synthesis of the reagent commenced with the treatment of BHT with 2,2,6-trimethyl-4H-1,3-dioxin-4-one. The keto ester **148** was obtained in 44% yield from this reaction as a mixture of keto and enol tautomers (45:55 keto/enol). This compound was then submitted to a reaction with tosyl azide to give intermediate **149**, which was not isolated but instead submitted to a hydrolysis reaction in 8% aq. KOH to produce the diazoester **150** in 66% yield. The cyclopropanation reaction was

performed on alkene **145** using diazoester **150**. The copper sources CuOTf or Cu(OTf)₂ were used along with the ligand **143** and catalyst loadings of 1 and 5 mol% were employed (Table 18, entries 3 and 4). Unfortunately, poor conversion was observed and the required cyclopropane was not obtained.

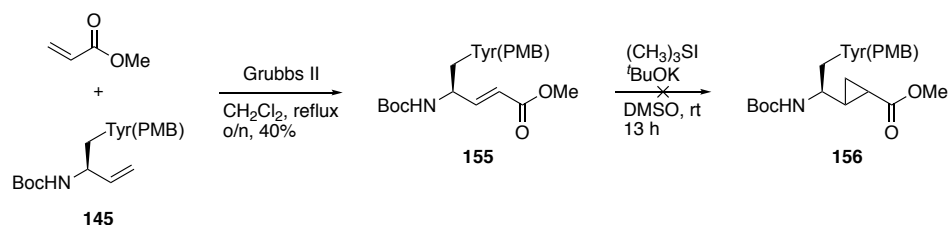
Cyclopropanation can be accelerated by the presence of an allylic alcohol in the substrate. The presence of a polar group results in coordination between the alcohol and the catalyst complex or reagent which delivers the reactant in an intramolecular fashion.¹⁹¹ In an attempt to exploit this reactivity, the allylic alcohol **151** and its corresponding protected version **152** were synthesised from alkene **145**, a compound obtained previously, by cross metathesis using Hoveyda-Grubbs second generation catalyst (Scheme 41). This reaction gave only the (*E*)-alkene isomer in modest yield and silyl protection afforded the alkene **152**



Scheme 41: Cross metathesis and subsequent cyclopropanation

The Simmons-Smith cyclopropanation reaction was performed on free alcohol **151** and on the protected alcohol **152**. Unfortunately, complex mixtures of products were obtained and neither of the required cyclopropanes **153** and **154** was obtained even after purification.

The final attempt to perform a cyclopropanation reaction involved the acrylate substrate **155** (Scheme 42). The substrate was synthesised from alkene **145** by cross metathesis using Grubbs II catalyst.



Scheme 42: Corey Chaykovsky Cyclopropanation

The (*E*)-alkene **155** was obtained in 40% yield and this compound was then submitted to a Corey-Chaykovsky cyclopropanation reaction.¹⁹² This procedure can be used for the synthesis of epoxides, aziridines and cyclopropanes and a chiral or achiral ylide salt can be reacted with α,β -unsaturated esters. Unfortunately, when alkene **155** was submitted to the cyclopropanation reaction, only traces of the compound **156** were detected by LCMS after column chromatography. Due to the failure of all routes to required cyclopropyl intermediate, this approach was abandoned.

Chapter 3

Tryptophan Zipper, turn replacement and analysis

3.1. Introduction

Results obtained by incorporation of cyclopropyl amide bond isosteres into small peptides were promising and there was evidence that {Gly Δ Gly} mimic was enhancing the formation a β -turn in some cases. However, short peptides rarely adopt stable secondary structure in solution.¹⁹³ and so was essential to identify a better system to evaluate the mimic. An ideal peptide would be longer, more stable, well-defined and fully characterised in literature, in order to evaluate the conformation adopted by the new peptide following incorporation of the dipeptide mimic and compare it to the native peptide.

To this end, the TrpZip peptide **157** was selected and its analogues were investigated. TrpZip stands for Tryptophan Zipper, a system designed by Cochran *at al.*¹⁹⁴ that is a water soluble 12-residue peptide (H-SWTWEGNKWTWK-NH₂). This peptide adopts a stable and monomeric β -hairpin, which is the minimal structural unit of an antiparallel β -sheet.¹⁹⁵ The hairpin is stabilised by two cross-strand Trp-Trp pairs, the indole groups of which stack in an edge-to-face manner (Figure 65).¹⁹⁶ Aromatic stacking is one of the strongest side-chain interactions in tertiary structure adopted by peptides and proteins.^{197,198} These interactions along with multiple intramolecular hydrogen bonds make the structure remarkably stable (T_m = 323 K) and TrpZip **153** has been reported to be the smallest peptide to adopt an unique tertiary structure without additional metal binding or formation of a disulfide bridge.¹⁹⁴

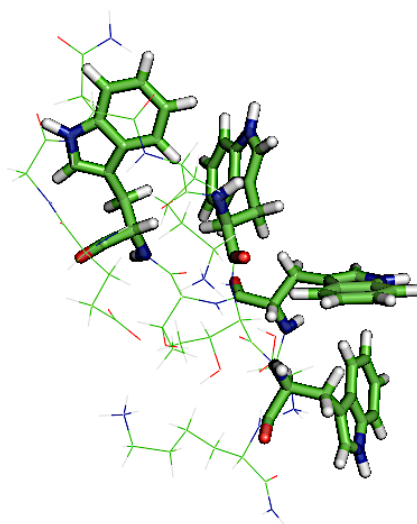


Figure 65: TrpZip 157 and Trp interactions

The interactions between indoles are considered to be hydrophobic in nature.¹⁹⁹ Folding of a β -hairpin can be initiated in two different ways: either the residues present in the peptide have a high propensity to form a turn structure which then brings the β -strands into close proximity (hydrogen bonds or side-chain interactions), or hydrophobic interactions between complementary residues on each strand allow formation of cross-strand hydrogen bonds which results in turn formation.²⁰⁰ Hydrophobic interactions are known to be a powerful driving force for formation of secondary structure²⁰¹ and TrpZip **157** has features which make it an excellent model for hydrophobic collapse and contribute to the structural stability of the β -hairpin.

Due to interactions between the indoles, its 3D structure and its overall sequence, TrpZip **157** displays a unique circular dichroism (CD) spectrum with intense positive-negative exciton coupled bands (Figure 66) in the far UV at 228 and 214 nm.²⁰²

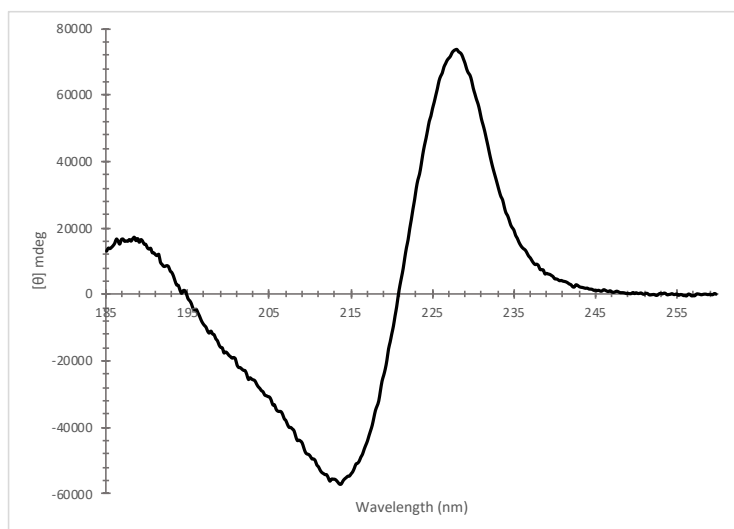


Figure 66: Far-UV CD spectrum of TrpZip 157

Because of the strong coupling of the chromophores in this region, the CD spectrum arising from their π - π^* transitions masks the weaker amide CD bands that are usually used for the determination of the secondary structure (positive bands at 195–220 nm).²⁰³ Which is why, the spectrum does not show the usual features expected of a β -sheet or a β -turn.

TrpZip and three analogues that vary in their turn sequence were synthesised and analysed (Figure 67). TrpZip was used as a reference peptide and GG-TrpZip **158** was synthesised in order to see the effect of replacing the Asn residue by a more flexible and achiral Gly residue. A new hybrid peptide **159** and **160** was then synthesised in which the turn sequence was replaced by the {Gly Δ Gly} dipeptide mimic described previously. The TrpZip analogues **158-160** were analysed and compared with the native form.

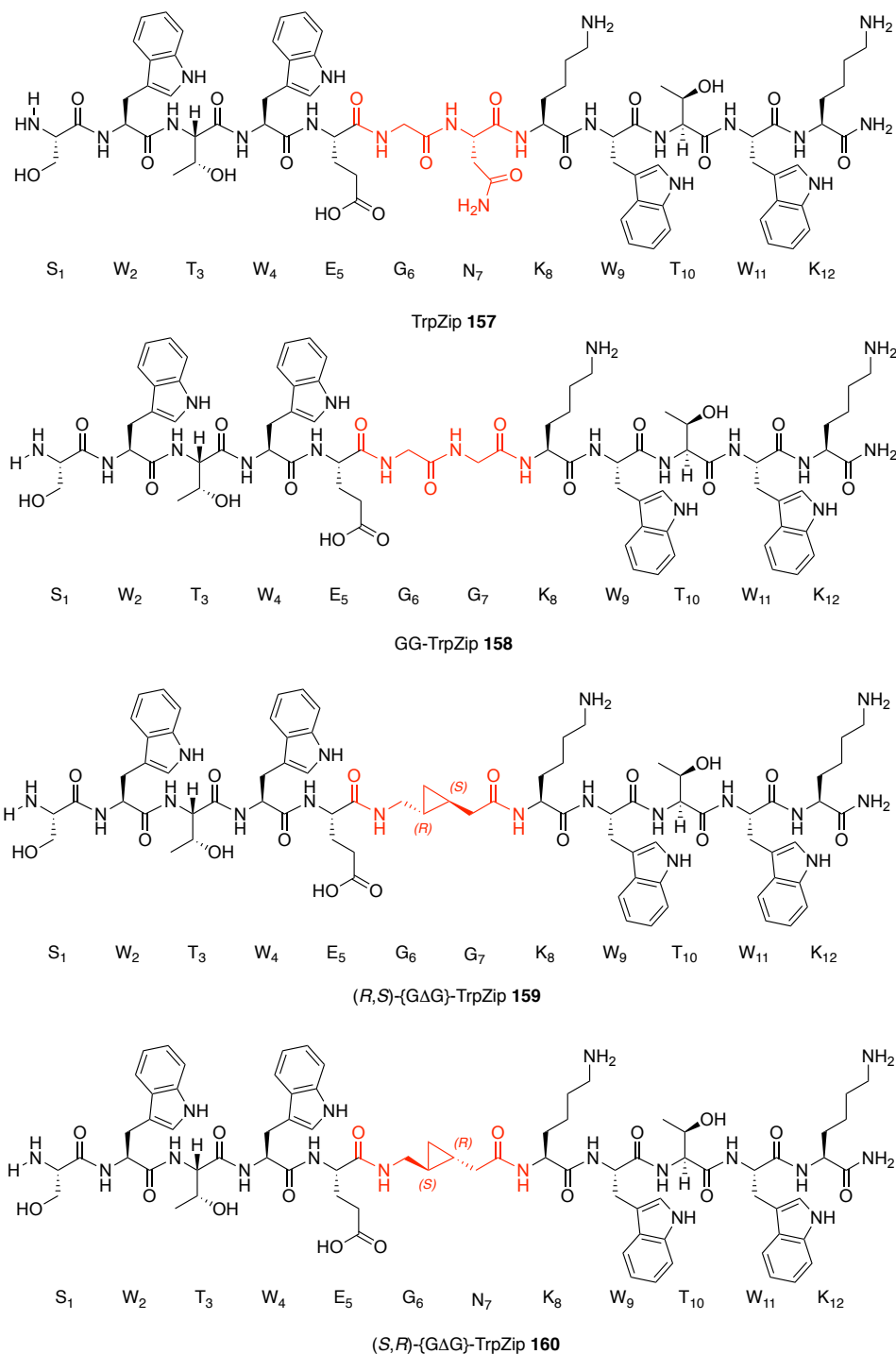


Figure 67: TrpZip and analogues synthesised

TrpZip was reported to fold to give a β -hairpin with a type II' turn involving the E-G-N-K amino acid sequence.¹⁹⁴ The aim of this study was to understand what happens when one or more of the amino acids is replaced in the turn sequence and to determine whether this is detrimental to β -hairpin formation.^{194,197,201,204} In particular, replacement of a peptide bond by a cyclopropane was to be explored to discover whether it stabilises the system or destabilises the β -hairpin to produce a random coil. To this end, all peptides were synthesised

and then analysed under the same conditions to obtain results that would permit direct comparison.

3.2. Synthesis of the TrpZip and its analogues

Microwave assisted solid phase peptide synthesis was used to synthesise the four compounds of interest. TrpZip **157** and GG-TrpZip **158** were synthesised using Tentagel S RAM resin (0.24 mmol/g loading) and Fmoc chemistry. A total of 4 equivalents of Fmoc protected L-amino acids and 4 equivalents of HCTU as coupling agent were used for the coupling reaction. After purification by reverse phase HPLC and lyophilisation, peptide content was determined by measuring the absorbance in 300 μ L of H₂O using a Nanodrop at 280 nm. The cycle in the synthesiser includes: Swelling of the resin, deprotection of the resin, coupling at 75 °C, deprotection of the amino acid that has been coupled, washing after each coupling and deprotection step, and precleavage in CH₂Cl₂. The resin was cleaved using TFA/TIS/H₂O (95:2.5:2.5) cocktail, which was then removed with a flow of N₂.

The synthesis of the {GΔG} analogues **159** and **160** was slightly different. H-KWTWK-Tentagel first sequence was synthesised on the peptide synthesiser using the method described before. Once the last Lys residue had been deprotected, (*R,S*)-Fmoc-{GlyΔGly}-OH **161** and (*S,R*)-Fmoc-{GlyΔGly}-OH **162** were coupled manually (1.1 and 2 equivalents respectively of dipeptide and 2 equivalents of HATU were used). The coupling was mixed overnight at rt for maximal conversion. Unreacted peptide was capped using acetic anhydride to avoid further coupling on it (truncated product was determined by LC-MS). The resin was then put in the synthesiser and the rest of the sequence was constructed following the same procedure as described previously.

3.3. Circular dichroism

3.3.1. Materials and methods

Far- and near-UV spectra were acquired with a Jasco J-810 spectropolarimeter using respectively a 0.01 cm and 0.1 cm pathlength cell. Peptide concentrations were determined by measuring the absorbance at 280 nm using a Nanodrop instrument (0.77–0.93 mg/mL in 20 mM phosphate buffer, pH 7). Thermal denaturation was measured in the near UV, using a 0.1 cm pathlength cell and the temperature varied from 5 °C to 80 °C in steps of 5 °C. Melting curves were acquired at 295 nm.

3.3.2. Results and discussion

TrpZip **157** exhibited a unique CD spectrum in near- and far-UV due to the interactions between the Trp residues. Two aromatic rings can interact to form a chiral pair of chromophores, which can be seen in the near UV (characteristic bands are observed between 250 and 320 nm),⁹ which indicated that the pairs of Trp of the peptides were in a chiral environment and in a well-defined tertiary structure. It was apparent that two cross-strand pairs of Trp were stacking with each other in this peptide resulting in bands at 287 and 295 nm. Bands in this region are generally taken as evidence for presence of a fixed and stable tertiary structure in proteins.

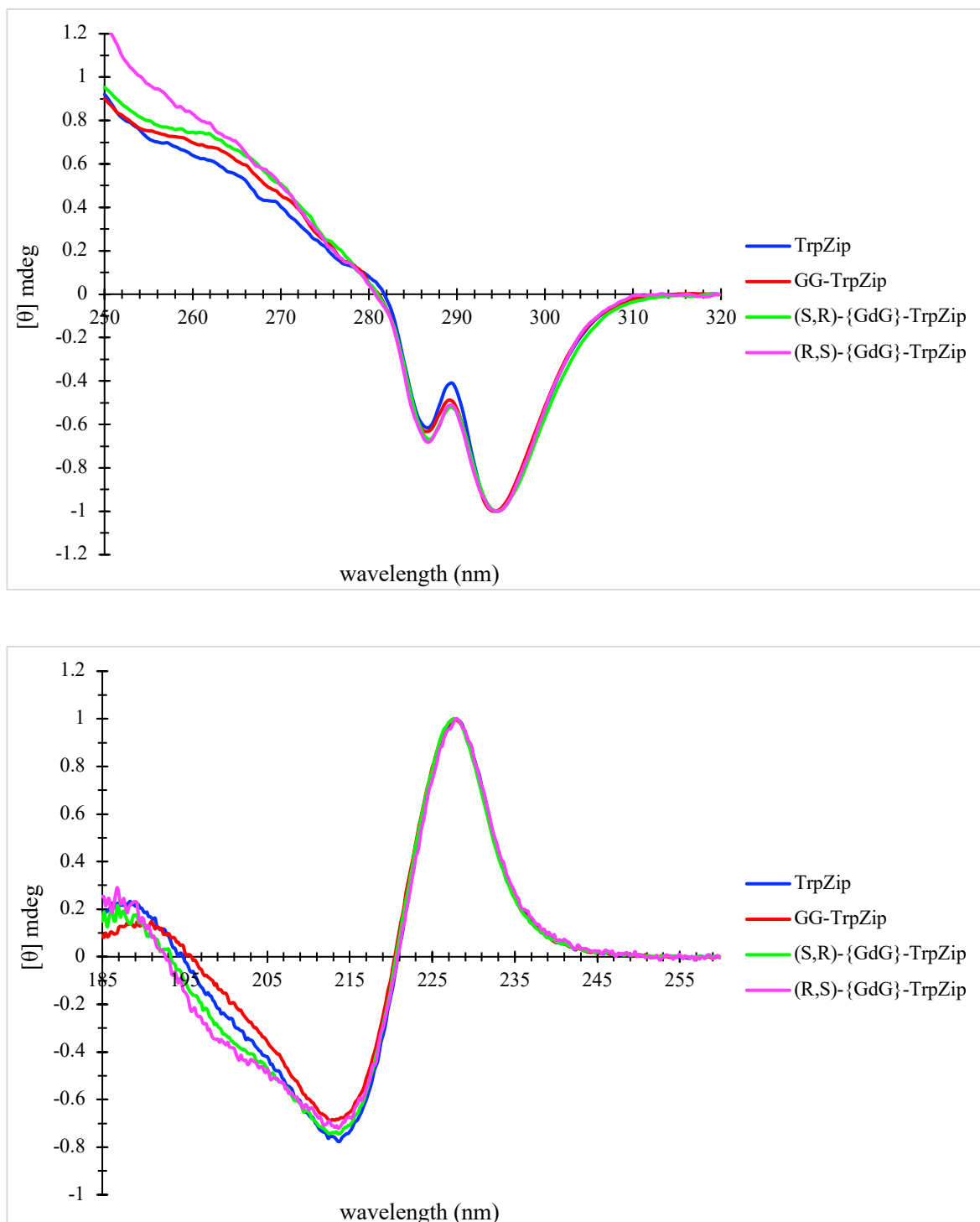
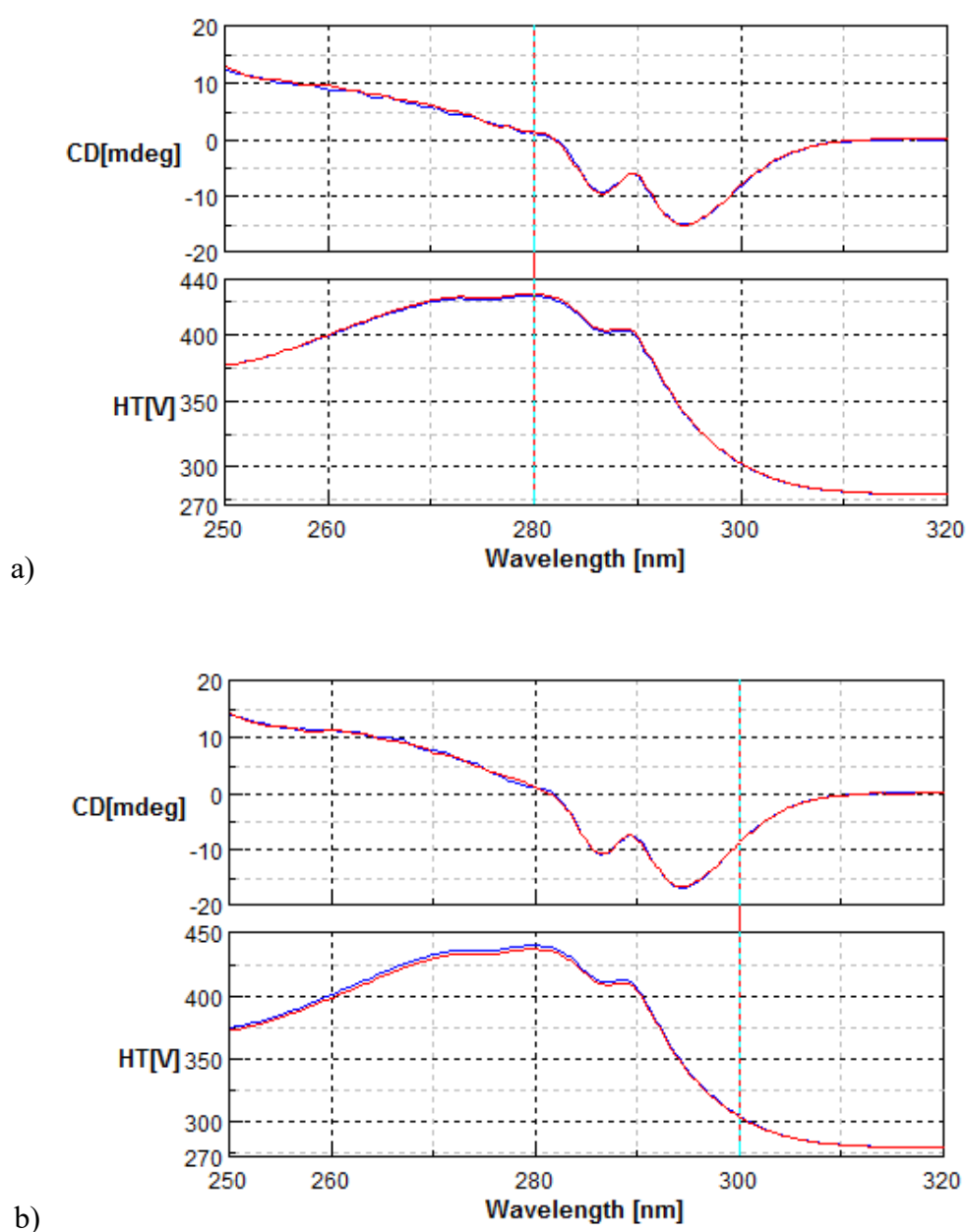


Figure 68: Near- and far-UV CD spectra, TrpZip 157 (blue), GG-TrpZip 158 (red), (R,S)-{GΔG}-TrpZip 159 (pink), (S,R)-{GΔG}-TrpZip 160 (green)

The CD spectra were normalised at the most intense peak for both regions (Figure 68). The exciton bands at 214 and 228 nm were observed in the far-UV as well as the two negative bands at 287 and 295 nm in the near-UV that were conserved in all the peptides. The interactions between the Trp were maintained and they were in the same environment. Comparison of the CD data for the analogues with that of the native form showed that the interactions were not changing in their nature; even though the turn sequence was modified,

either by swapping one residue or by replacing a planar peptide bond by a chiral non-planar cyclopropane unit. It was clear that cross-strand Trp pairs were still interacting with each other in the analogues **158**, **159** and **160**. Because this kind of interaction stabilises the β -hairpin and initiates the formation of it, it was possible to state that the analogues were also forming the β -hairpin. However, it was not clear whether they are as stable as the TrpZip **157**.

TrpZip peptide **157** had been reported to exhibit a reversible thermal unfolding. The CD spectra in the near-UV were recorded at 5 °C (blue), prior heating to 80 °C at which stage the peptide will be unfolded, and once it had been cooled back to 5 °C (red) (Figure 69).



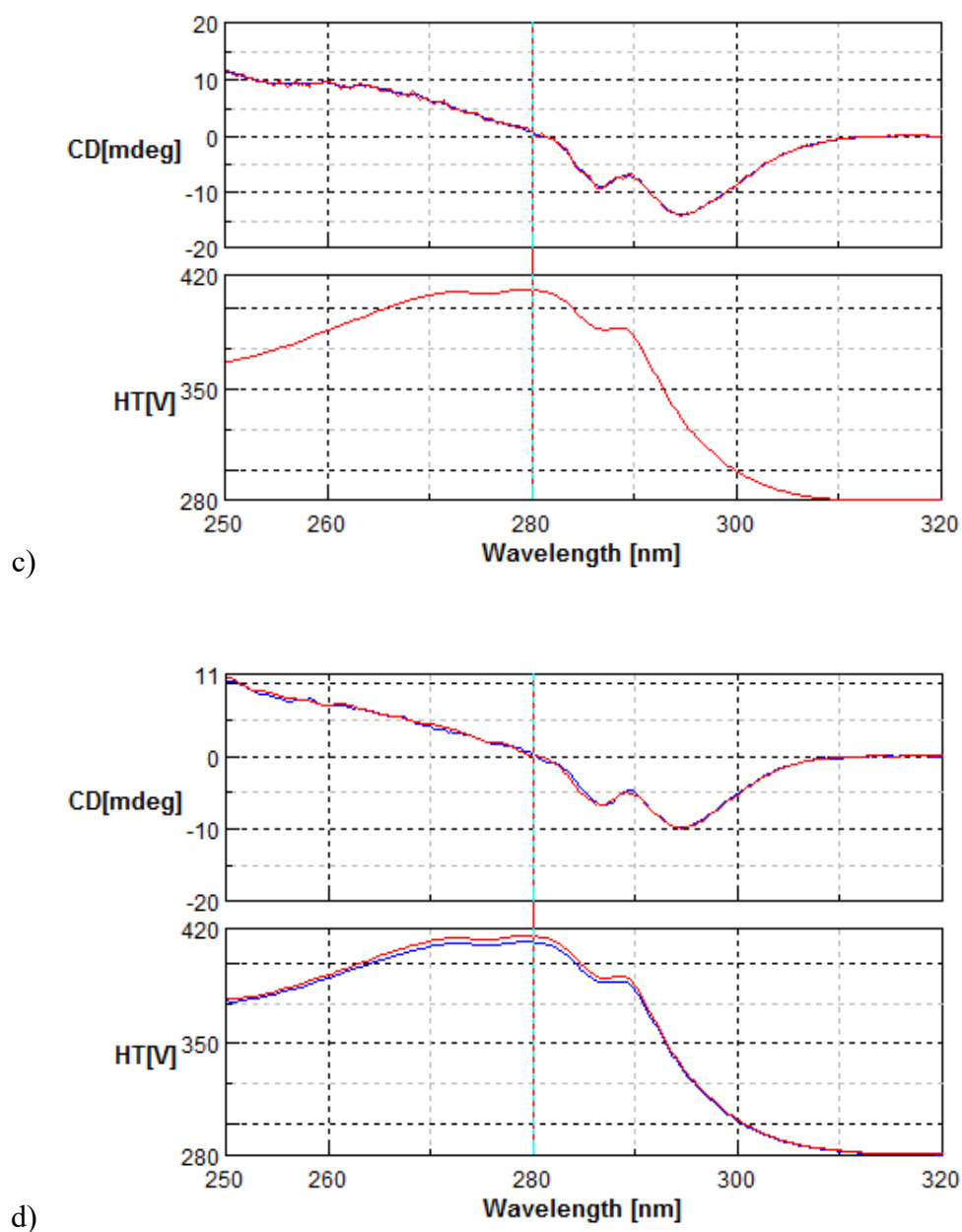


Figure 69: Near UV CD of a) TrpZip 157, b) GG-TrpZip 158, c) (S,R)-{GΔG}-TrpZip 160 and d) (R,S)-{GΔG}-TrpZip 159 at 5 °C, prior prior (blue) and following heating to 80 °C and cooling to 5 °C (red).

Following unfolding, the analogues behaved in a similar manner to the TrpZip **157** and they refolded to give exactly the same structure. The analogues all exhibited reversible thermal unfolding because the curves matched perfectly before and after heating. The near-UV CD spectrum is influenced by the behaviour of the side chains with regard to their position before and after heating. The data show that the interactions between the side chains were not modified after refolding. The analogues and the native peptide exhibited very similar stabilities in terms of their folding, which means they adopt the same preferred and stable conformation.

The evidence that the Trp side chains of the analogues were in a similar arrangement to those of the native form of TrpZip **157** prompted a more detailed study of the stability. The melting temperature (T_m) is the temperature at which 50% of the peptide is in an unfolded state. The higher it is, the greater the stability of the peptide. The data were acquired from 5 to 80 °C in increments of 5 °C for each peptide in the near UV (Figure 70). The arrow indicates the trend as a function of increasing temperature.

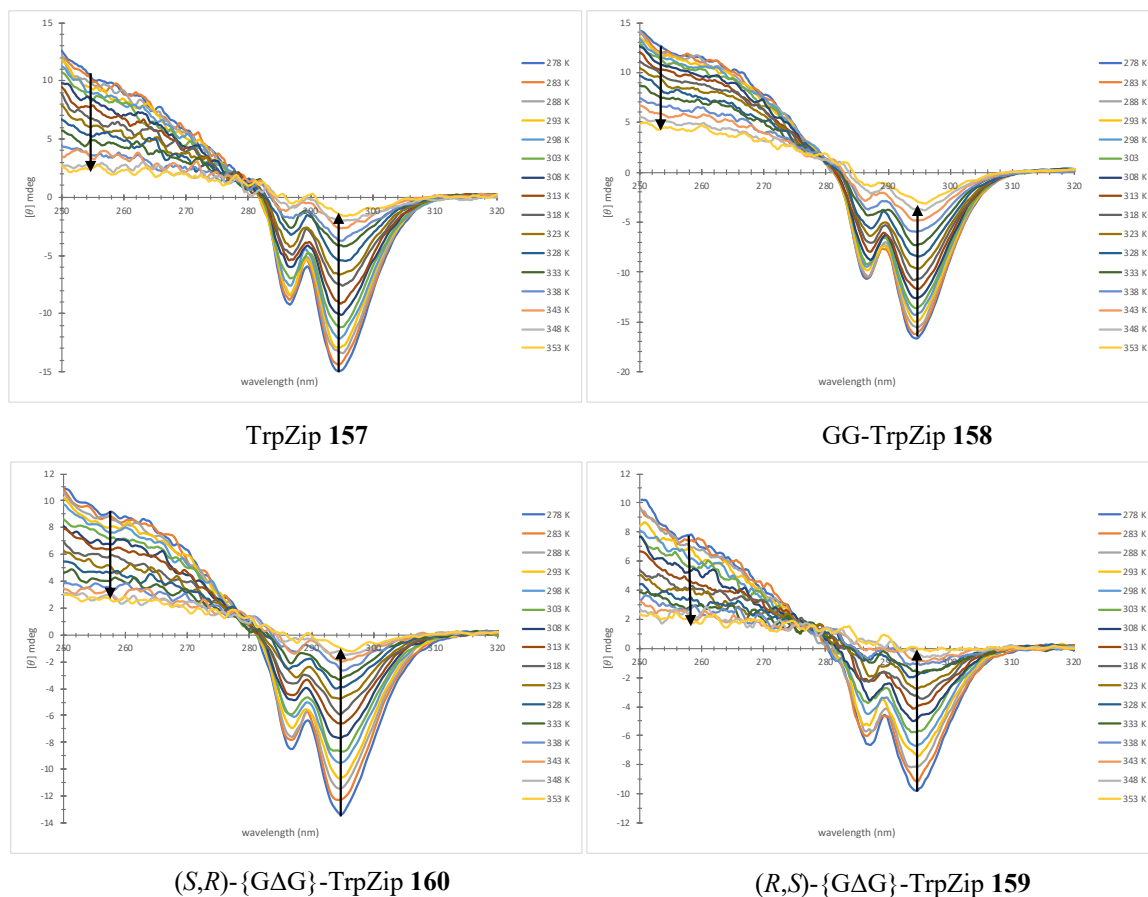


Figure 70: Thermal denaturation monitored by near-UV CD of TrpZip 157, GG-TrpZip 158, (S,R)-{GΔG}-TrpZip 160 and (R,S)-{GΔG}-TrpZip 159

All peptides followed the same trend and the CD intensities decreased upon heating, which indicates a secondary structural change from the hairpin to a disordered conformation by destabilising the intramolecular interactions. The data suggest a loss of the Trp cross-strand pairs interactions resulting in conformational mobility and a loss of signal. With this data it was possible to plot the thermal denaturation at a specific wavelength, which was chosen to be 295 nm (the most intense negative peak in near-UV, Figure 70), and also the fraction of peptide that is folded as function of the temperature, and thereby establish the stability of the peptides. Both sets of data demonstrated that the three analogues follow the same trend as the native peptide because the slope was similar for all peptides which indicates similar

stability (and consequently T_m). The two graphs allowed the degree of folding and the T_m to be estimated.

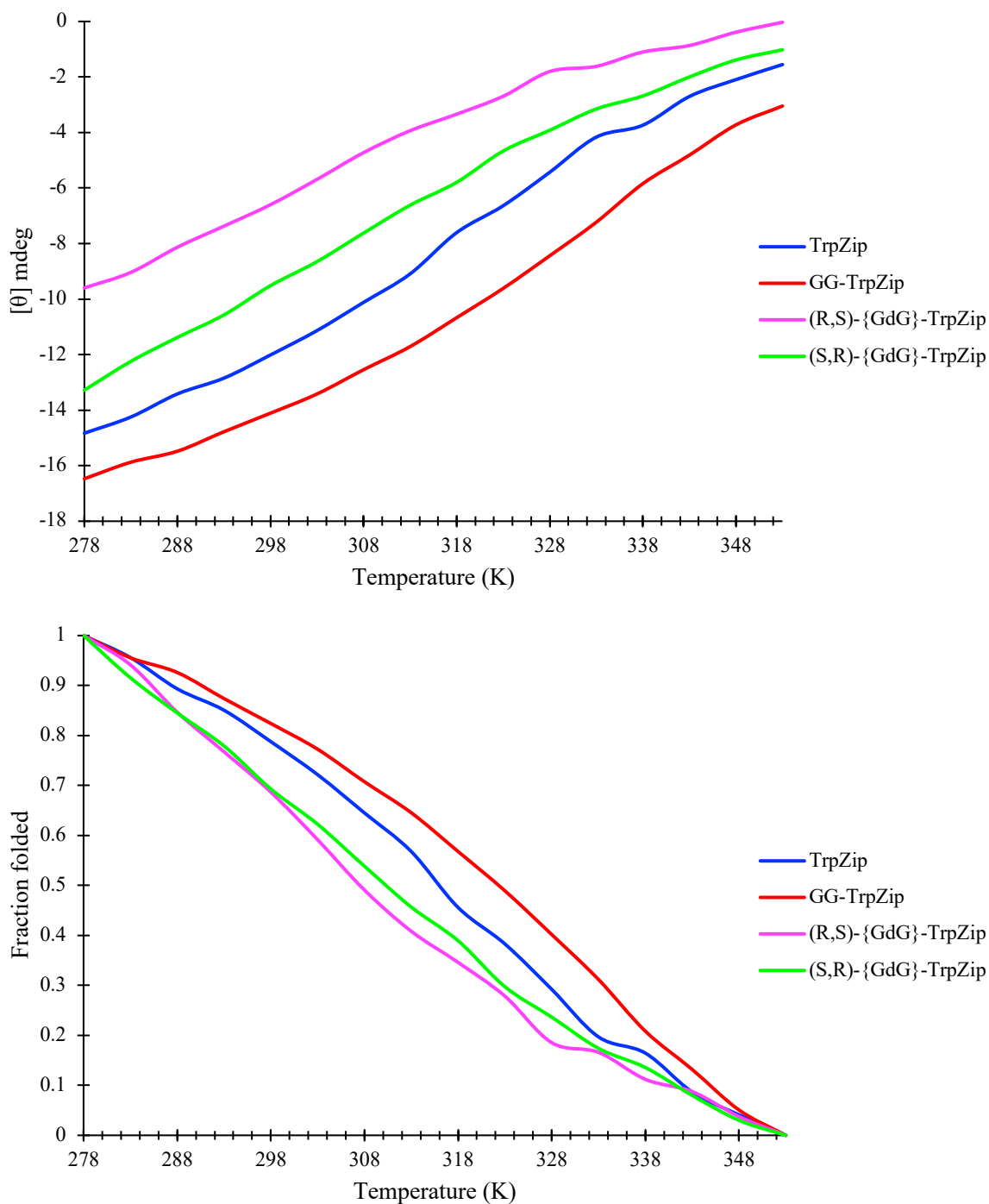


Figure 71: Thermal denaturation at 295 nm and fraction folded as function of the temperature of TrpZip 157 (blue), GG-TrpZip 158 (red), (R,S)-{GdG}-TrpZip 159 (pink), (S,R)-{GdG}-TrpZip 160 (green)

The fraction folded at any given temperature α was calculated by use of the following (equation 1):²⁰⁵

$$\alpha = \frac{\theta_t - \theta_U}{\theta_F - \theta_U}$$

Equation 1: fraction folded equation

Where θ_t is the observed ellipticity at any temperature, θ_F is the ellipticity of the fully folded form (chosen to be that at 278K), and θ_U is the ellipticity of the unfolded form (chosen to be that at 353 K, the highest temperature used). Subsequently, the T_m was calculated from the graph, it corresponds to the temperature where $\alpha = 0.5$. For the TrpZip native form **157**, the T_m was calculated to be 316.8 K (43.7 °C) which is similar to that reported in literature.¹⁹⁴ The GG-TrpZip analogue **158** showed slightly higher stability than the native peptide, with a T_m of 319.8 K (46.7 °C) i.e. 3 K higher than the original peptide. The Gly residue that had been used to replace the Asn residue in this analogue gave more flexibility in the turn sequence than that in the native peptide which results in less constraint in the interaction between the side chains of the peptide allowing it to adopt the most favourable and stable conformation. Both (R,S)-**159** and (S,R)-**160** (pink and green respectively in Figure 71) of the {GΔG} surrogate were incorporated into the peptide. The resulting analogues had similar stability with a T_m differing of less than 1.5 K (respectively 311.6 K/38.5 °C and 312.9 K/39.8 °C). Both of calculated T_m values were lower than for the native peptide and so they are slightly less stable than either the native or GG-TrpZip peptide **158**. This outcome is expected because replacement of the peptide bond with a cyclopropane delivers a more constrained system in which there is likely to be a difference in the strength or in the angle of the Trp interactions because the rings don't have the same degree of liberty to stack in the edge-to-face approach.

The results described above showed that there are stability differences between the various peptides but they adopt very similar conformations. The GG analogue **158** was found to have a higher stability than the native form, whereas the {GΔG} analogues **159** and **160** were found to be slightly less stable, suggesting a change in the interactions between the Trp, or a difference in the free energy of folding of the peptides (in ΔS or ΔH , and therefore in ΔG)

MD calculations were undertaken in order to understand the differences in the interactions (and thus the stability) and if these have an impact on the type of β -turn formed. Dr Drew Thomson has kindly provided all this data as part of a collaboration on this project.

3.4. MD calculation, a tool to understand the stability and folding pattern of peptides

The small size of this peptide allowed full-atom computation to be carried out. MD calculations have been performed in order to predict the conformation of the TrpZip **157** and its analogues **158-160**. Moreover, the measurements gave information on the nature of the β -turn formed. In this case, the turn sequence was examined closely by measuring the distance between the Glu-CO and Lys-NH and calculating the associated N-H-O angle (Figure 72), thus evaluating the formation of a crucial hydrogen bond within the turn or not.

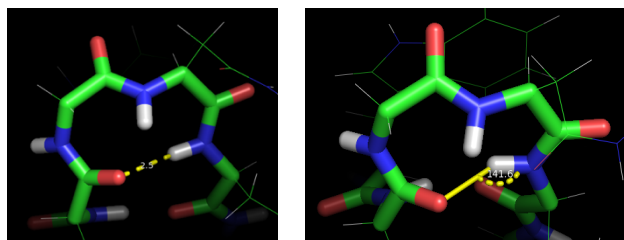


Figure 72: NH--OC distance and NHO angle within the turn studied

In proteins and peptides, the hydrogen bond between the CO_i and NH_{i+3} residues of the turn, has a length of 2.5 to 3.2 Å, the N-H-O angle from the same residues is about 130–180 °.²⁰⁶ Distance and angle were recorded for every 10th frame and plotted for each peptide (Figure 73). The red line corresponds to the maximum length of a hydrogen bond (3.2 Å).

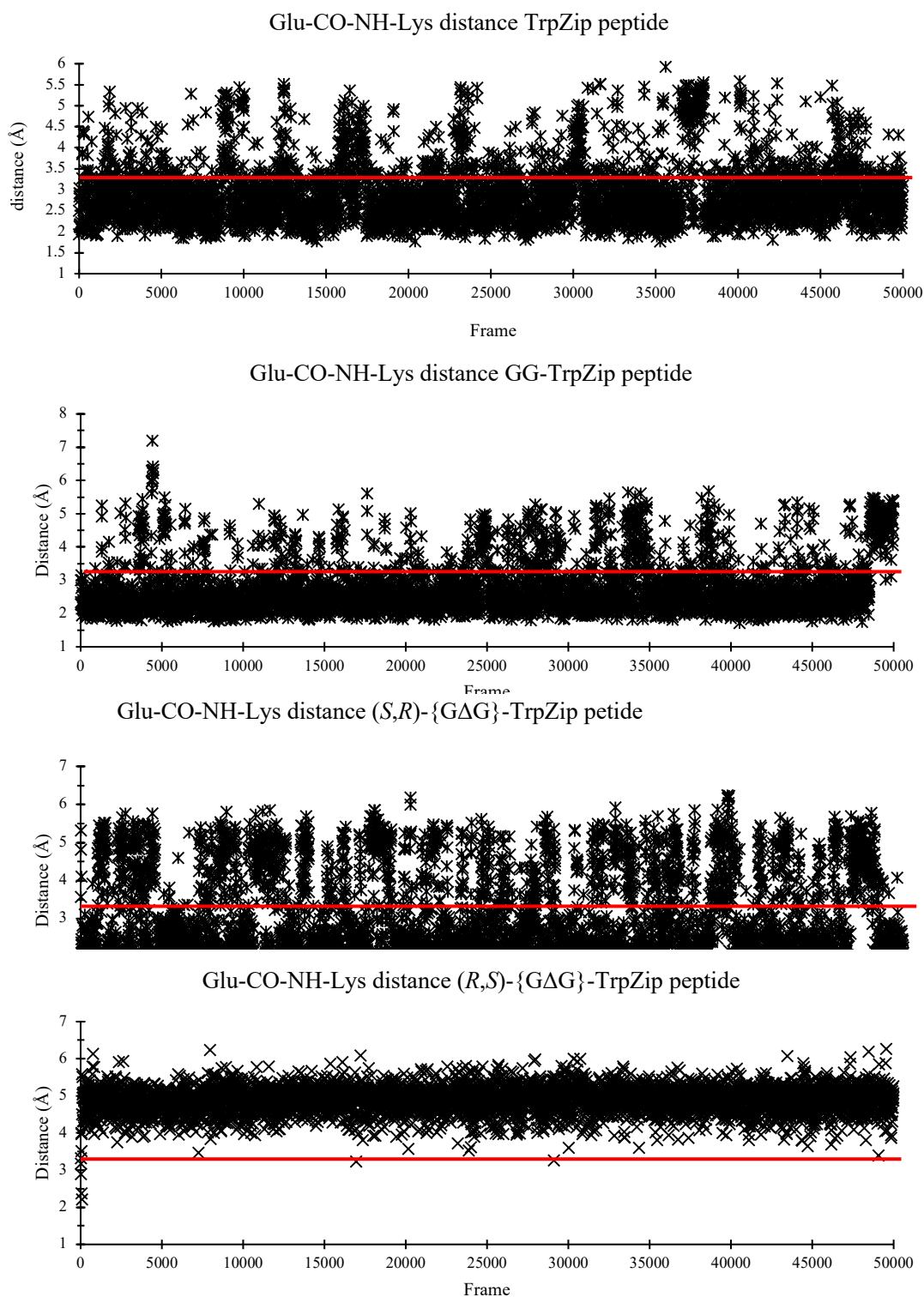


Figure 73: NH-CO distance in the turn for TrpZip 157, GG-TrpZip 158, (S,R)-{GΔG}-TrpZip 160 and (R,S)-{GΔG}-TrpZip 159

The distance between the Glu-CO and Lys-NH for the TrpZip peptide **157** (Figure 73, top graph), were within the range expected for a hydrogen bond (with an average distance of 2.91 Å within the 50000 frames). This vindicated our choice of the peptide as a reference because a β -turn was undoubtedly formed in this model system. GG-TrpZip **158** (Figure 73, 2nd graph) was for most of the frame within the hydrogen bond distance range (with an

average distance of 2.75 Å). It had been shown already that changing a residue within the turn was not detrimental to β -hairpin formation, but the results presented here supported this finding and showed that the crucial hydrogen bond is formed within the turn. (*S,R*)-{G Δ G}-TrpZip **160** (Figure 73, 3rd graph) showed a slightly different pattern and on average the distance was 3.07 Å (still within the range), but the graph showed more variation out of the range of distance with most of the frames having a distance smaller than 2.8 Å. This isomer brought the HBA and HBD groups into closer proximity than in the native peptide and thus enhanced hydrogen bond formation. In the case of (*R,S*)-{G Δ G}-TrpZip **159** (Figure 73, bottom graph), the simulation showed that the distance is out of the range for most of the frames (4.88 Å on average), suggesting that hydrogen bond could not be formed for this analogue. It corresponded to the analogue having the lowest *T_m* as measured by CD and so it is the least stable peptide (cf figure 71). Hydrogen bonds stabilise the secondary structure of peptides/proteins and so the higher the degree of hydrogen bonding, the higher will be the *T_m* because it will take more energy to break all of them when unfolding the peptide/protein. In a small system like TrpZip peptide, if a single hydrogen bond is missing, less energy is required to destabilise the whole system and so the *T_m* is lower. The lower stability of the system could be because the cyclopropane has separated the hydrogen bond donor and acceptor groups compared to native TrpZip **157** and so they might not be aligned with the required angle (between 130 and 180°). In order to explore this issue, the N-H-O angle of the hydrogen bond was measured (see Figure 72) for all peptides and they were shown to be within the expected range (Figure 74, only (*R,S*)-**159** peptide is shown as they are all similar).

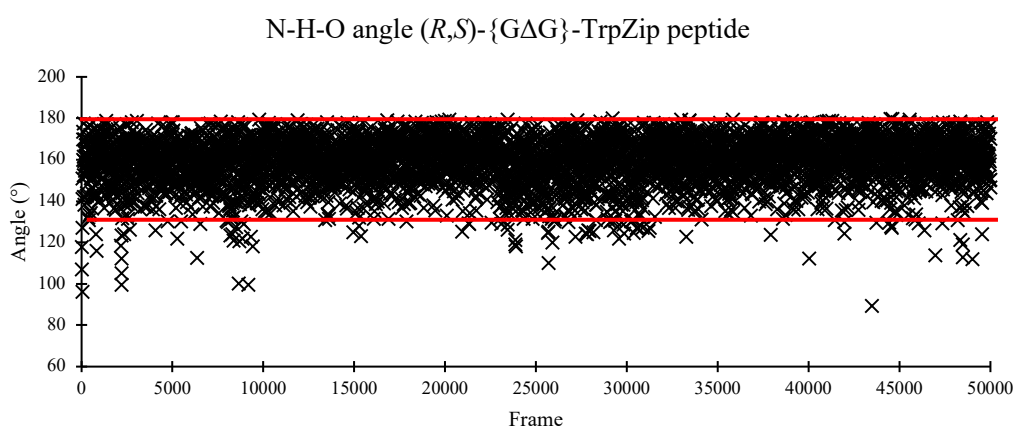


Figure 74: *N-H-O angle within turn of (*R,S*)-{G Δ G}-TrpZip 159*

Even though, (*R,S*)-{G Δ G}-TrpZip **159** had the correct angle in most of the frames of the simulation, the hydrogen bond donor and acceptor groups were located too far away in space.

Nevertheless, when the CD results are considered, the reduced hydrogen-bonding capabilities of the system did not appear to have any consequences with regard to formation of the β -hairpin (as the CD was very similar to that of the native peptide, see Figure 68). This finding supports the argument that the turn was not initiating the formation of the β -hairpin, but instead Trp-Trp interactions were initiating and stabilising the secondary structure leading to formation of the β -turn. The next challenge was to discover whether different types of turn were formed by determining the torsion angles within the turn.

The torsion angles (ϕ , ψ and ω) are the main factors in dictating how the protein folds. As already described in the introduction chapter, the ϕ angle of the i residue is defined by the torsion $C_{i-1}-N_i-C\alpha_i-C_i$, ψ by the torsion $N_i-C\alpha_i-C_i-N_{i+1}$, and ω by the torsion $C\alpha_i-C_i-N_{i+1}-C\alpha_{i+1}$ (Figure 75).²⁰⁷ The ϕ and ψ angles provide the flexibility required for the fold, ω is restricted due to the planarity of the peptide bond and is set to 180° .

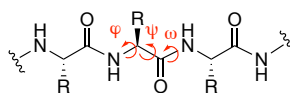


Figure 75: torsion angles in a peptide chain

Ramachandran plots are a convenient way in which to visualise the distribution of the dihedral angles (or torsion angles) of every amino acid in a protein structure (Figure 76).²⁰⁸ They are used to identify the secondary structure of a peptide or a protein. Ramachandran plots of a particular protein can also provide a good indication on the stability of its 3D structure.²⁰⁹ It is a PDB (protein data bank) distribution based on energy for all residues that comprise proteins.

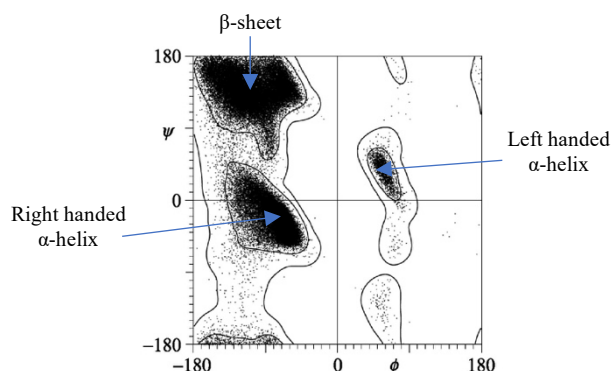


Figure 76: Ramachandran plot.²¹⁰

The plots are typically split in two regions: the forbidden and allowed regions. The forbidden region corresponds to the combination of angles where there would be unfavourable steric interactions between the atoms in the chain (white “background” in the figure). The allowed region represents the distribution of torsion angles favourable for formation of a stable secondary structure (black dots).²¹¹

β -Turns are classified according to the value of the dihedral angles of the central residues (in our case, Gly-6 and Gly-7, Asn-7 or Δ Gly-7). Three rules need to be respected for the system to be classified as a β -turn: the distance between the i and $i + 3$ C α s is less than 7 Å, the two central residues ($i + 1$ and $i + 2$) should not show helical properties (determined by their torsion angles), and a cross-strand hydrogen bond between residue i and $i + 3$ should be present.²¹²

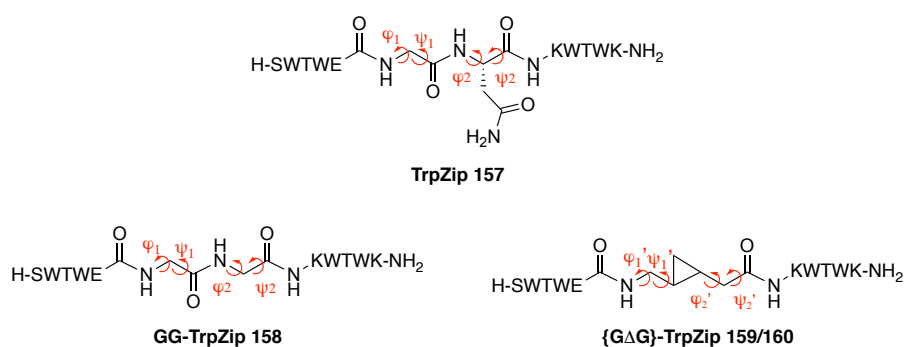


Figure 77: Dihedral angles in TrpZip and analogues

For the the $\{G\Delta G\}$ analogues **159** and **160**, the angles were measured following the same rules as for native peptides (*i.e.* defined by four points in space, through the atoms on the main chain of the turn, not through the methylene group of the cyclopropane); φ'_1 by the torsion C_E-N_G-C α -CH, ψ'_1 by the torsion N_G-C α -CH-CH, φ'_2 by the torsion CH-CH-C α -C_G

and ψ'_2 by the torsion CH-C α -C $_G$ -N $_K$). de Brevern has described and created Ramachandran plots for various types of β -turn (figure 78). The arrows represent the direction going from the $i+1$ residue's dihedral angle (ϕ_1, ψ_1) to the $i+2$ angles (ϕ_2, ψ_2). It is important to note that the dihedral angles chosen for the cyclopropane mimics cannot be used as a proof for β -turn formation. In the case of the analogues, a planar moiety has been replaced by a non-planar cyclopropane (sp^2 hybridized atoms are replaced by sp^3 centres) and so their physical and chemical properties are different. Consequently, the Ramachandran plots for the {G Δ G} analogues **159** and **160** provide qualitative rather than quantitative information.

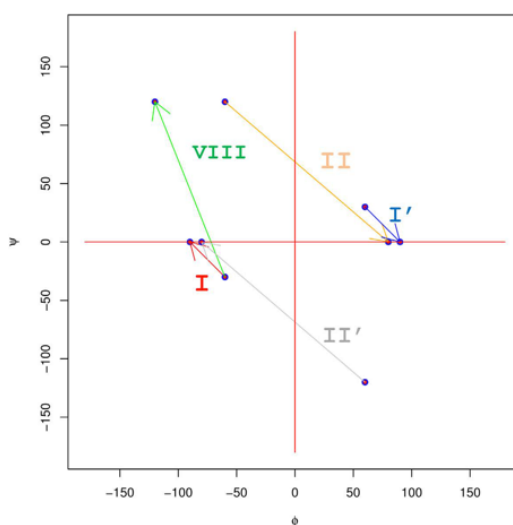


Figure 78: Ramachandran plot for different type of turn²¹²

The MD calculations provided by Dr. Drew Thomson, allowed the dihedral angles of the central residues of the turn to be measured for 5000 frames i.e. every 10th frame among 50,000. This allowed prediction of the type of turn adopted by the native form (and whether it corresponds to that reported by Cochran *et al.*) and by the GG-TrpZip **158**. The black dots correspond to the ϕ_1, ψ_1 angles ($i+1$ residue) and the blue dots to the ϕ_2, ψ_2 angles ($i+2$ residue).

The Ramachandran plot of TrpZip **157** (Figure 56) showed that a type II' β -turn is formed, a finding that agrees with the finding of Cochran *et al.*. The CD spectrum of GG-TrpZip **158** (see Figure 68) overlays closely with the native form of the TrpZip, and consequently they adopt the same conformation. However, the Ramachandran plots for the peptides are different which indicates that GG-TrpZip **158** adopts another type of turn. The ϕ_1, ψ_1 angles were found to be in the same region, which was expected as is it the unchanged Gly residue, and the rotations around the bonds (thus the torsion angles) were not impacted by

replacement of the adjacent residue. While, ϕ_2 and ψ_2 were found to have almost opposite values when compared to those of TrpZip **157**.

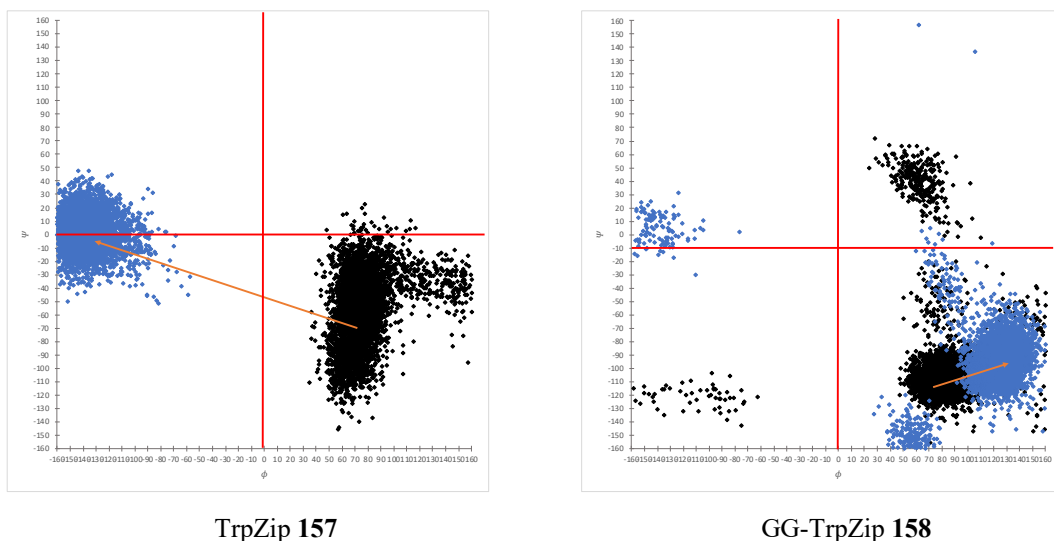


Figure 79: Ramachandran plots for TrpZip 157 and GG-TrpZip 158

The direction taken did not correspond to any of the types of turn that had been described by de Brevern. Several hypotheses may be ventured to explain this finding: another type of β -turn, not described in literature, could have been formed (possibly a new type IV turn); a turn other than a β -turn could have been formed (e.g., a γ -turn); or a turn has not been formed because the two Gly residues provide too much flexibility and so a turn is not crucial for a stable conformation to be adopted by the peptide.

(*S,R*)-{G Δ G}-TrpZip **160** (Figure 80) had ϕ'_1 and ψ'_1 angles that are the same region as the TrpZip. Pleasingly, the torsion angles measured on the C-ter of the dipeptide surrogate, ϕ'_2 and ψ'_2 , were also in the same region as the native form and so it appeared that this analogue was forming a type II' β -turn. This finding is in agreement with the CD spectrum in the near-UV (see figure 68), which matched that of TrpZip **153** perfectly and thereby showed the Trp were in the same chiral environment and interacting in the same way in both compounds. Because the Trp initiate formation of the β -hairpin, if the interactions are very similar the same type of turn would be expected.

For the (*R,S*)-**159** (figure 80), the key torsion angles were rotated by 180°. ϕ'_2 and ψ'_2 were found to have opposite values compare to the (*S,R*)-**160**. ϕ'_1 was found to be unchanged whereas ψ'_1 was also found to be the opposite. Fundamentally, all dihedral angles appear to be flipped except ϕ'_1 , resulting in a different type of turn that has the features of a type I'

turn when compared to de Brevern's Ramachandran plots. The stacking might be slightly deviating due to the rigidity of the cyclopropane. Surprisingly, despite the fact that the turn lacked a hydrogen bond (see Figure 73), a type of turn could still be discerned in the plot.

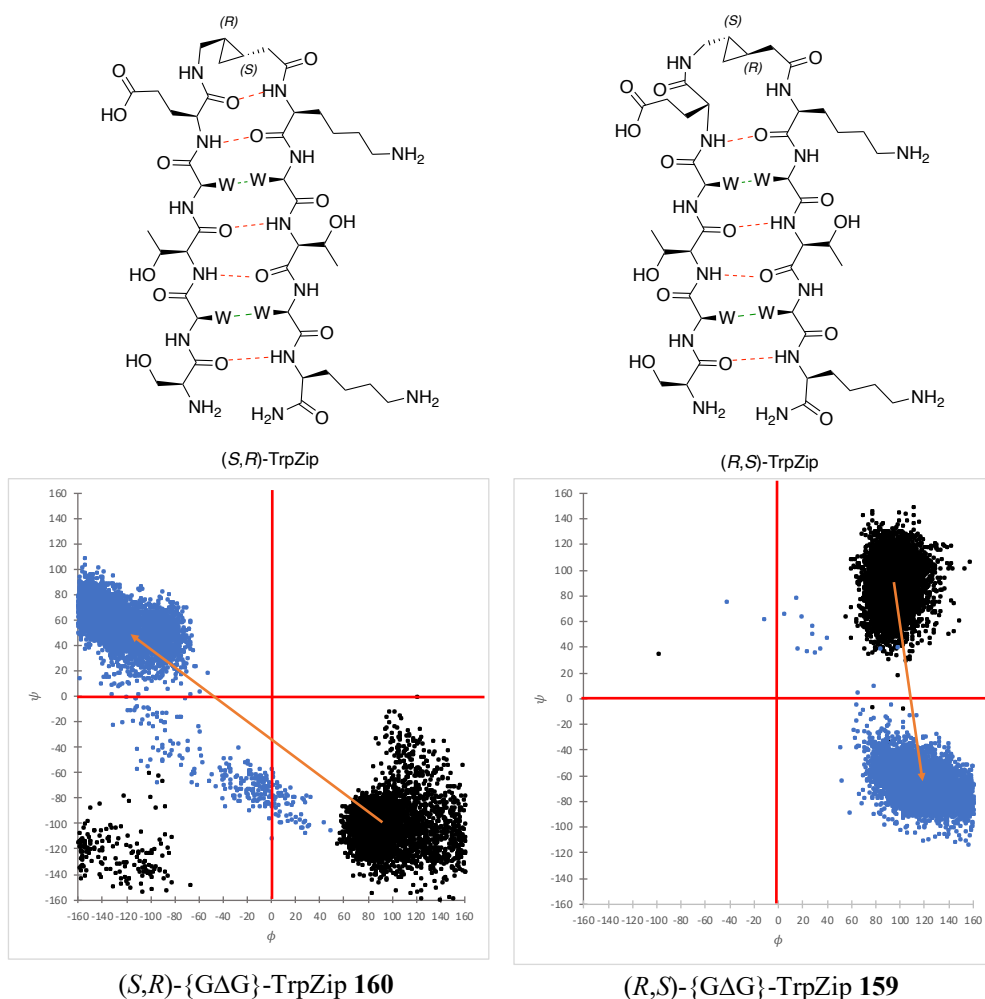


Figure 80: Ramachandran plot of cyclopropane analogues

The results presented above show that there are changes in the turn conformation of the analogues when compared to that of the native TrpZip **157**. However, these changes did not have an impact on the hairpin conformation adopted by all peptides (as shown by CD spectroscopy). The CD spectra were obtained in the near-UV region and show the Trp side chain contribution. Pleasingly, all peptides have essentially the same CD spectrum, which proves that the Trp side chains are in the same environment and interact in the same way as in TrpZip. Furthermore, the non-natural unit incorporated within the peptide is equally stabilising the β -hairpin (T_m slightly lower, which indicates similar stability). The cyclopropane is a rigid and compact group and the hypothesis is that the ΔH is similar to that of TrpZip **157** but ΔS (defined by the side chains) varies between the peptides. As a

consequence, the value of ΔG would be expected to vary, which could explain why the T_m values for the analogues are slightly different.

3.5. NMR conformational analysis

3.5.1. Material and method

NMR samples contained 0.25 to 1.30 mM peptide (measured by absorbance at 280 nm) in 95 % H_2O /5% D_2O -TSP (TSP used as chemical shift reference) in 10 mM pH 5.5 acetate buffer (AcOD was used for the preparation of the buffer and the pH was adjusted using aq. 10 mM KOH solution). All spectra were acquired on 600 MHz Bruker spectrometer at various temperatures (278–308 K). Double quantum filtered correlation spectroscopy (DQF-COSY), total correlation spectroscopy (TOCSY), and nuclear Overhauser effect (NOESY) spectroscopy were acquired with gradient selection and excitation sculpting for water suppression.

3.5.2. Results and discussion

Techniques in NMR spectroscopy have been well developed rapidly over the past 40 years.²¹³ Secondary structure can be determined by several methods: the proton ($H\alpha$) and carbon ($C\alpha$) chemical shifts,²¹⁴ the spin-spin coupling or $^3J_{NHC\alpha H}$ coupling constant and the Karplus equation,²¹⁵ NOE cross peaks,²¹⁶ etc... Furthermore, NMR spectroscopy is a great tool to use to determine whether the peptide is a monomer (concentration dependant study, chemical exchange), and to detect and differentiate between intra- and inter-molecular hydrogen bonds (chemical shift varying with temperature or hydrogen-deuterium exchange).²¹⁷

2D NOESY experiments are a convenient tool to determine the conformation adopted by a peptide. If the peptide adopts an antiparallel β -sheet, the NOESY spectrum shows intense sequential cross peaks between NH_i and $H\alpha_{i-1}$. 2D NOE experiments were investigated in this work in order to analyse the folding of TrpZip and its analogues. The protons were assigned using the sequential assignments method on 2D COSY and TOCSY spectra.²¹⁸ Characteristic sequential NOE cross peaks were observed for TrpZip **157**. The presence of long range $H\alpha$ - $H\alpha$ or NH - $H\alpha$ cross-peaks is a good indicator of secondary structure and backbone interactions that stabilise the system. It is particularly important in the case of TrpZip **157**, because its main structural characteristic is stacking between the indole groups of the Trp residues bringing the $H\alpha$ s of these residues in close proximity. Intense cross-peaks

were observed between H α s of Trp 2-Trp 11 and Trp 4-Trp 9 (Figure 81), indicating that these Trp residues were interacting with each other in this order confirming the conformation adopted by this peptide.

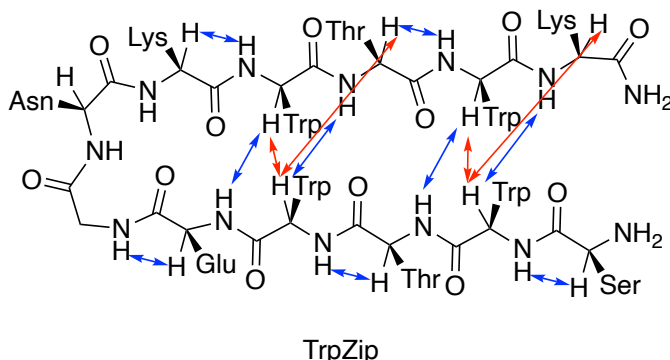


Figure 81: H α -H α cross-peaks (red) and NH-H α cross-peaks (blue) representation in TrpZip 157*

*In the interests of clarity, not all cross-peaks have been represented.

Some other H α -H α cross-peaks were observed between cross strand Trp-2 and Thr-10, supporting the interactions between Trp-4 and Trp-9. NH-H α cross peaks were also observed between residues located on both strands of the peptide (e. g. NH-Trp-2 with H α -Trp-11, blue in Figure 81). The observation of these cross-peaks in addition to the CD data that had been obtained provides conclusive confirmation that TrpZip **157** is adopting a β -hairpin conformation.

The aim was then to analyse the other peptides and identify the cross peaks observed. All of the peptides were assigned using the same method described previously (sequential assignments from COSY and TOCSY spectra). Sequential NH $_i$ -H α_{i-1} cross-peaks, which are a distinctive feature of antiparallel β -sheet, were observed for the all the analogues. Therefore, all analogues adopted the same conformation, which supported the the CD data that had been obtained. However, H α -H α NOESY cross-peaks for GG-TrpZip **158** were slightly different (Figure 82). In this case, Trp-Trp cross-peaks were present, showing that there are interactions between them, but there are also through-space interactions between Trp-4 and the two Gly residues that were not observed in TrpZip **158** (with Gly and Asn). The turn was more flexible due to the replacement of the Asn residue with Gly, allowing more interactions between the side chains around the turn and this was also showing that the Trp-4 is stacking on the top of Trp-9.

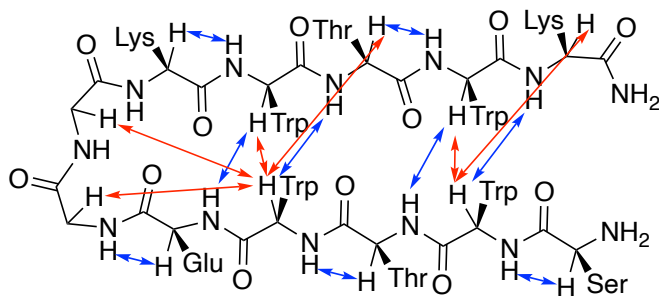


Figure 82: $H\alpha$ - $H\alpha$ cross-peaks (red) and NH - $H\alpha$ cross-peaks (blue) representation in GG-TrpZip 158*

*In the interests of clarity, not all cross-peaks have been represented.

More NH - $H\alpha$ NOESY cross-peaks were observed from residues on the two strands, which supports the hypothesis of a more stable flexible system, as determined by the CD spectra obtained and the higher T_m calculated (see Figure 71). Other expected cross-strand cross-peaks were also observed for this analogue.

When the 2D NOESY of the {G Δ G} analogues were analysed, that of (*S,R*)-{G Δ G}-TrpZip **160** exhibited an interesting feature (Figure 83). The NH s of the backbone, shown in the spectrum below, were exchanging with other NH s with smaller intensity (cross peaks highlighted in the figure).

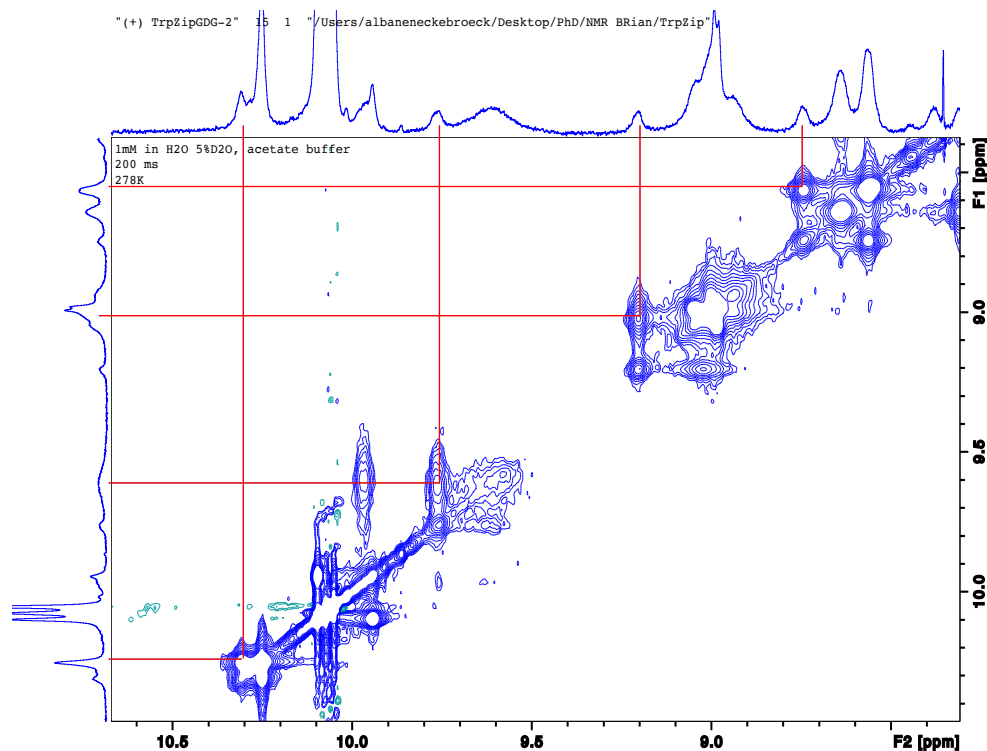


Figure 83: NOESY spectrum in NH region of (S,R)-{GΔG}-TrpZip 160

Two different circumstances could explain this: either the protons were exchanging with the protons of another molecule (intermolecular interactions), which implies dimer formation, or it was exchanging with another conformation adopted by the peptide. A concentration dependant NMR study was then undertaken to discover whether the “exchanged” peaks get smaller with the concentration. If the peaks are reduced in size with a decrease in the concentration, it means that the peptide is interacting with another molecule. To this end, ^1H NMR of the peptide was acquired at four different concentrations, from 0.125 mM to 1 mM (Figure 84).

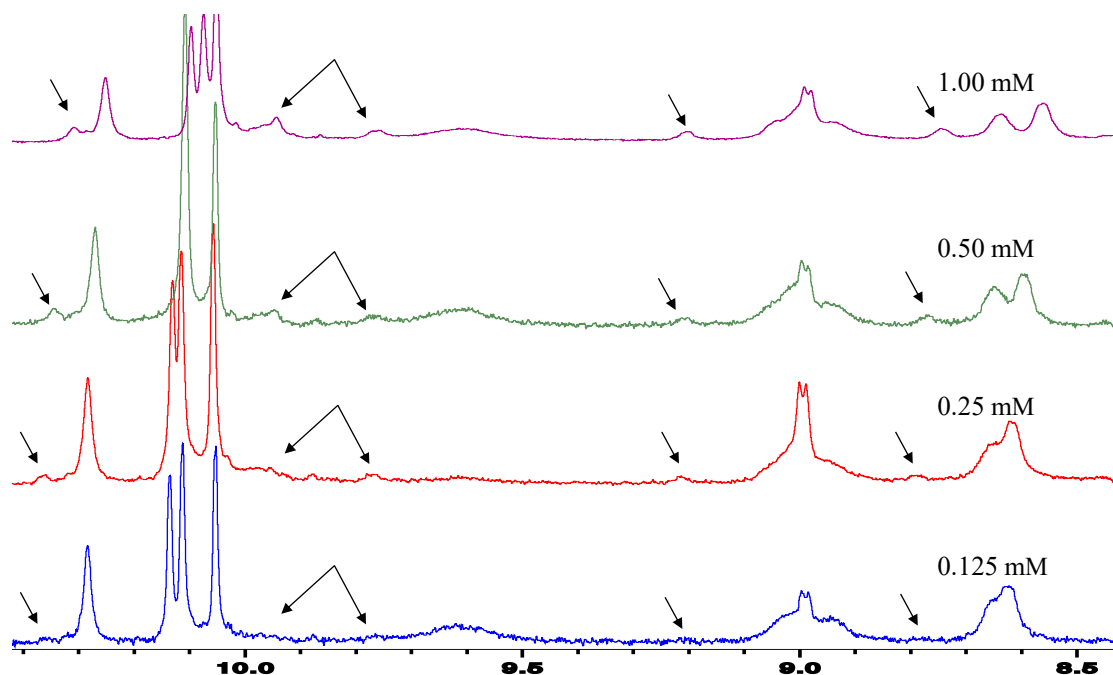


Figure 84: Concentration dependant NMR spectra of (S,R)-{GΔG}-TrpZip 160

The small peak (indicated with an arrow), became smaller with the concentration, which meant that this peptide was interacting with another molecule at higher concentration and forming a dimer. This observation might explain why a lower T_m was observed for this peptide. The 2D NMR experiments were performed at 0.25 mM because the signals were of better quality than those at lower concentration. The other enantiomer (R,S)-{GΔG}-TrpZip **159** did not show this concentration dependency and was behaving as expected for a monomer. Therefore, a higher concentration could be used for the 2D experiments and a 0.4 mM sample was prepared. For both analogues, long range NH-H α and H α -H α NOE cross peaks were not observed, but all sequential NH $_i$ -H α_{i-1} were present. The intensities of long-range NOE cross peaks are lower than those of the sequential cross peaks, so these peaks could probably not be observed at low concentration. It would be necessary to perform the NMR experiments at higher concentration in order to observe such cross peaks.

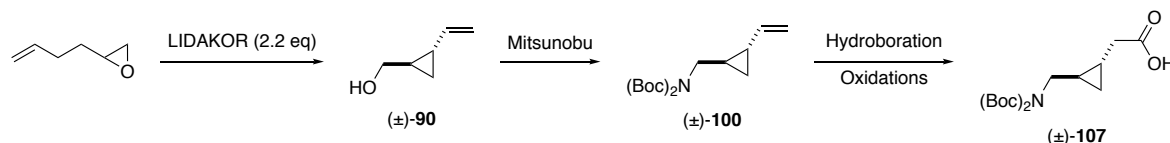
3.6. Conclusion

The β -hairpin conformation adopted by TrpZip peptide **157** has been confirmed by the combination of CD and NMR analysis. The replacement of the Asn-6 by a Gly did not prevent β -hairpin formation and the analogue was found to be slightly more stable than the native peptide with a higher T_m calculated. The analogues (*S,R*)-{G Δ G}-TrpZip **160** and (*R,S*)-{G Δ G}-TrpZip **159** also have features consistent with a β -hairpin conformation when analysed by CD and have similar stabilities to the native peptide. NMR analysis of (*S,R*)-{G Δ G}-TrpZip **160** showed that this analogue has concentration-dependent behaviour for and it appears to be interacting intermolecularly with another molecule and forming a dimer at higher concentrations. The spectra obtained from NOESY experiments did not exhibit any long-range cross peaks that had been observed for TrpZip **157** and GG-TrpZip **158**. However, characteristic sequential cross peaks were present in the spectra of both analogues. The promising CD data obtained for samples at higher concentration than used for NMR analysis, indicate that the NMR experiments would need to be performed at higher concentration in order to observe the expected long-range cross peaks. These experiments alongside other conformational analysis are currently undertaken by collaborators in order to better understand the folding properties of our analogues.

Chapter 4

Conclusions

In conclusion, the cyclopropane moiety was initially installed via a carbene mediated cyclopropanation, resulting in a mixture of *cis*- and *trans*-isomers. Epimerisation followed by resolution allowed to access to enantioenriched precursors **90**. Due to poor reproducibility and low overall yield, the route was revised towards the synthesis of racemic mixture of **90** in one step by using superbase-mediated rearrangement affording exclusively *trans*-**90** in a very good yield. It was then possible to install the N-terminus under Mitsunobu conditions. The terminal alkene present in the molecule allowed to access to the C-terminus by hydroboration and successive oxidations in decent overall yield. The racemic (\pm)-Boc₂-{GlyΔGly}-OH **106** was obtained in 4 steps (Scheme 43).



Scheme 43: (\pm)-Boc₂-{GlyΔGly}-OH **107** synthesis

Attempts to resolve the racemic mixture at different stage of the synthesis were investigated and the best route was found to be the amide coupling on carboxylic acid **85** using (*R*)-phenylglycinol after optimised oxidations. The two diastereoisomers were obtained in a reasonable yield (Scheme 44). After hydrolysis and reduction enantioenriched alcohol **90** was obtained, which then underwent the same reactions as the racemic mixture.

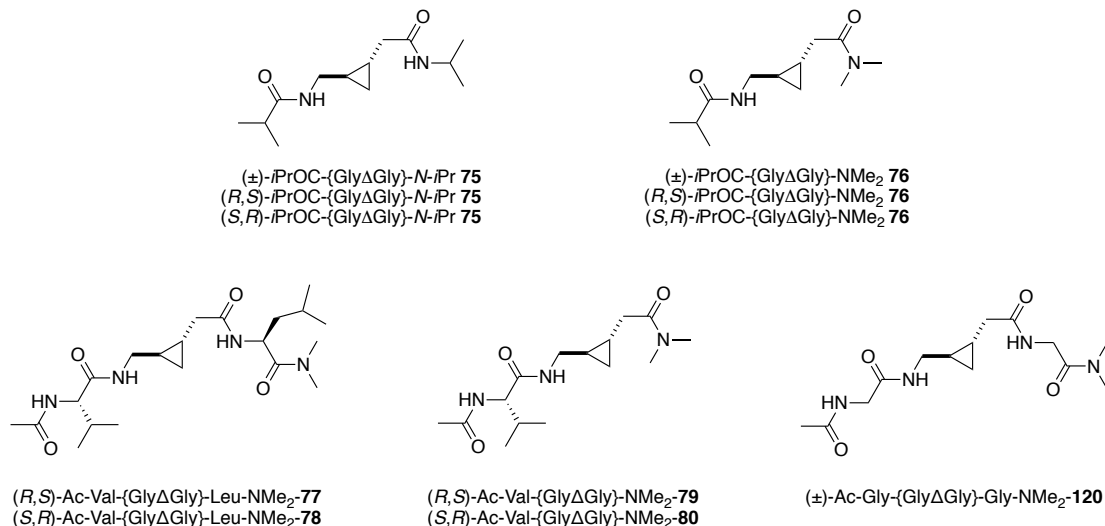


Figure 85: Peptides designed during this work

Esters (\pm) -*i*PrOCO-{Gly Δ Gly}-*N*-*i*Pr **127** and (\pm) -*i*PrOC-{Gly Δ Gly}-*O*-*i*Pr **129** were synthesised from intermediates previously obtained in this work. They allowed a better understanding of the hydrogen bonding network formed in the turn mimetics.

The {Gly Δ Gly} surrogate was proven to promote the formation of a turn by spectroscopic measurements by showing evidence of strong *intramolecular* hydrogen bonds in dipeptides as well as longer peptides. Furthermore, *i*PrOC-{Gly Δ Gly}-NMe₂ **76** variants were shown to be exclusively *intramolecularly* hydrogen bonded, implying an 8-membered ring hydrogen bonded system formation. This size of hydrogen bonding network is unusual for a β -turn suggesting the cyclopropane has a unique ability to stabilise this type of interaction. CD spectra added a supplementary information about the folding pattern of the tetrapeptides by displaying features found in type II β -turn. Nevertheless, in all solvent studied, a complex mixture of folded arrangements was adopted by the peptides (conformation I-IV in Figure 86).

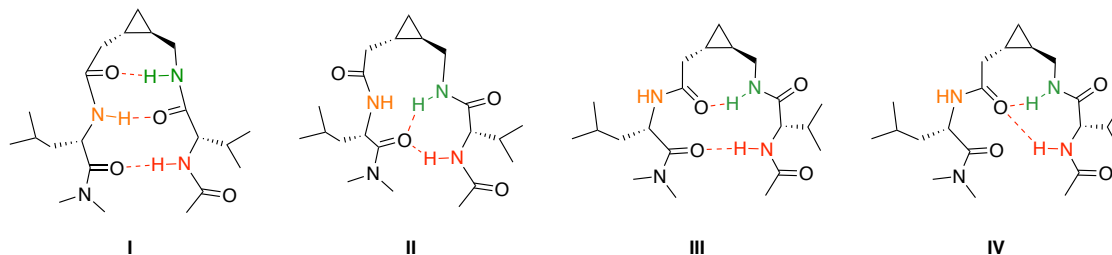


Figure 86: possible hydrogen bonding arrangements adopted by tetrapeptide 77/78

Further conformational NMR analysis of the tetrapeptides **77** and **78** showed folded conformation in CH_2Cl_2 and TFE but different interactions took place. As a matter of fact, Gly-NH was exchanging with TFE- d_3 solvent immediately, so it was not protected by intramolecular hydrogen bond as observed in CH_2Cl_2 . The 8-membered ring system was not formed in TFE. Therefore, the folding pattern of the mimetics designed was dependent on the solvent used. Overall, this suggests that cyclopropyl unit is efficient and compact tool to constrain small peptides to adopt a turn conformation stabilised by strong *intramolecular* hydrogen bonds. Folded conformation was determined for all enantioenriched compound synthesised. The stereochemistry on the cyclopropane did not impact the formation of the turn, and do not change the hydrogen bond network formed or the general conformation adopted as no differences have been observed by NMR, IR or CD.

To extend the study towards the formation of a reverse turn, dipeptide **107** was incorporated in the turn sequence of longer known peptides, in the 5-residue Leu-enkephalin **141** and 12-residue TrpZip **157**. {Gly Δ Gly}-Leu-enkephalin **132** and **133** were synthesised in 4 steps from enantioenriched variants of $\text{Boc}_2\text{-}\{\text{Gly}\Delta\text{Gly}\}\text{-OH}$ **107**. Conformational analysis did not reveal that these peptides adopted a defined and structured folded conformation. However, the analogues presented similar conformational features with the native peptide, proving the ability of the cyclopropane moiety to stabilise the conformation adopted by the peptide.

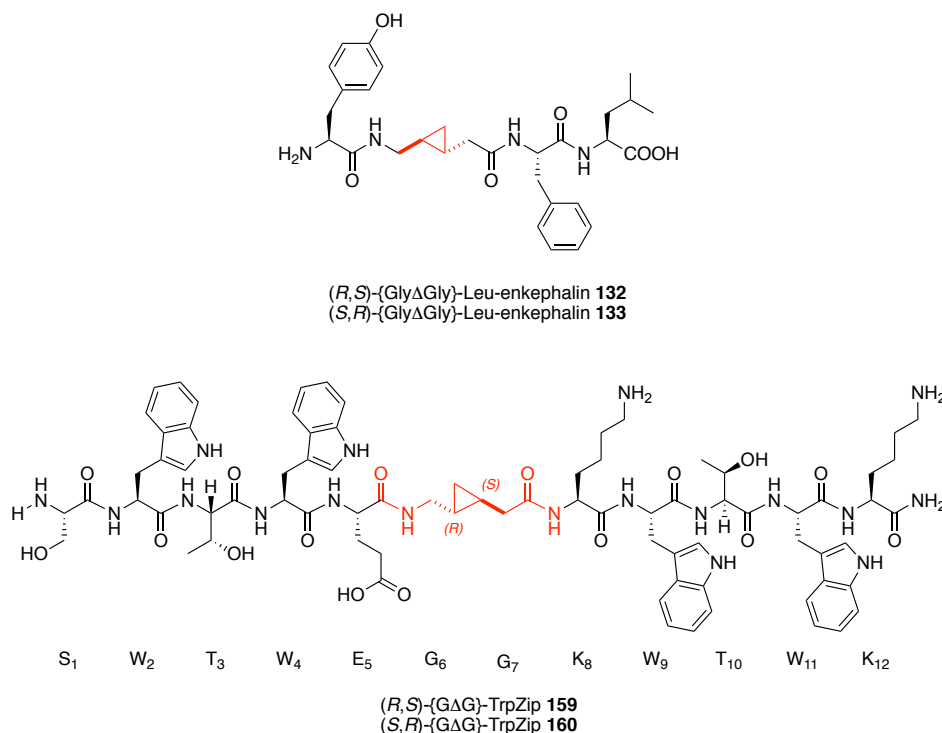


Figure 87: Leu-enkephalin and TrpZip analogues

The β -hairpin conformation adopted by native TrpZip peptide **157** has been confirmed by the combination of CD and NMR analysis. The analogues (R,S) -{G Δ G}-TrpZip **159** and (S,R) -{G Δ G}-TrpZip **160** have features consistent with a β -hairpin conformation when analysed by CD and have similar stabilities to the native peptide (determined by calculation of the T_m). However, the spectra obtained from NOESY experiments were not conclusive but characteristic sequential cross peaks of β -hairpin were present in the spectra of both analogues. The analogues were adopting a β -hairpin conformation but the intramolecular interactions are still to be determined. The NMR experiments would need to be performed at higher concentration in order to observe the expected long-range cross peaks. Other conformational analysis, such as CD recorded in the far-UV to understand the behaviour of the peptide backbone, analytical ultracentrifugation and other NMR experiments need to be undertaken to have better comprehension on the behaviour of the analogues synthesised. As well as shorter peptide, the stereochemistry of the cyclopropane did not impact a change on the formation of the β -hairpin, and stability of both analogues **159** and **160** was identical. However, MD calculation showed a difference in the turn and the hydrogen bond stabilising it (not present in the case of (S,R) -{G Δ G}-TrpZip **160**). Extra NMR measurements are currently running to understand which type of turn is formed and to obtain a 3D structure extracted from the NMR and MD calculation.

Overall, the cyclopropane used as a peptide bond isostere is an excellent tool to constrain a system into a turn conformation by stabilising the system with strong intramolecular hydrogen bond. When placed in a peptide adopting a β -hairpin conformation stabilised by cross-strand indoles stacking, the general folding adopted was similar. The dipeptide surrogate designed during this work promoted the turn formation or stabilised it.

Chapter 5

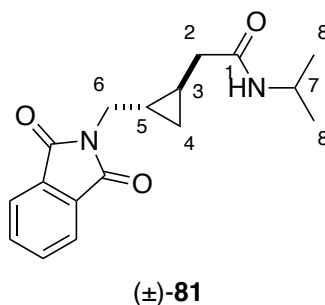
Experimental

General information

Air and/or moisture sensitive reactions were performed under an atmosphere of argon in flame dried apparatus. Tetrahydrofuran, toluene, dichloromethane, acetonitrile and diethyl ether were purified using a Pure-Solv™ 500 Solvent Purification System. Other dry organic solvents and starting materials were obtained from commercial sources and used as received. Petroleum ether used for column chromatography was the 40–60 °C fraction. All reactions were monitored by thin layer chromatography (TLC) using Merck silica gel 60 covered alumina plates F254. TLC plates were visualised under UV light and stained using either potassium permanganate solution, acidic ethanolic anisaldehyde or ninhydrine solution. Flash column chromatography was performed with silica gel (Merck 40–63 µm). Peptides were purified using a Gilson semi-preparative HPLC system equipped with a Phenomenex Synergi 10µ C18 80 Å, (250 x 21.2 mm) column. Peptides were lyophilized using a Christ Alpha 2–4 LDplus freeze-dryer.

IR spectra were recorded at ambient temperature using a Shimadzu IR instrument. All ¹H NMR spectra were recorded on Bruker 400 MHz Spectrospin, Bruker 500 MHz Spectrospin and Bruker 600 MHz Ultrashield 600 Plus spectrometers at ambient temperature. Data are reported as follows; chemical shift in ppm relative to CDCl₃ (7.26), CD₂Cl₂ (5.32) or D₂O (4.80) on the δ scale, integration, multiplicity (s = singlet, d = doublet, t = triplet, q = quartet, m = multiplet, br = broad, app. = apparent or a combination of these), coupling constant(s) *J* (Hz) and assignment. All ¹³C NMR spectra were recorded on a Bruker 400 MHz Spectrospin, Bruker 500 MHz Spectrospin and Bruker 600 MHz Ultrashield 600 Plus spectrometers at 101 MHz, 126 MHz and 151 MHz at ambient temperature. Data are reported as follows; chemical shift in ppm relative to CHCl₃ (77.16), CD₂Cl₂ (53.5) on the δ scale and assignment. Mass spectra were recorded using positive chemical ionization (CI+), positive ion impact (EI+), positive electrospray (ESI+), negative electrospray (ESI-) techniques on Jeol MStation JMS-700 instrument. The intensity of each peak is quoted as a percentage of the largest, where this information was available.

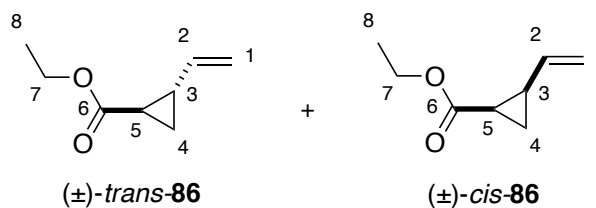
(±)-Phth-{GlyΔGly}-N-*i*-Pr **81**



A solution of (±)-NPhth-{GlyΔGly}-OH **59** (1.56 g, 6.01 mmol) in CH₂Cl₂ (280 mL) was treated with DMAP (730 mg, 6.01 mmol) at rt, EDCI (1.27 g, 6.60 mmol) and isopropyl amine (620 μL, 7.21 mmol) were added to the solution. The reaction mixture was stirred overnight at rt. The solvent was evaporated under vacuum, and the resulting oil was dissolved in EtOAc (50 mL), washed with H₂O (50 mL), 1 M aq. HCl (50 mL), sat. aq. NaHCO₃ (50 mL) and brine (30 mL). The organic phase was dried over MgSO₄, filtered and concentrated under vacuum to give the title compound (657 mg, 65%) as a brown solid.

R_f (EtOAc/PE 1:1) 0.38; m.p.: 176–177 °C; ν_{max} 3483, 1710, 1541, 1378, 1261, 1121 cm⁻¹; ¹H NMR (500 MHz; CDCl₃): δ 7.84 (2H, d, *J* = 5.5, 3.0 Hz, CH-Phthalimide), 7.72 (2H, dd, *J* = 5.5, 3.0 Hz, CH-Phthalimide), 5.67 (1H, d, *J* = 6.2 Hz, NH), 4.03–3.97 (1H, m, 1H, CH-C7), 3.71 (1H, dd, *J* = 14.2, 6.2 Hz, CH₂-C6), 3.52 (1H, dd, *J* = 14.2, 7.0 Hz, CH₂-C6), 2.15 (1H, dd, *J* = 16.2, 6.2 Hz, CH₂-C2), 2.05 (1H, dd, *J* = 16.2, 7.0 Hz, CH₂-C2), 1.11 (3H, d, *J* = 6.6 Hz, CH₃-C8), 1.07 (3H, d, *J* = 6.6 Hz, CH₃-C8), 1.08–1.04 (2H, m, CH-C3 + CH-C5), 0.67 (1H, ddd, *J* = 8.2, 5.2, 5.2 Hz, CH₂-C4), 0.43 (1H, ddd, *J* = 8.2, 5.3, 5.3 Hz, CH₂-C4); ¹³C NMR (126 MHz; CDCl₃): δ 170.9 (CO-C1), 168.7 (2 × CO-Phthalimide), 134.2 (C-Phthalimide), 134.0 (C-Phthalimide), 132.4 (CH-Phthalimide), 132.2 (CH-Phthalimide), 123.5 (CH-Phthalimide), 123.3 (CH-Phthalimide), 41.4 (CH-C7), 41.3 (CH₂-C6), 40.8 (CH₂-C2), 22.86 (CH₃-C8), 22.82 (CH₃-C8), 18.1 (CH-C5), 14.1 (CH-C3), 10.6 (CH₂-C4). HRMS (ESI+) for C₁₇H₂₀N₂NaO₃ [M+Na]⁺ calcd 323.1366, found 323.1353.

Ethyl-[(1*S,2*R**)-2-ethenylcyclopropane-1-carboxylate] and ethyl-[(1*R**,2*R**)-2-ethenylcyclopropane-1-carboxylate] **86****

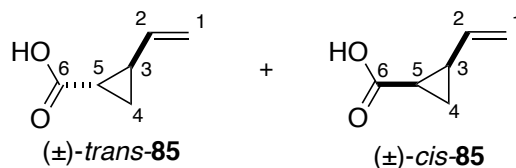


At $-4\text{ }^{\circ}\text{C}$, a solution of ethyl diazoacetate (5.00 g, 43.8 mmol) in CH_2Cl_2 (25 mL) was added dropwise (8 mL/h with a syringe pump) to a solution of butadiene (35.0 mL, 438 mmol) and $\text{Rh}_2(\text{OAc})_4$ (150 mg, 0.8 mol%) in CH_2Cl_2 (40 mL). The reaction mixture was stirred for one hour after the addition. Solvent was evaporated, and the crude material was dissolved in PE (100 mL) and filtered through a plug of silica gel. The solution was concentrated under vacuum to give the vinylcyclopropane (4.24 g, 69%) as a mixture of diastereoisomers (1:1 *dr*).

R_f (EtOAc/PE 1:1): 0.54; ν_{max} 2983, 1722, 1637, 1381, 1163 cm^{-1} ; ^1H NMR (400 MHz; CDCl_3) δ 5.82–5.72 (0.5H, m, CH-C2 *cis*), 5.39 (0.5H, ddd, $J = 17.1, 10.2, 8.4$ Hz, CH-C2 *trans*), 5.23 (0.5H, dd, $J = 17.2, 1.9$ Hz, CH₂-C1 *cis*), 5.16 (0.5H, dd, $J = 17.1, 0.9$ Hz, CH₂-C1 *trans*), 5.04 (0.5H, dd, $J = 10.3, 1.9$ Hz, CH₂-C1 *cis*), 4.98 (0.5H, dd, $J = 10.2, 1.6$ Hz, CH₂-C1 *trans*), 4.15–4.10 (2H, m, CH₂-C7 *cis* + CH₂-C7 *trans*), 2.03–1.98 (0.5H, m, CH-C3 *trans*), 1.95–1.89 (1H, m, CH-C3 *cis* + CH-C5 *cis*), 1.63 (0.5H, ddd, $J = 8.4, 5.2, 4.0$ Hz, CH-C5 *trans*), 1.36 (0.5H, ddd, $J = 8.9, 5.2, 4.3$ Hz, CH₂-C4 *cis*), 1.26 (1.5H, t, $J = 7.1$ Hz, CH₃-C8 *trans*), 1.25 (1.5H, t, $J = 7.1$ Hz, CH₃-C8 *cis*), 1.30–1.19 (1H, m, CH₂-C4 *cis* + CH₂-C4 *trans*), 0.96 (0.5H, ddd, $J = 8.3, 6.2, 4.4$ Hz, CH₂-C4 *trans*); ^{13}C NMR (101 MHz; CDCl_3): δ 173.5 (CO-C6 *trans*), 172.1 (CO-C6 *cis*), 138.3 (CH-C2 *trans*), 135.5 (CH-C2 *cis*), 116.2 (CH₂-C1 *cis*), 114.9 (CH₂-C1 *trans*), 60.72 (CH₂-C7 *trans*), 60.60 (CH₂-C7 *cis*), 25.7 (CH-C3 *trans*), 24.9 (CH-C3 *cis*), 22.0 (CH-C5 *trans*), 21.1 (CH-C5 *cis*), 15.7 (CH₂-C4 *trans*), 14.47 (CH₂-C4 *cis*), 14.38 (CH₃-C8 *trans*), 14.24 (CH₃-C8 *cis*); m/z (CI⁺) $[\text{M}+\text{H}]^+$ 141 (68%).*

*molecular weight too low to get accurate mass

(1*S,2*R**)-2-Ethenylcyclopropane-1-carboxylic acid and (1*R**,2*R**)-2-ethenylcyclopropane-1-carboxylic acid **85****



Procedure A:

Sodium solid (4.92 g, 214 mmol) was dissolved in anhydrous EtOH (40 mL). When the sodium was completely dissolved, a solution of ethyl-[(1*S**,2*R**)-2-ethenylcyclopropane-1-carboxylate] and ethyl-[(1*R**,2*R**)-2-ethenylcyclopropane-1-carboxylate] **86** (9.08 g, 64.8 mmol) in EtOH (20 mL) was added dropwise at rt. The reaction mixture was heated to reflux and stirred for 24 h. Et₂O (50 mL) was added to the reaction mixture and the solution was washed with sat. aq. NH₄Cl (3 × 20 mL), H₂O (3 × 20 mL), and brine (20 mL). The organic phase was dried over MgSO₄ and concentrated under vacuum. The aqueous phase was acidified to pH 1 using conc. aq. HCl and extracted with Et₂O (3 × 40 mL). The combined organic extracts were dried over MgSO₄, filtered and concentrated to give the carboxylic acid (4.22 g, 95%), as a dark oil with *trans*-**85** as the major isomer (9:1 *dr*).

Procedure B:

(1*R**,2*S**)-2-ethenyl-cyclopropanemethanol **90** (1.00 g, 10.2 mmol) and NMO·H₂O (11.9 g, 102 mmol) were dissolved in MeCN (41 mL). TPAP (358 mg, 1.02 mmol, 10 mol%) was added portionwise (20 mg/20min) at rt. The solution was stirred overnight at rt and the reaction was then quenched by the addition of an excess of isopropanol. H₂O (30 mL) was added and pH was carefully adjusted to 1 using 2 M aq. HCl. The aqueous phase was extracted with Et₂O (3 × 50 mL) and the combined organic extracts were then washed with brine (20 mL), dried over MgSO₄, filtered and concentrated under vacuum. The residue was purified by silica gel column chromatography (PE/EtOAc 1:1) to afford the title compound (371 mg, 30%) as a brown oil.

Procedure C:

A solution of DMSO (10.4 mL, 146 mmol) in CH₂Cl₂ (70 mL) was added dropwise at –78 °C, under Ar, to a solution of oxalyl chloride (6.1 mL, 73.1 mmol) in CH₂Cl₂ (50 mL). The solution was stirred at this temperature for 30 min and (1*R**,2*S**)-2-ethenyl-cyclopropanemethanol **90** (4.78 g, 48.7 mmol) in CH₂Cl₂ (50 mL) was added dropwise at –78 °C. The reaction mixture was stirred for 3 h at this temperature. Et₃N (40 mL, 292 mmol) was carefully added at –78 °C and the solution was allowed to warm to rt. H₂O (200 mL) and CH₂Cl₂ (200 mL) were added and the phases were separated. The organic phase was washed with 1 M aq. HCl. (3 × 150 mL), H₂O (150 mL), sat. aq. NaHCO₃ (150 mL) and brine (150 mL). The organic phase was dried over MgSO₄ and CH₂Cl₂ was removed by distillation. The resultant aldehyde was used without further purification.

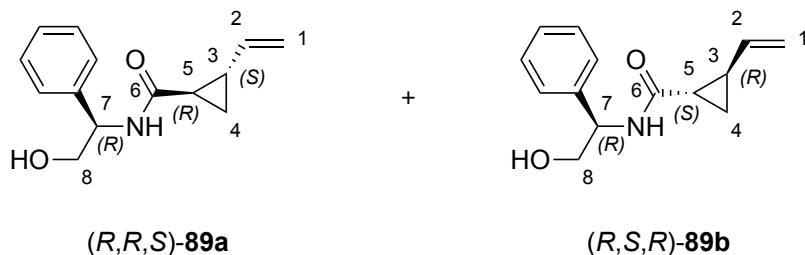
The aldehyde (48.7 mmol), 2-methyl-2-butene (52 mL, 487 mmol) and NaH₂PO₄·2H₂O (15.6 g, 97.4 mmol) were dissolved in *t*-BuOH (500 mL). The solution was cooled to 0 °C and NaClO₂ (15.4 g, 170 mmol) was added. The reaction mixture was stirred for 2 h at rt. The mixture was cooled to 0 °C and 1 M aq. HCl (20 mL) was added. The solution was extracted with CHCl₃ (3 × 60 mL). The combined organic extracts were washed with brine, dried over MgSO₄, filtered and concentrated under reduced pressure. The residue was purified by silica gel column chromatography (PE/EtOAc 1:1) to afford the title compound (3.76 g, 69% over 2 steps) as a yellow liquid.

Data for the major isomer is presented.

R_f(EtOAc/PE 1:1): 0.48; ν_{\max} 2957, 1692, 1229 cm^{–1}; ¹H NMR (400 MHz; CDCl₃): δ 10.99 (1H, bs, OH), 5.39 (1H, ddd, *J* = 17.0, 10.2, 8.3 Hz, CH-C2), 5.18 (1H, ddd, *J* = 17.0, 1.4, 0.6 Hz, CH₂-C1), 5.02 (1H, ddd, *J* = 10.2, 1.4, 0.4 Hz, CH₂-C1), 2.13–2.06 (1H, m, CH-C3), 1.64 (1H, ddd, *J* = 8.3, 5.0, 4.2 Hz, CH-C5), 1.43 (1H, ddd, *J* = 8.6, 5.0, 4.4 Hz, CH₂-C4), 1.06 (1H, ddd, *J* = 8.6, 6.4, 4.2 Hz, CH₂-C4); ¹³C NMR (126 MHz; CDCl₃): δ 179.9 (CO-C6), 137.6 (CH-C2), 115.4 (CH₂-C1), 26.6 (CH-C3), 21.7 (CH-C5), 16.3 (CH₂-C4). *m/z* (CI+) [M+H]⁺ 113 (72%).*

*molecular weight too low to get accurate mass

(1*R*,2*S*)-2-ethenyl-*N*-[(*R*)-2-hydroxy-1-phenylethyl]cyclopropanecarboxamide 89a and (1*S*,2*R*)-2-Ethenyl-*N*-[(*R*)-2-hydroxy-1-phenylethyl]cyclopropanecarboxamide 89b



To a well stirred solution of carboxylic acid (\pm)-**85** (4.0 g, 54 mmol) in THF (160 mL) were added dropwise, at $-20\text{ }^{\circ}\text{C}$, *N*-methylmorpholine (3.9 mL, 54 mmol), followed by *i*-BuOCOC₂Cl (4.6 mL, 54 mmol). The solution was stirred at this temperature for 15 min and (*R*)-phenylglycinol (4.9 g, 54 mmol) was added portionwise over a period of 30 min. The reaction mixture was stirred at $-20\text{ }^{\circ}\text{C}$ for 1 h and then allowed to warm to rt. The solvent was removed under vacuum. The residue was then dissolved in EtOAc (70 mL) and washed with H₂O (3 \times 20 mL), aq. sat. NaHCO₃ (3 \times 20 mL), 2 M aq. HCl (3 \times 20 mL) and brine (20 mL). The organic phase was dried over MgSO₄ and concentrated under reduced pressure. The crude product was then purified by silica gel on column chromatography (PE/EtOAc 1:0 to 0:1) to give (*R,R,S*)-**89a** (1.53 g, 37%) and (*R,S,R*)-**89b** (1.63 g, 39%). Each product was then recrystallized from EtOAc to obtain colourless crystals (100% recovery for both).

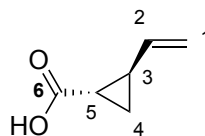
- **(*R,R,S*)-89a**

R_f (EtOAc/PE 1:1): 0.31; $[\alpha]_D^{20}$: -17.5 ($c = 1.05$, in CH_3Cl); ν_{max} (CHCl_3): 3310, 2961, 1634, 1545, 1059 cm^{-1} ; ^1H NMR (400 MHz; CDCl_3): δ 7.40–7.36 (2H, m, $2 \times \text{CH-Ph}$), 7.34–7.30 (3H, m, $3 \times \text{CH-Ph}$), 6.25 (1H, d, $J = 5.4$ Hz, NH), 5.42 (1H, ddd, $J = 17.0, 10.2, 8.5$ Hz, CH-C2), 5.18 (1H, dd, $J = 17.0, 1.5$ Hz, $\text{CH}_2\text{-C1}$), 5.07 (1H, td, $J = 6.2, 3.8$ Hz, OH), 5.00 (1H, dd, $J = 10.2, 1.5$ Hz, $\text{CH}_2\text{-C1}$), 3.97–3.87 (2H, m, $\text{CH}_2\text{-C8}$), 2.73 (1H, dd, $J = 7.3, 5.4$ Hz, CH-C7), 2.09–2.02 (1H, m, CH-C3), 1.47–1.37 (2H, m, CH-C5, $\text{CH}_2\text{-C4}$), 0.91 (1H, ddd, $J = 8.0, 6.2, 4.1$ Hz, $\text{CH}_2\text{-C4}$); ^{13}C NMR (126 MHz; CDCl_3): δ 172.8 (CO-C6), 139.0 (C-Ph), 138.6 (CH-C2), 129.1 ($2 \times \text{CH-Ph}$), 128.2 (CH-Ph), 126.9 ($2 \times \text{CH-Ph}$), 114.7 ($\text{CH}_2\text{-C1}$), 67.2 (CH-C7), 56.7 ($\text{CH}_2\text{-C8}$), 25.0 (CH-C3), 24.1 (CH-C5), 15.0 ($\text{CH}_2\text{-C4}$); HRMS (ESI $^-$) for $\text{C}_{14}\text{H}_{16}\text{NO}_2$ $[\text{M-H}]$ calcd 230.1186 found 230.1187.

- **(*R,S,R*)-89b**

R_f (EtOAc/PE 1:1): 0.20; $[\alpha]_D^{20}$: $+9.89$ ($c = 1.05$, CHCl_3); ν_{max} (CHCl_3): 3298, 2959, 1634, 1548, 1051 cm^{-1} ; ^1H NMR (400 MHz; CDCl_3): δ 7.40–7.37 (2H, m, $2 \times \text{CH-Ph}$), 7.34–7.30 (3H, m, $3 \times \text{CH-Ph}$), 6.23 (1H, d, $J = 5.4$ Hz, NH), 5.40 (1H, ddd, $J = 17.1, 10.2, 8.5$ Hz, CH-C2), 5.14 (1H, dd, $J = 17.1, 1.5$ Hz, $\text{CH}_2\text{-C1}$), 5.07 (1H, td, $J = 6.4, 4.0$ Hz, OH), 4.97 (1H, dd, $J = 10.2, 1.5$ Hz, $\text{CH}_2\text{-C1}$), 3.96–3.86 (2H, m, $\text{CH}_2\text{-C8}$), 2.77 (1H, dd, $J = 7.2, 5.4$ Hz, CH-C7), 2.05–2.01 (1H, m, CH-C3), 1.47–1.40 (2H, m, CH-C5, $\text{CH}_2\text{-C4}$), 0.97–0.93 (1H, m, $\text{CH}_2\text{-C4}$); ^{13}C NMR (126 MHz; CDCl_3): δ 172.6 (C-C6), 139.4 (C-Ph), 138.8 (CH-C2), 128.8 ($2 \times \text{CH-Ph}$), 127.8 (CH-Ph), 126.9 ($2 \times \text{CH-Ph}$), 114.4 ($\text{CH}_2\text{-C1}$), 66.7 (CH-C7), 56.4 ($\text{CH}_2\text{-C8}$), 24.6 (CH-C3), 23.9 (CH-C5), 14.9 ($\text{CH}_2\text{-C4}$); HRMS (ESI $^-$) for $\text{C}_{14}\text{H}_{16}\text{NO}_2$ $[\text{M-H}]$ calcd 230.1186 found 230.1187.

(1*S*,2*R*)-2-Ethenylcyclopropane-1-carboxylic acid 85



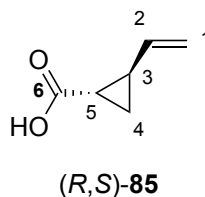
(*S,R*)-85

(1*S*,2*R*)-2-Ethenyl-*N*-[(*R*)-2-hydroxy-1-phenylethyl]cyclopropanecarboxamide **89b** (1.86 g, 8.08 mmol), was dissolved in a mixture of 10% KOH in MeOH (60 mL) and H₂O (30 mL). The solution was heated to reflux and stirred overnight. MeOH was then removed under vacuum and the aqueous solution was extracted with EtOAc (3 × 10 mL). The combined extracts were dried over MgSO₄ and concentrated under vacuum to recover (*R*)-phenylglycinol. The aqueous layer was acidified using conc. aq. HCl until pH 1, and the mixture was extracted with EtOAc (3 × 10 mL). The combined extracts were washed with brine (10 mL), dried over MgSO₄, filtered and the solvent was removed under reduced pressure to give the title compound (863 mg, 95%) as a colourless oil.

R_f (EtOAc/PE 1:1): 0.62; $[\alpha]_D^{26} +115$ (*c* = 1.00, CHCl₃); ν_{\max} 3219, 1697, 1462, 1198 cm⁻¹; ¹H NMR (400 MHz, CDCl₃): δ 11.27 (1H, bs, OH), 5.40 (1H, ddd, *J* = 17.0, 10.2, 8.3 Hz, CH-C2), 5.18 (1H, dd, *J* = 17.0, 1.6 Hz, CH₂-C1), 5.01 (1H, dd, *J* = 10.2, 1.6 Hz, CH₂-C1), 2.14–2.02 (1H, m, CH-C3), 1.64 (1H, ddd, *J* = 8.3, 5.1, 4.2 Hz, CH-C5), 1.43 (1H, ddd, *J* = 8.6, 5.1, 4.4 Hz, CH₂-C4), 1.05 (2H, ddd, *J* = 8.6, 6.4, 4.2 Hz, CH₂-C4); ¹³C NMR (126 MHz, CDCl₃): δ 179.6 (CO-C6), 137.7 (CH-C2), 115.4 (CH₂-C1), 26.6 (CH-C3), 21.8 (CH-C5), 16.3 (CH₂-C4); *m/z* (CI⁺) [M+H]⁺ 113 (80%).*

*molecular weight too low to get accurate mass

(1*R*,2*S*)-2-Ethenylcyclopropane-1-carboxylic acid **85**

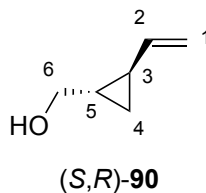


The procedure applied to the synthesis of (1*S*,2*R*)-2-ethenylcyclopropane-1-carboxylic acid **85** was followed using (1*R*,2*S*)-2-Ethenyl-*N*-[(*R*)-2-hydroxy-1-phenylethyl] cyclopropanecarboxamide **89a** (2.43 g, 10.5 mmol) to give the title compound (964 mg, 82%) as a yellow oil.

R_f (EtOAc/PE 1:1): 0.62; $[\alpha]_D^{20}$ -100 ($c = 1.00$, CHCl_3); ν_{max} 3219, 1697, 1462, 1198 cm^{-1} ; ^1H NMR (500 MHz, CDCl_3): δ 5.40 (1H, ddd, $J = 16.9, 10.2, 8.3$ Hz, CH-C2), 5.18 (1H, dt, $J = 16.9, 1.1$ Hz, CH_2 -C1), 5.02 (1H, dd, $J = 10.2, 1.1$ Hz, CH_2 -C1), 2.17–2.03 (1H, m, CH-C3), 1.64 (1H, ddd, $J = 8.5, 5.1, 4.1$ Hz, CH-C5), 1.44 (1H, ddd, $J = 8.8, 5.1, 5.1$ Hz, CH_2 -C4), 1.06 (1H, ddd, $J = 8.8, 6.4, 4.1$ Hz, CH_2 -C4). ^{13}C NMR (126 MHz, CDCl_3): δ 180.0 (CO-C6), 137.7 (CH-C2), 115.5 (CH_2 -C1), 26.6 (CH-C3), 21.8 (CH-C5), 16.3 (CH_2 -C4); m/z (EI+) $[\text{M}+\text{H}]^+$ 113 (99%).*

*molecular weight too low to get accurate mass

(1*S*,2*R*)-2-Ethenyl-cyclopropanemethanol 90

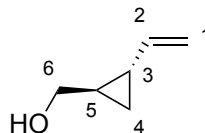


A solution of acid (*S,R*)-**85** (1.50 g, 13.3 mmol) in THF (19 mL) was added dropwise, at 0 °C, to a slurry of LiAlH₄ (1.10 g, 26.6 mmol) in THF (19 mL). The mixture was heated to reflux for 5 h. The reaction was then quenched by the sequential addition of H₂O (1 mL), 1 M aq. NaOH (1 mL) and H₂O (3 mL) at 0 °C. The resulting mixture was stirred for 15 min and an excess of MgSO₄ was added. The resulting suspension was stirred for extra further 15 min and filtered. The majority of the solvent was removed by distillation at atm. pressure to give (1*S*,2*R*)-2-ethenyl-cyclopropylmethanol **90** (1.18 g, 41 wt%, 59%) as a orange solution in THF.

R_f (PE/EtOAc 1:1, Anisaldehyde): 0.75; $[\alpha]_D^{26} +51$ ($c = 1.0$, CHCl₃); ν_{\max} 3333, 2924, 1636, 895 cm⁻¹; ¹H NMR (500 MHz, CDCl₃) δ 5.38 (1H, ddd, $J = 17.1, 10.2, 8.5$ Hz, CH-C2), 5.03 (1H, dd, $J = 17.1, 1.6$ Hz, CH₂-C1), 4.84 (1H, dd, $J = 10.2, 1.6$ Hz, CH₂-C1), 3.55–3.40 (2H, m, CH₂-C6), 1.34–1.29 (1H, m, CH-C3), 1.18–1.08 (1H, m, CH-C5), 0.70–0.56 (2H, m, CH₂-C4); ¹³C NMR (126 MHz, CDCl₃): δ 140.8 (CH-C2), 112.3 (CH₂-C1), 66.2 (CH₂-C6), 23.0 (CH-C5), 20.6 (CH-C3), 11.7 (CH₂-C4).*

*Molecular weight too low to obtain a nominal or accurate mass.

(1*R*,2*S*)-2-Ethenyl-cyclopropanemethanol **90**



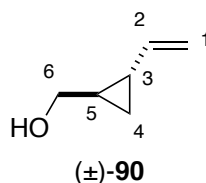
(*R,S*)-90

The procedure for the synthesis of the other enantiomer (*S,R*)-**90** was followed using acid (*R,S*)-**85** (1.40 g, 12.4 mmol) to give (1*R*,2*S*)-2-ethenyl-cyclopropylmethanol **90** (1.51 g, 49 wt%, 62%) as an orange solution in THF.

R_f (PE/EtOAc 1:1, Anisaldehyde): 0.88; $[\alpha]_D^{26} -61$ ($c = 1.0$, CHCl_3); ν_{max} 3337, 2924, 1636, 895 cm^{-1} ; ^1H NMR (500 MHz, CDCl_3) δ 5.37 (1H, ddd, $J = 17.1, 10.2, 8.7$ Hz, CH-C2), 5.02 (1H, dd, $J = 17.1, 1.6$ Hz, CH_2 -C1), 4.83 (1H, dd, $J = 10.2, 1.6$ Hz, CH_2 -C1), 3.47 (1H, dd, $J = 11.2, 6.8$ Hz, CH_2 -C6), 3.44 (1H, dd, $J = 11.2, 6.8$ Hz, CH_2 -C6), 1.31 (1H, dddd, $J = 8.7, 8.7, 4.6, 4.6$ Hz, CH-C3), 1.16–1.06 (1H, m, CH-C5), 0.67–0.57 (2H, m, CH_2 -C4); ^{13}C NMR (126 MHz, CDCl_3): δ 140.8 (CH-C2), 112.2 (CH_2 -C1), 66.1 (CH_2 -C6), 23.0 (CH-C5), 20.6 (CH-C3), 11.6 (CH_2 -C4).*

*Molecular weight too low to obtain a mass.

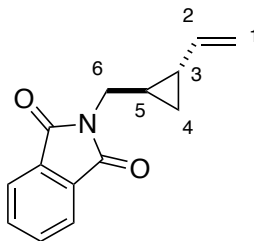
(1*R,2*S**)-2-Ethenyl-cyclopropanemethanol **90****



To THF (110 mL) cooled to $-78\text{ }^{\circ}\text{C}$ under Ar was added carefully, *n*-BuLi (40.0 mL of an 11 M solution in hexane, 440 mmol). The resultant solution was stirred for 10 min at this temperature. Diisopropylamine (62.0 mL, 440 mmol) was added dropwise followed by *t*-BuOK (49.0 g, 440 mmol). The reaction mixture was stirred at $-78\text{ }^{\circ}\text{C}$ for 45 min. 1,3-Epoxy-5-hexene (5.60 mL, 50.0 mmol) was added dropwise at $-78\text{ }^{\circ}\text{C}$ and the reaction mixture was allowed to stir for 15 h at $-50\text{ }^{\circ}\text{C}$. The reaction was quenched at $-50\text{ }^{\circ}\text{C}$ with H_2O (30 mL) and allowed to warm to rt. The solution was extracted with Et_2O ($3 \times 15\text{ mL}$), the combined organic layers were dried over MgSO_4 , and filtered. The majority of the solvent was removed by distillation at atm. pressure to afford (1*R**,2*S**)-2-ethenyl-cyclopropanemethanol **90** (35.13 g, 68 wt%, quant.) as a solution in THF as an orange solution in THF.

R_f (EtOAc/PE 1:1): 0.68; ν_{max} (CHCl_3): 3329, 2924, 1636, 1173, 1049, 1040 cm^{-1} ; ^1H NMR (500 MHz; CDCl_3): δ 5.41 (1H, ddd, $J = 17.1, 10.3, 8.5\text{ Hz}$, CH-C2), 5.06 (1H, dd, $J = 17.1, 1.6\text{ Hz}$, CH_2 -C1), 4.88 (1H, dd, $J = 10.3, 1.6\text{ Hz}$, CH_2 -C1), 3.54–3.47 (2H, m, CH_2 -C6), 1.51 (1H, bs, OH), 1.35 (1H, m, CH-C3), 1.21–1.13 (1H, m, CH-C5), 0.70–0.64 (2H, m, CH_2 -C4); ^{13}C NMR (126 MHz; CDCl_3): δ 140.7 (CH_2 -C2), 112.5 (CH-C1), 66.4 (CH_2 -C6), 23.1 (CH-C3), 20.7 (CH-C5), 11.7 (CH_2 -C4).

2-[(1*R,2*S**)-2-Ethenylcyclopropyl]methyl-2,3-dihydro-1*H*-isoindole-1,3-dione **94****

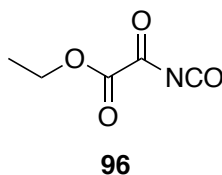


(±)-94

DEAD (3.60 mL, 22.8 mmol) was added dropwise at 0 °C to a solution of alcohol (±)-**90** (893 mg, 9.10 mmol), PPh₃ (5.98 g, 22.8 mmol) and phthalamide (3.35 g, 22.8 mmol) in dry THF (91 mL). The reaction mixture was heated to reflux and stirred overnight. Solvent was removed and the resulting residue was purified by silica gel column chromatography in PE/EtOAc (10:1 to 9:1) to afford the title compound (2.11 g, quant.) as an orange oil.

R_f (EtOAc/PE 1:1): 0.34; ν_{\max} (CHCl₃): 3466, 3080, 3001, 1771, 1709, 1635, 1393, 1037 cm⁻¹; ¹H-NMR (400 MHz; CDCl₃): δ 7.80–7.75 (2H, m, 2 × CH-Phth), 7.68–7.63 (2H, m, 2 × CH- Phth), 5.28 (1H, ddd, *J* = 17.1, 10.2, 8.6 Hz, CH-C2), 4.98 (1H, dd, *J* = 17.1, 1.7 Hz, CH₂-C1), 4.77 (1H, dd, *J* = 10.2, 1.7 Hz, CH-C1), 3.58 (1H, dd, *J* = 14.1, 7.1 Hz, CH₂-C6), 3.50 (1H, dd, *J* = 14.1, 7.3 Hz, CH₂-C6), 1.46 (1H, dddd, *J* = 8.6, 8.6, 4.9, 4.9 Hz, CH-C3), 1.26–1.19 (1H, m, CH-C5), 0.77 (1H, ddd, *J* = 8.5, 4.9, 4.9 Hz, 1 × CH₂-C4), 0.57 (1H, ddd, *J* = 8.5, 5.0, 5.0 Hz, CH₂-C4). ¹³C NMR (126 MHz; CDCl₃): δ 168.2 (2 × CO- Phth), 140.2 (CH-C2), 133.8 (4 × CH-Phth), 123.2 (2 × C-Phth), 112.5 (CH₂-C1), 41.4 (CH₂-C6), 21.6 (CH-C3), 19.7 (CH-C5), 12.6 (CH₂-C4). HRMS (ESI+) for C₁₄H₁₃NNaO₂ [M+Na]⁺ calcd 250.0838, found 250.0829.

Ethyl 2-isocyanato-2-oxoacetate **96**

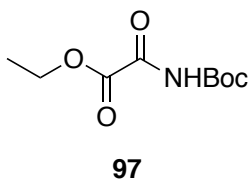


Oxalyl chloride (863 μL , 10.2 mmol) was added to a suspension of ethyl oxamate (1.00 g, 8.54 mmol) in CH_2Cl_2 (13 mL) at rt. The reaction mixture was heated to reflux and stirred overnight. The solvent was removed under vacuum to afford the isocyanate **96** (1.30 g, 100%) as a white solid.

R_f (EtOAc/PE 1:1) 0.15; ν_{max} 1790, 1732, 1713, 1306 cm^{-1} ; ^1H NMR (400 MHz; CDCl_3) δ 4.46 (2H, q, $J = 7.2$ Hz, $\text{CH}_2\text{-Et}$), 1.43 (3H, t, $J = 7.2$ Hz, $\text{CH}_3\text{-Et}$). ^{13}C (126 MHz, CDCl_3) δ 158.1 (CO-CONCO), 157.6 (CO-COOEt), 134.3 (NCO), 65.7 ($\text{CH}_2\text{-Et}$), 14.0 ($\text{CH}_3\text{-Et}$).*

*Product decomposed quickly, unable to obtain a mass of pure product without decomposition at rt and atm. pressure.

Ethyl 2-(*t*-butoxycarbonyl)amino-2-oxoacetate **97**

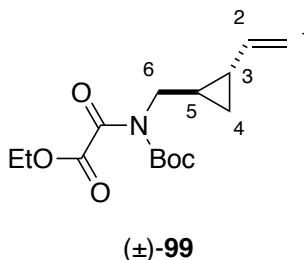


A solution of *t*-BuOH (1.23 mL, 12.8 mmol) in toluene (5 mL) was added to a solution of ethyl 2-isocyanato-2-oxoacetate **96** (8.54 mmol) in toluene (9 mL). The solution was heated to reflux and stirred for 24 h. The solvent was removed, and crude purified by silica gel column chromatography (PE/EtOAc from 9:1 to 1:1) affording the title compound (519 mg, 28%) as a colourless oil.

R_f (EtOAc/PE 1:1): 0.83; ν_{\max} (CHCl₃): 1734, 1705, 1248, 1152 cm⁻¹; ¹H NMR (400 MHz; CDCl₃): δ 10.42 (1H, bs, NH), 4.42 (2H, q, J = 7.1 Hz, CH₂-Et), 1.59 (9H, s, *t*-Bu), 1.41 (3H, t, J = 7.1 Hz, CH₃-Et); ¹³C NMR (126 MHz; CDCl₃): δ 158.4 (COEt + CONHBoc), 157.5 (CO-Boc), 86.4 (C-Boc), 63.5 (CH₂-Et), 27.8 (3 \times CH₃-Boc), 14.0 (CH₃-Et).*

*Values match what is reported in literature

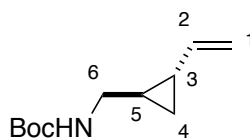
Ethyl 2-[(*t*-butoxycarbonyl)[(1*R,2*S**)-2-ethenylcyclopropyl]methylamino]-2-oxoacetate **99****



DEAD (2.17 mL, 13.8 mmol) was added dropwise at 0 °C to a solution of (±)-**90** (723 mg, 5.53 mmol), PPh₃ (3.62 g, 13.8 mmol) and ethyl 2-[(*t*-butoxy)carbonyl]amino-2-oxoacetate (3.00 g, 13.8 mmol) in THF (14 mL). The reaction mixture was heated to reflux and stirred overnight. Solvents were removed under vacuum and the resulting residue was purified by silica gel column chromatography in PE/EtOAc (10:1 to 9:1) to give the title compound (1.47 g, 90%) as an orange oil.

R_f (EtOAc/PE 1:1): 0.95; *v*_{max} (CHCl₃): 2982, 2938, 1740, 1698, 1636, 1369, 1145, 1024 cm⁻¹; ¹H NMR (400 MHz; CDCl₃): δ 5.35 (1H, ddd, *J* = 17.1, 10.2, 8.4 Hz, CH-C2), 5.04 (1H, dd, *J* = 17.1, 1.6 Hz, CH₂-C1), 4.86 (1H, dd, *J* = 10.2, 1.6 Hz, CH₂-C1), 4.34 (2H, q, *J* = 7.2 Hz, CH₂-Et), 3.64 (1H, dd, *J* = 14.0, 7.0 Hz, CH₂-C6), 3.59 (1H, dd, *J* = 14.0, 7.2 Hz, CH₂-C6), 1.52 (9H, s, *t*-Bu), 1.48-1.42 (1H, m, CH-C3), 1.36 (3H, t, *J* = 7.2 Hz, CH₃-Et), 1.10-1.02 (1H, m, CH-C5), 0.77 (1H, ddd, *J* = 8.6, 5.2, 5.2 Hz, CH₂-C4), 0.63 (1H, ddd, *J* = 8.6, 5.2, 5.2 Hz, CH₂-C4). ¹³C NMR (126 MHz; CDCl₃): 163.7 (COCOOEt), 162.0 (COCOOEt), 151.9 (CO-Boc), 140.4 (CH-C2), 112.7 (CH₂-C1), 85.3 (CH-Boc), 62.2 (CH₂-Et), 46.6 (CH₂-C6), 28.0 (3 × CH₃-Boc), 21.6 (CH-C3), 19.5 (CH-C5), 14.0 (CH₃-Et), 12.6 (CH₂-C4). HRMS (ESI+) for C₁₅H₂₃NNaO₅ [M+Na]⁺ calcd 320.1468, found 320.1460.

t*-Butyl-*N*-[(1*R**,2*S**)-2-ethenylcyclopropyl]methylcarbamate **93*

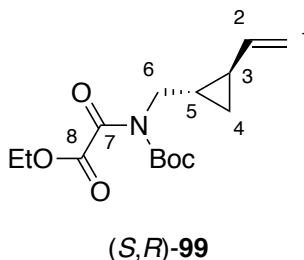


(±)-93

A solution of 4 M aq. LiOH (6.2 mL) was added dropwise to a solution of (±)-**99** (1.47 g, 4.95 mmol) in THF (2.20 mL). The reaction mixture was stirred overnight at rt. The solvent was then removed under reduced pressure and the residue was dissolved in CH₂Cl₂ (20 mL) and washed with sat. aq. NaHCO₃ (7 mL) and brine (7 mL). The organic phase was dried over MgSO₄, filtered and concentrated under vacuum to afford the title compound (801 mg, 82%) as a colourless liquid.

R_f (EtOAc/PE 1:1): 0.83; *v*_{max} (CHCl₃): 3356, 2083, 2001, 2978, 2934, 2877, 1694, 1636, 1368, 1169, 1030 cm⁻¹; ¹H NMR (500 MHz; CDCl₃): δ 5.37 (1H, ddd, *J* = 17.1, 10.2, 8.6 Hz, CH-C2), 5.04 (1H, dd, *J* = 17.1, 1.6, CH₂-C1), 4.86 (1H, dd, *J* = 10.2, 1.6 Hz, CH₂-C1), 4.62 (1H, s, NH), 3.10–2.98 (2H, m, CH₂-C6), 1.44 (9H, s, *t*-Bu), 1.30 (1H, dddd, *J* = 8.6, 8.6, 4.4, 4.4 Hz, CH-C3), 1.04–0.98 (1H, m, CH-C5), 0.65–0.59 (2H, m, CH₂-C4). ¹³C NMR (126 MHz; CDCl₃): δ 156.0 (CO-Boc), 140.8 (CH-C2), 112.4 (CH₂-C1), 79.3 (C-Boc), 44.5 (CH₂-C6), 28.6 (3 × CH₃-Boc), 21.2 (CH-C3), 20.7 (CH-C5), 12.6 (CH₂-C4). HRMS (ESI+) for C₁₁H₁₉NNaO₂ [M+Na]⁺ calcd 220.1308, found 220.1275.

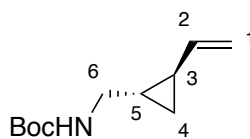
Ethyl 2-*[(t-butoxycarbonyl)[(1*S*,2*R*)-2-ethenylcyclopropyl]methylamino]-2-oxoacetate*
99



The procedure applied to the synthesis of (\pm)-**99** (AN-01-83) was followed using (*S,R*)-**90** (159 mg, 1.62 mmol), and ethyl 2-(*t*-butoxycarbonyl)amino-2-oxoacetate (879 mg, 4.05 mmol). The title compound (289 mg, 59%) was obtained as an orange oil.

R_f (EtOAc/PE 1:1): 0.95; $[\alpha]_D^{21} +73$ ($c = 0.01$, in CH_3Cl); ν_{max} (CHCl_3): 2982, 2938, 1740, 1698, 1636, 1369, 1145, 1024 cm^{-1} ; ^1H NMR (500 MHz; CDCl_3): δ 5.35 (1H, ddd, $J = 17.1$, 10.2, 8.4 Hz, CH-C2), 5.04 (1H, dd, $J = 17.1$, 1.1 Hz, CH_2 -C1), 4.86 (1H, dd, $J = 10.2$, 1.1 Hz, CH_2 -C1), 4.34 (2H, q, $J = 7.2$ Hz, CH_2 -Et), 3.64 (1H, dd, $J = 14.1$, 7.0 Hz, CH_2 -C6), 3.59 (1H, dd, $J = 14.1$, 7.2 Hz, CH_2 -C6), 1.52 (9H, s, *t*-Bu), 1.46–1.43 (1H, m, CH-C3), 1.36 (3H, t, $J = 7.2$ Hz, CH_3 -Et), 1.20–1.17 (1H, m, CH-C5), 0.77 (1H, ddd, $J = 8.6$, 5.2, 5.2 Hz, CH_2 -C4), 0.63 (1H, ddd, $J = 8.6$, 5.2, 5.2 Hz, CH_2 -C4); ^{13}C NMR (126 MHz; CDCl_3): δ 163.7 (CO-C7), 162.0 (CO-C8), 151.9 (CO-Boc), 140.4 (CH-C2), 112.7 (CH_2 -C1), 85.3 (C-Boc), 62.3 (CH_2 -Et), 46.7 (CH_2 -C6), 28.6 (C-Boc), 28.0 ($3 \times \text{CH}_3$ -Boc), 24.0 (CH-C3), 19.5 (CH-C5), 14.0 (CH_3 -Et), 12.6 (CH_2 -C4); HRMS (ESI+) for $\text{C}_{15}\text{H}_{23}\text{NNaO}_5$ $[\text{M}+\text{Na}]^+$ calcd 320.1468, found 320.1459.

t*-Butyl-*N*-[(1*S*,2*R*)-2-ethenylcyclopropyl]methylcarbamate **93*

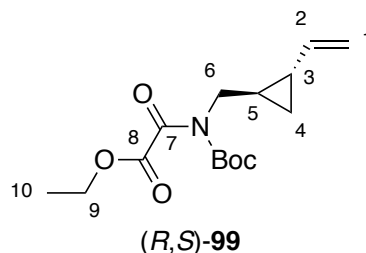


(*S,R*)-93

The procedure applied to the synthesis of (\pm)-**93** was followed using (*S,R*)-**99** (285 mg, 0.96 mmol). The title compound (99 mg, 32%) was obtained as a clear oil.

R_f (EtOAc/PE 1:1): 0.85; $[\alpha]_D^{21}$: +73 ($c = 0.10$, in CH_3Cl); ν_{max} (CHCl_3): 3348, 3078, 3003, 1695, 1636, 1366, 1271 cm^{-1} ; ^1H NMR (400 MHz; CDCl_3): δ 5.37 (1H, ddd, $J = 17.1, 10.2, 8.5$ Hz, CH-C2), 5.05 (1H, dd, $J = 17.1, 1.6$ Hz, CH_2 -C1), 4.86 (1H, dd, $J = 10.2, 1.6$ Hz, CH_2 -C1), 4.62 (1H, s, NH), 3.10–2.98 (2H, m, CH_2 -C6), 1.44 (9H, s, *t*-Bu), 1.34–1.27 (1H, m, CH-C3), 1.05–0.97 (1H, m, CH-C5), 0.66–0.59 (2H, m, CH_2 -C4); ^{13}C NMR (126 MHz; CDCl_3): δ 156.0 (CO-Boc), 140.8 (CH-C2), 112.4 (CH_2 -C1), 79.3 (C-Boc), 44.5 (CH_2 -C6), 28.6 ($3 \times \text{CH}_3$ -Boc), 21.2 (CH-C3), 20.7 (CH-C5), 12.6 (CH_2 -C4); HRMS (ESI+) for $\text{C}_{11}\text{H}_{19}\text{NNaO}_2$ $[\text{M}+\text{Na}]$ calcd 220.1308, found 220.1302.

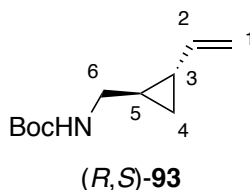
Ethyl 2-*[(t-butoxycarbonyl)[(1*R*,2*S*)-2-ethenylcyclopropyl]methylamino]-2-oxoacetate*
99



The procedure applied to the synthesis of (\pm)-**99** was followed using (*R,S*)-**2-90** (100 mg, 1.02 mmol), and ethyl 2-*(t*-butoxycarbonyl)amino-2-oxoacetate (879 mg, 4.05 mmol). The title compound (300 mg, 99%) was obtained as an orange oil.

R_f (EtOAc/PE 1:1): 0.95; [α]_D²⁵: -374 (c = 0.032, in CHCl₃); ν_{max} : 2982, 2938, 1740, 1698, 1636, 1369, 1145, 1024 cm⁻¹; ¹H NMR (500 MHz; CDCl₃): δ 5.35 (1H, ddd, J = 17.0, 10.2, 8.4 Hz, CH-C2), 5.04 (1H, dd, J = 17.0, 1.6 Hz, CH₂-C1), 4.86 (1H, dd, J = 10.2, 1.6 Hz, CH₂-C1), 4.34 (2H, q, J = 7.2 Hz, CH₂-Et), 3.64 (1H, dd, J = 14.1, 7.0 Hz, CH₂-C6), 3.59 (1H, dd, J = 14.1, 7.1 Hz, CH₂-C6), 1.52 (9H, s, *t*-Bu), 1.46–1.43 (1H, m, CH-C3), 1.36 (3H, t, J = 7.2 Hz, CH₃-Et), 1.21–1.16 (1H, m, CH-C5), 0.77 (1H, ddd, J = 8.6, 5.2, 5.2 Hz, CH₂-C4), 0.63 (1H, ddd, J = 8.6, 5.2, 5.2 Hz, CH₂-C4); ¹³C NMR (126 MHz; CDCl₃): δ 163.7 (CO-C7), 162.0 (CO-C8), 151.9 (CO-Boc), 140.4 (CH-C2), 112.7 (CH₂-C1), 85.3 (C-Boc), 62.3 (CH₂-Et), 46.6 (CH₂-C6), 28.0 (3 \times CH₃-Boc), 21.6 (CH-C3), 19.5 (CH-C5), 14.0 (CH₃-Et), 12.6 (CH₂-C4); HRMS (ESI+) for C₁₅H₂₃NNaO₅ [M+Na] calcd 320.1468, found 320.1455.

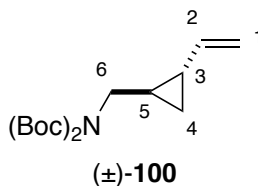
t*-Butyl-*N*-[(1*R*,2*S*)-2-ethenylcyclopropyl]methylcarbamate **93*



The procedure applied to the synthesis of (\pm)-**91** was followed using (*R,S*)-**2-99** (300 mg, 1.01 mmol). The title compound (132 mg, 66%) was obtained as a yellow oil.

R_f (EtOAc/PE 1:1): 0.85; $[\alpha]_D^{21}$: -374 ($c = 0.028$, in CH_3Cl); ν_{max} (CHCl_3): 3348, 3078, 3003, 1695, 1636, 1366, 1271 cm^{-1} ; ^1H NMR (400 MHz; CDCl_3): δ 5.37 (1H, ddd, $J = 17.1, 10.2, 8.6$ Hz, CH-C2), 5.04 (1H, dd, $J = 17.1, 1.6$ Hz, CH_2 -C1), 4.86 (1H, dd, $J = 10.2, 1.6$ Hz, CH_2 -C1), 4.62 (1H, s, NH), 3.09–3.02 (2H, m, CH_2 -C6), 1.44 (9H, s, *t*-Bu), 1.34–1.27 (1H, m, CH-C3), 1.04–0.98 (1H, m, CH-C5), 0.65–0.59 (2H, m, CH_2 -C4); ^{13}C NMR (126 MHz; CDCl_3): δ 156.0 (CO-Boc), 140.8 (CH-C2), 112.4 (CH_2 -C1), 79.3 (C-Boc), 44.5 (CH_2 -C6), 28.6 ($3 \times \text{CH}_3$ -Boc), 21.2 (CH-C3), 20.7 (CH-C5), 12.3 (CH_2 -C4); HRMS (ESI+) for $\text{C}_{11}\text{H}_{19}\text{NNaO}_2$ [$\text{M}+\text{Na}$] calcd 220.1308, found 220.1300.

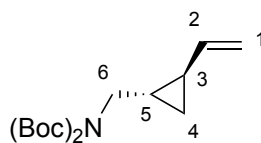
***t*-Butyl-*N*-(*t*-butoxycarbonyl-*N*-[(1*R**,2*S**)-2-ethenylcyclopropyl]methylcarbamate**
100



(±)-**90** (3.00 g, 30.6 mmol), HN(Boc)₂ (16.6 g, 76.5 mmol) and PPh₃ (20 g, 76.5 mmol) were dissolved in THF (310 mL). DEAD (12.1 mL, 76.5 mmol) was added dropwise at 0 °C. The mixture was warmed to rt and stirred for 12 h. The solvent was removed under vacuum, and the residue was purified by silica gel column chromatography (PE/EtOAc 10:0 to 9:1) to afford the title compound (6.05 g, 61%) as an orange oil.

R_f (EtOAc/PE 1:1): 0.96; *v*_{max} (CHCl₃): 3080, 2980, 2934, 1732, 1694, 1635, 1366, 1175, 1034 cm⁻¹; ¹H NMR (500 MHz; CDCl₃): δ 5.35 (1H, ddd, *J* = 17.1, 10.2, 8.6 Hz, CH-C2), 5.01 (1H, dd, *J* = 17.1, 1.6 Hz, CH₂-C1), 4.83 (1H, dd, *J* = 10.2, 1.6 Hz, CH₂-C1), 3.53 (2H, d, *J* = 7.5 Hz, CH₂-C6), 1.51 (18H, s, 2 × *t*-Bu), 1.47–1.40 (1H, m, CH-C3), 1.21 (1H, ddddd, *J* = 7.5, 5.0, 4.0, 1.1, 1.1 Hz, CH-C5), 0.73 (1H, ddd, *J* = 8.5, 5.2, 5.2 Hz, CH₂-C4), 0.58 (1H, ddd, *J* = 8.5, 5.0, 4.9 Hz, CH₂-C4); ¹³C NMR (126 MHz; CDCl₃): δ 152.9 (2 × CO-Boc), 141.0 (CH-C2), 112.2 (CH₂-C1), 82.3 (2 × C-Boc), 49.5 (CH₂-C6), 28.2 (6 × CH₃-Boc), 21.5 (CH-C3), 20.4 (CH-C5), 12.3 (CH₂-C4); HRMS (ESI+) for C₁₆H₂₇NNaO₄ [M+Na]⁺ calcd 320.1832, found 320.1819.

t*-Butyl *N*-(*t*-butoxycarbonyl)-*N*-[(1*S*,2*R*)-2-ethenylcyclopropyl]methylcarbamate **100*

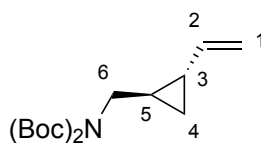


(*S,R*)-100

The procedure applied to the synthesis of (\pm)-**100** was followed using alcohol (*S,R*)-**90** (213 mg, 2.17 mmol), and DIAD (1.10 mL, 5.43 mmol) instead of DEAD. Purification by silica gel column chromatography (PE/EtOAc 99:1 to 85:15) afforded the title compound (412 mg, 64%) as an orange oil.

R_f (PE/EtOAc 1:1): 0.86; $[\alpha]_D^{26} +6.6$ ($c = 1.0$, CHCl₃); ν_{\max} 2978, 17.39, 1694, 1636, 1366, 1173, 1130, 856 cm⁻¹; ¹H NMR (400 MHz, CDCl₃) δ 5.35 (1H, ddd, $J = 17.1, 10.2, 8.5$ Hz, CH-C2), 5.01 (1H, dd, $J = 17.1, 1.7$ Hz, CH₂-C1), 4.83 (1H, dd, $J = 10.2, 1.7$ Hz, CH₂-C1), 3.53 (2H, d, $J = 6.9$ Hz, CH₂-C6), 1.50 (18H, s, 2 \times *t*-Bu), 1.46–1.40 (1H, m, CH-C3), 1.19 (1H, dddddd, $J = 8.6, 6.9, 6.9, 5.5, 4.5$ Hz, CH-C5), 0.73 (1H, ddd, $J = 8.6, 5.5, 4.8$ Hz, CH₂-C4), 0.58 (ddd, $J = 8.6, 4.9, 4.5$ Hz, CH₂-C4); ¹³C (126 MHz, CDCl₃): δ 141.0 (CH-C2), 112.2 (CH₂-C1), 82.3 (2 \times C-Boc), 49.5 (CH₂-C6), 28.2 (6 \times CH₃-Boc), 21.5 14.9 (CH-C3), 20.4 (CH-C5), 12.3 (CH₂-C4); HRMS (ESI⁺) calcd for C₁₆H₂₇NO₄Na [M+Na]⁺ 320.1832, found 320.1827.

t*-Butyl *N*-(*t*-butoxycarbonyl)-*N*-[(1*R*,2*S*)-2-ethenylcyclopropyl]methylcarbamate **100*

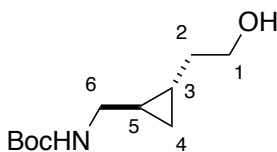


(*R,S*)-100

The procedure applied to the synthesis of (±)-**100** was followed using alcohol (*R,S*)-**90** (743 mg, 7.57 mmol). Purification by silica gel column chromatography (PE/EtOAc 99:1 to 90:10) gave the title compound (1.50 mg, 59%) as an orange oil.

R_f (PE/EtOAc 1:1): 0.86; $[\alpha]_D^{26} -6.3$ ($c = 1.0$, CHCl₃); ν_{\max} 2978, 1748, 1694, 1366, 1173, 1126, 853 cm⁻¹; ¹H NMR (500 MHz, CDCl₃) δ 5.35 (1H, ddd, $J = 17.1, 10.2, 8.5$ Hz, CH-C2), 5.01 (1H, ddd, $J = 17.1, 1.7, 0.6$ Hz, CH₂-C1), 4.83 (1H, dd, $J = 10.2, 1.7$ Hz, CH₂-C1), 3.53 (2H, d, $J = 6.9$ Hz, CH₂-C6), 1.50 (18 H, s, 2 × *t*-Bu), 1.46–1.39 (1H, dddd, $J = 8.6, 8.5, 5.1, 4.9$ Hz, CH-C3), 1.19 (1H, dddd, $J = 8.6, 6.9, 6.9, 5.1, 4.9$ Hz, CH-C5), 0.73 (1H, ddd, $J = 8.5, 5.1, 5.1$ Hz, CH₂-C4), 0.57 (1H, ddd, $J = 8.5, 4.9, 4.9$ Hz, CH₂-C4); ¹³C (126 MHz, CDCl₃): δ 152.9 (2 × CO-Boc), 141.0 (CH-C2), 112.2 (CH₂-C1), 82.3 (2 × C-Boc), 49.5 (CH₂-C6), 28.2 (6 × CH₃-Boc), 21.5 (CH-C3), 20.5 (CH-C5), 12.3 (CH₂-C4); HRMS (ESI⁺) calcd for C₁₆H₂₇NO₄Na [M+Na]⁺ 320.1832, found 320.1828.

t*-Butyl-*N*-[(1*R**,2*S**)-2-(2-hydroxyethyl)cyclopropyl]methylcarbamate **103*

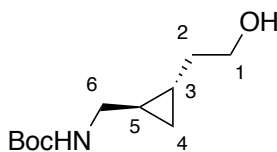


(±)-103

A flask with an argon inlet was charged with $\text{BH}_3 \cdot \text{THF}$ (1 M in THF, 2.60 mL, 2.60 mmol). A solution of (±)- **93** (340 mg, 1.71 mmol) in THF (2.10 mL) was added dropwise at rt. The reaction mixture was stirred overnight at rt. H_2O (4 mL) was then added carefully followed by pH 7 phosphate buffer solution (4 mL). Sodium perborate (526 mg, 3.42 mmol) was added and the reaction mixture was stirred for a further 2 h. The excess of sodium perborate was removed by filtration and the filtrate was concentrated under vacuum. The aqueous residue was extracted with Et_2O (3×10 mL). The combined organic extracts were washed with brine (10 mL), dried over MgSO_4 , filtered and concentrated under vacuum to give the corresponding alcohol (379 mg, quant.) as a colourless liquid.

R_f (EtOAc/PE 1:1): 0.51; ν_{max} (CHCl_3): 3329, 2976, 2928, 2874, 1688, 1366, 1171, 1042, 1020 cm^{-1} ; ^1H NMR (500 MHz; CDCl_3): δ 4.89 (1H, s, NH), 3.67 (2H, t, $J = 6.4$ Hz, $\text{CH}_2\text{-C1}$), 3.59 (1H, t, $J = 6.4$ Hz, OH), 3.11 (1H, ddd, $J = 13.7, 5.6, 5.6$ Hz, $\text{CH}_2\text{-C6}$), 2.84–2.80 (1H, m, $\text{CH}_2\text{-C6}$), 1.65–1.61 (1H, m, $1\text{H} \times \text{CH}_2\text{-C2}$), 1.43 (9H, s, *t*-Bu), 1.27–1.25 (1H, m, $\text{CH}_2\text{-C2}$), 0.72–0.67 (2H, m, $\text{CH-C5} + \text{CH-C3}$), 0.37–0.33 (1H, m, $\text{CH}_2\text{-C4}$), 0.31–0.27 (1H, m, $\text{CH}_2\text{-C4}$). ^{13}C NMR (126 MHz; CDCl_3): δ 156.4 (CO-Boc), 79.3 (C-Boc), 62.8 ($\text{CH}_2\text{-C1}$), 45.0 ($\text{CH}_2\text{-C6}$), 36.5 ($\text{CH}_2\text{-C2}$), 28.5 ($3 \times \text{CH}_3\text{-Boc}$), 18.4 (CH-C5), 15.0 (CH-C3), 10.0 ($\text{CH}_2\text{-C4}$). HRMS (ESI+) for $\text{C}_{11}\text{H}_{21}\text{NNaO}_3$ $[\text{M}+\text{Na}]^+$ calcd 238.1419 found, 238.1442.

t*-Butyl-*N*-[(1*R*,2*S*)-2-(2-hydroxyethyl)cyclopropyl]methylcarbamate **103*

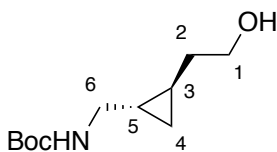


(*R,S*)-103

The procedure used for the hydroboration of (\pm)-**103** was followed using (*R,S*)-**93** (440 mg, 1.72 mmol). The title compound (379 mg, quant.) was obtained without any further purification as a colourless liquid.

R_f (EtOAc/PE 1:1): 0.51; ν_{\max} : 3354, 2928, 1715, 1514, 1244, 1173, 1022 cm^{-1} ; $^1\text{H-NMR}$ (500 MHz; CDCl_3): δ 4.95 (1H, s, NH), 3.64 (2H, t, $J = 6.3$ Hz, $\text{CH}_2\text{-C1}$), 3.59 (1H, t, $J = 6.6$ Hz, OH), 3.13–3.04 (1H, m, $\text{CH}_2\text{-C6}$), 2.85–2.77 (1H, m, $\text{CH}_2\text{-C6}$), 1.68–1.57 (1H, m, $\text{CH}_2\text{-C2}$), 1.40 (9H, s, *t*-Bu), 1.30–1.22 (1H, m, $\text{CH}_2\text{-C2}$), 0.72–0.62 (2H, m, CH-C5 + CH-C3), 0.35–0.30 (1H, m, $\text{CH}_2\text{-C4}$), 0.29–0.24 (1H, m, $\text{CH}_2\text{-C4}$). $^{13}\text{C NMR}$ (126 MHz; CDCl_3): δ 156.4 (CO-Boc), 79.3 (C-Boc), 62.7 ($\text{CH}_2\text{-C1}$), 44.9 ($\text{CH}_2\text{-C6}$), 36.5 ($\text{CH}_2\text{-C2}$), 28.5 (3 \times $\text{CH}_3\text{-Boc}$) 18.3 (CH-C5), 14.9 (CH-C3), 10.3 ($\text{CH}_2\text{-C4}$). HRMS (ESI+) for $\text{C}_{25}\text{H}_{21}\text{NNaO}_6$ [M+Na] calcd 464.2044 found 464.2041

t*-Butyl-*N*-[(1*S*,2*R*)-2-(2-hydroxyethyl)cyclopropyl]methylcarbamate **103*

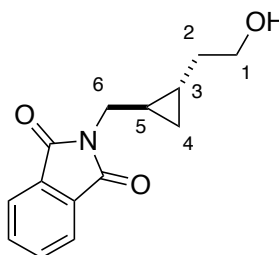


(*S,R*)-103

The procedure used for the hydroboration of (\pm)-**103** was followed using (*S,R*)-**93** (99.0 mg, 0.50 mmol). The title compound (66 mg, 61%) was obtained without any further purification as a colourless liquid.

R_f (EtOAc/PE 1:1): 0.54; $[\alpha]_D^{21}$: +0.52 ($c = 0.05$, in CH_3Cl); ν_{max} (CHCl_3): 3329, 2976, 2928, 2874, 1688, 1366, 1171, 1042, 1020 cm^{-1} ; ^1H NMR (500 MHz; CDCl_3): δ 4.99 (1H, s, NH), 3.61 (2H, t, $J = 6.2$ Hz, $\text{CH}_2\text{-C1}$), 3.56 (1H, t, $J = 6.2$ Hz, OH), 3.09–3.03 (1H, m, $1 \times \text{CH}_2\text{-C6}$), 2.80–2.78 (1H, m, $\text{CH}_2\text{-C6}$), 1.60–1.56 (1H, m, $\text{CH}_2\text{-C2}$), 1.38 (9H, s, *t*-Bu), 1.26–1.21 (1H, m, $\text{CH}_2\text{-C2}$), 0.68–0.63 (2H, m, CH-C5 + CH-C3), 0.32–0.29 (1H, m, $\text{CH}_2\text{-C4}$), 0.26–0.22 (1H, m, $\text{CH}_2\text{-C4}$); ^{13}C NMR (126 MHz; CDCl_3): δ 156.4 (CO-Boc), 79.2 (C-Boc), 62.5 ($\text{CH}_2\text{-C1}$), 44.9 ($\text{CH}_2\text{-C6}$), 36.5 ($\text{CH}_2\text{-C2}$), 28.4 ($3 \times \text{CH}_3\text{-Boc}$), 18.3 (CH-C5), 14.9 (CH-C3), 10.2 ($\text{CH}_2\text{-C4}$); HRMS (ESI+) for $\text{C}_{11}\text{H}_{21}\text{NNaO}_3$ $[\text{M}+\text{Na}]$ calcd 238.1419, found 238.1439.

[(1*R,2*S**)-(2-(2-Hydroxyethyl)cyclopropyl)methyl-2,3-dihydro-1*H*-isoindole-1,3-dione 104**

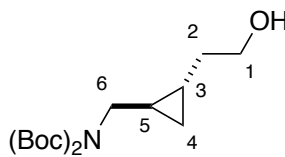


(±)-104

The procedure applied to the synthesis of compound (±)-**103** was followed using (±)-**94** (2.10 g, 9.23 mmol). The title compound (1.81 g, 80%) was obtained without any further purification as a as a yellow oil.

R_f (EtOAc/PE 1:1): 0.12; ν_{\max} (CHCl₃): 3381, 2930, 2874, 1771, 1705, 1395, 1059, 1042 cm⁻¹; ¹H-NMR (500 MHz; CDCl₃): δ 7.85–7.82 (2H, m, 2 \times CH-Pht), 7.72–7.69 (2H, m, 2 \times CH-Phth), 3.70–3.56 (3H, m, CH₂-C1 + 1 \times CH₂-C6), 3.44 (1H, dd, J = 14.1, 7.5 Hz, CH₂-C6), 1.39–1.31 (2H, m, CH₂-C2), 0.94–0.84 (2H, m, CH-C3 + CH-C5), 0.57 (1H, ddd, J = 8.3, 4.6, 4.6 Hz, CH₂-C4), 0.35 (1H, ddd, J = 8.3, 5.1, 5.1 Hz, CH₂-C4). ¹³C NMR (126 MHz; CDCl₃): δ 168.7 (2 \times CO-Phth), 134.1 (2 \times CH-Phth), 132.2 (2 \times C-Phth), 123.4 (2 \times CH-Pht), 62.8 (CH₂-C1), 42.1 (CH₂-C6), 19.0 (CH₂-C2), 17.5 (CH-C5), 15.3 (CH-C3), 10.5 (CH₂-C4). HRMS (ESI+) for C₁₄H₁₅NNaO₃ [M+Na]⁺ calcd 268.0944, found 268.0948.

t*-Butyl-*N*-(*t*-butoxycarbonyl)-*N*-[(1*R**,2*S**)-2-(2-hydroxyethyl)cyclopropyl]methylcarbamate **105*

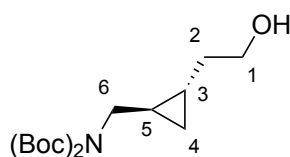


(±)-105

The procedure applied to the synthesis of (±)-**103** (AN-II-75) was applied using (±)-**100** (12.9 g, 43.6 mmol). The title compound (13.3 g, 97%) was obtained as a colourless liquid.

R_f (EtOAc/PE 1:1): 0.63; ν_{\max} (CHCl₃): 3464, 2980, 2934, 2674, 1732, 1692, 1368, 1172, 1126, 1096, 1036 cm⁻¹; ¹H NMR (500 MHz; CDCl₃): δ 3.66–3.64 (3H, m, CH₂-C1 + OH), 3.62–3.60 (1H, m, CH₂-C6), 3.34 (1H, dd, J = 14.3, 7.5 Hz, CH₂-C6), 1.63 (1H, dq, J = 13.6, 6.7 Hz, CH₂-C2), 1.50 (18H, s, 2 × *t*-Bu), 1.30–1.24 (1H, m, CH₂-C2), 0.90–0.87 (1H, m, CH-C5), 0.82–0.75 (1H, m, CH-C3), 0.47 (1H, ddd, J = 8.5, 4.8, 4.8 Hz, CH₂-C4), 0.31 (1H, ddd, J = 8.5, 5.0, 5.0 Hz, CH₂-C4); ¹³C NMR (126 MHz; CDCl₃): δ 153.3 (2 × CO-Boc), 82.4 (2 × C-Boc), 63.0 (CH₂-C1), 50.1 (CH₂-C6), 36.8 (CH₂-C2), 28.2 (6 × CH₃-Boc), 17.9 (CH-C5), 14.9 (CH-C3), 10.2 (CH₂-C4); HRMS (ESI+) for C₁₆H₂₉NNaO₅ [M+Na]⁺ calcd 338.1943, found 338.1917.

t*-Butyl *N*-(*t*-butoxycarbonyl)-*N*-[(1*R*,2*S*)-2-(2-hydroxyethyl)cyclopropyl]methylcarbamate **105*

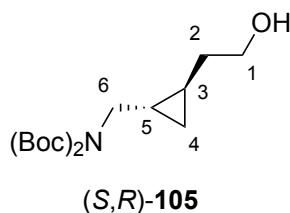


(*R,S*)-105

The procedure used for the hydroboration of (\pm)-**103** (AN-04-70) was applied using alkene (*R,S*)-**100** (1.32 g, 4.44 mmol). The mixture was stirred for 2 h before the oxidation reaction. The desired compound (1.27 g, 91%) was obtained as a colourless oil and used without further purification.

R_f (PE/EtOAc 1:1): 0.59; $[\alpha]_D^{27} +0.10$ ($c = 1.0$, CHCl₃); ν_{\max} 3522, 2978, 2932, 1732, 1694, 1366, 1173, 1130, 856 cm⁻¹; ¹H NMR (400 MHz, CDCl₃) δ 3.69–3.61 (3H, m, CH₂-C1 + 1 \times CH₂-C6), 3.34 (1H, dd, $J = 14.3, 7.5$ Hz, CH₂-C6), 1.67–1.60 (1H, m, CH₂-C2), 1.50 (18H, s, 2 \times *t*-Bu), 1.32–1.23 (1H, m, CH₂-C2), 0.94–0.85 (1H, m, CH-C5), 0.82–0.76 (1H, m, CH-C3), 0.47 (1H, ddd, $J = 8.6, 4.8$ Hz, 4.8 CH₂-C4), 0.31 (1H, ddd, $J = 8.6, 5.0, 5.0$ Hz, CH₂-C4); ¹³C (126 MHz, CDCl₃): δ 153.3 (2 \times CO-Boc), 82.4 (2 \times C-Boc), 63.0 (CH₂-C1), 50.1 (CH₂-C6), 36.8 (CH₂-C2), 28.2 (6 \times CH₃-Boc), 17.9 (CH-C5), 14.9 (CH-C3), 10.2 (CH₂-C4); HRMS (ESI+) calcd for C₁₆H₂₉NO₅Na [M+Na]⁺ 338.1938 found 338.1937.

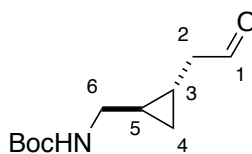
t*-Butyl *N*-(*t*-butoxycarbonyl)-*N*-[(1*S*,2*R*)-2-(2-hydroxyethyl)cyclopropyl]methylcarbamate **105*



The procedure used for the hydroboration/oxidation of (\pm)-**103** was applied using alkene (*S,R*)-**100** (1.01 g, 3.40 mmol). The reaction mixture was stirred for 2 h before the oxidation. The title compound (970 mg, 91%) was obtained as a colourless oil without any further purification.

R_f (PE/EtOAc 1:1): 0.59; $[\alpha]_D^{27} +0.5$ ($c = 1$, CHCl_3); ν_{max} 3522, 2978, 2931, 1732, 1685, 1366, 1172, 1126, 853 cm^{-1} ; ^1H NMR (400 MHz, CDCl_3) δ 3.69–3.59 (3H, m, $\text{CH}_2\text{-C1} + \text{CH}_2\text{-C6}$), 3.61 (1H, dd, $J = 8.5, 5.6$ Hz, $\text{CH}_2\text{-C6}$), 3.34 (1H, dd, $J = 14.3, 7.5$ Hz, $\text{CH}_2\text{-C2}$), 1.66–1.60 (1H, m, $\text{CH}_2\text{-C2}$), 1.50 (18H, s, $2 \times t\text{-Bu}$), 1.31–1.21 (1H, m, $\text{CH}_2\text{-C2}$), 0.91–0.85 (1H, m, CH-C5), 0.81–0.73 (1H, m, CH-C3), 0.47 (1H, ddd, $J = 8.5, 4.8, 4.8$ Hz, $\text{CH}_2\text{-C4}$), 0.31 (ddd, $J = 8.5, 5.0, 5.0$ Hz, $\text{CH}_2\text{-C4}$); ^{13}C (126 MHz, CDCl_3): δ 153.3 ($2 \times \text{CO-Boc}$), 82.4 ($2 \times \text{C-Boc}$), 63.0 ($\text{CH}_2\text{-C1}$), 50.1 ($\text{CH}_2\text{-C6}$), 36.8 ($\text{CH}_2\text{-C2}$), 28.2 ($6 \times \text{CH}_3\text{-Boc}$), 17.9 (CH-C5), 14.9 (CH-C3), 10.19 ($\text{CH}_2\text{-C4}$); HRMS (ESI $^+$) calcd for $\text{C}_{16}\text{H}_{29}\text{NO}_5\text{Na}$ $[\text{M}+\text{Na}]^+$ 338.1938, found 338.1932.

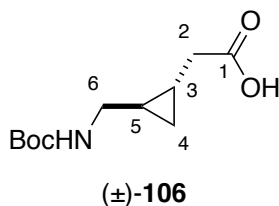
t*-Butyl [(1*R*,2*S*^{*})-2-(2-oxoethyl)cyclopropyl]methylcarbamate **102*



(±)-**103** (545 mg, 2.53 mmol) was dissolved in CH₂Cl₂ (13 mL). DMP (1.61 g, 3.80 mmol) was added to the solution at 0 °C. The reaction mixture was stirred overnight at rt. CH₂Cl₂ (10 mL) was added to the reaction mixture and the solution was washed with 1 M aq. NaOH (10 mL), aq. sat. NaHCO₃ (10 mL), and brine (10 mL). The organic phase was dried over MgSO₄, filtered and concentrated under vacuum. The crude was then purified by silica gel column chromatography (PE/EtOAc 1:1) to give the title compound (212 mg, 40%) as a yellow oil.

R_f (EtOAc/PE 1:1): 0.67; *v*_{max} (CHCl₃): 3360, 2978, 2930, 2726, 1695, 1366, 1169, 1051 cm⁻¹; ¹H NMR (500 MHz; CDCl₃): δ 9.79 (1H, t, *J* = 1.4 Hz, CHO-C1), 5.01 (1H, s, NH), 3.29–3.24 (1H, m, CH₂-C6), 2.85–2.80 (1H, m, CH₂-C6), 2.56 (1H, dd, *J* = 18.0, 5.5 Hz, CH₂-C2), 2.21 (1H, dd, *J* = 18.0, 7.1 Hz, CH₂-C2), 1.44 (9H, s, *t*-Bu), 0.88–0.81 (1H, m, CH-C3), 0.77 (1H, dddddd, *J* = 12.8, 11.0, 8.3, 5.5, 5.1 Hz, CH-C5), 0.53 (1H, ddd, *J* = 8.4, 5.1, 5.1 Hz, CH₂-C4), 0.40 (1H, ddd, *J* = 8.4, 5.5, 5.5 Hz, CH₂-C4); ¹³C NMR (126 MHz; CDCl₃): δ 202.1 (CO-C1), 156.1 (CO-Boc), 79.3 (C-Boc), 47.8 (CH₂-C2), 44.8 (CH₂-C6), 28.6 (3 × CH₃-Boc), 18.4 (CH-C5), 10.7 (CH-C3), 10.0 (CH₂-C4); HRMS (ESI+) for C₁₁H₁₉NNaO₃ [M+Na]⁺ calcd 236.1257, found 236.1252.

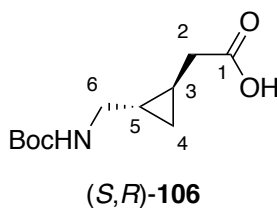
{{(1*R,2*S**)-2-([(*t*-butoxycarbonyl)amino]methylcyclopropyl}acetic acid [(*R**,*S**)-Boc-{GlyΔGly}-OH] 106**



(±)-**102** (212 mg, 0.99 mmol), 2-methyl-2-butene (2.10 mL, 19.8 mmol) and NaH₂PO₄·2H₂O (308 mg, 1.98 mmol.) were dissolved in *t*-BuOH (10 mL) and the resultant solution cooled to 0 °C. To the mixture was added NaClO₂ (313 mg, 3.47 mmol). The reaction mixture was stirred overnight at rt. The mixture was cooled down to 0 °C and 1 M aq. HCl was added to the solution until pH 1. The solution was extracted with CHCl₃ (3 × 15mL). The combined organic extracts were washed with brine, dried over MgSO₄, filtered and concentrated under reduced pressure. The residue was purified by silica gel column chromatography (PE/EtOAc 1:1) to afford (±)-**106** (176 mg, 77%) as a yellow oil.

R_f (EtOAc/PE 1:1): 0.55; *v*_{max} (CHCl₃): 3350, 2978, 1694, 1638, 1169 cm⁻¹. ¹H NMR (500 MHz; CDCl₃): δ 5.07 (1H, s, NH), 3.29 (1H, ddd, *J* = 12.5, 6.3, 6.3 Hz, CH₂-C6), 2.80–2.72 (1H, m, CH₂-C6), 2.54 (1H, dd, *J* = 16.9, 5.7 Hz, CH₂-C2), 2.08 (1H, dd, *J* = 16.9, 9.2 Hz, CH₂-C2), 1.44 (9H, s, *t*-Bu), 0.93–0.85 (1H, m, CH-C3), 0.83–0.79 (1H, m, CH-C5), 0.52 (1H, ddd, *J* = 8.4, 5.1, 5.1 Hz, CH₂-C4), 0.43 (1H, ddd, *J* = 8.4, 5.2, 5.2 Hz, CH₂-C4); ¹³C NMR (126 MHz; CDCl₃): δ 178.3 (CO-C1), 156.2 (CO-Boc), 79.3 (C-Boc), 44.8 (CH₂-C6), 37.9 (CH₂-C2), 28.6 (3 × CH₃-Boc), 18.5 (CH-C3), 12.9 (CH-C5), 10.3 (CH₂-C4); HRMS (ESI+) for C₁₁H₁₉NNaO₄ [M+Na]⁺ calcd 252.1206, found 252.1207.

(*R,S*)-Boc-{Gly Δ Gly}-OH 106

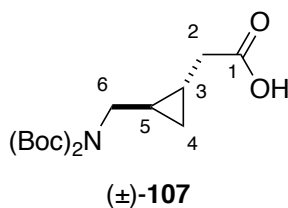


To a solution of (*S,R*)-**103** (56 mg, 0.26 mmol), DMSO (0.19 mL, 2.6 mmol) and DIPEA (0.18 mL, 1.04 mmol) in CH₂Cl₂ (3 mL) at 0 °C was added SO₃·pyridine (103 mg, 0.65 mmol) in two portions over 5 min. The reaction mixture was stirred for 15 min and then diluted with sat. aq. NaHCO₃ (5 mL). The phases were separated, and the organic phase was washed with sat. aq. NaHCO₃ (5 mL) and brine (5 mL), then dried over MgSO₄, filtered and concentrated under vacuum. The crude was used directly in the next step.

The procedure applied for the synthesis of (±)-**106** was then followed using the aldehyde previously obtained. The residue was purified by silica gel column chromatography (PE/EtOAc 1:1) to yield the acid (*S,R*)-**106** (5 mg, 22%) as dark yellow oil.

R_f (EtOAc/PE 1:1): 0.35; $[\alpha]_D^{21}$: +39 ($c = 0.10$, CH₃Cl), ν_{\max} (CHCl₃): 3335, 2978, 2930, 1711, 1368, 1171, 1026 cm⁻¹; ¹H NMR (500 MHz; CDCl₃): δ 5.03 (1H, s, NH), 3.30 (1H, ddd, $J = 12.7, 6.0, 6.0$ Hz, CH₂-C6), 2.83–2.73 (1H, m, CH₂-C6), 2.56 (1H, dd, $J = 16.8, 5.7$ Hz, CH₂-C2), 2.09 (1H, dd, $J = 16.8, 8.7$ Hz, CH₂-C2), 1.45 (9H, s, *t*-Bu), 0.95–0.86 (1H, m, CH-C3), 0.86–0.78 (1H, m, CH-C5), 0.53 (1H, ddd, $J = 8.5, 5.2, 5.2$ Hz, CH₂-C4), 0.44 (1H, ddd, $J = 8.5, 5.2, 5.2$ Hz, CH₂-C4); ¹³C NMR (126 MHz; CDCl₃): δ 178.3 (CO-C1), 156.2 (CO-Boc), 79.3 (C-Boc), 44.9 (CH₂-C6), 37.9 (CH₂-C2), 28.6 (3 × CH₃-Boc), 18.5 (CH-C3), 12.9 (CH-C5), 10.3 (CH₂-C4); HRMS (ESI+) for C₁₁H₁₉NNaO₄ [M+Na]⁺ calcd 252.1206, found 252.1203.

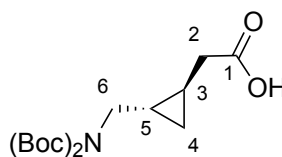
(±)-(Boc)₂-{GlyΔGly}-OH 107



(±)-**105** (1.46 g, 4.63 mmol) and NMO·H₂O (6.26 g, 46.3 mmol) were dissolved in MeCN (19 mL). TPAP (10 mol%, 162 mg, 0.46 mmol) was added portionwise (20 mg/20min) at rt. The reaction mixture was stirred overnight at rt. The reaction was then quenched by the addition of excess of isopropanol. H₂O (50 mL) was added and pH was carefully adjusted to 1 using 2 M aq. HCl. The aqueous phase was extracted with Et₂O (3 × 20 mL). The combined organic extracts were washed with brine, dried over MgSO₄, filtered and concentrated under vacuum to give the protected amino acid, which was used as crude for the next step.

R_f (EtOAc/PE 1:1): 0.08; ν_{max} (CHCl₃): 2980, 2936, 1709, 1694, 1368, 1171, 1126, 1034 cm⁻¹; ¹H NMR (500 MHz; CDCl₃): δ 3.52 (2H, dd, *J* = 6.9, 1.2 Hz, CH₂-C6), 2.28 (1H, dd, *J* = 16.2, 7.0 Hz, CH₂-C2), 2.21 (1H, dd, *J* = 16.2, 7.2 Hz, CH₂-C2), 1.50 (18H, s, 2 × *t*-Bu), 1.10–1.02 (2H, m, CH-C5 + CH-C3), 0.61 (1H, ddd, *J* = 8.5, 5.1, 5.1 Hz, CH₂-C4), 0.40 (1H, ddd, *J* = 8.5, 5.1, 5.1 Hz, CH₂-C4); ¹³C NMR (126 MHz; CDCl₃): δ 178.2 (C1), 153.0 (2 × CO-Boc), 82.4 (2 × C-Boc), 49.6 (CH₂-C6), 38.4 (CH₂-C2), 28.2 (6 × CH₃-Boc), 18.3 (CH-C5), 13.1 (CH-C3), 10.7 (CH₂-C4); HRMS (ESI+) for C₁₆H₂₇NNaO₆ [M+Na]⁺ calcd 352.1736, found 352.1680.

(*S,R*)-(Boc)₂-{GlyΔGly}-OH 107

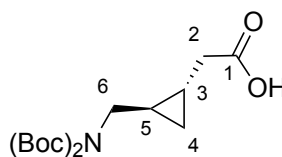


(*S,R*)-107

The procedure applied to the synthesis of (±)-**107** was followed using alcohol (*S,R*)-**105** (646 mg, 2.05 mmol). (*S,R*)-(Boc)₂-{GlyΔGly}-OH **107** (588 mg, 87%) was obtained as a black oil without any further purification.

R_f (PE/EtOAc 1:1): 0.15; $[\alpha]_D^{20} +0.72$ ($c = 1$, CHCl₃); ν_{\max} 2978, 2935, 1778, 1709, 1694, 1516, 1439, 1366, 1238, 1173, 1130, 853 cm⁻¹; ¹H NMR (400 MHz, CDCl₃) δ 3.52 (2H, dd, $J = 6.9, 5.6$ Hz, CH₂-C6), 2.30 (1H, dd, $J = 16.2, 6.7$ Hz, CH₂-C2), 2.19 (1H, dd, $J = 16.2, 7.3$ Hz, CH₂-C2), 1.50 (18H, s, 2 × *t*-Bu), 1.11–1.02 (2H, m, CH-C3 + CH-C5), 0.61 (1H, ddd, $J = 8.4, 5.2, 5.2$ Hz, CH₂-C4), 0.40 (1H, ddd, $J = 8.4, 5.2, 5.2$ Hz, CH₂-C4); ¹³C (126 MHz, CDCl₃): δ 177.9 (CO-C1), 152.9 (2 × CO-Boc), 82.4 (2 × C-Boc), 49.7 (CH₂-C6), 38.4 (CH₂-C2), 28.2 (6 × CH₃-Boc), 18.3 (CH-C5), 13.1 (CH-C3), 10.7 (CH₂-C4); HRMS (ESI+) for C₁₆H₂₇NO₆Na [M+Na]⁺ calcd 352.1731, found 352.1716.

(*R,S*)-(Boc)₂-{GlyΔGly}-OH **107**

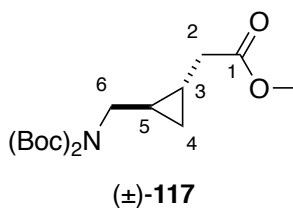


(*R,S*)-107****

The procedure used for the synthesis of (±)-**106** was applied using alcohol (*R,S*)-**105** (970 mg, 3.08 mmol) affording (*R,S*)-(Boc)₂-{GlyΔGly}-OH **107** (1.04 g, quant.) as a black oil. The compound was used without any further purification.

R_f (PE/EtOAc 1:1): 0.65; $[\alpha]_D^{27}$ -0.34 ($c = 1.0$, CHCl₃); ν_{\max} 3233, 2978, 2936, 1778, 1709, 1694, 1516, 1366, 1234, 1173, 1126, 853 cm⁻¹; ¹H NMR (400 MHz, CDCl₃) δ 3.52 (2H, dd, $J = 6.9, 1.6$ Hz, CH₂-C6), 2.29 (1H, dd, $J = 16.2, 6.9$ Hz, CH₂-C2), 2.21 (1H, dd, $J = 16.2, 7.1$ Hz, CH₂-C2), 1.50 (18H, s, 2 × *t*-Bu), 1.13–1.01 (2H, m, CH-C5 + CH-C3), 0.61 (1H, ddd, $J = 8.4, 5.2, 5.2$ Hz, CH₂-C4), 0.40 (1H, ddd, $J = 8.4, 5.1, 5.1$ Hz, CH₂-C4); ¹³C (126 MHz, CDCl₃): δ 178.4 (CO-C1), 153.0 (2 × CO-Boc), 82.4 (2 × C-Boc), 49.6 (CH₂-C6), 38.5 (CH₂-C2), 28.2 (6 × CH₃-Boc), 18.3 (CH-C5), 13.1 (CH-C3), 10.7 (CH₂-C4); HRMS (ESI+) for C₁₆H₂₇NO₆Na [M+Na]⁺ calcd 352.1731, found 352.1719.

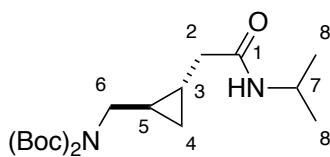
(±)-(Boc)₂-{GlyΔGly}-OMe 117



To a suspension of (±)-(Boc)₂-{GlyΔGly}-OH **107** (789 mg, 2.40 mmol) and NaHCO₃ (403 mg, 4.80 mmol) in anhydrous DMF (7.10 mL) was added MeI (750 μL, 12.0 mmol). The reaction mixture was stirred overnight at rt. H₂O (10.0 mL) was added dropwise and the mixture was then extracted with Et₂O (3 × 10 mL). The combined organic extracts were washed with H₂O (10 mL) and brine (10 mL), dried over MgSO₄, filtered and concentrated under vacuum. The residue was then purified by silica gel on column chromatography (PE/EtOAc, 95:5 to 85:15) to give (±)-(Boc)₂-{GlyΔGly}-OMe **117** (359 mg, 47%) as a yellow oil.

R_f (EtOAc/PE 1:1): 0.15; ν_{max} (CHCl₃): 2980, 2934, 2849, 1749, 1694, 1234, 1171, 1128, 1034 cm⁻¹; ¹H NMR (400 MHz; CDCl₃): δ 3.67 (3H, s, CH₃-OMe), 3.51 (2H, dd, *J* = 6.9, 3.6 Hz, CH₂-C6) [?], 2.25 (1H, dd, *J* = 15.7, 6.9 Hz, CH₂-C2), 2.17 (1H, dd, *J* = 15.7, 7.2 Hz, CH₂-C2), 1.51 (18H, s, 2 × *t*-Bu), 1.10–1.00 (2H, m, CH-C5 + CH-C3), 0.59 (1H, ddd, *J* = 8.5, 5.1, 5.1 Hz, CH₂-C4), 0.37 (1H, ddd, *J* = 8.5, 5.1, 5.1 Hz, 1 × CH₂-C4); ¹³C NMR (101 MHz; CDCl₃): δ 173.3 (CO-C1), 152.9 (2 × CO-Boc), 82.3 (2 × C-Boc), 51.8 (CH₃-OMe), 49.7 (CH₂-C6), 38.7 (CH₂-C2), 28.2 (6 × CH₃-Boc), 18.3 (CH-C3), 13.4 (CH-C5), 10.8 (CH₂-C4); HRMS (ESI+) for C₁₇H₂₉NNaO₆ [M+Na]⁺ calcd 366.1893, found 366.1883.

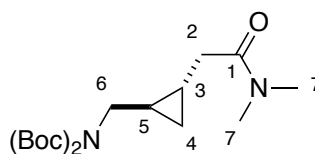
(±)-(Boc)₂-{GlyΔGly}-N-*i*Pr 118



(±)-(Boc)₂-{GlyΔGly}-OH **107** (700 mg, 2.13 mmol), *i*-PrNH₂ (370 μL, 4.26 mmol) and Et₃N (1.00 mL, 7.46 mmol) were dissolved in CH₂Cl₂ (11 mL). The solution was stirred for 15 min at rt and T3P (1.90 mL, of a 50% solution in EtOAc, 3.20 mmol) was added dropwise. The reaction mixture was stirred for 18 h at rt. The solution was washed with H₂O (3 × 10 mL) and the phases were separated. The organic phase was dried over MgSO₄, filtered and concentrated under vacuum. The residue was purified by silica gel on column chromatography (PE/EtOAc 1:1) to give the title compound (365 mg, 46%) as a colourless oil.

R_f (EtOAc/PE 1:1): 0.41; ν_{max} (CHCl₃): 3287, 2976, 2934, 2874, 1694, 1651, 1366, 1175, 1132, 1032 cm⁻¹; ¹H-NMR (400 MHz; CDCl₃): δ 5.91 (1H, d, *J* = 7.6 Hz, NH), 4.15–4.04 (1H, m, CH-C7), 3.63 (1H, dd, *J* = 14.4, 6.0 Hz, CH₂-C6), 3.52 (1H, dd, *J* = 14.4, 6.3 Hz, CH₂-C6), 2.19 (1H, dd, *J* = 16.3, 6.7 Hz, CH₂-C2), 2.07 (1H, dd, *J* = 16.3, 6.9 Hz, CH₂-C2), 1.50 (18H, s, 2 × *t*-Bu), 1.16 (6H, d, *J* = 6.6 Hz, 2 × CH₃-C8), 1.01–0.88 (2H, m, CH-C5 + CH-C3), 0.58 (1H, ddd, *J* = 8.6, 4.8, 4.8 Hz, CH₂-C4), 0.37 (1H, ddd, *J* = 8.6, 4.8, 4.8 Hz, CH₂-C4); ¹³C NMR (126 MHz; CDCl₃): 171.2 (CO-C1), 153.2 (2 × CO-Boc), 82.7 (2 × C-Boc), 49.1 (CH₂-C6), 41.3 (CH-C7), 41.1 (CH₂-C2), 28.2 (6 × CH₃-Boc), 22.9 (2 × CH₃-C8), 18.4 (CH-C5), 13.1 (CH-C3), 10.4 (CH₂-C4); HRMS (ESI+) for C₁₉H₃₄N₂NaO₅ [M+Na]⁺ calcd 393.2365 found, 397.2337.

(±)-(Boc)₂-{GlyΔGly}-NMe₂ 119

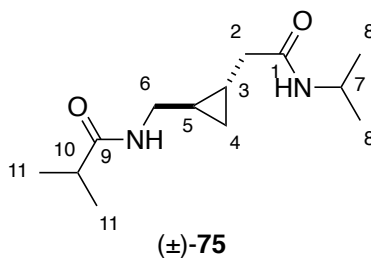


(±)-119

(±)-(Boc)₂-{GlyΔGly}-OH **107** (1.00 g, 3.04 mmol), HNMe₂ (1.60 mL of a 2 M solution in THF, 3.19 mmol) and Et₃N (1.50 mL, 10.6 mmol) were dissolved in CH₂Cl₂ (15 mL). The solution was stirred for 15 min at rt and T3P (2.70 mL of a 50% solution in EtOAc, 4.56 mmol) was added dropwise. The reaction mixture was stirred for 18 h at rt. The solution was washed with H₂O (3 × 10 mL) and phases separated. The organic phase was dried over MgSO₄, filtered and concentrated under vacuum. The residue was purified by silica gel column chromatography (PE/EtOAc 1:1) to give the title compound (400 mg, 37%) as a colourless oil.

R_f(EtOAc/PE 1:1): 0.17; ν_{max}(CHCl₃): 2978, 1740, 1694, 1649, 1368, 1132 cm⁻¹; ¹H NMR (500 MHz; CDCl₃): δ 3.58 (1H, dd, *J* = 14.4, 6.7 Hz, CH₂-C6), 3.46 (1H, dd, *J* = 14.4, 7.2 Hz, CH₂-C6), 2.97 (3H, s, CH₃-C7), 2.93 (3H, s, CH₃-C7), 2.43 (1H, dd, *J* = 15.3, 5.8 Hz, CH₂-C2), 2.11 (1H, dd, *J* = 15.3, 7.6 Hz, CH₂-C2), 1.50 (18H, d, *J* = 1.7 Hz, 2 × *t*-Bu), 1.13–1.05 (1H, m, CH-C3), 1.04–0.97 (1H, m, CH-C5), 0.62 (1H, ddd, *J* = 8.5, 5.1, 5.1 Hz, CH₂-C4), 0.38 (1H, ddd, *J* = 8.5, 5.1, 5.1 Hz, CH₂-C4); ¹³C NMR (126 MHz; CDCl₃): δ 172.3 (CO-C1), 152.9 (CO-Boc), 82.3 (C-Boc), 49.9 (CH₂-C6), 37.9 (CH₂-C2), 37.5 (CH₃-C7), 35.4 (CH₃-C7), 28.2 (6 × CH₃-Boc), 18.2 (CH-C5), 13.8 (CH-C5), 10.9 (CH₂-C4); HRMS (ESI+) for C₁₈H₃₂N₂NaO₅ [M+Na]⁺ calcd 379.2203, found 379.2190.

(±)-*i*PrOC-{GlyΔGly}-*N-i*Pr 75

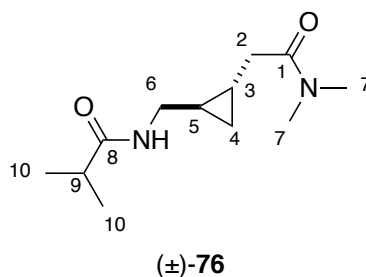


A solution of (±)-(Boc)₂-{GlyΔGly}-*i*Pr **118** (57 mg, 0.15 mmol) in CH₂Cl₂ (1.5 mL) was treated with TFA (115 μL, 9.90 mmol) dropwise at rt. The reaction mixture was stirred for 3 h at rt and solvent was removed under vacuum.

The resulting TFA salt (0.15 mmol) was dissolved in CH₂Cl₂ (380 μL) and Et₃N (40 μL, 0.28 mmol) was added. Isobutyric anhydride (46 μL, 0.28 mmol) was added dropwise at rt and the reaction mixture was stirred for 36 h. H₂O (10 mL) was added and phases were separated. The organic phase was washed with aq. sat. NaHCO₃ (3 × 10 mL) and brine (10 mL). The organic phase was dried over MgSO₄, filtered and concentrated under vacuum. The crude product was purified by silica gel column chromatography (PE/EtOAc 9:1 to 2:3) to afford the title compound (25 mg, 69% over two steps) as a white powder.

R_f (EtOAc/PE 1:1): 0.45; m.p.: 107–108 °C; ν_{max} (10 mM, CH₂Cl₂) 3429, 3325, 2974, 2932, 1663, 1516, 1277, 1265, 1258 cm⁻¹; ¹H NMR (400 MHz; CDCl₃): δ 6.77 (1H, s, NH-Gly), 5.42 (1H, s, NH-*i*Pr), 4.09 (1H, m, CH-C7), 3.72 (1H, ddd, *J* = 13.5, 6.0, 4.7 Hz, CH₂-C6), 2.61–2.47 (2H, m, CH₂-C6 + CH₂-C2), 1.18 (3H, d, *J* = 6.9 Hz, CH₃-C11), 1.17 (3H, d, *J* = 6.9 Hz, CH₃-C11), 1.17 (3H, d, *J* = 6.5 Hz, CH₃-C8), 1.16 (3H, d, *J* = 6.5 Hz, CH₃-C8), 2.43 (1H, hept, *J* = 6.9 Hz, CH-C10), 1.70 (1H, dd, *J* = 16.2, 9.4 Hz, CH₂-C2), 0.83–0.70 (2H, m, CH-C5 + CH-C3), 0.52 (1H, ddd, *J* = 8.2, 5.2, 5.2 Hz, CH₂-C4), 0.42 (1H, ddd, *J* = 8.2, 5.2, 5.2 Hz, CH₂-C4); ¹³C NMR (101 MHz; CDCl₃): δ 177.5 (CO-C1), 171.7 (CO-C9), 43.9 (CH₂-C6), 41.6 (CH-C7), 40.0 (CH₂-C2), 35.7 (CH-C10), 23.0 (2 × CH₃-C8), 19.8 (2 × CH₂-C11), 18.1 (CH-C3/5), 13.6 (CH-C3/5), 10.2 (CH₂-C4); HRMS (ESI⁺) for C₁₃H₂₄N₂NaO₂ [M+Na]⁺ calcd 262.1730, found 262.1727.

(±)-*i*PrOC-{GlyΔGly}-NMe₂ 76

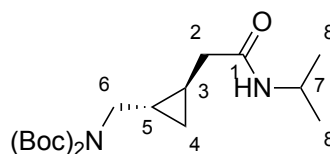


(±)-(Boc)₂-{GlyΔGly}-NMe₂ **119** (400 mg, 1.12 mmol) was dissolved in CH₂Cl₂ (11 mL) and treated with TFA (860 μL, 11.2 mmol). The reaction mixture was stirred for 3 h and solvent was removed under vacuum.

The resulting TFA·(±)-H-{GlyΔGly}-NMe₂ salt and Et₃N (164 μL, 1.18 mmol) were dissolved in CH₂Cl₂ (1.6 mL). Isobutyric anhydride (196 μL, 1.18 mmol) was added dropwise to the solution at rt. The reaction mixture was stirred for 18 h at rt. H₂O (10 mL) was added and the phases were separated. The organic phase was washed with sat. aq NaHCO₃ (3 × 10 mL), 1 M aq. NaOH (3 × 10 mL), 1 M aq. HCl (10 mL) and brine (10 mL), dried over MgSO₄, filtered and concentrated under vacuum. The residue was purified by silica gel column chromatography (CH₂Cl₂/MeOH 99:1 to 97:3) to afford the title compound (17 mg, 7% over 2 steps) as a colourless semi-solid.

R_f (PE/EtOAc 1:1): 0.08; ν_{max} (*c* = 10 mM, CH₂Cl₂) 3306, 3048, 2963, 2928, 2855, 1636, 1535 cm⁻¹; ¹H NMR (500 MHz, CDCl₃) δ 7.57 (1H, br s, NH), 3.91 (1H, ddd, *J* = 13.5, 6.3, 4.8 Hz, CH₂-C6), 2.96 (3H, s, CH₃-C7), 2.94 (3H, s, CH₃-C7), 2.88 (1H, dd, *J* = 17.0, 4.3 Hz, CH₂-C2), 2.46 (1H, hept, *J* = 6.9 Hz, CH-C9), 2.31 (1H, ddd, *J* = 13.5, 10.4, 1.9 Hz, CH₂-C6), 1.65 (1H, dd, *J* = 17.0, 10.1 Hz, CH₂-C2), 1.19 (3H, d, *J* = 6.9 Hz, CH₃-C10), 1.17 (3H, d, *J* = 6.9 Hz, CH₃-C10), 0.78 (1H, dddddd, *J* = 10.1, 8.4, 5.3, 5.3, 4.3 Hz, CH-C3), 0.63 (1H, dddddd, *J* = 9.6, 8.6, 5.1, 5.0, 4.8 Hz, CH-C5), 0.54 (1H, ddd, *J* = 8.3, 5.2, 5.2 Hz, CH₂-C4), 0.44 (1H, ddd, *J* = 8.3, 5.2, 5.2 Hz, CH₂-C4); ¹³C (126 MHz, CDCl₃): δ 177.5 (CO-C1), 172.9 (CO-C9), 44.5 (CH₂-C6), 37.3 (CH₂-C2), 36.9 (CH₃-C7), 35.5 (CH-C9), 35.5 (CH₃-C7), 19.8 (2 × CH₃-C10), 17.7 (CH-C5), 13.5 (CH-C3), 10.5 (CH₂-C4); HRMS (ESI⁺) for C₁₂H₂₂N₂O₂Na [M+Na]⁺ calcd 249.1573, found 249.1570.

(*S,R*)-Boc₂-{GlyΔGly}-N-*i*Pr 118

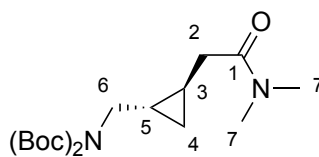


(*S,R*)-118

The procedure applied to the synthesis of (±)-(*Boc*)₂-{GlyΔGly}-*i*Pr **118** was followed using (*S,R*)-(*Boc*)₂-{GlyΔGly}-OH **107** (50 mg, 0.15 mmol). The crude was purified by silica gel column chromatography (PE/EtOAc 1:1) to give (*S,R*)-**118** (29 mg, 52%) as a colourless oil.

R_f (PE/EtOAc 1:1): 0.44; $[\alpha]_D^{17} +8.28$ ($c = 1.45$, CHCl₃); ν_{\max} 3308, 2975, 2934, 1728, 1700, 1642, 1368, 1174, 1132, 853 cm⁻¹; ¹H NMR (500 MHz, CDCl₃) δ 5.91 (1H, d, $J = 6.8$ Hz, NH), 4.15–4.05 (1H, m, CH-C7), 3.63 (1H, dd, $J = 14.4, 6.1$ Hz, CH₂-C6), 3.52 (1H, dd, $J = 14.4, 6.4$ Hz, CH₂-C6), 2.19 (1H, dd, $J = 16.5, 6.8$ Hz, CH₂-C2), 2.07 (1H, dd, $J = 16.5, 7.5$ Hz, CH₂-C2), 1.50 (18H, s, 2 × *t*-Bu), 1.16 (3H, d, $J = 6.3$ Hz, CH₃-C8), 1.16 (3H, d, $J = 6.6$ Hz, CH₃-C8), 1.01–0.88 (2H, m, CH-C5 + CH-C3), 0.59 (1H, ddd, $J = 8.5, 5.0, 5.0$ Hz, CH₂-C4), 0.38 (1H, ddd, $J = 8.5, 5.0, 5.0$ Hz, CH₂-C4); ¹³C (126 MHz, CDCl₃): δ 171.3 (CO-C1), 153.2 (2 × CO-Boc), 82.7 (C-Boc), 49.1 (CH₂-C6), 41.4 (CH-C7), 41.1 (CH₂-C2), 28.2 (6 × CH₃-Boc), 22.9 (CH₃-C8), 22.9 (CH₃-C8), 18.4 (CH-C5), 13.1 (CH-C3), 10.4 (CH₂-C4); HRMS (ESI+) for C₁₉H₃₄N₂O₅Na [M+Na]⁺ calcd 393.2360 found 393.2356.

(*S,R*)-(Boc)₂-{GlyΔGly}-NMe₂ 119

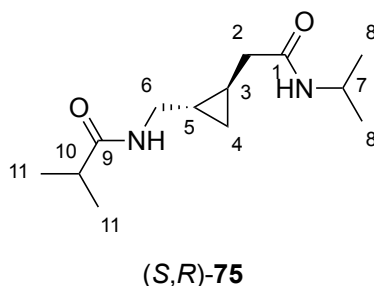


(*S,R*)-119

The procedure applied to the synthesis of (\pm)-(Boc)₂-{GlyΔGly}-NMe₂ **119** was followed using (*S,R*)-(Boc)₂-{GlyΔGly}-OH **107** (130 mg, 0.39 mmol). 2 equiv. of HNMe₂ (2 M in THF) were used in this case. The residue was purified by silica gel column chromatography (PE/EtOAc 1:1) to give (*S,R*)-(Boc)₂-{GlyΔGly}-NMe₂ **119** as a yellow oil (67 mg, 48%).

R_f (PE/EtOAc 1:1): 0.34; $[\alpha]_D^{22} +9.8$ ($c = 0.50$, CHCl₃); ν_{\max} 2977, 2932, 1744, 1734, 1693, 1646, 1368, 1171, 1131, 853 cm⁻¹; ¹H NMR (500 MHz, CDCl₃) δ 3.56 (1H, dd, $J = 14.4$, 6.6 Hz, CH₂-C6), 3.44 (1H, dd, $J = 14.4$, 7.2 Hz, CH₂-C6), 2.95 (3H, s, CH₃-C7), 2.91 (3H, s, CH₃-C7), 2.41 (1H, dd, $J = 15.3$, 5.8 Hz, CH₂-C2), 2.09 (1H, dd, $J = 15.3$, 7.5 Hz, CH₂-C2), 1.48 (18H, s, 2 \times *t*-Bu), 1.10–1.03 (1H, m, CH-C3), 1.01–0.96 (1H, m, CH-C5), 0.60 (1H, ddd, $J = 8.4$, 5.0, 5.0 Hz, CH₂-C4), 0.36 (1H, ddd, $J = 8.4$, 5.1, 5.1 Hz, CH₂-C4); ¹³C (126 MHz, CDCl₃): δ 172.2 (CO-C1), 152.9 (2 \times CO-Boc), 82.2 (CH-Boc), 49.9 (CH₂-C6), 37.8 (CH₂-C2), 37.4 (CH₃-C7), 35.4 (CH₃-C7), 28.2 (6 \times CH₃-Boc), 18.2 (CH-C5), 13.8 (CH-C3), 10.8 (CH₂-C4); HRMS (ESI⁺) for C₁₈H₃₂N₂O₅Na [M+Na]⁺ calcd 379.2203, found 379.2201.

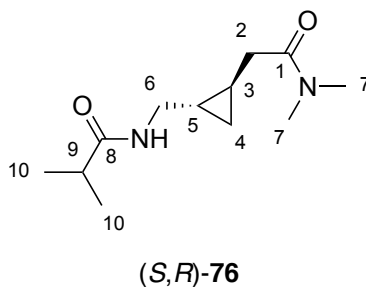
(*S,R*)-*i*Pr-{GlyΔGly}-*N-i*Pr 75



The procedure applied to the synthesis of (\pm)-*i*Pr-{GlyΔGly}-*N-i*Pr **75** was followed using (*S,R*)-(Boc)₂-{GlyΔGly}-*N-i*Pr **118** (74 mg, 0.20 mmol). After deprotection, 1.5 equiv. of Et₃N and isobutyric anhydride were used. Trituration of the residue with cold pentane and cold Et₂O in EtOAc afforded the title compound as a white solid (8 mg, 17% over 2 steps).

R_f (PE/EtOAc 1:1): 0.08; $[\alpha]_D^{21}$ -43 ($c = 0.28$, CHCl₃); m.p.: 134–135 °C; ν_{\max} 3300, 2970, 2924, 1639, 1547, 1238 cm⁻¹; ¹H NMR (500 MHz, CDCl₃) δ 6.78 (1H, br s, NH-C6), 5.39 (1H, br s, NH-C7), 4.10 (1H, dh, $J = 7.9, 6.5$ Hz, CH-C7), 3.73 (1H, ddd, $J = 13.5, 5.9, 4.8$ Hz, CH₂-C6), 2.60–2.50 (2H, m, CH₂-C6 + CH₂-C2), 2.43 (1H, h, $J = 7.0$ Hz, CH-C10), 1.70 (1H, dd, $J = 16.2, 9.4$ Hz, CH₂-C2), 1.18 (3H, d, $J = 7.0$ Hz, CH₃-C11), 1.18 (3H, d, $J = 7.0$ Hz, CH₃-C11), 1.17 (3H, d, $J = 6.5$ Hz, CH₃-C8), 1.16 (3H, d, $J = 6.5$ Hz, CH₃-C8), 0.83–0.71 (2H, m, CH-C3 + CH-C5), 0.53 (1H, ddd, $J = 8.1, 5.3, 5.3$ Hz, CH₂-C4), 0.42 (1H, ddd, $J = 8.1, 5.3, 5.3$ Hz, CH₂-C4); ¹³C (126 MHz, CDCl₃): δ 177.5 (CO-C9), 171.7 (CO-C1), 43.9 (CH₂-C6), 41.6 (CH-C7), 39.9 (CH₂-C2), 35.7 (CH-C10), 22.9 (CH₃-C8), 22.9 (CH₃-C8), 19.8 (2 \times CH₃-C11), 18.0 (CH-C5/3), 13.5 (CH-C3/5), 10.2 (CH₂-C4); HRMS (ESI⁺) for C₁₃H₂₄N₂O₂Na [M+Na]⁺ calcd 263.1730, found 263.1725.

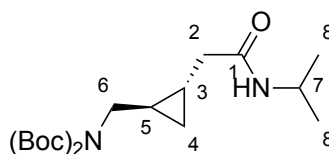
(*S,R*)-*i*Pr-{Gly Δ Gly}-NMe₂ **76**



The procedure applied to the synthesis of (\pm)-*i*Pr-{Gly Δ Gly}-NMe₂ **76** was followed using (1*R*,2*S*)-(Boc)₂-Gly Δ Gly}-NMe₂ **119** (90 mg, 0.25 mmol). After deprotection, 1.5 equiv. of Et₃N and isobutyric anhydride were used. The residue was purified by silica gel column chromatography (CH₂Cl₂/MeOH 100:0 to 97:3) to afford the title compound (37 mg, 65% over 2 steps) as a colourless semi-solid.

R_f (PE/EtOAc 1:1): 0.08; $[\alpha]_D^{28}$ -57 (c = 0.50, CHCl₃); ν_{\max} 3480, 3295, 2967, 2932, 1636, 1535, 1265, 1238 cm⁻¹; ¹H NMR (500 MHz, CDCl₃) δ 7.57 (1H, br s, NH), 3.92 (1H, ddd, J = 13.3, 6.3, 4.8 Hz, CH₂-C6), 2.97 (3H, s, CH₃-C7), 2.94 (3H, s, CH₃-C7), 2.88 (1H, dd, J = 17.0, 4.0 Hz, CH₂-C2), 2.46 (2H, h, J = 6.9 Hz, CH₂-C9), 2.32 (1H, ddd, J = 13.3, 10.2, 2.0 Hz, CH₂-C6), 1.65 (1H, dd, J = 17.0, 10.3 Hz, CH₂-C2), 1.18 (3H, d, J = 6.9 Hz, CH₃-C10), 1.17 (3H, d, J = 6.9 Hz, CH₃-C10), 0.78 (1H, dddddd, J = 10.3, 8.6, 5.3, 5.1, 4.0 Hz, CH-C3), 0.63 (1H, dddddd, J = 10.2, 8.6, 5.3, 5.1, 4.8 Hz, CH-C5), 0.55 (1H, ddd, J = 8.3, 5.1, 5.1 Hz, CH₂-C4), 0.45 (1H, ddd, J = 8.3, 5.3, 5.3 Hz, CH₂-C4); ¹³C (126 MHz, CDCl₃): δ 177.6 (CO-C1), 172.9 (CO-C8), 44.5 (CH₂-C6), 37.3 (CH₂-C2), 36.9 (CH₃-C7), 35.7 (CH-C9), 35.5 (CH₃-C7), 19.8 (2 \times CH₃-C10), 17.7 (CH-C5), 13.5 (CH-C3), 10.5 (CH₂-C4); HRMS (ESI+) for C₁₂H₂₂N₂O₂Na [M+Na]⁺ calcd 249.1573, found 249.1575.

(*R,S*)-Boc₂-{GlyΔGly}-N-*i*Pr 118

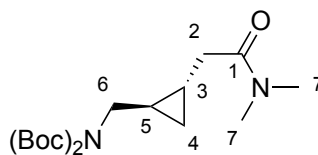


(*R,S*)-118

The procedure applied to the synthesis of (±)-(Boc)₂-{GlyΔGly}-N-*i*Pr **118** was followed using (*R,S*)-(Boc)₂-{GlyΔGly}-OH **107** (92 mg, 0.28 mmol). The crude was purified by silica gel column chromatography (PE/EtOAc 1:1) to give (*S,R*)-(Boc)₂-{GlyΔGly}-N-*i*Pr **118** (36 mg, 35%) as a colourless oil.

R_f (PE/EtOAc 1:1): 0.35; $[\alpha]_D^{17}$ -8.63 ($c = 1.80$, CHCl₃); ν_{\max} 3294, 2971, 2929, 1732, 1693, 1640, 1366, 1173, 1129, 853 cm⁻¹; ¹H NMR (400 MHz, CDCl₃) δ 5.96 (1H, d, $J = 8.1$ Hz, NH), 4.17–4.04 (1H, m, CH-C7), 3.60 (1H, dd, $J = 14.4, 6.0$ Hz, CH₂-C6), 3.50 (1H, dd, $J = 14.4, 6.2$ Hz, CH₂-C6), 2.16 (1H, dd, $J = 16.5, 6.7$ Hz, CH₂-C2), 2.04 (1H, dd, $J = 16.5, 7.2$ Hz, CH₂-C2), 1.48 (18H, s, 2 × *t*-Bu), 0.92 (3H, d, $J = 6.5$ Hz, CH₃-C8), 0.92 (3H, d, $J = 6.5$ Hz, CH₃-C8), 0.99–0.81 (2H, m, CH-C5 + CH-C3), 0.55 (1H, ddd, $J = 8.4, 5.0, 5.0$ Hz, CH₂-C4), 0.35 (1H, ddd, $J = 8.4, 5.1, 5.1$ Hz, CH₂-C4); ¹³C (101 MHz, CDCl₃): δ 171.2 (CO-C1), 153.2 (2 × CO-Boc), 82.6 (C-Boc), 49.1 (CH₂-C6), 41.3 (CH-C7), 41.0 (CH₂-C2), 28.2 (6 × CH₃-Boc), 22.8 (CH₃-C8), 22.8 (CH₃-C8), 18.4 (CH-C5), 13.1 (CH-C3), 10.4 (CH₂-C4); HRMS (ESI+) for C₁₉H₃₄N₂O₅Na [M+Na]⁺ calcd 393.2360, found 393.2359.

(*R,S*)-(Boc)₂-{GlyΔGly}-NMe₂ 119

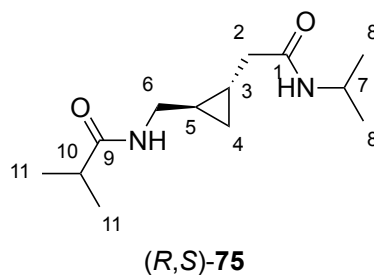


(*R,S*)-119

The procedure applied to the synthesis of (\pm)-(Boc)₂-{GlyΔGly}-NMe₂ **119** was followed using (*R,S*)-(Boc)₂-{GlyΔGly}-OH **107** (110 mg, 0.33 mmol). 2 equiv. of HNMe₂ (2 M solution in THF) were used in this case. The residue was purified by silica gel column chromatography (PE/EtOAc 1:1) to give (*S,R*)-(Boc)₂-{GlyΔGly}-NMe₂ **119** (87 mg, 74%) as a yellow oil.

R_f (PE/EtOAc 1:1): 0.27; $[\alpha]_D^{23}$ -16 (c = 0.50, CHCl₃); ν_{\max} 2981, 2943, 1736, 1692, 1646, 1368, 1171, 1131, 853 cm⁻¹; ¹H NMR (500 MHz, CDCl₃) δ 3.58 (1H, dd, J = 14.4, 7.1 Hz, CH₂-C6), 3.46 (1H, dd, J = 14.4, 7.1 Hz, CH₂-C6), 2.97 (3H, s, CH₃-C7), 2.93 (3H, s, CH₃-C7), 2.44 (1H, dd, J = 15.3, 5.0 Hz, CH₂-C2), 2.11 (1H, dd, J = 15.3, 7.6 Hz, CH₂-C2), 1.50 (18H, s, 2 \times *t*-Bu), 1.09 (1H, dddddd, J = 7.6, 7.1, 5.0, 5.0, 5.0 Hz, CH-C3), 1.01 (1H, dddddd, J = 7.1, 7.1, 7.1, 5.0, 5.0 Hz, CH-C5), 0.62 (1H, ddd, J = 8.5, 5.0, 5.0 Hz, CH₂-C4), 0.39 (1H, ddd, J = 8.5, 5.0, 5.0 Hz, CH₂-C4); ¹³C (126 MHz, CDCl₃): δ 172.3 (CO-C1), 153.0 (2 \times CO-Boc), 82.3 (CH-Boc), 49.9 (CH₂-C6), 37.9 (CH₂-C2), 37.5 (CH₃-C7), 35.4 (CH₃-C7), 28.2 (6 \times CH₃-Boc), 18.3 (CH-C5), 13.9 (CH-C3), 10.9 (CH₂-C4); HRMS (ESI+) for C₁₈H₃₂N₂O₅Na [M+Na]⁺ calcd 379.2203, found 379.2200.

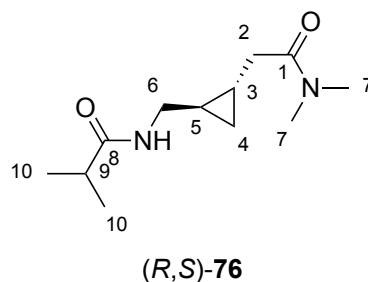
(*R,S*)-*i*PrOC-{GlyΔGly}-N-*i*Pr 75



The procedure applied to the synthesis of (\pm)-*i*PrOC-{GlyΔGly}-N-*i*Pr **75** was followed using (*R,S*)-(Boc)₂-{GlyΔGly}-N-*i*Pr **118** (70 mg, 0.19 mmol). After deprotection, 1.5 equiv. of Et₃N and isobutyric anhydride were used. Trituration of the residue with cold Et₂O in EtOAc yielded the title compound (15 mg, 31% over 2 steps) as a white solid.

R_f (PE/EtOAc 1:1): 0.08; $[\alpha]_D^{21} +48$ ($c = 0.30$, CHCl₃); m.p.: 134–135 °C; ν_{\max} (10 mM, CH₂Cl₂) 3429, 3325, 2974, 2932, 1663, 1516, 1277, 1265, 1258 cm⁻¹; ¹H NMR (500 MHz, CDCl₃) δ 6.78 (1H, br s, NH-C6), 5.40 (1H, br s, NH-C7), 4.10 (1H, dq, $J = 7.6, 6.5$ Hz, CH-C7), 3.73 (1H, ddd, $J = 13.5, 6.0, 4.7$ Hz, CH₂-C6), 2.60–2.48 (2H, m, CH₂-C6 + CH₂-C2), 2.43 (1H, h, $J = 6.9$ Hz, CH-C10), 1.70 (1H, dd, $J = 16.2, 9.4$ Hz, CH₂-C2), 1.18 (3H, d, $J = 6.9$ Hz, CH₃-C11), 1.18 (3H, d, $J = 6.9$ Hz, CH₃-C11), 1.17 (3H, d, $J = 6.5$ Hz, CH₃-C8), 1.16 (3H, d, $J = 6.5$ Hz, CH₃-C8), 0.83–0.71 (2H, m, CH-C3 + CH-C5), 0.53 (1H, ddd, $J = 8.1, 5.3, 5.3$ Hz, CH₂-C4), 0.42 (1H, ddd, $J = 8.1, 5.3, 5.3$ Hz, CH₂-C4); ¹³C (126 MHz, CDCl₃): δ 177.5 (CO-C9), 171.7 (CO-C1), 43.9 (CH₂-C6), 41.6 (CH-C7), 39.9 (CH₂-C2), 35.7 (CH-C10), 23.0 (CH₃-C8), 22.9 (CH₃-C8), 19.8 (2 \times CH₃-C11), 18.0 (CH-C5/3), 13.5 (CH-C3/5), 10.2 (CH₂-C4); HRMS (ESI+) for C₁₃H₂₄N₂O₂Na [M+Na]⁺ calcd 263.1730, found 263.1726.

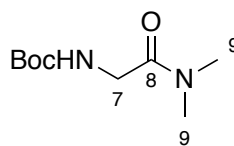
(*R,S*)-*i*Pr-{GlyΔGly}-NMe₂ 76



The procedure applied to the synthesis of (\pm)-*i*Pr-{GlyΔGly}-NMe₂ **76** was followed using (*R,S*)-(Boc)₂-{GlyΔGly}-NMe₂ **119** (122 mg, 0.34 mmol). After deprotection, 1.5 equiv. of Et₃N and isobutyric anhydride were used. The residue was purified by silica gel column chromatography (CH₂Cl₂/MeOH 100:0 to 97:3) to afford the title compound (31 mg, 40 % over 2 steps) as a colourless semi-solid.

R_f (PE/EtOAc 1:1): 0.08; $[\alpha]_D^{28} +68$ ($c = 0.50$, CHCl₃); ν_{\max} (10 mM, CH₂Cl₂) 3287, 2967, 2928, 1637, 1539, 1261, 1238 cm⁻¹; ¹H NMR (500 MHz, CDCl₃) δ 7.57 (1H, br s, NH), 3.92 (1H, ddd, $J = 13.5, 6.4, 4.9$ Hz, CH₂-C6), 2.97 (3H, s, CH₃-C7), 2.95 (3H, s, CH₃-C7), 2.89 (1H, dd, $J = 17.0, 3.8$ Hz, CH₂-C2), 2.47 (1H, h, $J = 7.0$ Hz, CH-C9), 2.32 (1H, ddd, $J = 13.5, 10.0, 2.0$ Hz, CH₂-C6), 1.65 (1H, dd, $J = 17.0, 10.5$ Hz, CH₂-C2), 1.18 (3H, d, $J = 7.0$ Hz, CH₃-C10), 1.18 (3H, d, $J = 7.0$ Hz, CH₃-C10), 0.83–0.75 (1H, m, CH-C3), 0.63 (1H, ddddd, $J = 10.0, 8.2, 4.9, 4.9, 4.9$ Hz, CH-C5), 0.55 (1H, ddd, $J = 8.3, 4.9, 4.9$ Hz, CH₂-C4), 0.45 (1H, ddd, $J = 8.3, 4.9, 4.9$ Hz, 1H \times CH₂-C4); ¹³C (126 MHz, CDCl₃): δ 177.6 (CO-C1), 173.0 (CO-C8), 44.5 (CH₂-C6), 37.3 (CH₂-C2), 36.9 (CH₃-C7), 35.7 (CH-C9), 35.5 (CH₃-C7), 19.8 (2 \times CH₃-C10), 17.7 (CH-C5), 13.5 (CH-C3), 10.5 (CH₂-C4); HRMS (ESI+) for C₁₂H₂₂N₂O₂Na [M+Na]⁺ calcd 249.1573 found 249.1566.

Boc-Gly-NMe₂ **121**

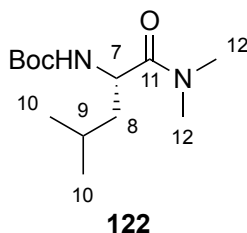


121

Boc-Gly-OH (3.00 g, 17.1 mmol), HNMe₂ (17.1 mL of a 2 M solution in THF, 34.2 mmol) and Et₃N (8.30 mL, 70.0 mmol) were dissolved in CH₂Cl₂ (100 mL). The solution was stirred for 15 min at rt and T3P (8.90 mL, of a 50% solution in EtOAc, 30.0 mmol) was added dropwise at 0 °C. H₂O (20 mL) was added and the phases were separated. The organic phase was washed with sat. aq. NaHCO₃ (20 mL), 1 M aq. HCl (20 mL), and brine (15 mL). The organic phase was dried over MgSO₄, filtered and concentrated under vacuum affording Boc-Gly-NMe₂ **121** (2.96 g, 86%) as a colourless solid.

R_f (EtOAc/PE 1:1): 0.27; m.p.: 129–130 °C, ν_{max} (CHCl₃): 3418, 1974, 1713, 1645, 1167 cm⁻¹; ¹H-NMR (500 MHz; CDCl₃): δ 5.51 (1H, s, NH), 3.94 (2H, d, J = 4.3 Hz, CH₂-C7), 2.97 (3H, s, CH₃-C9), 2.95 (3H, s, CH₃-C9), 1.44 (9H, s, *t*-Bu); ¹³C NMR (126 MHz; CDCl₃): δ 168.4 (CO-Boc), 156.0 (CO-C8), 79.7 (C-Boc), 42.4 (CH₂-C7), 36.0 (CH₃-C9), 35.7 (3 × CH₃-Boc), 28.5 (CH₃-C9); HRMS (ESI+) for C₉H₁₈N₂NaO₃ [M+Na]⁺ calcd 225.1210, found 225.1207.

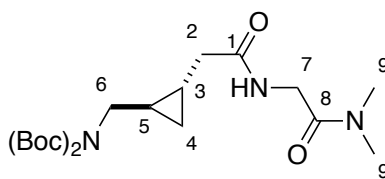
Boc-Leu-NMe₂ **122**



To a solution of Boc-Leu-OH (1.55 g, 6.70 mmol) in CH₂Cl₂ (10 mL) was added DCC (1.66 g, 8.04 mmol) portionwise at 0 °C, followed by HNMe₂ (6.70 mL of a 2 M solution in THF, 13.4 mmol). The mixture was heated to reflux and stirred for 8 h. The solid formed was filtered and washed with CH₂Cl₂, the filtrate was concentrated under vacuum. The resulting solid was purified by silica gel column chromatography (PE/EtOAc 1:1) to give Boc-Leu-NMe₂ **122** (1.12 g, 65%) as a white solid.

R_f (PE/EtOAc 1:1): 0.65; $[\alpha]_D^{21} +30$ ($c = 1.0$, CHCl₃); m.p.: 54–55 °C; ν_{\max} 3314, 2969, 1712, 1642, 1498, 1397, 1367, 1247, 1193 cm⁻¹; ¹H NMR (400 MHz, CDCl₃) δ 5.25 (1H, d, $J = 9.5$ Hz, NH), 4.64 (1H, ddd, $J = 9.5, 9.5, 3.9$ Hz, CH-C7), 3.07 (3H, s, CH₃-C12), 2.94 (3H, s, CH₃-C12), 1.80–1.65 (1H, m, CH-C9), 1.47 (1H, ddd, $J = 13.9, 9.5, 4.4$ Hz, CH₂-C8), 1.42 (9H, s *t*-Bu), 1.34 (1H, ddd, $J = 13.9, 9.3, 3.9$ Hz, CH₂-C8), 0.99 (3H, d, $J = 6.5$ Hz, CH₃-C10), 0.91 (3H, d, $J = 6.7$ Hz, CH₃-C10); ¹³C (126 MHz, CDCl₃): δ 173.1 (CO-C11), 155.8 (CO-Boc), 79.5 (C-Boc), 48.8 (CH-C7), 42.9 (CH₂-C8), 37.1 (CH₃-C12), 35.9 (CH₃-C12), 28.5 (3 × CH₃-Boc), 24.8 (CH-C9), 23.6 (CH₃-C10), 21.9 (CH₃-C10); HRMS (ESI⁺) for C₁₃H₂₆N₂O₃Na [M+Na]⁺ calcd 281.1836, found 281.1833.

(±)-(Boc)₂-{GlyΔGly}-Gly-NMe₂ 123



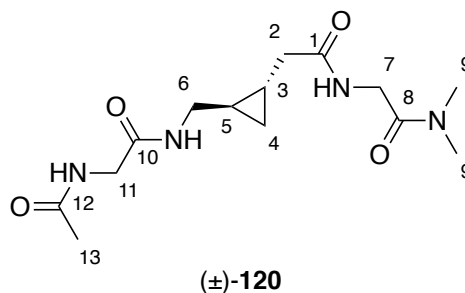
(±)-123

Boc-Gly-NMe₂ **121** (2.96 g, 14.6 mmol) was dissolved in CH₂Cl₂ (150 mL) and TFA (11.0 mL, 146 mmol) was added dropwise at rt. The reaction mixture was stirred overnight at rt and then the solvent was removed under vacuum to give TFA·H-Gly-NMe₂.

(±)-(Boc)₂-{GlyΔGly}-OH **107** (2.87 g, 8.72 mmol), TFA·H-Gly-NMe₂ (2.91 g, 14.6 mmol) and Et₃N (4.30 mL, 30.5 mmol) were dissolved in CH₂Cl₂ (43 mL). The solution was stirred for 15 min at rt and T3P (50% in EtOAc, 7.80 mL, 13.1 mmol) was added 0 °C. The reaction mixture was stirred for 16 h at rt. The solution was washed with H₂O (3 × 10 mL), sat. aq. NaHCO₃ (3 × 10 mL) and brine (10 mL). The phases were separated, and the organic phase was dried over MgSO₄, filtered and concentrated under vacuum. The residue was purified by silica gel column chromatography (PE/EtOAc 1:1) to give the title compound (3.26 mg, 63%) as a colourless oil.

R_f (EtOAc/PE 1:1): 0.22; ν_{max} (CHCl₃): 3312, 2978, 2933, 1690, 1644, 1366, 1125, 1030, 853 cm⁻¹; ¹H-NMR (500 MHz; CDCl₃): δ 6.90 (1H, t, *J* = 4.0 Hz, NH), 4.03 (2H, d, *J* = 4.0 Hz, CH₂-C7), 3.62 (1H, dd, *J* = 14.4, 6.0 Hz, CH₂-C6), 3.45 (1H, dd, *J* = 14.4, 6.9 Hz, CH₂-C6), 2.98 (3H, s, CH₃-C9), 2.97 (3H, s, CH₃-C9), 2.37 (1H, dd, *J* = 16.0, 5.7 Hz, CH₂-C2), 2.01 (1H, dd, *J* = 16.0, 7.8 Hz, CH₂-C2), 1.48 (18H, s, 2 × *t*-Bu), 1.07–0.97 (2H, m, CH-C3 + CH-C5), 0.68 (ddd, *J* = 8.0, 5.1, 5.1 Hz, CH₂-C4), 0.42 (ddd, *J* = 8.0, 5.1, 5.1 Hz, CH₂-C4); ¹³C NMR (126 MHz; CDCl₃): δ 172.2 (CO-C1), 168.1 (CO-C8), 152.9 (CO-Boc), 82.3 (C-Boc), 49.5 (CH₂-C6), 41.4 (CH₂-C7), 40.6 (CH₂-C2), 36.0 (CH₃-C9), 35.7 (CH₃-C9), 28.2 (6 × CH₃-Boc), 18.4 (CH-C5), 13.8 (CH-C3), 10.8 (CH₂-C4); HRMS (ESI+) for C₂₀H₃₅N₃NaO₆ [M+Na]⁺ calcd 436.2418, found 436.2402.

(±)-Ac-Gly- $\{\text{Gly}\Delta\text{Gly}\}$ -Gly-NMe₂ **120**

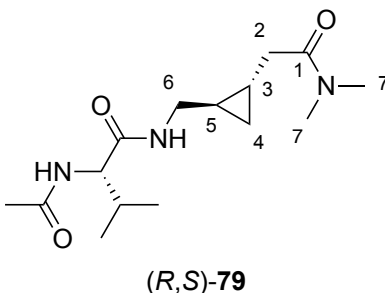


(±)-(Boc)₂- $\{\text{Gly}\Delta\text{Gly}\}$ -Gly-NMe₂ **123** (2.26 g, 5.47 mmol) was dissolved in CH₂Cl₂ (55 mL) and TFA (4.20 mL, 54.7 mmol) was added dropwise at rt. The reaction mixture was stirred overnight at rt and the solvent was then removed under vacuum. The resulting TFA salt was then used without further purification in the next coupling.

TFA·(±)-H- $\{\text{Gly}\Delta\text{Gly}\}$ -Gly-NMe₂ (200 mg, 0.61 mmol), Et₃N (300 μ L, 2.14 mmol) and Ac-Gly-OH (143 mg, 1.22 mmol) were dissolved in CH₂Cl₂ (3.00 mL). The solution was stirred for 15 min at rt and T3P (550 μ L of a 50% solution in EtOAc, 0.92 mmol) was added dropwise. The reaction mixture was heated to reflux and stirred overnight. The reaction mixture was then cooled and washed with H₂O (3 \times 5 mL). The organic phase was dried over MgSO₄, filtered and concentrated under vacuum. The residue was triturated with cold PE in EtOAc to afford (±)-Ac-Gly- $\{\text{Gly}\Delta\text{Gly}\}$ -Gly-NMe₂ **120** (100 mg, 52% over two steps) as a white solid.

R_f (EtOAc/PE 1:1): 0.19; m.p.: 138–140 °C; ν_{max} (20 mM in CHCl₃): 3408, 3319, 1053, 2984, 1659, 1651, 1514, 1271, 1263 cm⁻¹; ¹H-NMR (400 MHz; CDCl₃): δ 7.68 (1H, s, NH-C6), 6.75 (1H, s, NH-C7), 6.56 (1H, s, NH-C11), 4.10 (1H, dd, J = 17.4, 4.3 Hz, CH₂-C7), 4.04 (1H, dd, J = 17.4, 4.4 Hz, CH₂-C7), 3.95 (2H, d, J = 4.8 Hz, CH₂-C11), 3.93–3.86 (1H, m, CH₂-C6), 3.03 (6H, s, 2 \times CH₃-C9), 2.79 (1H, dd, J = 16.6, 3.4 Hz, CH₂-C2), 2.45 (1H, ddd, J = 13.7, 10.0, 3.2 Hz, CH₂-C6), 2.03 (3H, s, CH₃-C13), 1.68 (1H, dd, J = 16.6, 10.4 Hz, CH₂-C2), 0.86–0.78 (2H, m, CH-C5 + CH-C3), 0.56 (1H, ddd, J = 8.2, 5.3, 5.3 Hz, CH₂-C4), 0.47 (1H, ddd, J = 8.2, 5.4, 5.4 Hz, CH₂-C4); ¹³C NMR (126 MHz; CDCl₃): δ 172.6 (CO-C1), 170.4 (CO-C12), 168.9 (CO-C10), 168.4 (CO-C8), 44.2 (CH₂-C6), 42.9 (CH₂-C11), 41.3 (CH₂-C7), 39.7 (CH₂-C2), 36.2 (CH₃-C9), 35.9 (CH₃-C9), 23.2 (CH₃-C13), 18.1 (CH-C5), 14.0 (CH-C3), 10.4 (CH₂-C4); HRMS (ESI⁺) for C₁₄H₂₄N₄NaO₄ [M+Na]⁺ calcd 335.1690, found 335.1688.

(*R,S*)-Ac-Val-{GlyΔGly}-NMe₂ 79



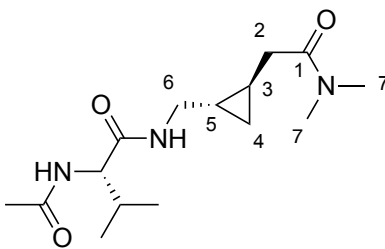
(*R,S*)-79

(*R,S*)-(Boc)₂-{GlyΔGly}-NMe₂ **119** (87 mg, 0.24 mmol) was dissolved in CH₂Cl₂ (3 mL) and TFA (184 μL, 2.40 mmol) was added to the solution. The reaction mixture was stirred at rt for 8 h. The solvent was then removed, and the compound was used for the subsequent coupling without purification.

To a solution of TFA·(*R,S*)-H-{GlyΔGly}-NMe₂ (0.24 mmol) in CH₂Cl₂ (1 mL), was added DIPEA (125 μL, 1.35 mmol) dropwise. Ac-Val-OH (38 mg, 0.24 mmol) was added, followed by HATU (91 mg, 0.24 mmol). The reaction mixture was stirred overnight at rt. The solution was washed with H₂O (3 × 5 mL). The organic phase was dried over MgSO₄ and filtered. The solvent was removed under vacuum and the resulting brown oil was purified by silica gel column chromatography (CH₂Cl₂/MeOH 99:1 to 96:4) to afford (*R,S*)-Ac-Val-{GlyΔGly}-NMe₂ **79** (10 mg, 14%) as a white powder.

R_f (CH₂Cl₂/MeOH 9:1):0.57; $[\alpha]_D^{21} +41$ ($c = 0.13$, CH₂Cl₂); m.p.: 123–125 °C; ν_{\max} ($c = 10$ mM, CH₂Cl₂) 3410, 3306, 2963, 2932, 1678, 1659, 1632, 1551, 1513, 1269, 1261 cm⁻¹; ¹H NMR (500 MHz, CD₂Cl₂) δ 8.16 (1H, s, NH-Gly), 6.70 (1H, d, $J = 9.2$ Hz, NH-Val), 4.34 (1H, dd, $J = 9.2, 5.0$ Hz, CH α -Val), 3.98 (1H, ddd, $J = 13.4, 7.0, 4.4$ Hz, CH₂-C6), 2.97 (3H, s, CH₃-C7), 2.93 (3H, s, CH₃-C7), 2.97–2.92 (1H, m, CH₂-C2), 2.24–2.15 (2H, m, CH₂-C6 + CH β -Val), 2.03 (3H, s, CH₃-Ac), 1.63 (1H, dd, $J = 17.5, 10.5$ Hz, CH₂-C2), 0.93 (3H, d, $J = 6.9$ Hz, CH₃ γ -Val), 0.86 (3H, d, $J = 6.9$ Hz, CH₃ γ -Val), 0.77–0.71 (1H, m, CH-C3), 0.62–0.56 (2H, m, CH-C5 + CH₂-C4), 0.52–0.47 (1H, m, CH₂-C4); ¹³C (126 MHz, CD₂Cl₂): δ 173.6 (CO-C1), 171.5 (CO-Ac), 170.6 (CO-Val), 59.0 (CH α -Val), 44.6 (CH₂-C6), 37.5 (CH₂-C2), 37.3 (CH₃-C7), 35.9 (CH₃-C7), 31.5 (CH β -Val), 23.6 (CH₃-Ac), 19.7 (CH₃ γ -Val), 18.5 (CH₃ γ -Val), 17.8 (CH-C5), 13.6 (CH-C3), 10.8 (CH₂-C4); HRMS (ESI⁺) for C₁₅H₂₇N₃O₃Na [M+Na]⁺ calcd 320.1945, found 320.1934.

(*S,R*)-Ac-Val-{GlyΔGly}-NMe₂ 80

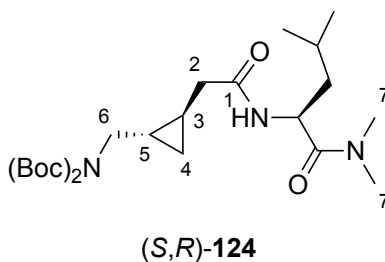


(*S,R*)-80

The procedure applied to the synthesis of (*R,S*)-Ac-Val-{GlyΔGly}-NMe₂ **79** was followed using (*S,R*)-(Boc)₂-{GlyΔGly}-NMe₂ **119** (161 mg, 0.45 mmol). After the work up, cold Et₂O (5 mL) was added to the residue and a precipitate was formed. Et₂O was filtered and this was repeated another time to give (*S,R*)-Ac-Val-{GlyΔGly}-NMe₂ **80** (16 mg, 12%) as a white powder.

R_f (CHCl₃/MeOH 95:5): 0.69; [α]_D²¹ -39 (*c* = 0.55, CHCl₃); m.p.: 130–131 °C; ν_{max} (*c* = 10 mM, CH₂Cl₂) 3418, 3294, 2963, 2932, 1678, 1659, 1632, 1547, 1504, 1273, 1265, 1258 cm⁻¹; ¹H NMR (500 MHz, CD₂Cl₂) δ 8.18 (1H, bs, NH-Gly), 6.51 (1H, d, *J* = 9.3 Hz, NH-Val), 4.33 (1H, dd, *J* = 9.3, 5.3 Hz, CH α -Val), 3.80 (1H, dd, *J* = 13.1, 5.2, 5.2 Hz, CH₂-C6), 2.96 (3H, s, CH₃-C7), 2.98–2.95 (1H, m, CH₂-C2), 2.93 (3H, s, CH₃-C7), 2.32 (1H, ddd, *J* = 13.1, 10.6, 2.1 Hz, CH₂-C6), 2.17–2.09 (1H, m, CH β -Val), 2.02 (3H, s, CH₃-Ac), 1.63 (1H, dd, *J* = 17.3, 11.2 Hz, CH₂-C2), 0.93 (3H, d, *J* = 6.9 Hz, CH₃ γ -Val), 0.88 (3H, d, *J* = 6.9 Hz, CH₃ γ -Val), 0.74–0.68 (1H, m, CH-C3), 0.68–0.63 (1H, m, CH-C5), 0.58 (1H, ddd, *J* = 8.3, 5.1, 5.1 Hz, CH₂-C4), 0.50 (1H, ddd, *J* = 8.3, 5.2, 5.2 Hz, CH₂-C4); ¹³C (126 MHz, CD₂Cl₂): δ 173.5 (CO-C1), 171.6 (CO-Ac), 170.4 (CO-Val), 58.9 (CH α -Val), 45.0 (CH₂-C6), 37.5 (CH₂-C2), 37.3 (CH₃-C7), 35.9 (CH₃-C7), 31.9 (CH β -Val), 23.7 (CH₃-Ac), 19.6 (CH₃ γ -Val), 17.9 (CH₃ γ -Val), 17.6 (CH-C5), 13.8 (CH-C3), 11.1 (CH₂-C4); HRMS (ESI⁺) for C₁₅H₂₇N₃O₃Na [M+Na]⁺ calcd 320.1945, found 320.1933.

(*S,R*)-(Boc)₂-{GlyΔGly}-Leu-NMe₂ 124

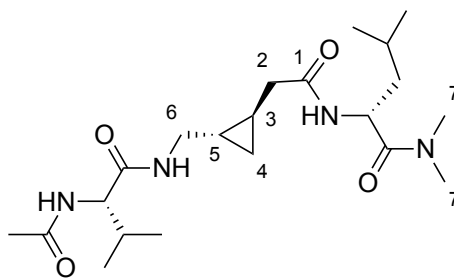


Boc-Leu-NMe₂ **122** (1.12 g, 4.34 mmol) was dissolved in CH₂Cl₂ (44 mL) and TFA (1.7 mL, 21.7 mmol) was added at rt. The reaction mixture was stirred for 8 h at this temperature. The solvent was removed under vacuum and the residue was used in the next step without further purification.

TFA·NH₂-Leu-NMe₂ (130 mg, 0.39 mmol) was dissolved in CH₂Cl₂ (1.3 mL), DIPEA (203 μL, 1.17 mmol) was added followed by (*S,R*)-(Boc)₂-{GlyΔGly}-OH **107** (106 mg, 0.39 mmol). The mixture was stirred for 15 min and HATU (148 mg, 0.39 mmol) was added. The reaction mixture was stirred overnight at rt and H₂O (10 mL) was added. The phases were separated and the organic phase was washed with sat. aq. NaHCO₃ (10 mL), brine (10 mL), dried over MgSO₄ and filtered. The solvent was removed under vacuum and the residue was purified by silica gel column chromatography (PE/EtOAc 1:1) to afford (*S,R*)-(Boc)₂-{GlyΔGly}-Leu-NMe₂ **124** (131 mg, 72%) as a yellow oil.

R_f (PE/EtOAc 1:1): 0.35; [α]_D²² +15 (*c* = 0.25, CHCl₃); ν_{max} 3287, 2926, 1711, 1634, 1506, 1366, 1248, 1173 cm⁻¹; ¹H NMR (400 MHz, CDCl₃) δ 6.52 (1H, d, *J* = 8.6 Hz, NH-Leu), 5.01 (1H, ddd, *J* = 12.8, 8.6, 4.0 Hz, CH α -Leu), 3.66 (1H, dd, *J* = 14.4, 5.7 Hz, CH₂-C6), 3.47 (1H, dd, *J* = 14.4, 6.9 Hz, CH₂-C6), 3.09 (3H, s, CH₃-C7), 2.94 (3H, s, CH₃-C7), 2.34 (1H, dd, *J* = 15.9, 5.7 Hz, CH₂-C2), 1.98 (1H, dd, *J* = 15.9, 7.7 Hz, CH₂-C2), 1.70–1.60 (1H, m, CH γ -Leu), 1.49 (18H, s, 2 \times *t*-Bu), 1.45–1.36 (2H, m, CH₂ β -Leu), 1.02–0.95 (2H, m, CH-C3 + CH-C5), 0.99 (3H, d, *J* = 6.5 Hz, CH₃ δ -Leu), 0.91 (3H, d, *J* = 6.8 Hz, CH₃ δ -Leu), 0.65 (1H, ddd, *J* = 7.8, 5.1, 5.1 Hz, CH₂-C4), 0.40 (1H, ddd, *J* = 7.8, 5.1, 5.1 Hz, CH₂-C4); ¹³C NMR (126 MHz, CDCl₃): δ 172.6 (CO-C1), 171.6 (CO-Leu), 152.87 (2 \times CO-Boc), 82.3 (2 \times C-Boc), 49.2 (CH₂-C6), 47.3 (CH α -Leu), 42.2 (CH₂ β -Leu), 40.6 (CH₂-C2), 37.0 (CH₃-C7), 35.7 (CH₃-C7), 28.1 (6 \times CH₃-Boc), 24.7 (CH γ -Leu), 23.4 (CH₃ δ -Leu), 21.8 (CH₃ δ -Leu), 18.3 (CH-C5), 13.4 (CH-C3), 10.5 (CH₂-C4); HRMS (ESI⁺) for C₂₄H₄₃N₃O₆Na [M+Na]⁺ calcd 492.3044, found 492.3028.

(*S,R*)-Ac-Val-{GlyΔGly}-Leu-NMe₂ 78



(*S,R*)-78

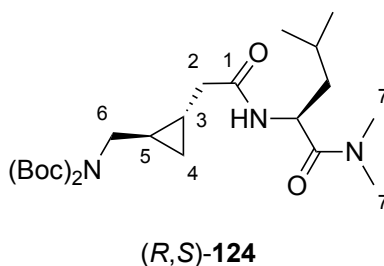
(*R,S*)-(Boc)₂-{GlyΔGly}-Leu-NMe₂ **124** (310 mg, 0.66 mmol) was dissolved in CH₂Cl₂ (3 mL) and TFA (505 μL, 6.60 mmol) was added to the solution. The reaction mixture was stirred at rt for 8 h. The solvent was then removed, and the product was used for the coupling reaction without purification.

To a solution of TFA·(1*R*,2*S*)-H-{GlyΔGly}-Leu-NMe₂ (0.66 mmol) in CH₂Cl₂ (3 mL) was added DIPEA (345 μL, 1.98 mmol) dropwise. Ac-Val-OH (105 mg, 0.66 mmol) was added followed by HATU (251 mg, 0.66 mmol). The reaction mixture was stirred overnight at rt. The solution was washed with H₂O (3 × 10 mL) and phases were separated. The organic phase was dried over MgSO₄ and filtered. The solvent were removed under vacuum and the resulting brown oil was purified by silica gel column chromatography (CH₂Cl₂/MeOH 99:1 to 90:10) to afford (*S,R*)-Ac-Val-{GlyΔGly}-Leu-NMe₂ **78** (130 mg, 76% over two steps) as a white powder.

R_f (CH₂Cl₂/MeOH 9:1): 0.95; [α]_D²¹ −17 (*c* = 0.55, CHCl₃); m.p.: 155–156 °C; ν_{max} (*c* = 10 mM, CH₂Cl₂) 3422, 3306, 2963, 2874, 1659, 1639, 1508, 1278, 1269 cm^{−1}; ¹H NMR (600 MHz, CD₂Cl₂) δ 7.74 (1H, bs, NH-Gly), 6.63 (1H, d, *J* = 8.6 Hz, NH-Leu), 6.43 (1H, d, *J* = 8.8 Hz, NH-Val), 5.01 (1H, ddd, *J* = 10.6, 8.6, 3.7 Hz, CHα-Leu), 4.31 (1H, dd, *J* = 8.8, 6.4 Hz, CHα-Val), 3.65 (1H, ddd, *J* = 13.8, 4.2, 4.2 Hz, CH₂-C6), 3.11 (3H, s, CH₃-C7), 2.96 (3H, s, CH₃-C7), 2.74 (1H, dd, *J* = 17.0, 3.8 Hz, CH₂-C2), 2.57 (1H, ddd, *J* = 13.8, 10.2, 4.2 Hz, CH₂-C6), 2.12–2.00 (1H, m, CHβ -Val), 1.97 (3H, s, CH₃-Ac), 1.70–1.60 (2H, m, CHγ-Leu + CH₂-C2), 1.54 (1H, ddd, *J* = 14.1, 10.6, 4.3 Hz, CH₂β -Leu), 1.41 (1H, ddd, *J* = 14.1, 9.5, 3.7 Hz, 1H × CH₂β -Leu), 0.99 (3H, d, *J* = 6.5 Hz, CH₃δ-Leu), 0.93 (3H, d, *J* = 6.2 Hz, CH₃γ-Val), 0.92 (3H, d, *J* = 6.2 Hz, CH₃δ-Leu), 0.89 (3H, d, *J* = 6.9 Hz, CH₃γ-Val), 0.82–0.73 (2H, m, CH-C3 + CH-C5), 0.54 (1H, ddd, *J* = 10.2, 5.4, 5.4 Hz, CH₂-C4), 0.46 (1H, ddd, *J* = 10.2, 5.4, 5.4 Hz, CH₂-C4); ¹³C (151 MHz, CD₂Cl₂): δ 174.1 (CO-C1), 173.3 (CO-Ac), 172.5 (CO-Leu), 171.9 (CO-Val), 58.7 (CHα-Val), 48.0 (CHα-Leu), 44.4 (CH₂-C6),

42.3 (CH₂β -Leu), 40.2 (CH₂-C2), 37.5 (CH₃-C7), 36.2 (CH₃-C7), 32.0 (CHβ -Val), 25.3 (CHγ-Leu), 23.7 (CH₃-Ac), 23.6 (CH₃δ-Leu), 22.0 (CH₃δ-Leu), 19.6 (CH₃γ-Val), 18.5 (CH₃γ-Val), 18.4 (CH-C5), 14.0 (CH-C3), 11.2 (CH₂-C4); HRMS (ESI+) for C₂₁H₃₈N₄O₄Na [M+Na]⁺ calcd 433.2785, found 433.2782.

(*R,S*)-(Boc)₂-{GlyΔGly}-Leu-NMe₂ 124

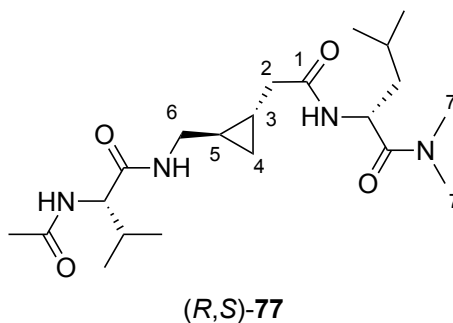


Boc-Leu-NMe₂ **122** (1.12g, 4.34 mmol) was dissolved in CH₂Cl₂ (44 mL) and TFA (1.7 mL, 21.7 mmol) was added at rt. The reaction mixture was stirred for 8 h at this temperature. The solvent was removed under vacuum and the residue was used in the next step without further purification.

(*R,S*)-(Boc)₂-{GlyΔGly}-OH **107** (90 mg, 0.33 mmol) was dissolved in CH₂Cl₂ (1 mL). DIPEA (200 μL, 0.99 mmol) was added followed by TFA·H-Leu-NMe₂ (110 mg, 0.33 mmol). The mixture was stirred for 15 min and HATU (125 mg, 0.33 mmol) was added. The reaction mixture was stirred overnight at rt. H₂O (10 mL) was added and the phases were separated. The organic phase was washed with sat. aq. NaHCO₃ (10 mL), brine (10 mL), dried over MgSO₄ and filtered. The solvent was removed under vacuum and the residue was purified by silica gel column chromatography (PE/EtOAc 1:1) to afford (*S,R*)-(Boc)₂-{GlyΔGly}-Leu-NMe₂ **124** (131 mg, 85%) as a yellow oil.

R_f (PE/EtOAc 1:1): 0.20; $[\alpha]_D^{23}$ -13 (*c* = 0.50, CHCl₃); ν_{\max} 3304, 2930, 1711, 1634, 1508, 1366, 1248, 1173 cm⁻¹; ¹H NMR (500 MHz, CDCl₃) δ 6.52 (1H, d, *J* = 8.6 Hz, NH), 5.02 (1H, ddd, *J* = 9.5, 8.6, 3.9 Hz, CH α -Leu), 3.65 (1H, dd, *J* = 14.3, 5.8 Hz, CH₂-C6), 3.45 (1H, dd, *J* = 14.3, 7.1 Hz, CH₂-C6), 3.09 (3H, s, CH₃-C7), 2.95 (3H, s, CH₃-C7), 2.41 (1H, dd, *J* = 16.0, 5.3 Hz, CH₂-C2), 1.92 (dd, *J* = 16.0, 8.0 Hz, 1H, CH₂-C2), 1.71–1.61 (1H, m, CH γ -Leu), 1.51 (18H, s, 2 \times *t*-Bu), 1.46–1.40 (2H, m, CH₂ β -Leu), 1.04–0.98 (2H, m, CH-C5 + CH-C3), 1.00 (3H, d, *J* = 6.5 Hz, CH₃ δ -Leu), 0.92 (3H, d, *J* = 6.6 Hz, CH₃ δ -Leu), 0.70 (1H, ddd, *J* = 8.0, 5.1, 5.1 Hz, CH₂-C4), 0.43 (ddd, *J* = 8.0, 5.2, 5.2 Hz, CH₂-C4); ¹³C (126 MHz, CDCl₃): δ 172.7 (CO-C1), 171.7 (CO-Leu), 153.0 (2 \times CO-Boc), 82.4 (2 \times C-Boc), 49.5 (CH₂-C6), 47.3 (CH α -Leu), 42.8 (CH₂ β -Leu), 40.8 (CH₂-C2), 37.2 (CH₃-C12), 35.9 (CH₃-C12), 28.2 (6 \times CH₃-Boc), 24.9 (CH γ -Leu), 23.6 (CH₃ δ -Leu), 22.1 (CH₃ δ -Leu), 18.4 (CH-C5), 13.7 (CH-C3), 10.8 (CH₂-C4); HRMS (ESI⁺) for C₂₄H₄₃N₃O₆Na [M+Na]⁺ calcd 492.3044, found 492.3026.

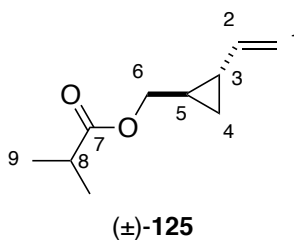
(*R,S*)-Ac-Val-{GlyΔGly}-Leu-NMe₂ 77



The procedure applied to the synthesis of (*S,R*)-Ac-Val-{GlyΔGly}-Leu-NMe₂ **78** was followed using (*R,S*)-(Boc)₂-{GlyΔGly}-Leu-NMe₂ **124**. The crude product was purified by silica gel column chromatography (CH₂Cl₂/MeOH 99:1 to 94:6) to afford (*R,S*)-Ac-Val-{GlyΔGly}-Leu-NMe₂ **77** (20 mg, 17%) as a white powder.

R_f (CH₂Cl₂/MeOH 9:1): 0.90; $[\alpha]_D^{21} +47$ ($c = 0.90$, CH₂Cl₂); m.p.: 95–97 °C; ν_{\max} ($c = 10$ mM, CH₂Cl₂) 3418, 3302, 3051, 2963, 1659, 1643, 1512, 1504, 1269, 1261, 1254 cm⁻¹; ¹H NMR (500 MHz, CDCl₃) δ 7.82 (1H, d, $J = 6.7$ Hz, NH-Gly), 6.44 (1H, d, $J = 8.6$ Hz, NH-Leu), 6.37 (1H, d, $J = 8.7$ Hz, NH-Val), 5.03 (1H, ddd, $J = 10.5, 8.6, 3.6$ Hz, CH α -Leu), 4.42 (1H, dd, $J = 8.7, 6.0$ Hz, CH α -Val), 3.97 (1H, ddd, $J = 13.8, 6.7, 4.3$ Hz, CH₂-C6), 3.13 (3H, s, CH₃-C7), 2.98 (3H, s, CH₃-C7), 2.69 (1H, dd, $J = 16.3, 3.6$ Hz, CH₂-C2), 2.35 (1H, ddd, $J = 13.8, 9.8, 2.7$ Hz, CH₂-C6), 2.14–2.02 (1H, m, CH β -Val), 2.01 (3H, s, CH₃-Ac), 1.75–1.69 (2H, m, CH γ -Leu + CH₂-C2), 1.53–1.42 (2H, m, CH₂ β -Leu), 1.02 (3H, d, $J = 6.6$ Hz, CH₃ δ -Leu), 0.94 (3H, d, $J = 6.8$ Hz, CH₃ γ -Val), 0.92 (3H, d, $J = 6.6$ Hz, CH₃ δ -Leu), 0.90 (3H, d, $J = 6.8$ Hz, CH₃ γ -Val), 0.85–0.74 (2H, m, CH-C3 + CH-C5), 0.54 (1H, ddd, $J = 8.3, 5.2, 5.2$ Hz, CH₂-C4), 0.46 (1H, ddd, $J = 8.3, 5.4, 5.4$ Hz, CH₂-C4); ¹³C (126 MHz, CD₂Cl₂): δ 172.9 (CO-C1), 172.4 (CO-Ac), 171.4 (CO-Leu), 169.8 (CO-Val), 58.1 (CH α -Val), 47.6 (CH α -Leu), 44.0 (CH₂-C6), 42.4 (CH₂ β -Leu), 39.7 (CH₂-C2), 37.2 (CH₃-C7), 36.0 (CH₃-C7), 32.0 (CH β -Val), 24.9 (CH γ -Leu), 23.6 (CH₃-Ac), 23.6 (CH₃ δ -Leu), 21.8 (CH₃ δ -Leu), 19.3 (CH₃ γ -Val), 18.5 (CH₃ γ -Val), 18.3 (CH-C5), 14.2 (CH-C3), 10.2 (CH₂-C4); HRMS (ESI+) for C₂₁H₃₈N₄O₄Na [M+Na]⁺ calcd 433.2785, found 433.2768.

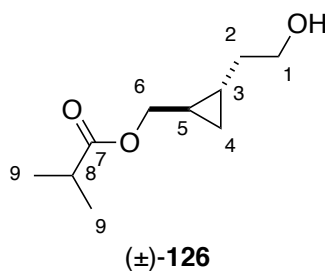
(1*R,2*S**)-(2-Ethenylcyclopropyl)methyl isobutyrate 125**



To a cooled solution of DMAP (24.0 mg, 200 μ mol) in pyridine (5.00 mL) at 0 °C, was added (±)-**90** (1.00 g, 10.2 mmol). Isobutyric anhydride (3.40 mL, 20.4 mmol) was added dropwise to the solution and the reaction mixture was stirred for 48 h at rt. H₂O (15 mL) was added and the resulting aqueous solution was extracted with Et₂O (3 \times 15 mL). The combined organic extracts were washed with sat. aq. NH₄Cl (10 mL), H₂O (10 mL) and brine (10 mL), dried over MgSO₄, filtered and concentrated under vacuum. The residue was purified by silica gel column chromatography (PE/EtOAc 20:1) to afford the title compound (819 mg, 48%) as a colourless liquid.

R_f (EtOAc/PE 1:1): 0.46; ν_{\max} (CHCl₃): 2972, 2362, 1732, 1190, 1152, 897 cm⁻¹; ¹H NMR (500 MHz; CDCl₃): δ 5.39 (1H, ddd, J = 17.0, 10.3, 8.5 Hz, CH-C2), 5.05 (1H, dd, J = 17.0, 1.5 Hz, CH₂-C1), 4.87 (1H, dd, J = 10.3, 1.5 Hz, CH₂-C1), 3.97 (1H, dd, J = 11.3, 6.9 Hz, CH₂-C6), 3.94 (1H, dd, J = 11.3, 6.9 Hz, CH₂-C6), 2.54 (1H, p, J = 7.0 Hz, CH-C8), 1.45–1.34 (1H, m, CH-C3), 1.22–1.17 (1H, m, CH-C5), 1.16 (6H, d, J = 7.0 Hz, 2 \times CH₃-C9), 0.72 (1H, ddd, J = 8.5, 5.3, 5.3 Hz, CH₂-C4), 0.67 (1H, ddd, J = 8.5, 5.1, 5.1 Hz, CH₂-C4); ¹³C NMR (126 MHz; CDCl₃): δ 177.4 (CO-C7), 140.3 (CH-C2), 112.8 (CH₂-C1), 67.5 (CH₂-C6), 34.2 (CH-C8), 20.9 (CH-C3), 19.4 (CH-C5), 19.1 (2 \times CH₃-C9), 12.0 (CH₂-C4); HRMS (ESI+) for C₁₀H₁₆NaO₂ [M+Na]⁺ calcd 191.1043, found 191.1043.

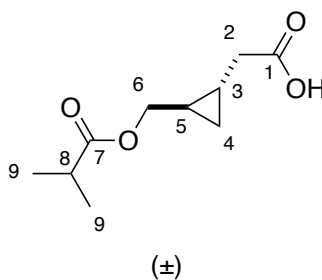
[(1*R,2*S**)-2-(2-Hydroxyethyl)cyclopropyl]methyl isobutyrate **126****



A flask equipped with an argon inlet was charged with $\text{BH}_3 \cdot \text{THF}$ (10.0 mL of a 1 M solution in THF, 10.0 mL, 9.74 mmol). A solution of (±)-**125** (819 mg, 4.87 mmol) in THF (18 mL) was added dropwise at 0 °C. The reaction mixture was stirred for 4 h at this temperature. H_2O (9 mL) was then added carefully followed by pH 7 phosphate buffer solution (9 mL). Sodium perborate (2.20 g, 14.6 mmol) was added and the reaction mixture was stirred for a further 2 h. The excess of sodium perborate was removed by filtration and the solvent was removed under vacuum. The aqueous phase was extracted with Et_2O (3×20 mL). The combined organic extracts were washed with brine (20 mL), dried over MgSO_4 , filtered and concentrated under vacuum. The residue was purified by silica gel column chromatography (PE/EtOAc 1:1) to give the corresponding alcohol (83 mg, 9%) as a yellow oil.

R_f (EtOAc/PE 1:1): 0.58; ν_{max} (CHCl_3): 3422, 2931, 1732, 1471, 1192, 1155, 1072, 1044 cm^{-1} . ^1H NMR (500 MHz; CDCl_3): δ 4.09 (1H, dd, $J = 11.4, 6.2$ Hz, $\text{CH}_2\text{-C6}$), 3.75 (1H, dd, $J = 11.4, 8.3$ Hz, $\text{CH}_2\text{-C6}$), 3.69 (2H, ddd, $J = 6.8, 6.1, 2.4$ Hz, $\text{CH}_2\text{-C1}$), 2.55 (1H, hept, $J = 7.0$ Hz, CH-C8), 1.65 (1H, dddd, $J = 13.5, 12.8, 6.1, 6.1$ Hz, $\text{CH}_2\text{-C2}$), 1.36 (1H, dddd, $J = 14.3, 12.8, 6.8, 6.8$ Hz, $\text{CH}_2\text{-C2}$), 1.17 (3H, d, $J = 7.0$ Hz, $\text{CH}_3\text{-C9}$), 1.17 (3H, d, $J = 7.0$ Hz, $\text{CH}_3\text{-C9}$), 1.00–0.87 (1H, m, CH-C5), 0.80–0.69 (1H, m, CH-C3), 0.49 (1H, ddd, $J = 8.5, 4.9, 4.9$ Hz, $\text{CH}_2\text{-C4}$), 0.42 (1H, ddd, $J = 8.5, 5.1, 5.1$ Hz, $\text{CH}_2\text{-C4}$); ^{13}C NMR (126 MHz; CDCl_3): δ 177.5 (CO-C7), 68.6 ($\text{CH}_2\text{-C6}$), 63.0 ($\text{CH}_2\text{-C1}$), 36.4 ($\text{CH}_2\text{-C2}$), 34.2 (CH-C8), 19.2 ($2 \times \text{CH}_3\text{-C9}$), 17.1 (CH-C5), 14.7 (CH-C3), 9.7 ($\text{CH}_2\text{-C4}$); HRMS (ESI+) for $\text{C}_{10}\text{H}_{18}\text{NaO}_3$ $[\text{M}+\text{Na}]^+$ calcd 209.1148, found 209.1150.

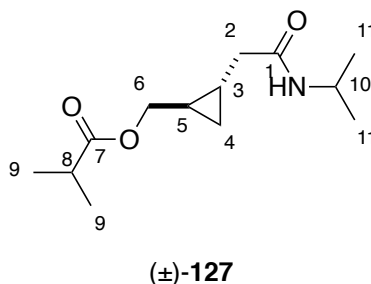
(±)-*i*PrCOO-{GlyΔGly}-OH



The procedure applied to the synthesis of (±)-**107** was followed using (±)-2-(2-hydroxyethyl)cyclopropyl]methyl isobutyrate **126** (83 mg, 0.45 mmol). The title compound (95 mg) was obtained as a black oil and used as crude for the next step.

R_f (EtOAc/PE 1:1): 0.38; ^1H NMR (500 MHz; CDCl_3): δ 3.97 (1H, dd, $J = 11.5, 6.7$ Hz, $\text{CH}_2\text{-C6}$), 3.92 (1H, dd, $J = 11.6, 7.0$ Hz, $\text{CH}_2\text{-C6}$), 2.54 (1H, hept, $J = 7.0$ Hz, CH-C8), 2.30 (2H, dd, $J = 14.0, 6.9$ Hz, $\text{CH}_2\text{-C2}$), 1.16 (3H, d, $J = 7.1$ Hz, $\text{CH}_3\text{-C9}$), 1.16 (3H, d, $J = 7.1$ Hz, $\text{CH}_3\text{-C9}$), 1.09–1.00 (2H, m, $\text{CH-C3} + \text{CH-C5}$), 0.60 (1H, ddd, $J = 8.3, 5.3, 5.3$ Hz, $\text{CH}_2\text{-C4}$), 0.50 (1H, ddd, $J = 8.3, 5.3, 5.3$ Hz, $\text{CH}_2\text{-C4}$); ^{13}C NMR (126 MHz; CDCl_3): δ 178.3 (CO-C1), 177.4 (CO-C7), 67.6 ($\text{CH}_2\text{-C6}$), 38.1 ($\text{CH}_2\text{-C2}$), 34.2 (CH-C8), 19.1 ($\text{CH}_3\text{-C9}$), 19.1 ($\text{CH}_3\text{-C9}$), 17.4 (CH-C5), 12.9 (CH-C3), 10.2 ($\text{CH}_2\text{-C4}$); HRMS (ESI+) for $\text{C}_{10}\text{H}_{16}\text{NaO}_4$ $[\text{M}+\text{Na}]^+$ calcd 223.0941, found 223.0944.

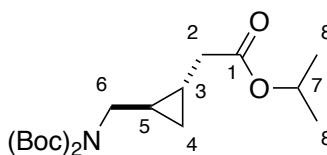
(±)-*i*PrCOO-{GlyΔGly}-*i*Pr 127



The procedure applied to the synthesis of (±)-**118** was applied using (±)-**126** (95 mg, 0.47 mmol). The title compound was obtained as a white solid (55 mg, 51% over 2 steps) after the work up.

R_f (EtOAc/PE 1:1): 0.41; m.p.: > 400 °C; ν_{\max} (10 mM in CH₂Cl₂): 3429, 3059, 2970, 2928, 2870, 1724, 1663, 1512, 1466, 1270, 1161, 1157 cm⁻¹; ¹H NMR (500 MHz; CDCl₃): δ 5.71 (1H, bs, NH), 4.14–4.10 (1H, m, CH-C10), 4.08 (1H, dd, J = 11.6, 6.4 Hz, CH₂-C6), 3.81 (1H, dd, J = 11.6, 7.6 Hz, CH₂-C6), 2.55 (1H, hept, J = 7.0 Hz, CH-C8), 2.18 (1H, dd, J = 16.1, 6.9 Hz, CH₂-C2), 2.11 (1H, dd, J = 16.1, 7.3 Hz, CH₂-C2), 1.18–1.13 (12H, m, 2 × CH₃-C9 + 2 × CH₃-C11), 1.05–0.90 (2H, m, CH-C5 + CH-C3), 0.59 (1H, ddd, J = 8.4, 5.0, 5.0 Hz, CH₂-C4), 0.48 (1H, ddd, J = 8.4, 5.1, 5.1 Hz, CH₂-C4); ¹³C NMR (126 MHz; CDCl₃): δ 177.4 (CO-C1), 170.9 (CO-C7), 67.8 (CH₂-C6), 41.4 (CH-C10), 40.7 (CH₂-C2), 34.1 (CH-C8), 22.9 (2 × CH₃-C9), 19.2 (2 × CH₃-C11), 17.5 (CH-C5), 13.6 (CH-C3), 10.2 (CH₂-C4); HRMS (ESI+) for C₁₃H₂₃NNaO₃ [M+Na]⁺ calcd 264.1570, found 264.1572.

(±)-(Boc)₂-{GlyΔGly}-O-*i*Pr 128

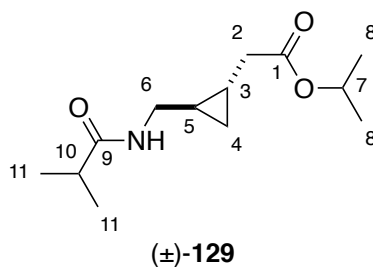


(±)-128

(±)-(Boc)₂-{GlyΔGly}-OH **107** (90 mg, 0.27 mmol) was dissolved in CH₂Cl₂ (1.4 mL). DCC (62 mg, 0.30 mmol) and *i*-PrOH (23 μL, 0.30 mmol) were added to the solution. The reaction mixture was stirred overnight at rt. The solvent was removed under vacuum. The residue was purified by silica gel column chromatography (PE/EtOAc 1:1) to afford the title compound as a mixture 0.3:1 NHBoc/N(Boc)₂ (87 mg). Only the major compound is reported.

R_f (EtOAc/PE 1:1): 0.41; ¹H NMR (500 MHz; CDCl₃): δ 5.05 (1H, hept, *J* = 6.4 Hz, CH-C7), 3.37–3.28 (1H, m, CH₂-C6), 2.71 (1H, ddd, *J* = 13.0, 8.4, 4.0 Hz, CH₂-C6), 2.48–2.44 (1H, m, CH₂-C2), 1.96 (1H, dd, *J* = 16.8, 9.0 Hz, CH₂-C2), 1.44 (18H, s, 2 × *t*-Bu), 1.03 (3H, d, *J* = 6.3 Hz, CH₃-C8), 1.03 (3H, d, *J* = 6.3 Hz, CH₃-C8), 0.88–0.82 (1H, m, CH-C3), 0.81–0.75 (1H, m, CH-C5), 0.48 (1H, ddd, *J* = 8.6, 5.2, 5.2 Hz, CH₂-C4), 0.40 (1H, ddd, *J* = 8.6, 5.2, 5.2 Hz, CH₂-C4); ¹³C NMR (126 MHz; CDCl₃): δ 172.7 (CO-C1), 152.9 (2 × CO-Boc), 82.3 (2 × C-Boc), 68.0 (CH-C7), 45.0 (CH₂-C6), 38.7 (CH₂-C2), 28.6 (6 × CH₃-Boc), 22.0 (2 × CH₃-C8), 18.3 (CH-C5), 13.3 (CH-C3), 10.2 (CH₂-C4); HRMS (ESI+) for C₁₉H₃₃N₂NaO₆ [M+Na]⁺ calcd 394.2200, found 394.2186.

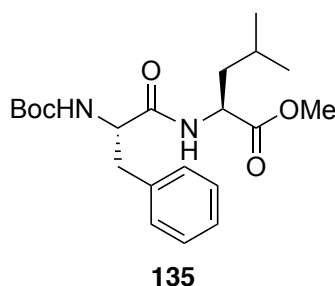
(±)-*i*Pr-{GlyΔGly}-O*i*Pr 129



(±)- (Boc)₂-{GlyΔGly}-O*i*Pr **128** (88 mg, 0.24 mmol) was dissolved in CH₂Cl₂ (2.4 mL) and TFA (200 μL, 2.40 mmol) was added dropwise. The reaction mixture was stirred for 3 h and the solvent was removed under vacuum. The residue was taken up in CH₂Cl₂ (0.34 mL) and Et₃N (50 μL, 0.36 mmol) was added followed by isobutyric anhydride (60 μL, 0.36 mmol) at rt. The mixture was stirred overnight at rt and H₂O (5 mL) was added. The phases were separated and the organic phase was washed with sat. aq. NaHCO₃ (5 mL), 1 M aq. HCl (5 mL), brine (5 mL), dried over MgSO₄ and concentrated under reduced pressure. The residue was purified by silica gel column chromatography (Et₂O/PE 9:1 to 7:3) to give the title compound (29 mg, 65% over 3 steps) as a colourless solid.

R_f(Et₂O/PE 1:1): 0.63; m.p.: 103–104 °C; ν_{max} (10 mM in CH₂Cl₂): 3437, 3356, 3048, 2982, 2928, 2866, 1713, 1666, 1516, 1192, 1107 cm⁻¹; ¹H NMR (500 MHz; CDCl₃): δ 6.56 (1H, bs, NH), 5.03 (1H, hept, *J* = 6.6 Hz, CH-C7), 3.72 (1H, ddd, *J* = 13.6, 5.7, 5.7 Hz, CH₂-C6), 2.67 (1H, dd, *J* = 17.3, 4.6 Hz, CH₂-C2), 2.51 (1H, ddd, *J* = 13.6, 9.6, 2.9 Hz, CH₂-C6), 2.41 (1H, hept, *J* = 7.0 Hz, CH-C10), 1.79 (1H, dd, *J* = 17.3, 9.9 Hz, CH₂-C2), 1.24 (3H, d, *J* = 6.6 Hz, CH₃-C8), 1.24 (3H, d, *J* = 6.6 Hz, CH₃-C8), 1.17 (3H, d, *J* = 7.0 Hz, CH₃-11), 1.17 (3H, d, *J* = 7.0 Hz, CH₃-11), 0.82–0.76 (1H, m, CH-C3), 0.76–0.69 (1H, m, CH-C5), 0.53 (1H, ddd, *J* = 8.5, 5.2 Hz, CH₂-C4), 0.44 (1H, ddd, *J* = 8.5, 5.2 Hz, CH₂-C4); ¹³C NMR (126 MHz; CDCl₃): δ 177.2 (CO-C9), 173.5 (CO-C1), 68.1 (CH-C7), 44.1 (CH₂-C6), 38.2 (CH₂-C2), 35.8 (CH-C10), 22.0 (2 × CH₃-C8), 19.8 (2 × CH₃-C11), 17.8 (CH-C5), 13.2 (CH-C3), 10.4 (CH₂-C4); HRMS (ESI+) for C₁₃H₂₃NNaO₃ [M+Na]⁺ calcd 264.1570, found 264.1563.

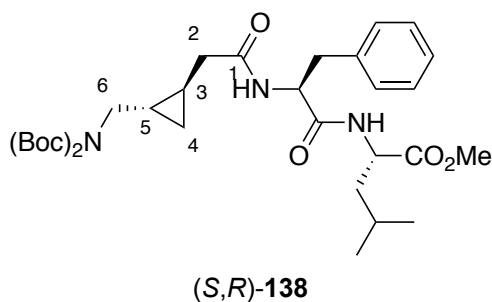
Boc-Phe-Leu-OMe 135



To a solution of Boc-Phe-OH (1.00 g, 3.77 mmol) in CH_2Cl_2 (13 mL) was added HCl·H-Leu-OMe (685 mg, 3.77 mmol) followed by DIPEA (1.97 mL, 3.77 mmol). The solution was stirred for 10 min and HATU (1.40 g, 3.77 mmol) was added. The reaction mixture was stirred for 6 h at rt. H_2O (30 mL) was added and the phases were separated. The organic phase was dried over MgSO_4 and filtered. The solvents were removed under vacuum and the resulting brown oil was purified by silica gel column chromatography (PE/EtOAc 1:1) to yield Boc-Phe-Leu-OMe **135** (1.30 g, 88%) as a white powder.

R_f (PE/EtOAc 1:1): 0.88; $[\alpha]_D^{22}$ -28 ($c = 1.0$, MeOH); m.p.: 109–110 °C; ν_{max} 3287, 2957, 1748, 1682, 1645, 1535, 1366, 1250, 1171 cm^{-1} ; ^1H NMR (500 MHz, CDCl_3) δ 7.36–7.20 (5H, m, $5 \times \text{CH-Ph}$), 6.23 (1H, d, $J = 8.3$ Hz, NH-Leu), 5.01 (1H, s, NH-Phe), 4.59 (1H, ddd, $J = 8.6, 8.3, 4.8$ Hz, $\text{CH}\alpha$ -Leu), 4.36 (d, $J = 5.6$ Hz, $\text{CH}\alpha$ -Phe), 3.72 (3H, s, OCH_3), 3.12 (1H, dd, $J = 13.7, 6.6$ Hz, $\text{CH}_2\beta$ -Phe), 3.08 (1H, dd, $J = 13.7, 5.6$ Hz, $\text{CH}_2\beta$ -Phe), 1.65–1.52 (2H, m, $\text{CH}\gamma$ -Leu + $\text{CH}_2\beta$ -Leu), 1.54–1.44 (1H, m, $\text{CH}_2\beta$ -Leu), 1.44 (9H, s, t -Bu), 0.93 (3H, d, $J = 6.2$ Hz, $\text{CH}_3\delta$ -Leu), 0.91 (3H, d, $J = 6.3$ Hz, $\text{CH}_3\delta$ -Leu); ^{13}C (126 MHz, CDCl_3): δ 172.3 (CO-Phe), 171.0 (CO-Boc), 169.7 (CO-Leu), 129.5 ($2 \times \text{CH-Ph}$), 128.8 ($2 \times \text{CH-Ph}$), 126.48 (CH-Ph), 110.0 (C-Ph), 79.5 (C-Boc), 53.4 ($\text{CH}\alpha$ -Phe), 52.4 (OCH_3), 50.9 ($\text{CH}\alpha$ -Leu), 41.8 ($\text{CH}_2\beta$ -Leu), 39.2 ($\text{CH}_2\beta$ -Phe), 28.4 ($3 \times \text{CH}_3$ -Boc), 24.8 ($\text{CH}\gamma$ -Leu), 22.9 ($\text{CH}_3\delta$ -Leu), 22.0 ($\text{CH}_3\delta$ -Leu); HRMS (ESI+) for $\text{C}_{21}\text{H}_{32}\text{N}_2\text{NaO}_5$ $[\text{M}+\text{Na}]^+$ calcd 415.2203, found 415.2197.

(*S,R*)-(Boc)₂-{GlyΔGly}-Phe-Leu-OMe 138



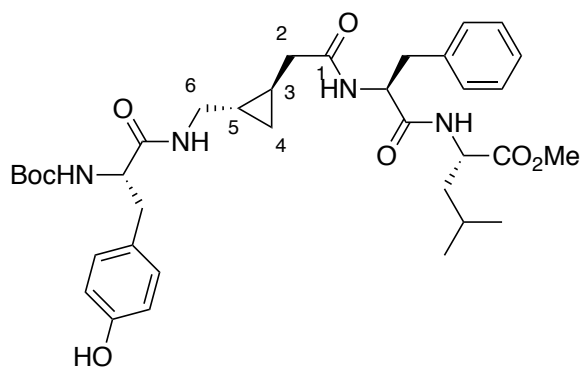
Boc-Phe-Leu-OMe **135** (260 mg, 0.66 mmol) was dissolved in CH₂Cl₂ (6.6 mL) and TFA (100 μL, 0.99 mmol) was added. The reaction mixture was stirred for 5 h at rt and the solvent was removed under vacuum.

TFA·H-Phe-Leu-OMe (122 mg, 0.30 mmol) was dissolved in CH₂Cl₂ (1 mL) and DIPEA (160 μL, 0.90 mmol) was added followed by (*S,R*)-(Boc)₂-{GlyΔGly}-OH **107** (100 mg, 0.30 mmol). The mixture was stirred for 15 min and HATU (114 mg, 0.30 mmol) was added. The reaction mixture was stirred for 5 h at rt. H₂O (10 mL) was added and the phases were separated. The organic phase was washed with 1 M aq. HCl (10 mL), H₂O (10 mL), brine (10 mL), dried over MgSO₄ and filtered. The solvent was removed under vacuum and the residue was purified by silica gel column chromatography (PE/EtOAc 9:1 to 1:1) to afford (*S,R*)-(Boc)₂-GlyΔGly}-Phe-Leu-OMe **138** (108 mg, 60%) as a colourless solid.

R_f (PE/EtOAc 1:1): 0.68; $[\alpha]_D^{16} -10$ ($c = 0.40$, CHCl₃); m.p.: 153–154 °C; ν_{\max} 3281, 2957, 1746, 1694, 1641, 1553, 1368, 1175, 1128 cm⁻¹; ¹H NMR (500 MHz, CDCl₃) δ 7.27–7.16 (5H, m, 5 × CH-Ph), 6.45 (1H, d, $J = 7.2$ Hz, NH-Phe), 6.25 (1H, d, $J = 8.3$ Hz, NH-Leu), 4.64 (1H, ddd, $J = 14.5, 7.2, 7.2$ Hz, CH α -Phe), 4.48 (1H, ddd, $J = 8.5, 8.3, 5.2$ Hz, CH α -Leu), 3.66 (3H, s, OCH₃), 3.55 (1H, dd, $J = 14.3, 6.0$ Hz, CH₂-C6), 3.42 (1H, dd, $J = 14.3, 6.8$ Hz, CH₂-C6), 3.07 (2H, d, $J = 7.2$ Hz, CH₂ β -Phe), 2.30 (1H, dd, $J = 16.4, 6.1$ Hz, CH₂-C2), 1.87 (1H, dd, $J = 16.4, 8.3$ Hz, CH₂-C2), 1.60–1.40 (3H, m, CH γ -Leu + CH₂ β -Leu), 1.46 (18H, s, 2 × *t*-Bu), 0.93–0.82 (2H, m, CH-C5 + CH-C3), 0.85 (6H, d, $J = 6.3$ Hz, 2 × CH₃ δ -Leu), 0.52 (1H, ddd, $J = 8.4, 5.0, 5.0$ Hz, CH₂-C4), 0.23 (1H, ddd, $J = 8.4, 5.1, 5.1$ Hz, CH₂-C4); ¹³C NMR (126 MHz, CDCl₃) δ 172.9 (CO-Leu), 172.3 (CO-C1), 170.7 (CO-Phe), 153.1 (2 × CO-Boc), 136.7 (C-Ph), 129.5 (C-Ph), 128.8 (2 × Ph), 127.1 (2 × CH-Ph), 82.5 (C-Boc), 54.4 (CH α -Phe), 52.4 (OCH₃), 51.1 (CH α -Leu), 49.0 (CH₂-C6), 41.5 (CH₂ β -Leu), 40.7 (CH₂-C2), 37.8 (CH₂ β -Phe), 28.2 (6 × CH₃-Boc), 24.9 (CH γ -Leu), 22.8 (CH₃ δ -Leu).

Leu), 22.1 (CH₃δ-Leu), 18.5 (CH-C5), 13.2 (CH-C3), 10.4 (CH₂-C4); HRMS (ESI+) for C₃₂H₄₉N₃NaO₈ [M+Na]⁺ calcd 626.3412, found 626.3389.

(*S,R*)-Boc-Tyr- $\{\text{Gly}\Delta\text{Gly}\}$ -Phe-Leu-OMe **140**



(*S,R*)-140

(*S,R*)-(Boc)₂- $\{\text{Gly}\Delta\text{Gly}\}$ -Phe-Leu-OMe **138** (108 mg, 0.18 mmol) was dissolved in CH₂Cl₂ (2 mL) and TFA (140 μ L, 1.80 mmol) was added to the solution. The reaction mixture was stirred at rt for 12 h. The solvent was then removed, and the compounds was used for the coupling without purification.

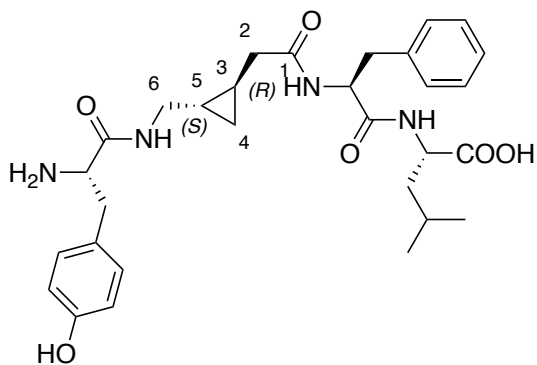
To a solution of TFA·(*S,R*)-H- $\{\text{Gly}\Delta\text{Gly}\}$ -Phe-Leu-OMe (0.18 mmol) in DMF (600 μ L) was added DIPEA (94 μ L, 0.54 mmol) dropwise. Boc-Tyr-OH (76 mg, 0.27 mmol) was added followed by HATU (68 mg, 0.18 mmol). The reaction mixture was stirred overnight at rt. The solution was washed with 5% aq. LiCl (4 \times 5 mL), 1 M aq. HCl (5 mL) and sat. aq. NaHCO₃ (5 mL). The organic phase was dried over MgSO₄ and filtered. The solvent was removed under vacuum and the resulting oil was purified by silica gel column chromatography (CH₂Cl₂/MeOH 99:1 to 95:5) to afford (*S,R*)-Boc-Tyr- $\{\text{Gly}\Delta\text{Gly}\}$ -Phe-Leu-OMe **140** (90 mg, 75%) as a white powder.

R_f (CH₂Cl₂/MeOH 9:1): 0.76; $[\alpha]_D^{15} +38$ ($c = 0.05$, CHCl₃); m.p.: 152–153 °C; ν_{max} 3276, 2955, 1732, 1701, 1656, 1519, 1342, 1172, 1129 cm⁻¹; ¹H NMR (500 MHz, CDCl₃) δ 7.33–7.18 (5H, m, 5 \times CH-Ph), 7.04 (2H, bd, $J = 8.3$ Hz, 2 \times CH-Arom-Tyr), 6.71 (2H, d, $J = 8.3$ Hz, 2 \times CH-Arom-Tyr), 6.68 (1H, bs, NH-Gly), 6.60 (1H, bs, NH-Phe), 6.38 (1H, bs, NH-Leu), 5.43 (1H, d, $J = 8.3$ Hz, NH-Tyr), 4.68 (1H, bs, CH α -Phe), 4.56 (1H, bs, CH α -Leu), 4.34 (1H, dd, $J = 8.3, 6.7$ Hz, CH α -Tyr), 3.71 (3H, s, OCH₃), 3.48 (1H, bs, 1H \times CH₂-C6), 3.09 (2H, bd, $J = 5.7$ Hz, CH₂ β -Phe), 3.01 (1H, bs, 1H \times CH₂ β -Tyr), 2.92 (1H, bs, 1H \times CH₂ β -Tyr), 2.67–2.59 (1H, m, 1H \times CH₂-C6), 2.29 (2H, bd, $J = 16.7$ Hz, 1H \times CH₂-C2), 1.91–1.81 (1H, m, 1H \times CH₂-C2), 1.66–1.48 (3H, m, CH γ -Leu + CH₂ β -Leu), 1.41 (9H, s, *t*-Bu), 0.90 (6H, d, $J = 6.0$ Hz, 2 \times CH₃ δ -Leu), 0.54 (2H, m, CH-C5 + CH-C3), 0.39 (1H, bs, CH₂-C4), 0.31 (1H, bs, CH₂-C4)**; ¹³C (126 MHz, CDCl₃): 173.0 (CO-OCH₃), 172.7 (CO-

Leu), 171.7 (CO-C1), 171.4 (CO-Phe), 155.6 (CO-Boc), 155.2 (C-Tyr), 136.5 (CH-Arom-Phe), 130.7 ($2 \times$ CH-Arom-Tyr), 129.5 ($2 \times$ CH-Ph), 128.8 (CH-Ph), 128.6 (CH-Ph), 127.3 (C-Ph), 115.7 ($2 \times$ CH-Arom-Tyr), 80.0 (C-Boc), 56.3 (CH α -Tyr), 54.6 (CH α -Phe), 52.6 (OCH₃), 51.3 (CH α -Leu), 43.0 (CH₂-C6), 41.4 (CH₂ β -Leu), 39.8 (CH₂-C2), 38.4 (CH₂ β -Tyr), 38.2 (CH₂ β -Phe), 28.5 ($3 \times$ CH₃-Boc), 24.9 (CH γ -Leu), 22.0 ($2 \times$ CH₃ δ -Leu), 18.0 (CH-C5), 13.0 (CH-C3), 10.7 (CH₂-C4); HRMS (ESI+) for C₃₆H₅₀N₄NaO₈ [M+Na]⁺ calcd 689.3521, found 689.3503.

**Most of the signal are shown broad due to exchange in conformation for this peptide.

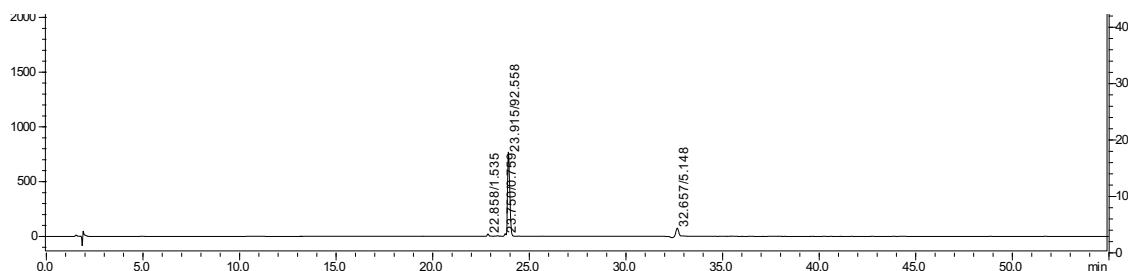
(*S,R*)-H-Tyr-{GlyΔGly}-Phe-Leu-OH 133

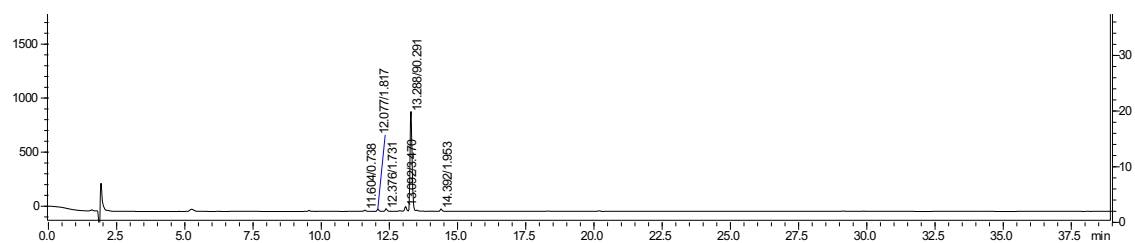


(*S,R*)-133

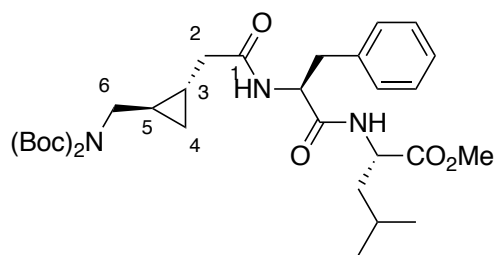
(*S,R*)-Boc-Tyr-{GlyΔGly}-Phe-Leu-OMe **140** (20.0 mg, 0.03 mmol) was dissolved in THF (0.10 mL) and 4 M aq. HCl (0.50 mL). The reaction mixture was stirred overnight at rt. The solution was then lyophilised. The crude peptide was purified using semi-preparative HPLC system with a flow rate of 8 mL/min. A linear gradient of buffer A (H₂O and 0.1% TFA) to buffer B (MeCN and 0.1% TFA) was used over 40 min from 35 to 65%. UV detection wavelengths were 214 and 280 nm. The title compound was obtained as a white solid (8 mg, 48%).

$[\alpha]_D^{20}$ -0.87 (c = 0.12, MeOH); HRMS (ESI+) for C₂₈H₃₈N₅O₇ [M+H]⁺ calcd 556.2766 found 556.2752. HPLC: purity 92.56% (50 mins gradient), 90.29% (20 mins gradient); m.p.: 107–108 °C.





(*R,S*)-(Boc)₂-{GlyΔGly}-Phe-Leu-OMe 137

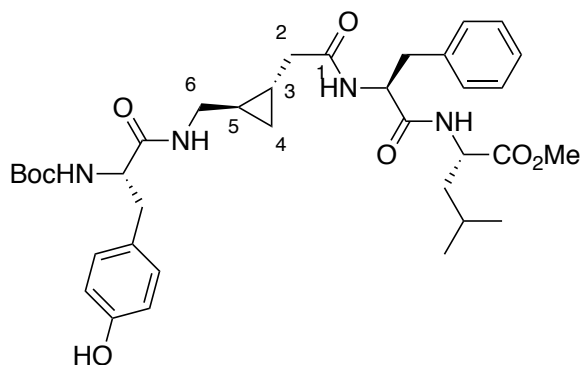


(*R,S*)-137

The procedure applied to the synthesis of (*S,R*)-(Boc)₂-{GlyΔGly}-Phe-Leu-OMe **138** on exactly the same scale. The residue was purified by silica gel column chromatography (PE/EtOAc 9:1 to 1:1) to afford (*R,S*)-(Boc)₂-{GlyΔGly}-Phe-Leu-OMe **137** (118 mg, 65%) as a white solid.

R_f (PE/EtOAc 1:1): 0.68; $[\alpha]_D^{20}$ -23 ($c = 0.90$, CHCl₃); m.p.: 122–123 °C; ν_{\max} 3275, 3067, 2957, 1746, 1694, 1639, 1553, 1437, 1368, 1238, 1128 cm⁻¹; ¹H NMR (500 MHz, CDCl₃) δ 7.32–7.22 (5H, m, 5 × CH-Ph), 6.52 (1H, d, $J = 7.4$ Hz, NH-Phe), 6.23 (1H, d, $J = 8.2$ Hz, NH-Leu), 4.67 (1H, ddd, $J = 14.8, 7.4, 7.4$ Hz, CH α -Phe), 4.51 (1H, ddd, $J = 8.2, 8.2, 5.3$ Hz, CH α -Leu), 3.70 (3H, s, OCH₃), 3.60 (1H, dd, $J = 14.4, 5.8$ Hz, CH₂-C6), 3.44 (1H, dd, $J = 14.4, 6.8$ Hz, CH₂-C6), 3.12 (2H, dd, $J = 7.4, 3.9$ Hz, CH₂ β -Phe), 2.33 (1H, dd, $J = 16.4, 6.2$ Hz, CH₂-C2), 1.95 (1H, dd, $J = 16.4, 8.1$ Hz, CH₂-C2), 1.65–1.41 (3H, m, CH γ -Leu + CH₂ β -Leu), 1.50 (18H, s, 2 × *t*-Bu), 0.95–0.82 (2H, m, CH-C5 + CH-C3), 0.89 (3H, d, $J = 6.3$ Hz, CH₃ δ -Leu), 0.89 (3H, d, $J = 6.3$ Hz, CH₃ δ -Leu), 0.57 (1H, ddd, $J = 8.5, 5.1, 5.1$ Hz, CH₂-C4), 0.31 (1H, ddd, $J = 8.5, 5.1, 5.1$ Hz, CH₂-C4); ¹³C (126 MHz, CDCl₃): δ 172.9 (CO-Leu), 172.3 (CO-C1), 170.8 (CO-Phe), 153.1 (2 × CO-Boc), 136.8 (C-Ph), 129.5 (C-Ph), 128.8 (2 × CH-Ph), 127.1 (2 × CH-Ph), 82.5 (2 × C-Boc), 54.3 (CH α -Phe), 52.4 (OCH₃), 51.1 (CH α -Leu), 48.9 (CH₂-C6), 41.5 (CH₂ β -Leu), 40.7 (CH₂-C2), 37.8 (CH₂ β -Phe), 28.2 (6 × CH₃-Boc), 24.9 (CH γ -Leu), 22.8 (CH₃ δ -Leu), 22.1 (CH₃ δ -Leu), 18.4 (CH-C5), 13.1 (CH-C3), 10.4 (CH₂-C4); HRMS (ESI+) for C₃₂H₄₉N₃NaO₈ [M+Na]⁺ calcd 626.3412, found 626.3381.

(*R,S*)-Boc-Tyr-{GlyΔGly}-Phe-Leu-OMe 139



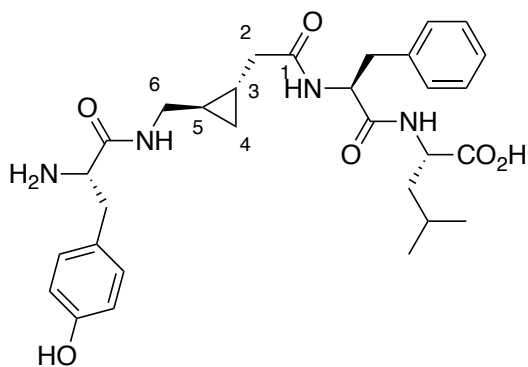
(*R,S*)-139

The procedure applied to the synthesis of (*S,R*)-Boc-Tyr-{GlyΔGly}-Phe-Leu-OMe **140** was followed using (*R,S*)-(Boc)₂-{GlyΔGly}-Phe-Leu-OMe **137** (107 mg, 0.18 mmol). The residue was purified by silica gel column chromatography (CH₂Cl₂/MeOH 99:1 to 98:2) to afford (*R,S*)-Boc-Tyr-{GlyΔGly}-Phe-Leu-OMe **139** (130 mg, 76%) as a white powder.

R_f (CH₂Cl₂/MeOH 9:1): 0.93; [α]_D²⁰ −5.5 (*c* = 0.20, CHCl₃); m.p.: 167–168 °C; ν_{max} 3287, 2953, 2926, 1725, 167, 1533, 1516, 1449, 1368, 1246, 1167 cm^{−1}; ¹H NMR (500 MHz, CDCl₃) δ 7.33–7.19 (5H, m, 5 × CH-Ph), 7.05 (2H, d, *J* = 8.3 Hz, 2 × CH-Arom-Tyr), 6.72 (2H, d, *J* = 8.3 Hz, 2 × CH-Arom-Tyr), 6.41 (1H, d, *J* = 7.2 Hz, NH-Phe), 6.38 (1H, d, *J* = 8.2 Hz, NH-Leu), 6.04 (1H, bs, NH-Gly), 5.43 (1H, d, *J* = 8.3 Hz, NH-Tyr), 4.70 (1H, m, CH α -Phe), 4.60–4.51 (1H, m, CH α -Leu), 4.29–4.22 (1H, m, CH α -Tyr), 3.71 (3H, s, OCH₃), 3.49 (1H, bd, *J* = 13.5 Hz, CH₂-C6), 3.08 (2H, d, *J* = 7.2 Hz, CH₂ β -Phe), 3.07–3.01 (1H, m, CH₂ β -Tyr), 2.80 (1H, bdd, *J* = 11.3, 11.3 Hz, CH₂ β -Tyr), 2.42 (1H, m, CH₂-C6), 2.00–1.86 (2H, m, CH₂-C2), 1.65–1.45 (3H, m, CH γ -Leu + CH₂ β -Leu), 1.42 (9H, s, *t*-Bu), 0.90 (3H, d, *J* = 6.1 Hz, CH₃ δ -Leu), 0.89 (3H, d, *J* = 6.2 Hz, CH₃ δ -Leu), 0.57–0.33 (4H, m, CH-C5 + CH-C3 + CH₂-C4)**; ¹³C (126 MHz, CDCl₃): δ 172.9 (CO-OCH₃), 172.5 (CO-Leu), 171.6 (CO-C1), 171.2 (CO-Phe), 155.4 (C-Tyr), 151.8 (CO-Boc), 136.4 (CH-Ph), 130.6 (2 × CH-Arom-Tyr), 129.5 (2 × CH-Arom-Phe), 128.8 (CH-Ph), 128.7 (CH-Ph), 127.3 (C-Ph), 115.9 (2 × CH-Arom-Tyr), 80.0 (C-Boc), 56.6 (CH α -Tyr), 54.7 (CH α -Phe), 52.6 (OCH₃), 51.2 (CH α -Leu), 43.7 (CH₂-C6), 41.5 (CH₂ β -Leu), 39.9 (CH₂-C2), 39.0 (CH₂ β -Tyr), 38.4 (CH₂ β -Phe), 28.5 (3 × CH₃-Boc), 24.9 (CH γ -Leu), 22.9 (CH₃ δ -Leu), 22.0 (CH₃ δ -Leu), 17.2 (CH-C5), 13.7 (CH-C3), 10.8 (CH₂-C4); HRMS (ESI⁺) for C₃₆H₅₀N₄NaO₈ [M+Na]⁺ calcd 689.3521, found 689.3493.

**Almost all peaks are shown broad or multiplet due to exchange in conformation for this peptide.

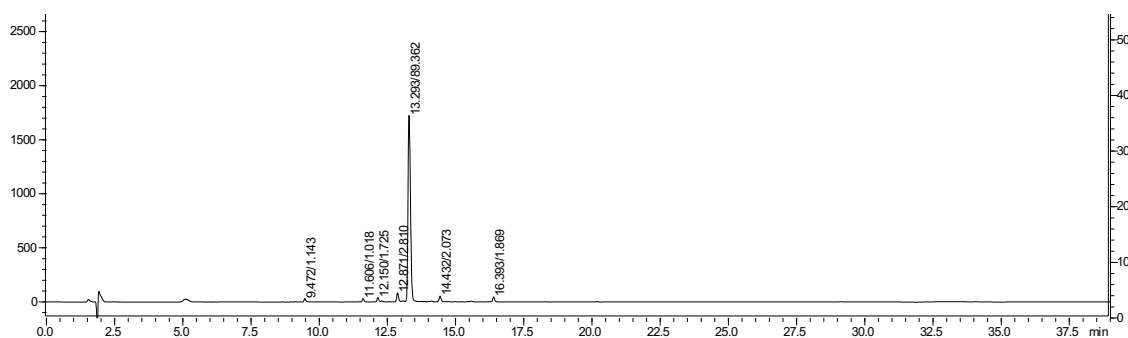
(*R,S*)-H-Tyr-{GlyΔGly}-Phe-Leu-OH 132

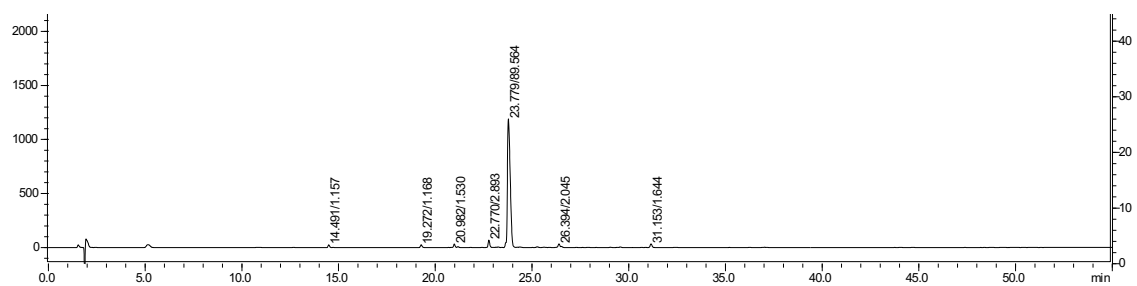


(*R,S*)-132

(*R,S*)-Boc-Tyr-{GlyΔGly}-Phe-Leu-OMe **139** (59.0 mg, 0.09 mmol) was dissolved in a mixture of THF (2 mL) and 4 M aq. HCl (2.25 mL). The reaction mixture was stirred overnight at rt. The solution was then lyophilised, and the crude peptide was then purified using semi-preparative HPLC system with a flow rate of 8 mL/min. A linear gradient of buffer A (H₂O and 0.1% TFA) to buffer B (MeCN and 0.1% TFA) was used over 40 min from 35 to 65%. UV detection wavelengths were 214 and 280 nm. The title compound (20 mg, 40%) was obtained as a colourless solid.

$[\alpha]_D^{20} +9.5$ ($c = 0.22$, MeOH); HRMS (ESI⁺) for C₃₀H₄₁N₄O₆ [M+H]⁺ calcd 553.3021, found 553.3013. HPLC: purity 89.56% (50 mins gradient), 89.36% (20 mins gradient), m.p.: 129–130 °C.





Microwave Assisted Solid Phase Peptide Synthesis:

Following peptides were synthesised using an Automated Biotage Initiator + Alstra microwave synthesizer on 0.1 mmol scale using Tentagel S RAM resin (0.24 mmol/g loading) or Fmoc-Leu Wang resin (0.84 mmol/g loading). L-amino acids were used for peptide synthesis with *N*-Fmoc protecting groups (4 equiv.). Analytical HPLC was undertaken on a Shimadzu SIL-20AHT equipped with a dual wavelength UV detector and a Phenomenex Aeris 5 μ m C18 (150 x 46 mm) column at a flow rate of 1 mL/min. A linear gradient of buffer A (95:5 H₂O/MeCN and 0.1% TFA) to buffer B (95:5 MeCN/H₂O and 0.1% TFA) was used over 20 min and 50 min from 0 to 100% and 100 to 0%. UV measurements were recorded at 214 nm and 280 nm. Peptides were purified using a Gilson semi-preparative HPLC system equipped with a Phenomenex Synergi 10u C18 80 Å, (250 x 21.2 mm) column with a flow rate of 8 mL/min. Peptides were lyophilized using a Christ Alpha 2–4 LDplus freeze-dryer. Peptide content was determined using a Nanodrop 2000c using UV absorbance at 280 nm when mentioned.

Peptides were synthesised *via* the following general procedure on the peptide synthesiser:

Resin Swelling – Resin swollen in DMF at 70 °C for 20 min.

Coupling – Coupling reactions were performed using 4 equiv. of amino acid, 4 equiv. of HCTU (0.5 M in DMF) and 8 equiv. of DIPEA (2 M in NMP). Natural amino acids were coupled at 75 °C for 5 min.

Deprotection – Fmoc deprotections were carried out using 20% piperidine in DMF, spiked with 5% formic acid at 75 °C for 30 s. A second deprotection was then undertaken at 70 °C for 3 min.

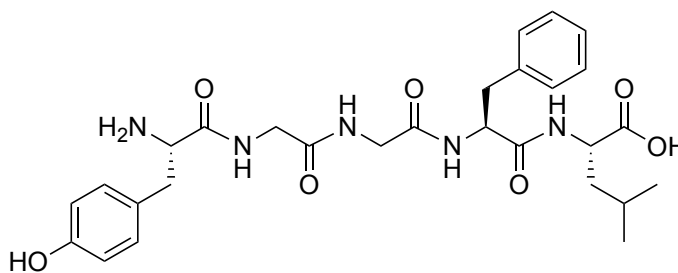
Washing – Resin was washed with DMF after each coupling and deprotection step.

Peptide Cleavage – Resin bound peptide was cleaved and protecting groups removed upon addition of 3 mL TFA/TIS/H₂O (95:2.5:2.5) and spun for 3 h.

After filtration through a sintered frit, the cleavage cocktail was evaporated using a stream of N₂ and the peptide was precipitated with ice cold Et₂O and centrifuged at 4500 rpm for 5 min. After decanting the supernatant, the Et₂O wash was repeated a further 2 times. The

crude peptide dissolved in 50% MeCN/H₂O with 0.1% TFA and was lyophilized before purification.

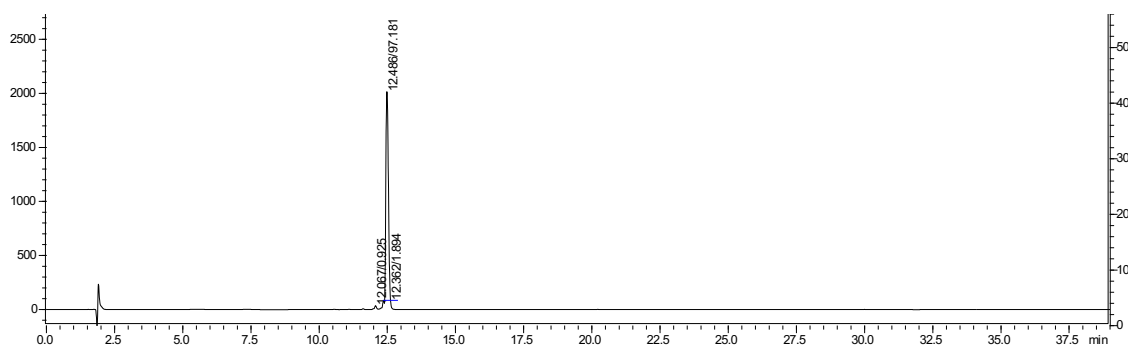
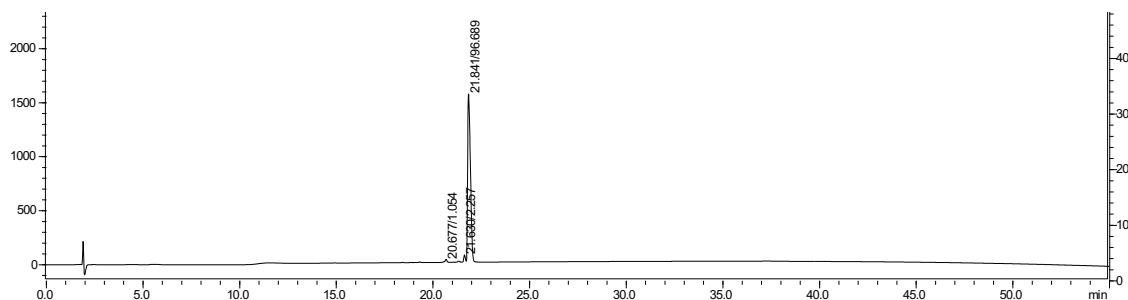
Leu-enkephalin **141**



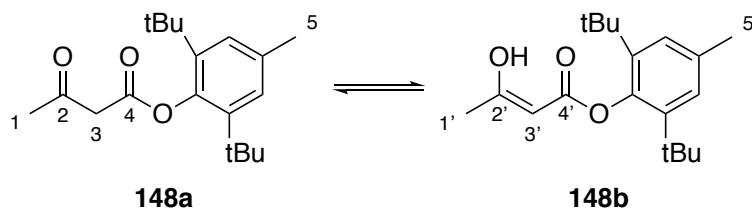
141

Following the procedure described for for SPPS using Fmoc-Leu Wang resin (0.84 mmol/g loading), the crude peptide was purified using semi-preparative HPLC system with a flow rate of 8 mL/min. A linear gradient of buffer A (H₂O and 0.1% TFA) to buffer B (MeCN and 0.1% TFA) was used over 40 min from 20 to 70%. UV detection wavelengths were 214 and 280 nm. Leu-enkephalin **137** (24 mg, 43%) was obtained as a white solid.

HRMS (ESI⁺) for C₂₈H₃₈N₅O₇ [M+H]⁺ calcd 556.2766, found 556.2752. HPLC: purity 96.69% (50 min gradient), 97.18% (20 min gradient), m.p.: 157–160 °C.



2,6-Di-*t*-butyl-4-methylphenyl-3-oxobutanoate 148

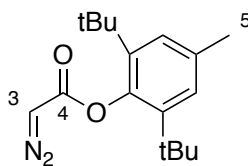


A mixture of 2,6-di-*t*-butyl-4-methylphenol (5.00 g, 22.7 mmol) and 2,2,6-trimethyl-4H-1,3-dioxin-4-one (3.00 mL, 22.7 mmol) in xylene (5 mL) was stirred at 140 °C for 2 h. Solvents were removed under reduced pressure and the residue was purified by silica gel column chromatography (PE/EtOAc 9:1) to give an orange solid which was recrystallised from PE to afford the title compound (3.07 g, 44%) as white solid as a mixture (45:55) of keto **148a**/enol **148b** compounds.

R_f (EtOAc/PE 1:1): 0.58; m.p.: 97–98 °C; ^1H NMR (500 MHz; CDCl_3): δ 12.15 (0.55H, s, OH enol), 7.13 (2H, s, CH-Arom), 5.33 (0.55H, d, $J = 0.8$ Hz, CH-C3'), 3.73 (0.9H, s, CH_2 -C3), 2.40 (1.35H, s, CH_3 -C1), 2.33 (3H, s, CH_3 -C5 + CH_3 -C5'), 2.07 (1.65, s, CH_3 -C1'), 1.34 (8.1H, s, 2 \times *t*Bu enol form), 1.33 (9.9H, s, 2 \times *t*Bu keto form); ^{13}C NMR (126 MHz; CDCl_3): δ 200.2 (CO-C2), 177.6 (CO-C4'), 167.8 (CO-C4), 145.5 (C-Ar), 145.1 (C-Ar), 142.4 (C-Ar), 142.0 (C-Ar), 135.2 (C-Ar), 134.8 (C-Ar), 127.3 (C-Ar), 127.1 (C-Ar), 90.6 (CH-C3'), 50.9 (CH_2 -C3), 35.4 (CH_3 -C1'), 34.4 (CH_3 -C1), 31.7 (*t*Bu keto form), 31.6 (*t*Bu keto form), 30.9 (3 \times *t*Bu keto form), 21.7 (*t*Bu enol form), 21.7 (CH_3 -C5), 21.3 (CH_3 -C5'); HRMS (ESI+) for $\text{C}_{19}\text{H}_{28}\text{NaO}_3$ $[\text{M}+\text{Na}]^+$ calcd 327.1931 found 327.1934.*

*Values match what has been reported in literature.^{ref}

2,6-Di-*t*-butyl-4-methylphenyl 2-diazoacetate **150**



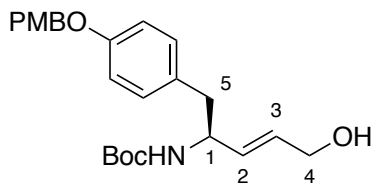
150

To a solution of 2,6-di-*t*-butyl-4-methylphenyl-3-oxobutanoate **148** (3.07 g, 10.1 mmol) in MeCN (13 mL) was added Et₃N (1.8 mL). The solution was cooled to 0 °C and TsN₃ (2.20 g, 11.3 mmol) in MeCN (13 mL) was added dropwise. The reaction mixture was allowed to warm to rt and stirred overnight at rt. The solvents were removed and the residue was dissolved in Et₂O. The solution was washed with 8% aq. KOH solution (3 × 40 mL) and the organic phase was dried over MgSO₄ and concentrated under vacuum. The residue was dissolved in MeCN (15 mL) and 8% aq. KOH (25 mL) was added. The mixture was stirred for 4 h at rt. H₂O (15 mL) was added and the mixture extracted with Et₂O (3 × 20 mL). The combined extracts were dried over MgSO₄ and concentrated under vacuum. The crude product was purified by column chromatography on silica gel (PE/Et₂O 30:1) to afford the title product (1.92 g, 66%) as a bright yellow solid.

R_f(EtOAc/PE 1:1): 0.58; m.p.: 153–154 °C; ν_{max} 2961, 2914, 2110, 1705, 1366, 1335, 1184, 1144, 1107 cm⁻¹; ¹H NMR (500 MHz; CDCl₃): δ 7.11 (2H, s, CH-Arom), 2.32 (3H, s, CH₃-C5), 1.35 (18H, s, 2 × *t*Bu); ¹³C NMR (126 MHz, CDCl₃) δ 142.6 (CO-C4), 134.9 (2 × CH-Arom), 130.9 (C-Arom), 127.2 (CH-C3), 35.4 (C-*t*Bu), 31.7 (2 × *t*Bu), 21.7 (CH₃-C5); HRMS (ESI+) for C₁₉H₂₈NaO₃ [M+Na]⁺ calcd 327.1931, found 327.1934.*

*Values match what has been reported in literature.^{ref}

t*-Butyl-(4*S,E*)-{5-hydroxy-1-[4-(4-methoxybenzyloxy)phenyl]pent-3-en-2-yl}carbamate **151*

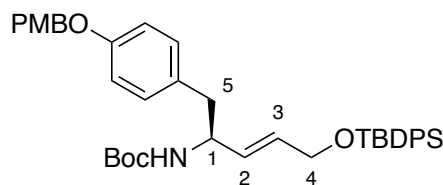


151

(4*S*)-*t*-Butyl-1-[4-(4-methoxybenzyloxy)phenyl]but-3-en-2-yl}carbamate **145** (50.0 mg, 0.13 mmol) previously synthesised following a known procedure, [REF](#) was dissolved in degassed CH₂Cl₂ (2 mL) and butenediol (39 μ L, 0.65 mmol) was added. The solution was degassed and Hoveyda-Grubbs 2nd generation catalyst (3 mg, 3.5 mol%) was added. The reaction mixture was stirred at reflux for 18 h. The solvents were removed and the residue was purified by silica gel column chromatography (PE/EtOAc 9:1 to 1:1) to give the title compound (23 mg, 43%) as a white solid.

R_f(PE/EtOAc 1:1): 0.38; $[\alpha]_D^{18} +13$ ($c = 1.0$, CHCl₃); ν_{\max} 3294, 2971, 2929, 1732, 1693, 1640, 1366, 1173, 1129 cm⁻¹; ¹H NMR (400 MHz, CDCl₃) δ 7.35 (2H, d, $J = 8.6$ Hz, 2 \times CH-Ph-PMB), 7.08 (2H, d, $J = 8.6$ Hz, 2 \times CH-Ph-PMB), 6.90 (4H, dd, $J = 10.2, 8.6$ Hz, 4 \times CH-Ph), 5.75–5.62 (2H, m, CH-C2 + CH-C3), 4.96 (2H, s, CH₂-PMB), 4.48 (1H, bs, NH), 4.38 (1H, bs, CH-C1), 4.11 (2H, d, $J = 3.9$ Hz, CH₂-C4), 3.81 (3H, s, OCH₃-PMB), 2.77 (2H, d, $J = 6.3$ Hz, CH₂-C5), 1.40 (9H, s, CH₃-Boc); ¹³C (101 MHz, CDCl₃): δ 159.6 (CO-Boc), 157.7 (2 \times C-Ph-PMB), 155.3 (2 \times C-Ph), 131.8 (CH-C3), 130.6 (2 \times CH-Ph), 129.8 (CH-C2), 129.4 (2 \times CH-Ph), 114.9 (2 \times CH-Ph), 114.1 (2 \times CH-Ph), 80.0 (C-Boc), 70.0 (CH₂-PMB), 63.2 (CH₂-C4), 55.5 (OCH₃-PMB), 52.9 (CH-C1), 40.9 (CH₂-C5), 28.5 (3 \times CH₃-Boc); HRMS (ESI+) for C₂₄H₃₁NO₅Na [M+Na]⁺ calcd, 436.2094 found 436.2088.

t*-Butyl-(4*S,E*)-{5-(*t*-butyldiphenylsilyloxy)-1-[4-(4-methoxybenzyloxy)phenyl]pent-3-en-2-yl}carbamate **152*

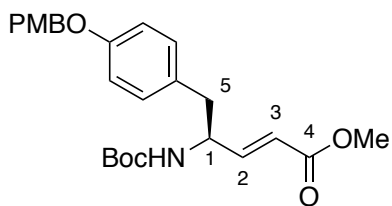


152

TPBDPSCl (15 μ L, 0.06 mmol) was slowly added to a solution of *t*-butyl-(4*S,E*)-{5-hydroxy-1-[4-(4-methoxybenzyloxy)phenyl]pent-3-en-2-yl}carbamate **151** (20 mg, 0.05 mmol) and imidazole (7 mg, 0.09 mmol) in CH_2Cl_2 (0.50 mL). The reaction mixture was stirred for 24 h at rt. H_2O (7 mL) was added and the phases were separated. The organic phase was dried over Na_2SO_4 , filtered and concentrated under vacuum. The resulting oil was purified by silica gel column chromatography (PE/EtOAc 1:1) yielding the title compound (33 mg, quant.) as a clear oil

R_f (PE/EtOAc 1:1): 0.79; ν_{max} 2982, 2864, 1715, 1550, 1436, 1248, 1173, 1129 cm^{-1} ; ^1H NMR (400 MHz, CDCl_3) δ 7.73–7.70 (4H, m, 4 \times CH-Ph-TBDPS), 7.65 (4H, ddd, J = 8.1, 1.6, 1.6 Hz, 4 \times CH-Ph-TBDPS), 7.41–7.36 (2H, m, 2 \times CH-Ph-TBDPS), 7.35 (2H, d, J = 8.7 Hz, 2 \times CH-Ph-PMB), 7.17 (1H, s, NH), 7.07 (2H, d, J = 8.7 Hz, 2 \times CH-Ph PMB), 6.91 (2H, d, J = 8.6 Hz, 2 \times CH-Ph), 6.87 (1H, d, J = 8.6 Hz, 2 \times CH-Ph), 5.69 (1H, dd, J = 15.5, 5.2 Hz, CH-C2), 5.59 (1H, ddd, J = 15.5, 4.8, 3.5 Hz, CH-C3), 4.94 (2H, s, CH_2 -PMB), 4.42–4.36 (1H, m, CH-C1), 4.16 (2H, d, J = 3.5 Hz, CH_2 -C4), 3.81 (3H, s, CH_3 -PMB), 2.80–2.69 (2H, m, CH_2 -C5), 1.42 (9H, s, *t*-Bu-Boc), 1.04 (9H, s, *t*-Bu-TBDPS); ^{13}C NMR (126 MHz, CDCl_3) δ 159.6 (CO-Boc), 157.7 (2 \times C-Ph-PMB), 135.7 (4 \times CH-Ph), 134.9 (4 \times CH-Ph), 130.7 (2 \times CH-Ph), 129.8 (CH-C2 + CH-C3), 129.6 (2 \times C-Ph), 129.4 (2 \times CH-Ph), 127.9 (2 \times C-Ph), 114.8 (2 \times CH-Ph), 114.1 (2 \times CH-Ph), 83.1 (CH-Boc), 70.0 (CH_2 -PMB), 63.9 (CH_2 -C4), 55.5 (OCH_3 -PMB), 41.0 (CH_2 -C5), 34.0 (C-TBDPS), 28.6 (*t*-Bu-Boc), 27.0 (*t*-Bu-TBDPS); HRMS (ESI+) for $\text{C}_{40}\text{H}_{49}\text{NO}_5\text{NaSi}$ $[\text{M}+\text{Na}]^+$ calcd 674.3272, found 674.3252.

Methyl-(4*S,E*)-4-[(*t*-butoxycarbonyl)amino]-5-[4-(4-methoxybenzyloxy)phenyl]pent-2-enoate **155**

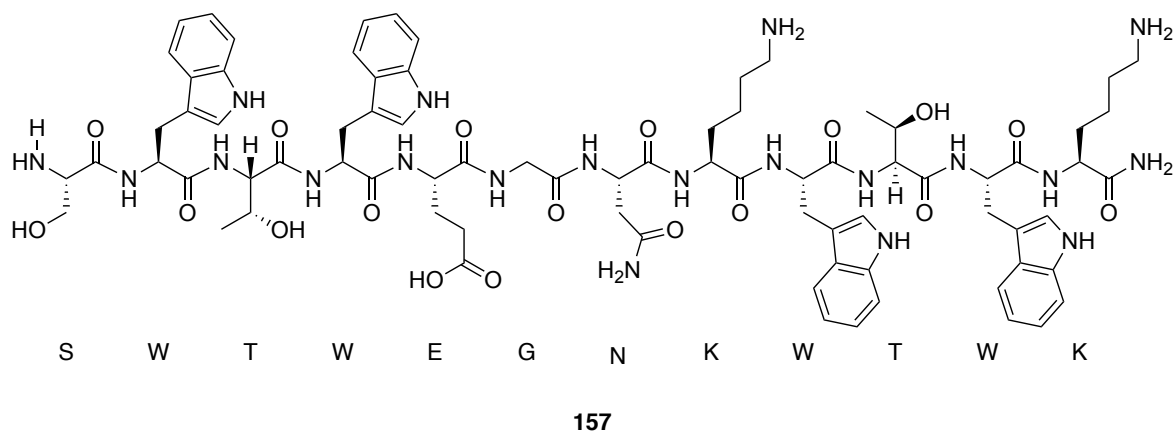


151

A solution of *t*-butyl {1-[4-(4-methoxybenzyloxy)phenyl]but-3-en-2-yl} carbamate **145** (50 mg, 0.13 mmol) in CH₂Cl₂ (300 μ L) and a solution of methyl acrylate (20 μ L, 0.23 mmol) in CH₂Cl₂ (300 μ L) were added simultaneously to a suspension of degassed Grubbs II catalyst (3.3 mg, 3 mol%) in CH₂Cl₂ (700 μ L). The reaction mixture was degassed again and stirred for 48 h at reflux. Solvents were removed and the residue was purified by silica gel column chromatography (PE/EtOAc 9:1 to 1:4) to give the title compound (23 mg, 40%) as a clear oil.

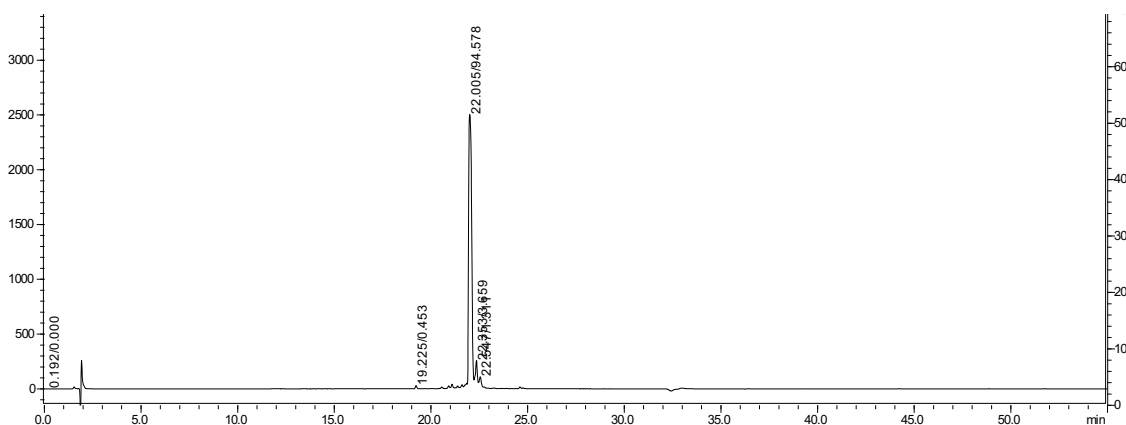
R_f (PE/EtOAc 1:1): 0.48; $[\alpha]_D^{18} +6.2$ ($c = 0.75$, CHCl₃), ν_{\max} 3354, 2974, 2928, 1714, 1514, 1368, 1244, 1172, 1022 cm⁻¹; ¹H NMR (500 MHz, CDCl₃) 7.35 (2H, d, $J = 8.7$ Hz, 2 \times CH-Arom PMB), 7.07 (2H, d, $J = 8.6$ Hz, 2 \times CH-Arom), 6.92 (2H, d, $J = 6.8$ Hz, 2 \times CH-Arom-PMB), 6.90 (2H, d, $J = 7.1$ Hz, 2 \times CH-Arom), 5.85 (1H, dd, $J = 15.7, 1.7$ Hz, CH-C2), 4.96 (2H, s, CH₂-PMB), 4.56 (1H, bs, CH-C1), 4.49 (1H, bs, CH-C3), 3.82 (3H, s, CH₃-PMB), 3.73 (3H, s, CO₂CH₃), 2.83 (2H, d, $J = 6.6$ Hz, CH₂-C5), 1.40 (9H, s, *t*-Bu); ¹³C NMR (126 MHz, CDCl₃) δ 166.8 (CO-Ac), 159.6 (2 \times C-Arom-PMB), 158.0 (CO-Boc), 155.1 (2 \times CH-Arom), 130.6 (2 \times CH-Arom), 129.4 (2 \times CH-Arom-PMB), 129.2 (2 \times C-Arom), 120.8 (CH-C1), 115.1 (2 \times CH-Arom), 114.2 (2 \times CH-Arom-PMB), 83.1 (C-Boc), 67.0 (CH₂-PMB), 55.5 (CH₃-PMB), 51.8 (CO₂CH₃), 39.5 (CH₂-C5), 28.5 (*t*-Bu); HRMS (ESI+) for C₂₅H₃₁NO₆Na [M+Na]⁺ calcd 464.2044, found 464.2041.

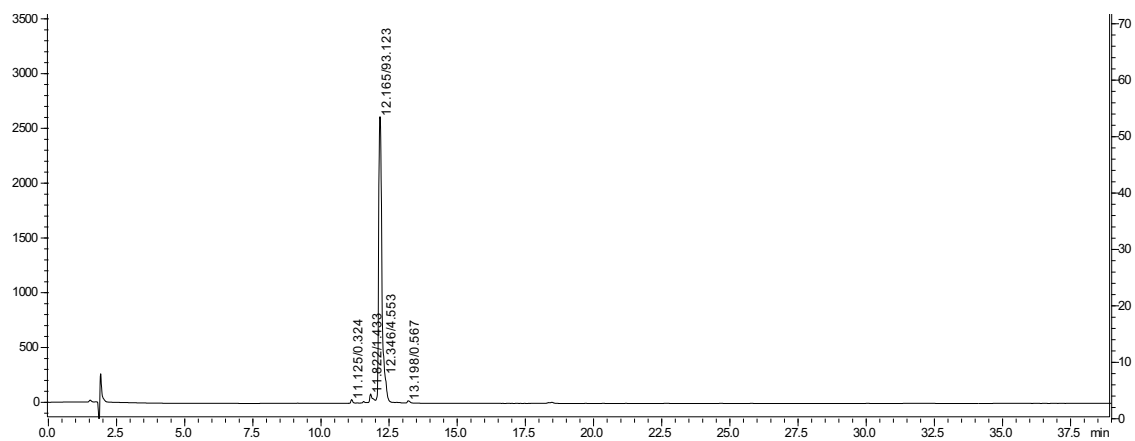
TrpZip 157



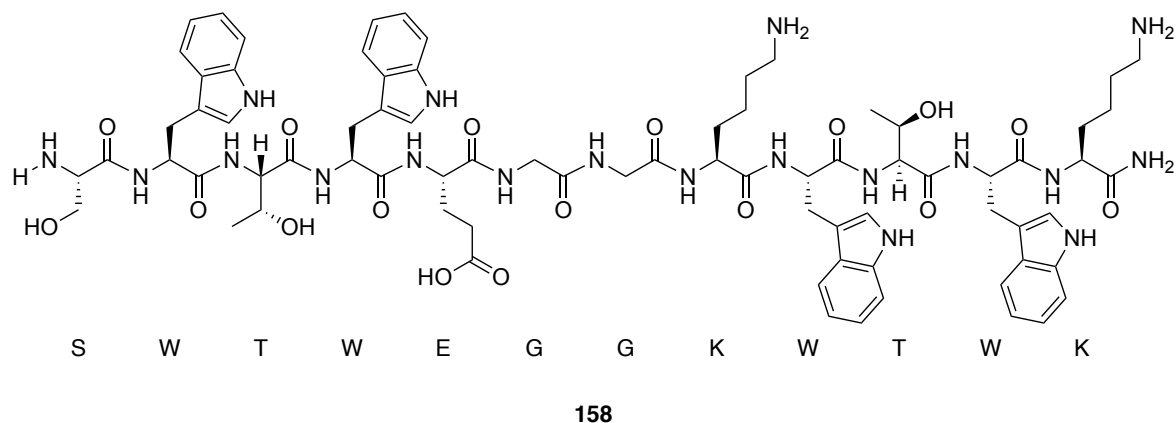
Following the general procedure for SPPS using TentaGel S RAM resin (0.24 mmol/g loading). The crude peptide was purified using semi-preparative HPLC system with a flow rate of 8 mL/min. A linear gradient of buffer A (H₂O and 0.1% TFA) to buffer B (MeCN and 0.1% TFA) was used over 55 min from 20 to 70%. UV detection wavelengths were 214 and 280 nm. TrpZip **157** (15 mg, 9%) was obtained as a colourless solid.

HRMS (ESI⁺) for C₇₈H₁₀₄N₂₀O₁₈ [M+2H]²⁺ calcd 804.3913, found 804.3943. HPLC: purity 94.58% (50 min gradient), 93.12% (20 min gradient).



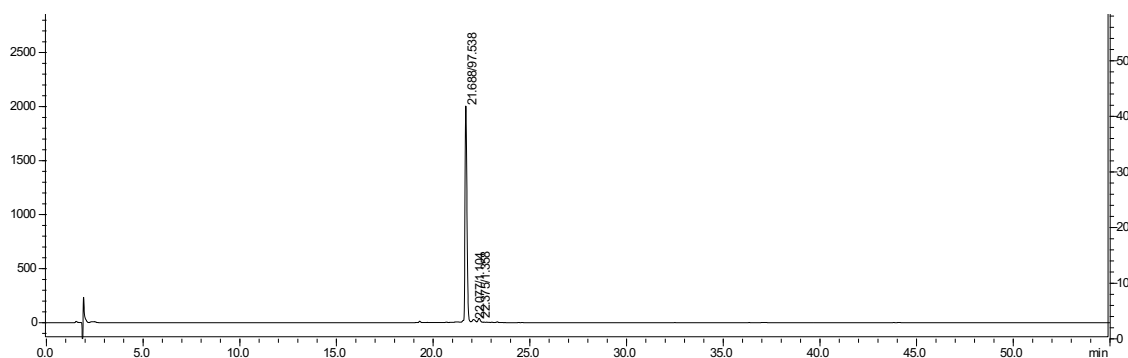


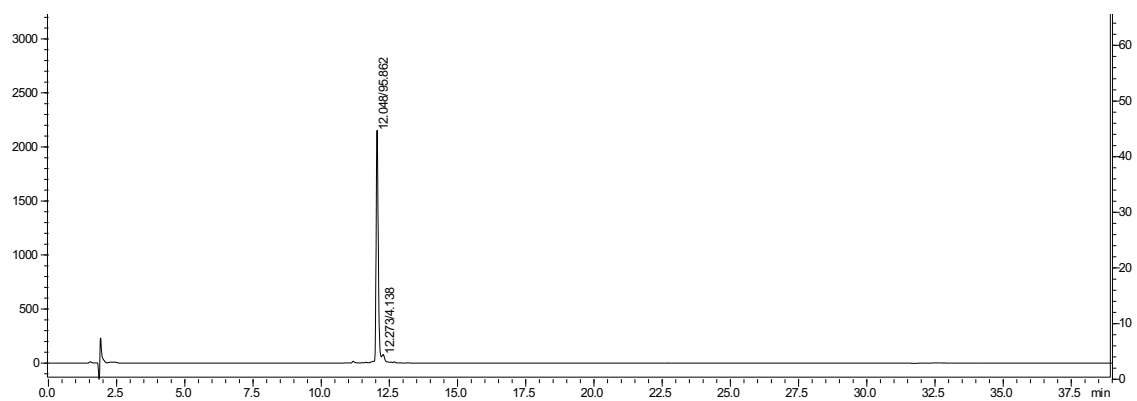
GG TrpZip 158



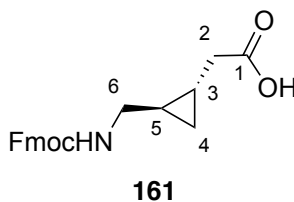
Following the general procedure for SPPS using TentaGel S RAM resin (0.24 mmol/g loading). The crude peptide was purified using semi-preparative HPLC system with a flow rate of 8 mL/min. A linear gradient of buffer A (H₂O and 0.1% TFA) to buffer B (MeCN and 0.1% TFA) was used over 55 mins from 20-70%. UV detection wavelengths were 214 and 280 nm. GG TrpZip **158** (28 mg, 18%) was obtained as a white solid. Peptide content was determined by measuring the absorbance at 280 nm.

HRMS (ESI⁺) for C₇₆H₁₀₁N₁₉O₁₇ [M+2H]²⁺ calcd 775.8806, found 775.8832. HPLC: purity 97.54% (50 min gradient), 95.86% (20 min gradient).





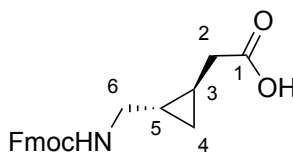
(*R,S*)-Fmoc-{GlyΔGly}-OH 161



(*R,S*)-(Boc)₂-{GlyΔGly}-OH **107** (248 mg, 0.75 mmol) was dissolved in CH₂Cl₂ (8 mL) and TFA (0.6 mL) was added. The solution was stirred for 3 h at rt and the solvent was removed. The resulting TFA salt was dissolved in a dioxane/H₂O mixture (3:1, 13 mL) and K₂CO₃ (310 mg, 2.25 mmol) was added. The solution was stirred for 30 min at rt and FmocOSu (304 mg, 0.900 mmol) was added. The reaction mixture was stirred overnight at rt. The mixture was diluted in 2 M aq. K₂CO₃ (5 mL) and extracted with EtOAc (3 × 5 mL). The aq. phase was then acidified carefully to pH 1 using 1 M aq. HCl and then extracted with EtOAc (3 × 5 mL). The combined extracts were dried over MgSO₄, filtered and concentrated under vacuum. The residue was purified by silica gel on column chromatography (PE/EtOAc 1:1) to give the title compound (40 mg, 15%) as a yellow oil.

R_f (Et₂O/PE 1:1): 0.27; $[\alpha]_D^{22} +25$ (*c* = 0.50, CHCl₃); ν_{\max} 3335, 3067, 2932, 1703, 1520, 1450, 1242, 1034 cm⁻¹; ¹H NMR (400 MHz; CDCl₃): δ 7.75 (2H, d, *J* = 7.5 Hz, 2 × CH-Arom-Fmoc), 7.61 (2H, d, *J* = 7.5 Hz, 2 × CH-Arom-Fmoc), 7.39 (2H, t, *J* = 7.5 Hz, 2 × CH-Arom-Fmoc), 7.30 (2H, t, *J* = 7.5 Hz, 2 × CH-Arom-Fmoc), 5.39 (1H, bs, NH), 4.35 (2H, d, *J* = 6.9 Hz, CH₂-Fmoc), 4.22 (1H, t, *J* = 6.9 Hz, CH-Fmoc), 3.42 (1H, ddd, *J* = 12.5, 6.1, 6.1 Hz, CH₂-C6), 2.78 (1H, ddd, *J* = 12.5, 8.4, 4.2 Hz, CH₂-C6), 2.60 (1H, dd, *J* = 17.3, 5.5 Hz, CH₂-C2), 2.04 (1H, dd, *J* = 17.3, 8.8 Hz, CH₂-C2), 0.92–0.77 (2H, m, CH-C3 + CH-C5), 0.53 (1H, ddd, *J* = 9.5, 5.3, 5.3 Hz, CH₂-C4), 0.45 (1H, ddd, *J* = 9.5, 5.4, 5.4 Hz, CH₂-C4); ¹³C NMR (126 MHz; CDCl₃): δ 178.6 (CO-C1), 156.6 (CO-Fmoc), 144.2 (2 × C-Arom-Fmoc), 141.4 (2 × C-Arom-Fmoc), 127.8 (2 × CH-Arom-Fmoc), 127.2 (2 × CH-Arom-Fmoc), 125.3 (2 × CH-Arom-Fmoc), 120.1 (2 × CH-Arom-Fmoc), 66.9 (CH-Fmoc), 47.4 (CH₂-Fmoc), 45.3 (CH₂-C6), 37.8 (CH₂-C2), 18.4 (CH-C5), 12.9 (CH-C3), 10.3 (CH₂-C4); HRMS (ESI⁺) for C₂₁H₂₁NNaO₄ [*M*+Na]⁺ calcd 374.1363, found 374.1356.

(*S,R*)-Fmoc-{GlyΔGly}-OH 162

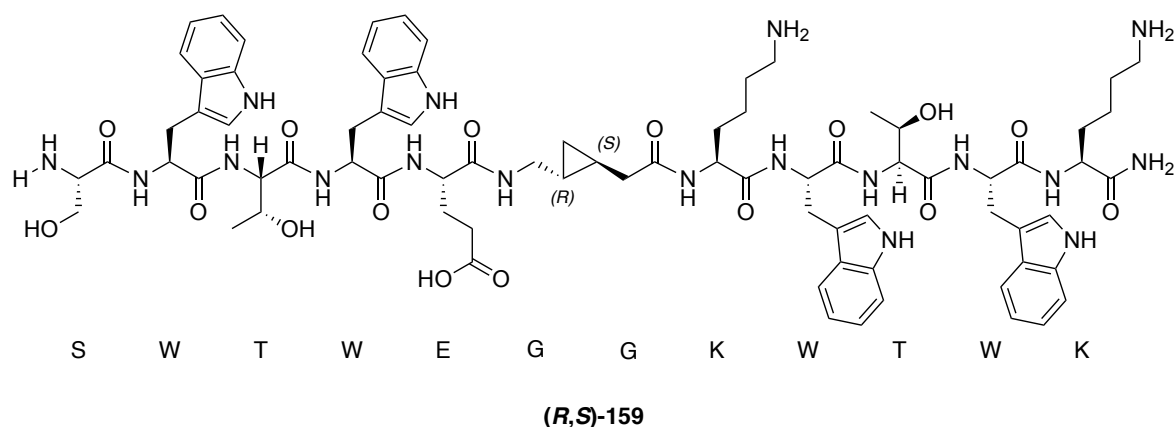


162

(*S,R*)-(Boc)₂-{GlyΔGly}-OH **107** (203 mg, 0.61 mmol) was dissolved in CH₂Cl₂ (6 mL) and TFA (0.50 mL, 6.1 mmol) was added. The solution was stirred for 3 h at rt and solvent were removed. The resulting TFA salt was dissolved in a dioxane/H₂O mixture (3:1, 12 mL) and K₂CO₃ (253 mg, 1.83 mmol) was added. The solution was stirred for 30 min at rt and FmocOSu (250 mg, 0.730 mmol) was added. The reaction mixture was stirred overnight at rt. The mixture was diluted in 2 M aq. K₂CO₃ (5 mL) and extracted with EtOAc (3 × 5 mL). The aq. phase was then acidified carefully using 1 M aq. HCl to pH 1 and extracted with EtOAc (3 × 5 mL). The combined extracts were dried over MgSO₄, filtered and concentrated under vacuum. The residue was purified by silica gel on column chromatography (PE/EtOAc 1:1) to give the title compound as a yellow oil (70 mg, 27%).

R_f (Et₂O/PE 1:1): 0.27; [α]_D¹⁹ -18 (*c* = 0.50, CHCl₃); ν_{max} 3325, 3065, 2926, 1707, 1522, 1451, 1246, 1033 cm⁻¹; ¹H NMR (400 MHz; CDCl₃): δ 7.76 (2H, d, *J* = 7.4 Hz, 2 × CH-Arom-Fmoc), 7.62 (2H, d, *J* = 7.4 Hz, 2 × CH-Arom-Fmoc), 7.39 (2H, t, *J* = 7.4 Hz, 2 × CH-Arom-Fmoc), 7.31 (2H, dddd, *J* = 7.4, 7.4, 1.1, 1.1 Hz, 2 × CH-Arom-Fmoc), 5.38 (1H, bs, NH), 4.37 (2H, d, *J* = 7.2 Hz, CH₂-Fmoc), 4.23 (1H, t, *J* = 7.2 Hz, CH-Fmoc), 3.44 (1H, ddd, *J* = 12.4, 5.5, 5.5 Hz, CH₂-C6), 2.77 (1H, ddd, *J* = 12.4, 8.2, 4.5 Hz, 1H × CH₂-C6), 2.62 (1H, dd, *J* = 17.6, 5.1 Hz, CH₂-C2), 2.11–1.97 (1H, m, CH₂-C2), 0.90–0.77 (2H, m, CH-C3 + CH-C5), 0.55 (1H, ddd, *J* = 8.2, 5.2, 5.2 Hz, CH₂-C4), 0.46 (1H, ddd, *J* = 8.2, 4.0, 4.0 Hz, CH₂-C4); ¹³C NMR (126 MHz; CDCl₃): δ 177.0 (CO-C1), 156.6 (CO-Fmoc), 144.2 (2 × C-Arom-Fmoc), 141.5 (2 × C-Arom-Fmoc), 127.8 (2 × CH-Arom-Fmoc), 127.2 (2 × CH-Arom-Fmoc), 125.3 (2 × CH-Arom-Fmoc), 120.1 (2 × CH-Arom-Fmoc), 66.9 (CH-Fmoc), 47.4 (CH₂-Fmoc), 45.3 (CH₂-C6), 37.5 (CH₂-C2), 18.5 (CH-C5), 13.0 (CH-C3), 10.4 (CH₂-C4); HRMS (ESI+) for C₂₁H₂₁NNaO₄ [M+Na]⁺ calcd, 374.1363 found 374.1353.

(*R,S*)-{GlyΔGly}-TrpZip 159



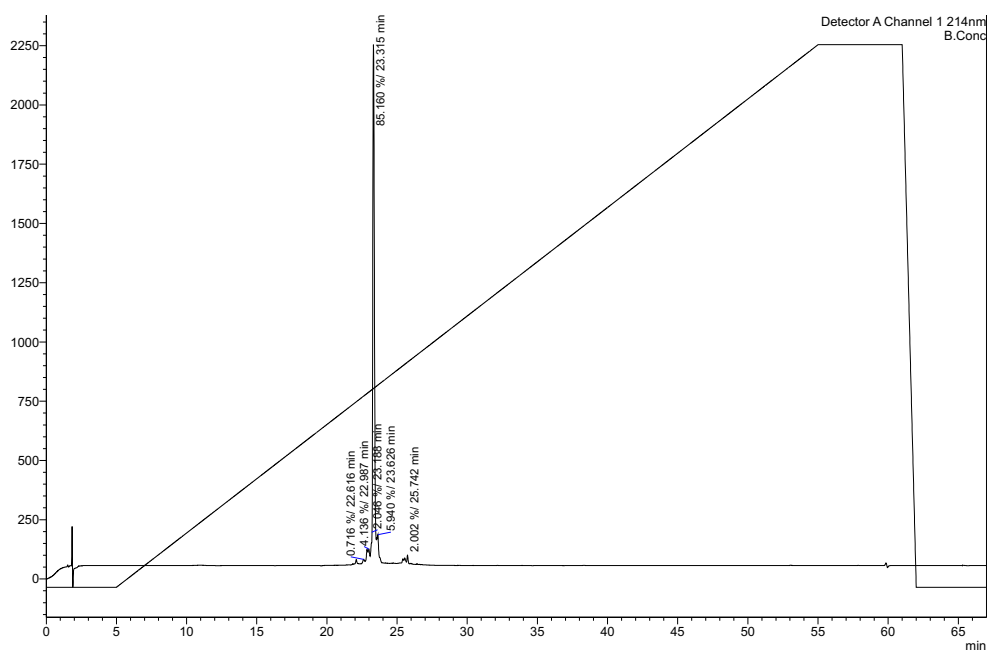
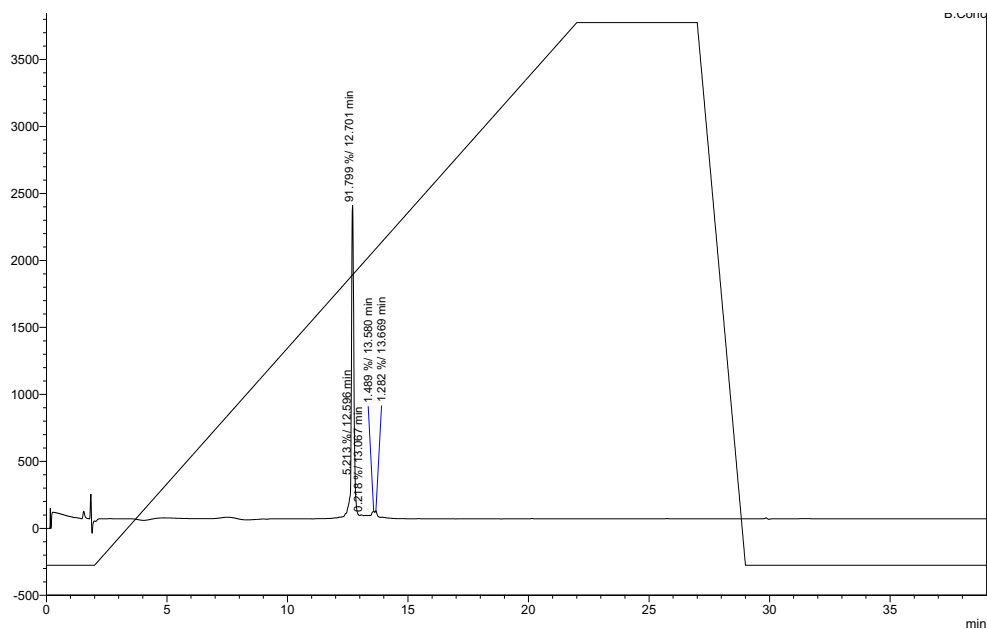
Following the general procedure for SPPS using TentaGel S RAM resin (0.24 mmol/g loading), H-K₁-W₃-T₂-W₄-K₂-resin sequence was synthesised. This was not cleaved from the resin for the next coupling.

(1*S*,2*R*)-Fmoc-{GlyΔGly}-OH (39.0 mg, 0.11 mmol, 1.1 equiv.) and HATU (76.0 mg, 0.20 mmol) were dissolved in 5 mL of DMF. DIPEA (70 μL, 0.40 mmol) was then added. The solution was stirred for 5 min for preactivation and then it was added to the resin and spun overnight. The reaction was monitored by LCMS ([*M*+Na] 556.92 g/mol). Unreacted peptide was capped using 0.4 mL of acetic acid in 0.6 mL of pyridine and spun for 40 min. the resin was then washed with DMF (4 × 10 mL) through a sintered frit.

The coupling of the rest of the sequence (Fmoc-S-W₁-T₁-W₂-E-OH) to the resin was carried out following the procedure for SPPS on a 0.050 mmol scale.

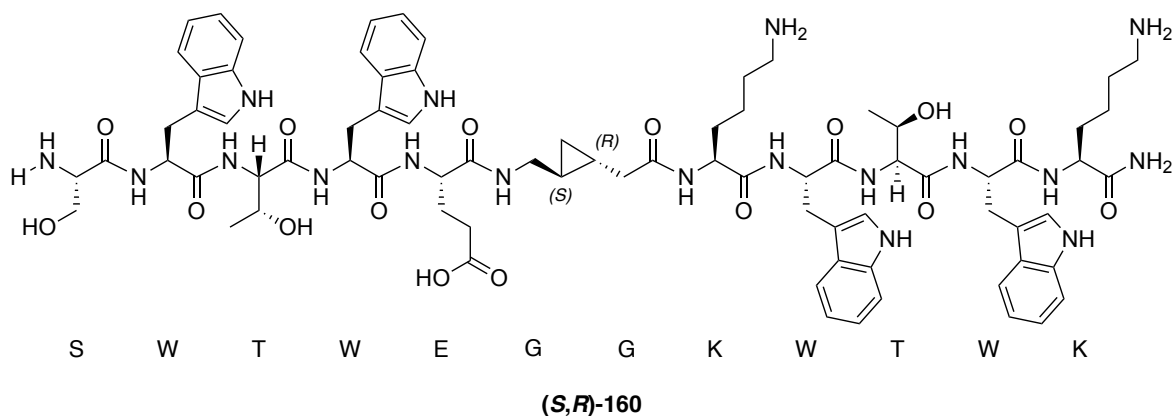
The crude peptide was purified using semi-preparative HPLC system with a flow rate of 8 mL/min. A linear gradient of buffer A (H₂O and 0.1% TFA) to buffer B (MeCN and 0.1% TFA) was used over 50 min from 20 to 70%. UV detection wavelengths were 214 and 280 nm. (1*S*,2*R*)-{GlyΔGly}-TrpZip (15 mg, 19%) was obtained as a colourless solid. Peptide content was determined by measuring the absorbance at 280 nm.

HRMS (ESI+) for $C_{78}H_{104}N_{18}O_{16}$ $[M+2H]^{2+}$ calcd 774.3948, found 774.3944. HPLC: purity 91.80% (20 min gradient), 85.16% (50 min gradient).



C:\LabSolutions\Data\Drew\Albane\AN-VI-38-3-44_

(*S,R*)-{GlyΔGly}-TrpZip 160



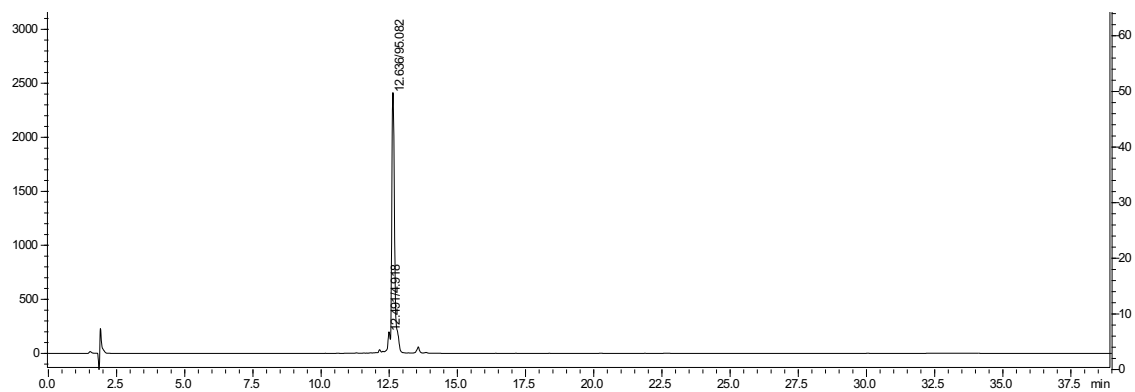
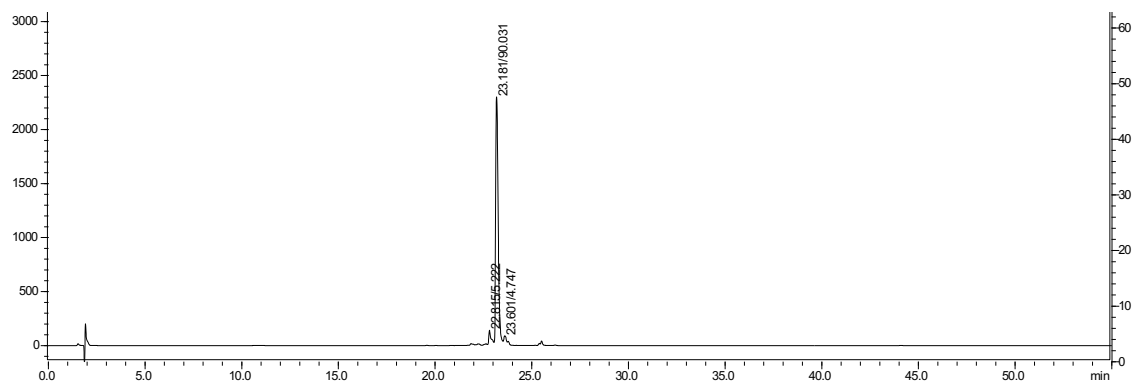
Following the general procedure for SPPS using TentaGel S RAM resin (0.24 mmol/g loading), H-K₁-W₃-T₂-W₄-K₂-resin sequence was synthesised. This was not cleaved from the resin for the next coupling.

(*S,R*)-Fmoc-{GlyΔGly}-OH (70 mg, 0.20 mmol, 2 equiv.) and HATU (76 mg, 0.20 mmol) were dissolved in 5 mL of DMF. DIPEA (70 μL, 0.40 mmol) was then added. The solution was stirred for 5 min for preactivation and then it was added to the resin and spun overnight. The reaction was monitored by LCMS ([M+Na] 556.92 g/mol). Unreacted peptide was capped using 0.4 mL of acetic acid in 0.6 mL of pyridine and spun for 40 min. The resin was then washed with DMF (4 × 10 mL) through a sintered frit.

The coupling of the rest of the sequence (Fmoc-S-W₁-T₁-W₂-E-OH) to the resin was carried out following the procedure for SPPS on a 0.050 mmol scale.

The crude peptide was purified using semi-preparative HPLC system with a flow rate of 8 mL/min. A linear gradient of buffer A (H₂O and 0.1% TFA) to buffer B (MeCN and 0.1% TFA) was used over 50 min from 20 to 70%. UV detection wavelengths were 214 and 280 nm. (*S,R*)-{GlyΔGly}-TrpZip **155** (15 mg, 19%) was obtained as a colourless solid. Peptide content was determined by measuring the absorbance at 280 nm.

HRMS (ESI⁺) for C₂₈H₃₈N₅O₇ [M+H]⁺ calcd 556.2766, found 556.2752. HPLC: purity 90.03% (50 min gradient), 95.08% (20 min gradient).



LIST OF REFERENCES

- ¹ T. C. Gasser, R. W. Ogden, G. A. Holzapfel, *J. R. Soc. Interface*, **2006**, 3, 15–35.
- ² U. B Hendgen-Cotta, M. Kelm, T. Rassaf, *Nitric Oxide*, **2010**, 22, 75–82.
- ³ J. J. Collins, X. Hou, E. V. Romanova, B. G. Lambrus, C. M. Miller, A. Saberi, J. V. Sweedler, P. A. Newmark, *PLOS Biology*, **2010**, 8, 1–21.
- ⁴ S. M. Heissler, J. Selvadurai, L. M. Bond, R. Fedorov, J. Kendrick-Jones, F. Buss, D. J. Manstein, *FEBS letters*, **2012**, 586, 3208–3214.
- ⁵ M. Yoshimoto, H. Sakamoto, H. Shirakami, *Colloids Surf., B*, **2009**, 69, 281–287.
- ⁶ G. A. Chasse, A. M. Rodriguez, M. L. Mak, E. Deret, A. Perczel, C. P. Sosa, R. D. Enriz, I. G. Csizmadia, *J. Mol. Struct.*, **2001**, 537, 319–361.
- ⁷ I. Wagner, H. Musso, *Angew. Chem.*, **1983**, 22, 816–828.
- ⁸ R. D. Semba, M. Shardell, F. A. Sakr Ashour, R. Moaddel, I. Trehan, K. M. Maleta, M. I. Ordiz, K. Kraemer, M. A. Khadeer, L. Ferrucci, M. J. Manary, *EBiomedicine*, **2016**, 6, 246–252.
- ⁹ D. M. Driscoll, P. R. Copeland, *Annu. Rev. Nutrition*, **2003**, 23, 17–40.
- ¹⁰ J. A. Krzycki, *Curr. Opin. Microbiol.*, **2005**, 8, 706–712.
- ¹¹ E. D. Zanders, *Methods in Molecular Biology, Chemical Genomics*, **2005**, Vol. 310.
- ¹² D. A. Evans, T. C. Britton, R. L. Dorow, J. F. Dellaria, *J. Am. Chem. Soc.*, **1986**, 108, 6395–6397.
- ¹³ H. B. Vickery, C. L. A. Schmidt, *Chemical Review*, **1931**, 169–318.
- ¹⁴ C. A. Lipinski, F. Lombardo, B. W. Dominy, P. J. Freeney, *Adv. Drug Delivery Rev.*, **2001**, 46, 3–26.
- ¹⁵ T. Kenakin, *Pharmacology in Drug Discovery and Development*, 2nd Edition, **2017**, Chap. 11, 275–299.
- ¹⁶ M. Yusuf, A. Hardianto, M. Muchtaridi, R. F. Nuwarda, T. Sobruto, *Encyclopedia of Bioinformatics and Computational Biology*, **2019**, Vol. 2, 688–699.
- ¹⁷ T. J. Sereda, C. T. Mant, A. M. Quinn, R. S. Hodges, *J. Chromatogr. A*, **1993**, 646, 17–30.
- ¹⁸ J. C. Bulinski, International Review of Cytology, *Peptide antibodies: new tools for cell biology*, **1986**, Vol. 103, 281–302.
- ¹⁹ R. M. J. Liskamp, D. Rijkers, J. Kruijtz, J. Kemmink, *Chem. Bio. Chem.*, **2011**, 12, 1626–1653.
- ²⁰ G. N. Ramachandran, V. Sasisekharan, *Adv. Prot. Chem.*, **1968**, 23, 282–427.
- ²¹ M. S. Weiss, A. Jabs, R. Hilgenfeld, *Nature Struc. Biol.*, **1998**, 5, 676.
- ²² G. J. Kleywegt, T. A. Jones, *Structure*, **1996**, 12, 1395–1400.
- ²³ A. Jabs, M. S. Weiss, R. Hilgenfeld, *J. Mol. Biol.*, **1999**, 286, 291–304.
- ²⁴ E. Erez, D. Fass, E. Bibi, *Nature*, **2009**, 459, 371–378.
- ²⁵ J. Westermarck, J. Ivaska, G. L. Corthals, *Mol. Cell. Proteomic*, **2013**, 12, 1752–1763.
- ²⁶ D. Ramu, R. Jain, R. R. Kumar, V. Sharma, S. Garg, R. Ayana, T. Lythra, P. Yadav, S. Sen, S. Singh, *Arch. Pharm.*, **2019**, 352, 1–15.
- ²⁷ A. Boeijsen, J. van Ameijde, R. M. J. Liskamp, *J. Org. Chem.*, **2001**, 66, 8454–8462.
- ²⁸ V. D. Bock, D. Speijer, H. Hiemstra, J. H. van Maarseveen, *Org. Biomol. Chem.*, **2007**, 5, 971–975.
- ²⁹ A. Choudhary, R. T. Raines, *Chem. Bio. Chem.*, **2011**, 12, 1801–1807.
- ³⁰ T. Takekiyo, L. Wu, Y. Yoshimura, A. Shimizu, T. A. Keiderling, *Biochemistry*, **2009**, 48, 1543–1552.
- ³¹ A. Tkatchenko, M. Scheffler, *Phys. Rev. Lett.*, **2009**, 102, 1–4.
- ³² P. D. Ross, S. Subramanian, *Biochem.*, **1981**, 20, 3096–3102.
- ³³ L. Pauling, R. B. Corey, H. R. Branson, *Proc. Natl. Acad. Sci. USA*, **1951**, 37, 205–211.
- ³⁴ C. N. Pace, J. M. Scholtz, *Biophys. J.*, **1998**, 75, 422–427.
- ³⁵ A. J. Wilson, *Prog. Biophys. Mol. Biol.*, **2015**, 119, 33–40.
- ³⁶ U. Heinemann, W. Saenger, *Nature*, **1982**, 299, 27–31.
- ³⁷ M.-A. Meyers, P.-Y. Chen, A. Y.-M. Lin, Y. Seki, *Prog. Mater. Sci.*, **2008**, 53, 1–206.
- ³⁸ K.-C. Chou, H. A. Scheraga, *Proc. Natl. Acad. Sci. USA*, **1982**, 79, 7047–7051.
- ³⁹ F. U. Hartl, *Nature*, **1996**, 381, 571–580.
- ⁴⁰ W. T. Godbey, An introduction to Biotechnology, *Chapter II: Proteins*, **2014**, 9–33.
- ⁴¹ J. D. Tyndall, B. Pfeiffer, G. Abbenante, D. P. Fairlie, *Chem. Rev.*, **2005**, 105, 793–826.
- ⁴² J. S. Hutchinson, J. M. Thornton, *J. M. Protein Sci.*, **1994**, 3, 2207–2216.
- ⁴³ A.-M. C. Morcelino, L. M. Gierasch, *Biopolymers.*, **2008**, 89, 380–391.
- ⁴⁴ K. S. Rotondi, L. M. Gierasch, *Biopolymers*, **2006**, 84, 13–22.
- ⁴⁵ L. R. Whitby, Y. Ando, V. Setola, P. K. Vogt, B. L. Roth, D. L. Boger, *J. Am. Chem. Soc.*, **2011**, 133, 10184–10194.
- ⁴⁶ A. Giannis, T. Kolter, *Angew. Chem. Int. Ed. Engl.*, **1993**, 32, 1244–1267.
- ⁴⁷ H. J. Dyson, P. E. Wright, *Curr. Opin. Struct. Biol.*, **1993**, 3, 60–65.
- ⁴⁸ E. Vass, M. Hollósi, F. Besson, R. Buchet, *Chem. Rev.*, **2003**, 103, 1917–1954.
- ⁴⁹ A. Elliot, E. J. Ambrose, *Nature*, **1950**, 165, 921–922.
- ⁵⁰ P. L. Haris, D. Chapman, *Trends Biochem. Sci.*, **1992**, 17, 328–333.

- ⁵¹ J. L. R. Arrondo, A. Muga, J. Castresana, F. M. Goñi, *Prog. Biophys. Molec. Biol.*, **1993**, *59*, 23–56.
- ⁵² W. K. Surewicz, H. H. Mantsch, *Biochim. Biophys. Acta*, **1988**, *952*, 115–130.
- ⁵³ D. M. Byler, H. Susi, *Biopol.*, **1986**, *25*, 469–487.
- ⁵⁴ S. H. Gellman, G. P. Dado, G.-B. Liang, B. R. Adams, *J. Am. Chem. Soc.*, **1991**, *113*, 1164–1173.
- ⁵⁵ S. Brahms, J. Brahms, *J. Mol. Biol.*, **1980**, *138*, 149–178.
- ⁵⁶ Redrawn from S. Brahms, J. Brahms, *J. Mol. Biol.*, **1980**, *138*, 149–178 with permission from Elsevier.
- ⁵⁷ N. Sreerama, R. W. Woody, *Anal. Biochem.*, **2000**, *287*, 252–260.
- ⁵⁸ M. Kawai, G. Fasman, *J. Am. Chem. Soc.*, **1978**, *100*, 3630–3632.
- ⁵⁹ C. A. Busch, S. K. Sarkar, K. D. Kopple, *Biochem.*, **1978**, *17*, 4951–4954.
- ⁶⁰ P. Xie, Q. Zhou, M. Diem, *J. Am. Chem. Soc.*, **1995**, *117*, 9502–9508.
- ⁶¹ A. Perczel, M. Hollósi, B. M. Foxman, G. D. Fasman, *J. Am. Chem. Soc.*, **1991**, *113*, 9772–9784.
- ⁶² A. Mitra, P. J. Seaton, R. Ali Assarpour, T. Williamson, *Tetrahedron*, **1998**, *54*, 15489–15498.
- ⁶³ R. R. Gardner, G.-B. Liang, S. H. Gellman, *J. Am. Chem. Soc.*, **1995**, *117*, 3280–3281.
- ⁶⁴ S. H. Gellman, G. P. Dado, G.-B. Liang, B. R. Adams, *J. Am. Chem. Soc.*, **1991**, *113*, 1164–1173.
- ⁶⁵ S. W. Englander, T. R. Sosnick, J. J. Englander, L. Mayne, *Curr. Opin. Struct. Biol.*, **1996**, *6*, 18–23.
- ⁶⁶ M. Qabar, J. Urban, C. Sia, M. Klein, M. Kahn, *Lett. Pept. Sci.*, **1996**, *3*, 25–30.
- ⁶⁷ R. A. Wiley, D. H. Rich, *Med. Res. Rev.*, **1993**, *13*, 327–384.
- ⁶⁸ K. Burgess, *Acc. Chem. Res.*, **2001**, *34*, 826–835.
- ⁶⁹ J. Eichler, *Curr. Opin. Chem. Biol.*, **2008**, *12*, 707–713.
- ⁷⁰ T. Klabunde, G. Hessler, *Chem. Bio. Chem.*, **2002**, *3*, 928–944.
- ⁷¹ E. Ko, J. Liu, L. M. Perez, G. Lu, A. Schaefer, K. Burgess, *J. Am. Chem. Soc.*, **2011**, *133*, 462–477.
- ⁷² S. Hanessian, L. Auzzas, *Acc. Chem. Res.*, **2008**, *41*, 1241–1251.
- ⁷³ R. De Wachter, L. brans, S. Ballet, I. Van Den Eynde, D. Feytens, A. Keresztes, G. Toth, Z. Urbanczyk-Lipkowska, D. Tourwé, *Tetrahedron*, **2009**, *65*, 2266–2278.
- ⁷⁴ C. Chothia, A. M. Lesk, A. Tramontano, M. Levitt, S. J. Smith-Gill, G. Air, S. Sheriff, E. A. Padlan, E. A. Davies D., W. R. Tulip, P. M. Colman, S. Spinelli, P. M. Alzari, R. J. Poljak, *Nature*, **1989**, *342*, 877–883.
- ⁷⁵ M. Favre, K. Moehle, L. Jiang, B. Pfeiffer, J. A. Robinson, *J. Am. Chem. Soc.*, **1999**, *121*, 2679–2685.
- ⁷⁶ R. R. Gardner, G.-B. Liang, S. H. Gellman, *J. Am. Chem. Soc.*, **1999**, *121*, 1806–1816.
- ⁷⁷ Adapted with permission from R. R. Gardner, G.-B. Liang, S. H. Gellman, *J. Am. Chem. Soc.*, **1999**, *121*, 1806–1816, copyright 1999 American Chemical Society
- ⁷⁸ J. C. Froehlich, *Alcohol Health and research World*, **1997**, *21*, 132–135.
- ⁷⁹ A. D. Corbett, G. Henderson, A. T. McKnight, S. J. Paterson, *Br. J. Pharmacol.*, **2006**, *147*, S153–S162.
- ⁸⁰ L. R. Whitby, Y. Ando, V. Setola, P. K. Vogt, B. L. Roth, D. L. Boger, *J. Am. Chem. Soc.*, **2011**, *133*, 10184–10194.
- ⁸¹ J. Hughes, T. W. Smith, H. W. Kosterlitz, L. A. Fothergill, B. A. Morgan, H. R. Morris, *Nature*, **1975**, *258*, 577–579.
- ⁸² G. D. Smith, J. F. Griffin, *Science*, **1978**, *199*, 1214–1216.
- ⁸³ A. Aubry, C. Sakarellos, *Biopol.*, **1989**, *28*, 27–40.
- ⁸⁴ A. Proteau-Gagné, V. Bournival, K. Rochon, Y. Dory, L. Gendron, *ACS Chem. Neurosci.*, **2010**, *1*, 757–769.
- ⁸⁵ A. Proteau-Gagné, K. Rochon, M. Roy P.-J. Albert, B. Guérin, L. Gendron, Y. L. Dory, *Bioorg. Med. Chem. Lett.*, **2013**, *23*, 5267–5269.
- ⁸⁶ M. Eguchi, R. Y. W. Shen, J. P. Shea, M. S. Lee, M. Kahn, *J. Med. Chem.*, **2002**, *45*, 1395–1398.
- ⁸⁷ W. A. Noyes, D. B. Forman, *J. Am. Chem. Soc.*, **1933**, *116*, 3493–3494.
- ⁸⁸ A. A. Virgilio, J. A. Ellman, *J. Am. Chem. Soc.*, **1991**, *116*, 11580–11581.
- ⁸⁹ F. Mohamadi, N. G. J. Richards, W. C. Guida, R. Liskamp, C. Caufield, T. Hendrickson, W. C. Still, *J. Comput. Chem.*, **1991**, *11*, 440–467.
- ⁹⁰ B. E. Fink, P. R. Kym, J. A. Katzenellenbogen, *J. Am. Chem. Soc.*, **1998**, *120*, 4334–4344.
- ⁹¹ A. Mizuno, S. Miura, M. Watanabe, Y. Ito, S. Yamada, T. Odagami, Y. Kogami, M. Arisawa, S. Shuto, *Org. Lett.*, **2013**, *15*, 1686–1689.
- ⁹² A. Reichelt, F. Martin, *Acc. Chem. Res.*, **2006**, *39*, 433–442.
- ⁹³ A. D. Walsh, *Transactions of the Faraday Society*, **1949**, *45*, 179–190.
- ⁹⁴ W. A. Donaldson, *Tetrahedron*, **2001**, *57*, 8589–8627.
- ⁹⁵ J. E. Baldwin, R. M. Adlington, D. Bebbington, A. T. Russell, *Tetrahedron*, **1994**, *50*, 12015–12028.
- ⁹⁶ S. A. Savage, G. S. Jones, S. Kolotuchin, S. A. Ramrattant, T. Vu, R. E. Waltermire, *Org. Process Res. Dev.*, **2009**, *6*, 1169–1176.
- ⁹⁷ M. S. Kuo, R. J. Zielinski, J. I. Cialdella, C. K. Marschke, M. J. Dupuis, G. P. Li, D. A. Kloosterman, C. H. Spilman, V. P. marshall, *J. Am. Chem. Soc.*, **1995**, *117*, 10629–10634.
- ⁹⁸ A. Freund, *J. Prak. Chem.*, **1882**, *26*, 367–377.
- ⁹⁹ H. E. Simmons, R. D. Smith, *J. Am. Chem. Soc.*, **1958**, *80*, 5323–5324.
- ¹⁰⁰ A. B. Charrette, H. Juteau, H. Lebel, C. Molinaro, *J. Am. Chem. Soc.*, **1998**, *120*, 11943–11952.
- ¹⁰¹ A. B. Charrette, H. Lebel, *J. Am. Chem. Soc.*, **1996**, *118*, 10327–10328.
- ¹⁰² J. C. Lorenz, J. Long, Z. Yang, S. Xue, Y. Xie, Y. Shi., *J. Org. Chem.*, **2004**, *69*, 327–334.

- ¹⁰³ S. Chuprakov, S. W. Kwok, L. Zhang, L. Lercher, V. V. Fokin, *J. Am. Chem. Soc.*, **2009**, *131*, 18034–18035.
- ¹⁰⁴ S. Chantamath, D. T. Nguyen, K. Shibatomi, S. Iwasa, *Org. Lett.*, **2013**, *15*, 772–775.
- ¹⁰⁵ E. Rossi, P. Woehl, M. Maggini, *Process. Res. Dev.*, **2012**, *16*, 1146–1149.
- ¹⁰⁶ A. B. Charette, M. K. Janes, H. Lebel, *Tetrahedron Asymmetry*, **2003**, *14*, 867–872.
- ¹⁰⁷ B. Morandi, E. M. Carreira, *Science*, **2012**, *335*, 1471–1474.
- ¹⁰⁸ R. J. Mattson, J. D. Catt, D. J. Denhart, J. A. Deskus, J. L. Ditta, M. A. Higgins, L. R. Marcin, C. P. Sloan, B. R. Beno, Q. Gao, M. A. Cunningham, G. K. Mattson, T. F. Molski, M. T. Taber, N. J. Lodge, *J. Med. Chem.*, **2005**, *48*, 6023–6034.
- ¹⁰⁹ Derek Strokes, PhD thesis, *Towards the Synthesis of a protein β -turn Mimetic based on the Opioid Pentapeptide Leu-enkephalin*, **2012**.
- ¹¹⁰ X. J. Zhang, Y. S. Zhang, Y. S. Huang, R. P. Hsung, K. C. M. Kurtz, J. Oppenheimer, M. E. Petersen, I. K. Sagamanova, L. C. Shen, M. R. Tracey, *J. Org. Chem.*, **2006**, *71*, 4170–4177.
- ¹¹¹ B. Yao, Z. Liang, T. Niu, Y. Zhang, *J. Org. Chem.*, **2009**, *74*, 4630–4633.
- ¹¹² A. L. Kohnen, J. R. Dunetz, R. L. Danheiser, *Org. Synth.*, **2007**, *84*, 88–101.
- ¹¹³ B. M. Trost, D. T. Stiles, *Org. Lett.*, **2005**, *7*, 2117–2120.
- ¹¹⁴ A. B. Evans, D. W. Knight, *Tet. Lett.*, **2001**, *42*, 6947–6948.
- ¹¹⁵ S. J. Butler, K. A. Jolliffe, *Org. Biomol. Chem.*, **2011**, *9*, 3471–3483.
- ¹¹⁶ A. Ajamian, J. L. Gleason, *Org. Lett.*, **2001**, *3*, 4161–4164.
- ¹¹⁷ R. Campagne, Master Thesis, **2014**.
- ¹¹⁸ M. A. Blanchette, W. Choy, J. T. Davis, A. P. Essenfeld, S. Masamune, W. R. Roush, T. Sakai, *Tet. Lett.*, **1984**, *25*, 2183–2186.
- ¹¹⁹ D. Seebach, M. Overhand, F. N. M. Kühnle, B. Martinoni, *Helv. Chim. Acta*, **1996**, 913–941.
- ¹²⁰ C. Angus, Bsc. Thesis, **2015**.
- ¹²¹ W. C. Still, C. Gennari, *Tetrahedron Lett.*, **1983**, *24*, 4405–4408.
- ¹²² J. Rizo, L. M. Gierasch, *Annu. Rev. Biochem.*, **1992**, *61*, 387–418.
- ¹²³ J. A. Robinson, *Curr. Opin. Chem. Biol.*, **2011**, *15*, 379–386.
- ¹²⁴ A. Grauer, B. König, *Eur. J. Org. Chem.*, **2009**, 5099–5111.
- ¹²⁵ S. Oishi, H. Kamitani, Y. Kodera, K. Watanabe, K. Kobayashi, T. Narumi, K. Tomita, H. Ohno, T. Naito, E. Kodama, M. Matsuoka, N. Fujii, *Org. Biomol. Chem.*, **2009**, *7*, 2872–2877.
- ¹²⁶ R. R. Gardner, G.-B. Liang, S. H. Gellman, *J. Am. Chem. Soc.*, **1999**, *121*, 1806–1816. (REF 64 IN INTRO)
- ¹²⁷ V. A. Rassadin, V. V. Sokolov, A. F. Khlebnikov, N. V. Ulin, S. I. Kozhushkov, A. de Meijere, *Synthesis*, **2012**, *44*, 372–376.
- ¹²⁸ V. F. Gareev, R. M. Sultanova, R. Z. Biglova, V. A. Dokichev, Y. V. Tomilov, *Russ. Chem. Bull., Int. Ed.*, **2008**, *57*, 1784–1786.
- ¹²⁹ T. Kajiwarra, Y. Sasaki, F. Kimura, A. Hatanaka, *Agric. Biol. Chem.*, **1981**, *45*, 1461–1466.
- ¹³⁰ P. Müller, C. Baud, D. Ené, S. Motallebi, *Helv. Chim. Acta*, **1995**, *78*, 459–470.
- ¹³¹ F. Lv, Z.-F. Li, W. Hu, X. Wu, *Bioorg. Med. Chem.*, **2015**, *23*, 7661–7670.
- ¹³² C. Morrill, R. H. Grubbs, *J. Org. Chem.*, **2003**, *68*, 6031–6034.
- ¹³³ S. Chantamath, D. T. Nguyen, K. Shibatomi, S. Iwasa, *Org. Lett.*, **2013**, *15*, 772–775. (REF 86 INTRO)
- ¹³⁴ W. Kirmse, P. Van Chiem, P.-G. Henning, *Tetrahedron*, **1985**, *41*, 1441–1451.
- ¹³⁵ S. Xiao, X.-X. Shi, J. Xing, J.-J. Yan, S.-L. Liu, *Eur. J. Org. Chem.*, **2010**, 1711–1716.
- ¹³⁶ T. Schotten, W. Boland, L. Jaenicke, *Helv. Chim. Acta.*, **1985**, *68*, 1186–1192.
- ¹³⁷ C. L. Bailey, A. Y. Joh, Z. Q. Hurley, C. L. Anderson, B. Singaram, *J. Org. Chem.*, **2016**, *81*, 3619–3628.
- ¹³⁸ A. Mordini, D. Peruzzi, F. Russo, M. Valacchi, G. Reginato, A. Brandi, *Tetrahedron*, **2005**, *61*, 3349–3360.
- ¹³⁹ M. von Delius, F. Hauke, A. Hirsch, *Eur. J. Org. Chem.*, **2008**, *24*, 4109–4119.
- ¹⁴⁰ Y.-C. Wong, Z. Ke, Y.-Y. Yeung, *Org. Lett.*, **2015**, *17*, 4944–4947.
- ¹⁴¹ S. E. Sen, S. L. Roach, *Synthesis*, **1995**, 756–758.
- ¹⁴² F. Berrée, G. Michelot, M. Le Corre, *Tet. Lett.*, **1998**, *39*, 8275–8276.
- ¹⁴³ S. B. Daval, C. Valant, D. Bonnet, E. Kellenberger, M. Hibert, J.-L. Galzi, B. Ilien, *J. Med. Chem.*, **2012**, *55*, 2125–2143.
- ¹⁴⁴ Z. Wang, R. B. Silverman, *J. Enzyme Inhib.*, **2004**, *19*, 293–301.
- ¹⁴⁵ I. Koppel, J. Koppel, F. Degerbeck, L. Grehn, U. Ragnarsson, *J. Org. Chem.*, **1991**, *56*, 7172–7174.
- ¹⁴⁶ K. Seehafer, C. C. Malakar, M. Bender, J. Qu, C. Liang, G. Helmchen, *Eur. J. Org. Chem.*, **2016**, 493–501.
- ¹⁴⁷ E. Hohn, J. Paleček, J. Pietruszka, W. Frey, *Eur. J. Org. Chem.*, **2009**, 3765–3782.
- ¹⁴⁸ F. Lv, Z.-F. Li, W. Hu, X. Wu, *Bioorg. Med. Chem.*, **2015**, 7661–7670.
- ¹⁴⁹ Z. K. Wickens, B. Morandi, R. H. Grubbs, *Angew. Chem. Int. Ed.*, **2013**, *52*, 11257–11260.
- ¹⁵⁰ F. Lv, Z.-F. Li, W. Hu, X. Wu, *Bioorg. Med. Chem.*, **2015**, *23*, 7661–7670.
- ¹⁵¹ X. Camps, E. Dietel, A. Hirsch, S. Pyo, L. Echegoyen, S. Hacknarth, B. Röder, *Chem. Eur. J.*, **1999**, *5*, 2362–2373.
- ¹⁵² G. W. Kabalka, T. M. Shoup, N. M. Goudgaon, *J. Org. Chem.*, **1989**, *54*, 5930–5933.
- ¹⁵³ J. S. Clark, M. C. Kimber, J. Robertson, C. S. P. McErlean, C. Wilson, *Angew. Chem.*, **2005**, *44*, 6157–6162.

- ¹⁵⁴ E. M. Flamme, W. R. Roush, *Org. Lett.*, **2005**, 7, 1411–1414.
- ¹⁵⁵ T. Seki, S. Tanaka, M. Kitamura, *Org. Lett.*, **2012**, 14, 608–611.
- ¹⁵⁶ P. Langer, *J. Prakt. Chem.*, **2000**, 342, 728–730.
- ¹⁵⁷ A.-K. C. Schmidt, C. B. W. Stark, *Org. Lett.*, **2011**, 13, 4164–4167.
- ¹⁵⁸ E. N. Jacobsen, *Acc. Chem. Res.*, **2000**, 33, 421–431.
- ¹⁵⁹ M. Tokunaga, J. F. Iarrow, F. Kakiuchi, E. N. Jacobsen, *Science*, **1997**, 277, 936–938.
- ¹⁶⁰ B. Neises, W. Steglich, *Angew. Chem. Int. Ed. Engl.*, **1978**, 17, 522–524.
- ¹⁶¹ J. K. Whitesell, D. Reynolds, *J. Org. Chem.*, **1983**, 48, 3548–3551.
- ¹⁶² K. Avula, D. K. Mohapatra, *Tet. Let.*, **2016**, 57, 1715–1717.
- ¹⁶³ Q. Zhao, H. N. Wong, *Tetrahedron*, **2007**, 63, 6296–6305.
- ¹⁶⁴ L.-X. Zhao, J. G. Park, Y.-S. Moon, A. Basnet, J. Choi, E.-K. Kim, T. C. Jeong, Y. Jahng, E.-S. Lee, *IL FARMACO*, **2004**, 59, 381–388.
- ¹⁶⁵ D. He, J. Ma, X. Shi, C. Zhao, M. Hou, Q. Guo, S. Ma, X. Li, P. Zhao, W. Liu, Z. Yang, J. Mou, P. Song, Y. Zhang, J. Li, *Chem. Pharma. Bull.*, **2014**, 62, 967–978.
- ¹⁶⁶ A. Dondoni, S. Franco, F. Junquera, F. F. L. Merchá, P. Merino, T. Tejero, *J. Org. Chem.*, **1997**, 62, 5497–5507.
- ¹⁶⁷ Y. S. Klausner, M. Bodansky, *Synthesis*, **1972**, 9, 453–463.
- ¹⁶⁸ A. L. Llaness García, *synlett.*, **2007**, 8, 1328–1329.
- ¹⁶⁹ J. Christoffers, A. Mann, *Chem. Eur. J.*, **2001**, 7, 1014–1027.
- ¹⁷⁰ D. X. Hu, P. Grice, S. V. Ley, *J. Org. Chem.*, **2012**, 77, 5198–5202.
- ¹⁷¹ A. B. Smith, J. J. Chruma, Q. Han, J. Barbosa, *Bioorg. Med. Chem. Lett.*, **2004**, 14, 1697–1702.
- ¹⁷² L. A. Carpino, A. El-Faham, F. Albericio, *Tetrahedron Lett.*, **1994**, 35, 2279–2282.
- ¹⁷³ W. F. Vranken, W. Rieping, *Struct. Biol.*, **2009**, 9, 1–10.
- ¹⁷⁴ C. Laurence, M. Berthelot, *Perspect. Drug Discovery Des.*, **2000**, 18, 39–60.
- ¹⁷⁵ CROSS REF 42 intro
- ¹⁷⁶ M. Crisma, G. D. Fasman, H. Balaram, P. Balaram, *Int. J. Peptide Protein Res.*, **1984**, 23, 411–419.
- ¹⁷⁷ A. Perczel, M. Hollósi, B. M. Foxman, G. D. Fasman, *J. Am. Chem. Soc.*, **1991**, 113, 9772–9784.
- ¹⁷⁸ A. Perczel, M. Hollósi, P. Sándor, G. D. Fasman, *Int. J. Peptide Protein Res.*, **1993**, 41, 223–236.
- ¹⁷⁹ A. Perczel, G. D. Fasman, *Protein Sci.*, **1992**, 1, 378–395.
- ¹⁸⁰ Redrawn from A. Perczel, G. D. Fasman, *Protein Sci.*, **1992**, 1, 378–395 with permission from Wiley and Sons.
- ¹⁸¹ E. Czinki, A. G. Császár, A. Perczel, *Chem. Eur. J.*, **2003**, 9, 1182–1189.
- ¹⁸² P. J. Fuchs, A. M. J. J. Bonvin, B. Boicchio, A. Pepe, *Biophys. J.*, **2006**, 90, 2745–2759.
- ¹⁸³ P. Morales, M. Angeles Jiménez, *Arch. Biochem. Biophys.*, **2019**, 661, 149–167.
- ¹⁸⁴ CROSS REF TO REF 66 INTRO JC froelich
- ¹⁸⁵ J. Podlech, D. Seebach, *Angew. Chem. Int. Ed. Eng.*, **1995**, 34, 471–472.
- ¹⁸⁶ J. Cesar, M. Sollner Dolenc, *Tetrahedron Lett.*, **2001**, 42, 7099–7102.
- ¹⁸⁷ CROSS REF LORENZ
- ¹⁸⁸ CROSS REF MATTSON
- ¹⁸⁹ D. A. Evans, K. A. Woerpel, Mé H. Hinman, A. A. Faul, *J. Am. Chem. Soc.*, **1991**, 113, 726–728.
- ¹⁹⁰ D. P. hari, J. Waser, *J. Am. Chem. Soc.*, **2017**, 139, 8420–8423.
- ¹⁹¹ H. Lebel, J.-F. Marcoux, C. Molinaro, A. B. Charette, *Chem. Rev.*, **2003**, 103, 977–1050.
- ¹⁹² A.-H. Li, L.-X. Dai, V. K. Aggarwal, *Chem. Rev.*, **1997**, 97, 2341–2372.
- ¹⁹³ P. Bruzdziak, A. Panuszko, B. Piotrowski, J. Stangret, *Journal of Molecular Liquids*, **2019**, 277, 532–540.
- ¹⁹⁴ A. D. Cochran, N. J. Skelton, M. A. Starovashnik, *PNAS*, **2001**, 98, 5578–5583.
- ¹⁹⁵ V. Muñoz, E.R. Henry, J. Hofrichter, W.A. Eaton, *PNAS*, **2008**, 95, 5872–5879.
- ¹⁹⁶ C. Krejtschi, R. Huang, T. A. Keiderling, K. Hauser, *Vibrational Spectroscopy*, **2008**, 48, 1–7.
- ¹⁹⁷ W. Y. Yang, J. W. Pitera, W. C. Swope, M. Gruebele, *J. Mol. Biol.*, **2004**, 336, 241–251.
- ¹⁹⁸ N. Kannan S. Vishveshwara, *Protein Eng.*, **2000**, 13, 753–761.
- ¹⁹⁹ C. A. Hunter K. R. lawson, J. Perkins, C. J. Urch, *J. Chem. Soc., Perkin Trans. 2*, **2001**, 651–669.
- ²⁰⁰ R. Huang, L. Wu, D. McElheny, P. Bour, A. Roy, T. A. Keiderling, *J. Phys. Chem. B*, **2009**, 113, 5661–5674.
- ²⁰¹ W. F. Degrado, C. M. Summa, V. Pavone, F. Natri, A. Lombardi, *Annu. Rev. Biochem.*, **1999**, 68, 779–819.
- ²⁰² R. Huang, L. Wu, D. McElheny, R. Huang, T. A. Keiderling, *Biochemistry*, **2009**, 48, 10362–10371.
- ²⁰³ A. Roy, P. Bour, T. A. Keiderling, *Chirality*, **2009**, 21, E163–E171.
- ²⁰⁴ G. Hopping, J. Kellock, B. Caughey, V. Daggett, *ACS Med. Chem. Lett.*, **2013**, 4, 824–828.
- ²⁰⁵ N. J. Greenfield, *Nat. Protoc.*, **2006**, 1, 2527–2535.
- ²⁰⁶ M. Meot-Ner, *Chem. Rev.*, **2005**, 105, 213–284.
- ²⁰⁷ G. J. Kleywegt, T. A. Jones, *Structure*, **1996**, 12, 1395–1400.
- ²⁰⁸ G. N. Ramachandran, C. Ramakrishnan, V. Sasisekharan, *J. Mol. Biol.*, **1963**, 7, 95–99.
- ²⁰⁹ R. W. W. Hooft, C. Sander, G. Vriend, *Bioinformatics*, **1997**, 13, 425–430.
- ²¹⁰ Reprinted from *New Tool and Data for Improving Structures*, Vol 374, J. S. Richardson, W. B. Arendal III, D. C. Richardson, 385–412, 2003, with permission from Elsevier

-
- J. S. Richardson, W. B. Arendal III, D. C. Richardson, *Methods in Enzymology*, **2003**, 374, 385–412.
- ²¹¹ F. Carrascoza, S. Zaric, R. Silaghi-Dumitrescu, *J. Mol. Graph. Model.*, **2014**, 50, 125–133.
- ²¹² A.G. de Brevern, *Scientific Reports*, **2016**, 6, article number 33191.
- ²¹³ J. L. Thomas, D. Volker, S. Uli, *Methods in enzymol. Part A and B: NMR of Biological molecules*, Vol. 338 and 339, **2001**.
- ²¹⁴ D. S. Wishart, B. D. Sykes, F. M. Richards, *J. Mol. Biol.*, **1991**, 222, 311–333.
- ²¹⁵ M. Karplus, *J. Chem. Phys.*, **1959**, 30, 11–15.
- ²¹⁶ J.-C. Hus, D. Marion, M. Blackledge, *J. Mol. Biol.*, **2000**, 298, 927–936.
- ²¹⁷ S. Raghothama, *Journal of the Indian Institute of Science*, **2010**, 90, 145–161.
- ²¹⁸ N. J. Skelton, K. C. Garcia, D. V. Goeddel, C. Quan, J. P. Burnier, *Biochemistry*, **1994**, 33, 13581–13592.